Group 4 Transition-Metal and Lanthanide Complexes Supported by Bulky Amido Ligands

KU, Ka Wai

A Thesis Submitted in Partial Fulfillment

of the Requirements for the Degree of

Doctor of Philosophy

in

Chemistry

The Chinese University of Hong Kong

May 2011

UMI Number: 3497774

All rights reserved

INFORMATION TO ALL USERS
The quality of this reproduction is dependent on the quality of the copy submitted.

In the unlikely event that the author did not send a complete manuscript
and there are missing pages, these will be noted. Also, if material had to be removed,
a note will indicate the deletion.

UMI
Dissertation Publishing

UMI 3497774

Copyright 2012 by ProQuest LLC.

All rights reserved. This edition of the work is protected against
unauthorized copying under Title 17, United States Code.

ProQuest

ProQuest LLC.
789 East Eisenhower Parkway
P.O. Box 1346
Ann Arbor, MI 48106 - 1346

Thesis Committee

Professor Kevin W. P. LEUNG (Chair)

Professor Dennis K. P. NG (Committee Member)

Professor Hung Kay LEE (Thesis Supervisor)

Professor Peter JUNK (External Examiner)

Professor Chak-Po LAU (Additional External Examiner)

Abstract

This present research work focuses on the coordination chemistry of three different types of anionic nitrogen-containing ligands, namely the bulky arylamido ligands $[N(C_6H_3R_2–2,6)(CH_2Bu^t)]^-$ (R = Me, Pr^i), the benzamidinato ligand $[PhC(NC_6H_3Pr^i_2–2,6)(NSiMe_3)]^-$, and the *2*-pyridylamido ligand $[N(C_6H_3Pr^i_2–2,6)(2–C_5H_3N–6–Me)]^-$.

Chapter 1 gives a brief introduction to metal complexes supported by amido and amidinato ligands.

Chapter 2 describes the synthesis, structural characterization, and reactivity of Group 4 metal complexes of the bulky *N*-alkylated arylamido ligands $[N(C_6H_3R_2–2,6)(CH_2Bu^t)]^-$ [R = Me (L^1), Pr^i (L^2)]. Direct reactions of MCl_4 (M = Zr, Hf) with $[LiL^n(tmeda)]$ [*n* = 1 (**5**), *n* = 2 (**6**)] afforded heterobimetallic complexes $[M(L^n)_2Cl(\mu–Cl)_2Li(tmeda)]$ [M = Zr, *n* = 1 (**8**), *n* = 2 (**9**); M = Hf, *n* = 1 (**10**), *n* = 2 (**11**)]. Neutral, mononuclear bis(amide) complexes $[M(L^2)_2Cl_2]$ [M = Ti (**12**), Zr (**13**), Hf (**14**)] were obtained by treatment of $MCl_4(thf)_x$ (M = Ti, x = 2; M = Zr, Hf, x = 0) with the tmeda-free lithium salt $LiL^2(thf)_2$ (**7**). Ligand substitution reactions of **13** and **14** with $LiNMe_2$ afforded the corresponding tetra(amido) complexes $[M(L^2)_2(NMe_2)_2]$ [M = Zr (**15**), Hf (**16**)]. Subsequent reactions of complexes **15** and **16** with methyl iodide led to a mixture of the corresponding monoiodide (**17** and **19**) and diiodide (**18** and **20**) complexes. The bis(amido) dimethyl complexes $[M(L^2)_2Me_2]$ [M = Zr (**21**), Hf (**22**)] were prepared by the reactions of **13** and **14** with LiMe. Ti(III) amide-chloride complexes $[Ti(L^1)_2(\mu–Cl)_2Li(tmeda)]$ (**23**) and $[Li(tmeda)_2]^+[Ti(L^2)_2Cl_2]^-$

(**24**) were also synthesized by the reactions of $TiCl_3(thf)_3$ with lithium reagents **5** and **6**, respectively.

Chapter 3 reports on the synthesis, structure, and reactivity of Ti(III), Ti(IV), Zr(IV) and Hf(IV) complexes containing the unsymmetrical benzamidinate ligand $[PhC(NC_6H_3Pr^i_2–2,6)(NSiMe_3)]^-$ (L^3). Reaction of $TiCl_3(thf)_3$ with $[LiL^3(thf)_2]$ (**29**) gave the Ti(III) complex $[Ti(L^3)_2Cl]$ (**31**). Treatment of **31** with LiMe led to the corresponding methyl derivative $[Ti(L^3)_2Me]$ (**32**). The reaction of $TiCl_4(thf)_2$ with $[LiL^3(tmeda)]$ (**28**) led to $[Ti(L^3)(NC_6H_3Pr^i_2–2,6)(\mu–Cl)_2Li(tmeda)]$ (**33**). Treatment of MCl_4 (M = Zr, Hf) with complex **28** yielded the corresponding neutral complexes $[M(L^3)_2Cl_2]$ [M = Zr (**34**), Hf (**35**)]. Ligand substitution reaction of **34** with LiMe gave the bis(methyl) complex $[Zr(L^3)_2Me_2]$ (**36**). The mono(benzyl) complex $[Zr(L^3)_2(CH_2Ph)Cl]$ (**37**) was obtained via the reaction of **34** with $PhCH_2MgCl$.

Chapter 4 describes the coordination chemistry of the 2-pyridylamido ligand $[N(C_6H_3Pr^i_2–2,6)(2–C_5H_3N–6–Me)]^-$ (L^4) with divalent lanthanide ions [Sm(II), Eu(II) and Yb(II)]. Metathetical reactions of $LnI_2(thf)_2$ (Ln = Yb, Eu) with potassium amide $[\{KL^4(OEt_2)\}_2]$ (**42**) led to divalent lanthanide complexes $[Yb(L^4)_2(thf)_2]$ (**44**) and $[Eu(L^4)(\mu–L^4)_2(thf)_2]$ (**45**), respectively. On the other hand, treatment of $SmI_2(thf)_2$ with **42** led to the homoleptic Sm(III) derivative $[Sm(L^4)_3]$ (**46**). Oxidation of **44** and **45** with iodine yielded Ln(III) complexes $[Yb(L^4)_2(I)(thf)]$ (**47**) and $[Eu(L^4)_3]$ (**48**), respectively. Yb(III) complex **47** was also prepared by the reaction of **44** with CuI. Reactions of **44** with PhEEPh (E = S, Se, Te) resulted in the isolation of Yb(III) tris(amido) complex $[Yb(L^4)_3]$ (**49**). Treatment of complex **47** with $KOBu^t$ also gave $[Yb(L^4)_3]$ (**49**) as the only isolable product.

摘要

本項研究主要針對具有立體位阻的芳胺基配體 $[N(C_6H_3R_2\text{–}2,6)(CH_2Bu^t)]^-$ (R = Me, Pr^i)、不對稱的苯脒基配體 $[PhC(NC_6H_3Pr^i_2\text{–}2,6)(NSiMe_3)]^-$ 及 2–吡啶胺基配體 $[N(C_6H_3Pr^i_2\text{–}2,6)(2\text{–}C_5H_3N\text{–}6\text{–}Me)]^-$ 的配位化學。

第一章 概括介紹胺基和脒基配體，以及由它們所衍生的金屬配合物。

第二章 描述具有立體位阻的芳胺基配體 $[N(C_6H_3R_2\text{–}2,6)(CH_2Bu^t)]^-$ [R = Me (L^1), Pr^i (L^2)] 所衍生的第四族金屬配合物的合成、結構表徵和反應性能。通過無水四氯化物 MCl_4 (M = Zr, Hf) 和胺基鋰 [LiL^n(tmeda)] [n = 1 (**5**), n = 2 (**6**)] 的反應，雙核配合物 $[M(L^n)_2Cl(\mu\text{–}Cl)_2Li(tmeda)]$ [M = Zr, n = 1 (**8**), n = 2 (**9**); M = Hf, n = 1 (**10**), n = 2 (**11**)] 成功被合成。利用不含四甲基乙二胺的胺基鋰 $LiL^2(thf)_2$ (**7**)，中性單核的雙胺基金屬配合物 $[M(L^2)_2Cl_2]$ [M = Ti (**12**), Zr (**13**), Hf (**14**)] 亦可由上述反應製備。中性的雙胺基金屬配合物 $[M(L^2)_2Cl_2]$ [M = Zr (**13**), Hf (**14**)] 與二甲胺基鋰的配體取代反應生成相應的四胺基金屬配合物 $[M(L^2)_2(NMe_2)_2]$ [M = Zr (**15**), Hf (**16**)]。進一步把四胺基金屬配合物 **15** 和 **16** 與碘代甲烷反應，可得出相應包含單取代碘配合物和雙取代碘配合物的混合物。通過雙胺基金屬配合物 $[M(L^2)_2Cl_2]$ [M = Zr (**13**), Hf (**14**)] 與甲基鋰的反應，雙取代甲基–胺基金屬配合物 $[M(L^2)_2Me_2]$ [M = Zr (**21**), Hf (**22**)] 被成功合成。三價鈦配合物 $[Ti(L^1)_2(\mu\text{–}Cl)_2Li(tmeda)]$ (**23**) 和 $[Li(tmeda)_2]^+[Ti(L^2)_2Cl_2]^-$ (**24**) 亦由 $TiCl_3(thf)_3$ 和相應的胺基鋰 [LiL^n(tmeda)] [n = 1 (**5**), n = 2 (**6**)] 的反應成功製備。

第三章 闡述由不對稱的苯脒基配體 $[PhC(NC_6H_3Pr^i_2\text{–}2,6)(NSiMe_3)]^-$ (L^3) 所衍生的第四族金屬配合物的合成、結構表徵和反應性能。通過 $TiCl_3(thf)_3$ 和 $[LiL^3(thf)_2]$ (**29**) 的反應，成功合成三價鈦配合物 $[Ti(L^3)_2Cl]$ (**31**)。配合物 **31** 與甲基鋰的反應生成相應的甲基配合物 $[Ti(L^3)_2Me]$ (**32**)。通過 $TiCl_4(thf)_2$ 和

$[LiL^3(tmeda)]$ (**28**) 的反應，成功製備 $[Ti(L^3)(NC_6H_3Pr^i_2\text{–}2,6)(\mu\text{–}Cl)_2Li(tmeda)]$ (**33**)。中性配合物 $[M(L^3)_2Cl_2]$ [M = Zr (**34**), Hf (**35**)] 則由 MCl_4 (M = Zr, Hf) 與化合物 **28** 的反應成功合成。胺基鋯配合物 $[Zr(L^3)_2Cl_2]$ (**34**) 和甲基鋰的配體取代反應得到雙取代甲基配合物 $[Zr(L^3)_2Me_2]$ (**36**)。通過 $[Zr(L^3)_2Cl_2]$ (**34**) 和格氏試劑苄基氯鎂的反應，單苄基配合物 $[Zr(L^3)_2(CH_2Ph)Cl]$ (**37**) 成功被製備。

第四章 描述 2–吡啶胺基配體 $[N(C_6H_3Pr^i_2\text{–}2,6)(2\text{–}C_5H_3N\text{–}6\text{–}Me)]^-$ (L^4) 對於二價鑭系金屬離子(釤、銪和鐿) 的配位化學，以及由 L^4 配體所衍生的二價鑭系金屬配合物的反應化學。通過 $LnI_2(thf)_2$ (Ln = Yb, Eu) 和鉀配合物 $[\{KL^4(OEt_2)\}_2]$ (**42**) 的反應，成功合成相應的二價鑭系金屬配合物 $[Yb(L^4)_2(thf)_2]$ (**44**) 和 $[Eu(L^4)(\mu\text{–}L^4)_2(thf)_2]$ (**45**)。另一方面，$SmI_2(thf)_2$ 與 **42** 的反應則得出三價配合物 $[Sm(L^4)_3]$ (**46**)。用碘把二價鑭系金屬配合物 **44** 和 **45** 氧化，可以得到相應的三價鑭系金屬配合物 $[Yb(L^4)_2(I)(thf)]$ (**47**) 和 $[Eu(L^4)_3]$ (**48**)。配合物 **47** 亦可由二價鐿配合物 **44** 和碘化亞銅的反應製備。另外，二價鐿配合物 **44** 與二苯基硫族化合物 PhEEPh (E = S, Se, Te) 的反應則可以得到三價鐿配合物 $[Yb(L^4)_3]$ (**49**)。而鐿配合物 **47** 和叔丁醇鉀的反應亦生成三胺基三價鐿配合物 **49**。

Acknowledgement

I would like to express my deepest gratitude to my supervisor, Prof. Hung Kay Lee, for his guidance and valuable advice throughout the course of my study and the preparation of this thesis. Prof. Lee is very patient with students. His continuous support means a lot to me.

I am grateful to Prof. Thomas C. W. Mak and Ms. Bella H. S. Chan for their assistance and advice on the X-ray crystallography. Ms. Chan is very nice and she taught me a lot on X-ray structure analysis. Thanks should also be given to Mr. Chi Chung Lee and Ms. Sarah H. Y. Ng for the measurement of mass spectra.

I would also like to express my appreciation to all the members in Prof. Lee's research group. I appreciate Dr. Ho Yu Au-Yeung for his kind assistance. Dr. Au-Yeung is always willing to help. He has taught me lots of experimental skills since the very beginning of my research work. I am thankful to Dr. Shuang Yao, Mr. George Fai Wong and Ms. Lai Fong Yeung for their encouragement, assistance and useful discussion during my study. Help from Ms. Yin Man Lai is also acknowledged. I would also like to thank my new friends, Mr. Chi Wai Au, Mr. Kevin Yat Kit Chen and Mr. Lei Yun, for their kind assistance and the enjoyable working environment they brought.

Finally, my family members and friends are greatly acknowledged for their continuous encouragement and support. They always stand by me, bringing me confidence and strength for challenges in life.

Ka Wai Ku
February 2011

Table of Contents

Abbreviations

Ligands and Substituents

Me	methyl
Et	ethyl
Pr^i	*iso*-propyl
Bu^n	*n*-butyl
Bu^t	*tert*-butyl
Ph	phenyl
Py	pyridyl
Cp	cyclopentadienyl
Cy	cyclohexyl
Ar	aryl
Mes	2,4,6-trimethylphenyl
OTf	triflate

Compounds

thf	tetrahydrofuran
tmeda	*N,N,N'N'*,-tetramethylethylenediamine
dme	1,2-dimethoxyethane
dmpe	bis(dimethylphosphino)ethane

NMR Spectroscopy

s	singlet
d	doublet
dd	double of doublet
t	triplet
q	quartet
sept	septet
m	multiplet
br	broad signal
δ	chemical shift
J	coupling constant
ppm	part per million

Miscellaneous

r.t.	room temperature
h	hour(s)
d	day(s)
M.p.	melting point
dec.	decomposed
Anal.	analysis
Calc.	calculated

List of Compounds

Compound **13**	$[Zr(L^2)_2Cl_2]$	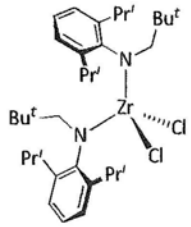	p. 36
Compound **13a**	$[Zr(L^2)_2Cl(\mu\text{–}Cl)_2Li(thf)_2]$	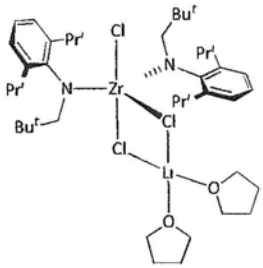	p. 37
Compound **14**	$[Hf(L^2)_2Cl_2]$	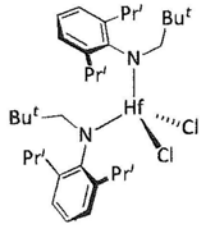	p. 36
Compound **15**	$[Zr(L^2)_2(NMe_2)_2]$	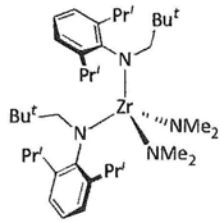	p. 54
Compound **16**	$[Hf(L^2)_2(NMe_2)_2]$	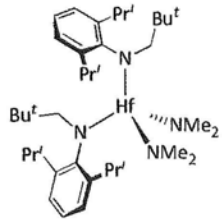	p. 54
Compound **17**	$[Zr(L^2)_2(NMe_2)(I)]$	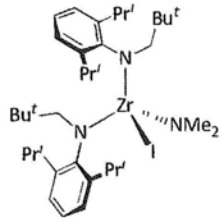	p. 54

Compound **18**	$[Zr(L^2)_2I_2]$	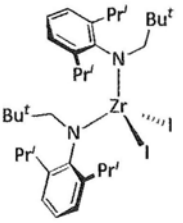	p. 54
Compound **19**	$[Hf(L^2)_2(NMe_2)(I)]$	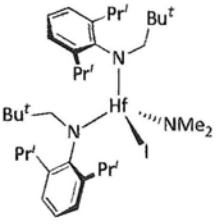	p. 54
Compound **20**	$Hf(L^2)_2I_2$		p. 54
Compound **21**	$[Zr(L^2)_2Me_2]$	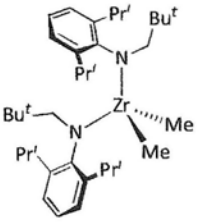	p. 67
Compound **22**	$[Hf(L^2)_2Me_2]$	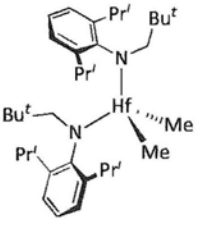	p. 67
Compound **23**	$[Ti(L^1)_2(\mu\text{–}Cl)_2Li(tmeda)]$	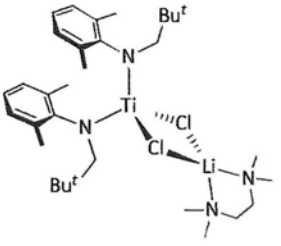	p. 74

Compound **24**	$[Li(tmeda)_2]^+[Ti(L^2)_2Cl_2]^-$	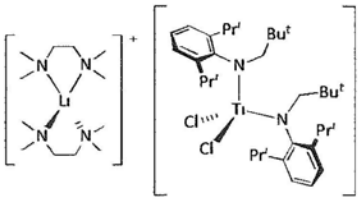	p. 74
Compound **29**	$LiL^3(thf)_2$		p. 98
Compound **31**	$[Ti(L^3)_2Cl]$	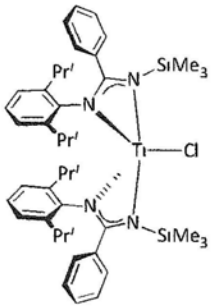	p. 100
Compound **32**	$[Ti(L^3)_2Me]$	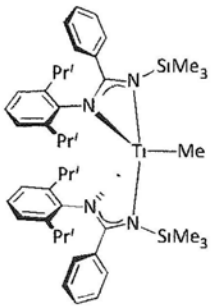	p. 101
Compound **33**	$[Ti(L^3)(NC_6H_3Pr^i{}_2\text{–}2,6)(\mu\text{–}Cl)_2Li(tmeda)]$	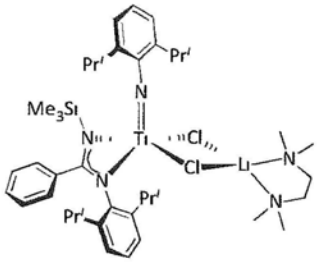	p. 106
Compound **34**	$[Zr(L^3)_2Cl_2]$	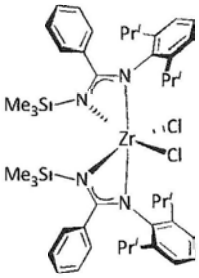	p. 110

Compound **35**	$[Hf(L^3)_2Cl_2]$	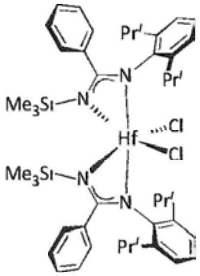	p. 110
Compound **36**	$[Zr(L^3)_2Me_2]$	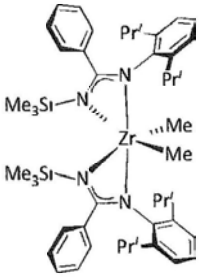	p. 115
Compound **37**	$[Zr(L^3)_2(CH_2Ph)Cl]$	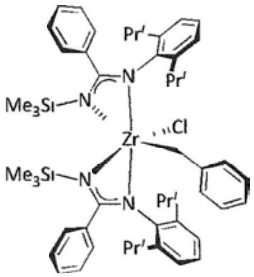	p. 115
Compound **39**	$[Mg(L^3)_2(thf)]$	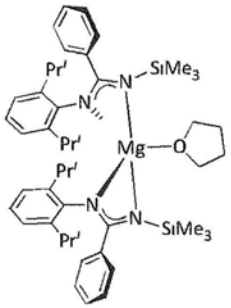	p. 123
Compound **40**	$[Ca(L^3)_2(thf)]$	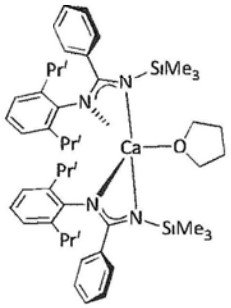	p. 124

Compound **41**	$[HL^4]$	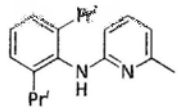	p. 148
Compound **42**	$[\{KL^4(OEt_2)\}_2]$	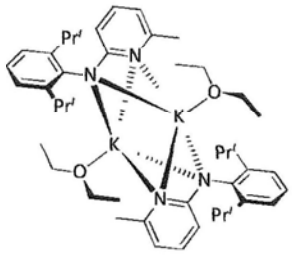	p. 148
Compound **43**	$KL^4(thf)_2$		p. 148
Compound **44**	$[Yb(L^4)_2(thf)_2]$	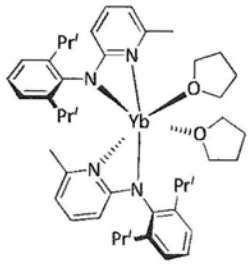	p. 153
Compound **45**	$[Eu(L^4)(\mu\text{–}L^4)_2K(thf)]$	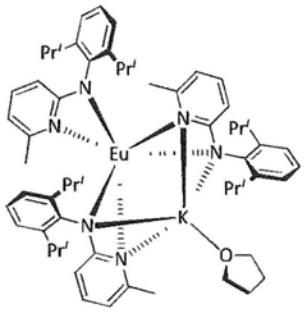	p. 153
Compound **46**	$[Sm(L^4)_3]$	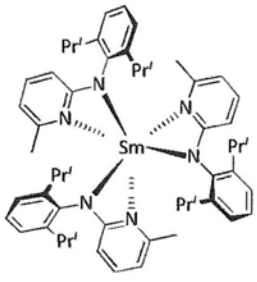	p. 153

Chapter 1

An Overview on Amido and Amidinato Ligands

Amide and amidinate are nitrogen-containing ligands with the general formula of $[NR_2]^-$ *and* $[RC(NR')(NR'')]^-$ *(R, R', R'' = H, alkyl, aryl or silyl), respectively. As alternatives to the ubiquitous metallocenes, metal complexes derived from these ligands have received considerable attention in past decades. The work described in this thesis is focused on Group 4 metal and lanthanide complexes supported by sterically demanding amido and amidinato ligands. In this introductory chapter, a brief account on amido and amidinato ligands is given.*

Background

In the last century, studies of complexes containing metal–carbon bonds have been a popular topic in organometallic chemistry.[1a] On the other hand, complexes containing metal–nitrogen bonds have received relatively less attention. In the 70s and 80s, tremendous efforts were devoted to the chemistry of cyclopentadienyl ligands. The reactivity of metal-cyclopentadienyl complexes, with alkene polymerization in particular, was extensively investigated. After an exhaustive study on cyclopentadienyl and related complexes, the development for alternative ligand systems for cyclopentadienides has attracted an increasing research interest. Among various cyclopentadienyl alternatives, nitrogen donating ligands such as amides[1a–f,l] and amidinates[1g–l] have been extensively studied due to their unique properties.

There are two advantages for using amido and amidinato ligands in coordination chemistry: (i) the electronic and steric requirements of these ligands can be readily modified to tailor properties of interest,[1d–h] and (ii) nitrogen-based ligands are kinetically more robust than halide, hydride or alkyl ligands, thereby affording metal complexes with definite reaction sites without dissociation of the supporting ligands.[1f,g]

Amido Ligands

A. General Features

Amido ligands are generally represented by the formula of –NRR', in which R and R' can be a H, alkyl, aryl, silyl or boryl group (Chart 1–1).[1a–c] By virtue of the possibility of double substitution, the steric and electronic properties of amido ligands can be readily modified. The diversity of ligand design accounts for the good compatibility of amido ligands with a wide range of metal ions.

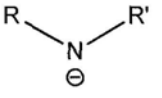

Chart 1–1

B. Development

The first metal amide, $Zn(NEt_2)_2$, was synthesized by Frankland in 1856.[2] After the report of the first transition metal amide, namely $[Ti(NPh_2)_4]$, by Dermer and Fernelius in 1934,[8a] the chemistry of transition metal amides remained stagnant for more than a decade. Until 1959, Bradley initiated a systematic study on transition metal dialkylamides.[1a] Later in the 70s, the chemistry of lanthanide metal amides was explored.[1b]

The foundations of metal amide chemistry were laid by the pioneering work of Bürger, Wannagat, Bradley and Lappert.[1a–f] Over the past decades, a variety of amido ligands have been developed for supporting various metal ions. The ligands of interest are usually bulky and free of β-hydrogen. Apart from monodentate

amides, multidentate amido ligands such as 2-pyridylamides have also been developed.

C. The Bis(trimethylsilyl)amido Ligand — $[N(SiMe_3)_2]^-$

The chemistry of bis(trimethylsilyl)amido ligand, $[N(SiMe_3)_2]^-$, has been extensively studied over the past decades.[1a,3–7] The $[N(SiMe_3)_2]^-$ ligand is an extremely versatile ligand. It can provide a great steric protection and is also electronically compatible with a variety of metal ions.

Early in 1960s, bis(trimethylsilyl)amido complexes of the types ML_3 [M = Al, Ga, Cr, Fe; L = $N(SiMe_3)_2$], ML_2 (M = Be, Mn, Co, Ni, Zn, Cd, Hg) and ML (M = Li, Na, Cu) were reported by Bürger and Wannagat.[1a]

In 1973, trivalent rare-earth complexes $[LnL_3]$ (Ln = Sc, Y, La, Ce, Pr, Nd, Sm, Eu, Gd, Ho, Yb, Lu) were isolated by Bradley[4a] and Hursthouse.[4b] Later, monomeric lanthanide(II) complexes of the type $[LnL_2X_2]$ (Ln = Sm, Eu, Yb; X = thf, Et_2O, dme) were reported by the groups of Zalkin,[5a] Andersen[5b–c] and Evans.[5d] These divalent lanthanide silylamides served as valuable starting materials for other organolanthanide(II) compounds.

Using the $[N(SiMe_3)_2]^-$ ligand, Bradley and Andersen have reported a few early transition metal amides of the types $[ML_3]$ (M = Ti, V)[1a] and $[ML_3X]$ (M = Zr, Hf; X = Cl, Me),[6] respectively. The chemistry of the $[N(SiMe_3)_2]^-$ ligand has attracted an increasing attention since the reports of the low-coordinate late transition metal complexes $[M\{N(SiMe_3)_2\}_3]$ and $[M\{N(SiMe_3)_2\}_2]_2$ (M = Mn, Co).[7]

D. Arylamido Ligands

Arylamido ligands contain one or two aryl substituent(s) attached to the amido nitrogen (Chart 1–2). There are two advantages of using arylamido ligands in the studies of metal amide complexes. It is noteworthy that delocalization of the lone-pair electron density on the amido nitrogen onto the aryl substituents may enhance the stability of the metal complexes.[1f] Moreover, ligand modification is easy as a wide variety of aryl substituents with different steric and electronic properties are readily available.

1. Anilides

A few examples of anilido ligands are shown in Chart 1–2.[8–15] The first metal anilide, $[Ti(NPh_2)_4]$, was prepared in 1934.[8a] Over the years, a number of main-group,[9] transition metal[10–14] and lanthanide[15] anilido complexes have been synthesized and structurally characterized.

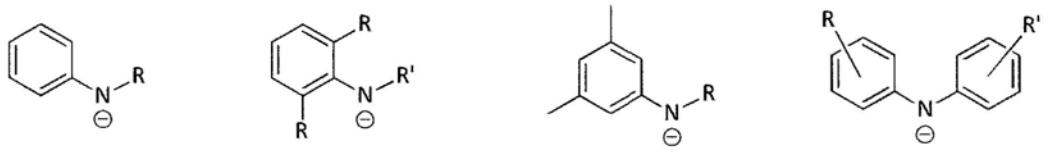

R = H, Bu^t, $CH(Bu^t)_2$, $SiMe_3$

R = Me, Pr^i
R' = H, CH_2Bu^t, $SiMe_3$

R = Bu^t, Ad, $CMe(CD_3)_2$, $CPh(CD_3)_2$,

R/R' = H/H, Pr^i_2–2,6/F–2
F_5/F_5, $F_5/SiMe_3$

Chart 1–2

A number of studies on Group 4 metal anilides have been reported due to their potential applications as catalysts in olefin polymerization.[9–12] For example, Ti(IV), Zr(IV) and Hf(IV) complexes supported by the $[N(C_6H_3Pr^i_2\text{–}2,6)(SiMe_3)]^-$ ligand were shown to be active catalysts towards polymerization of ethylene.[11c–e] The

reducing property of Ti(III) anilides have also been investigated.[9,12] A detailed discussion on Group 4 metal anilides is given in Chapter 2.

Stabilization of late transition metal amides, in which a π-conflict exist between the *d* electrons of the metal ions and the amido nitrogen, was regarded as a challenge in the past decades.[1b,f] It is believed that the π-conflict can be relieved by using arylamido ligands because of the delocalization of the lone-pair electron density on the nitrogen onto the aromatic ring.[1f] Recently, the coordination chemistry of the $[N(R)(C_6H_3R'_2\text{–}2,6)]^-$ (R = $SiMe_3$, CH_2Bu^t, C_6F_5; R′ = Me, Pr′) ligands towards the first-row late transition metal has been examined by our research group (Chart 1–3).[13]

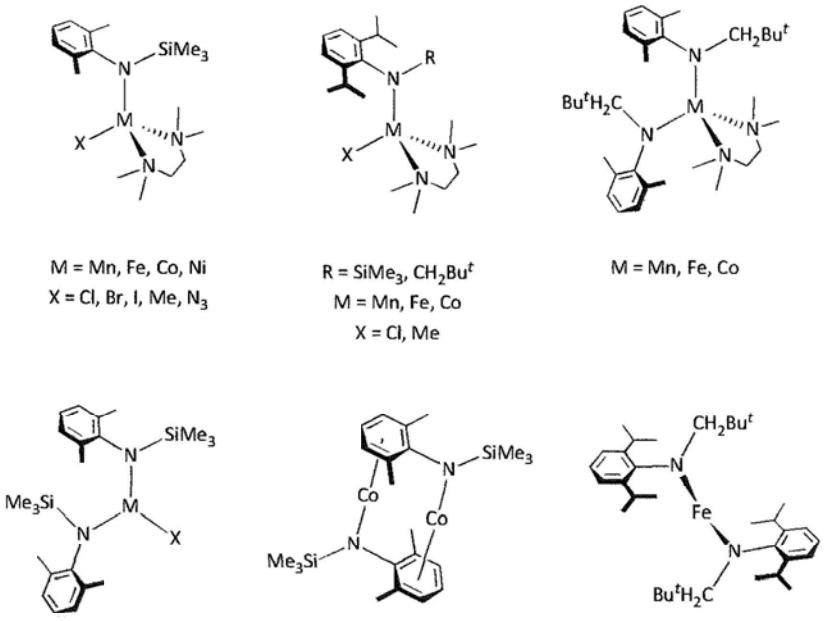

Lee *et al.*[13]

Chart 1–3

Successful isolation of coordinatively unsaturated complexes has also been

achieved by using sterically very bulky arylamido ligands. Power and co-workers have reported a few *quasi*-two-coordinate Mn(II)[14a] and Fe(II)[14b] complexes, as well as a stable one-coordinate Tl(I) complex,[14c] of very bulky terphenyl amido ligands. By using the bulky $[N(CH_2Bu^t)(C_6H_3Pr^i_2\text{-}2,6)]^-$ ligand, a two-coordinate Fe(II) complex has also been prepared by our research group (Chart 1–3).[13a]

Stabilization of large lanthanide ions by anilido ligands has been reported.[15] For example, neutral Y(III), Nd(III) and Yb(III) complexes of the $[NH(C_6H_3Pr^i_2\text{–}2,6)]^-$ ligand were reported by Evans and co-workers in 1996.[15a] Furthermore, monomeric divalent lanthanide complexes derived from the $[N(SiMe_3)(C_6H_3Pr^i_2\text{–}2,6)]^-$ ligand have been reported by Schumann and co-workers in 1997.[15h] More recently, Sm(II) and Yb(II) complexes of the less bulky $[N(Ph)(SiMe_3)]^-$ ligands were synthesized in Shen's laboratory through reduction of the corresponding trivalent precursors.[15i] All of these complexes are heteroleptic and contain solvent molecules coordinated to the metal centers.

2. 2-Pyridylamides

The coordination chemistry of 2-pyridylamido ligands has attracted much attention due to their flexible binding modes.[1e,16a] They can act as monodentate, *N,N'*-chelating or *N,N'*-bridging ligands (Chart 1–4), leading to metal complexes with interesting structures.

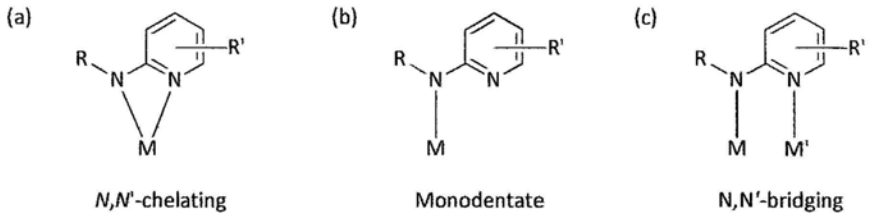

N,N'-chelating Monodentate N,N'-bridging

Chart 1–4

The steric properties and solubility behavior of 2-pyridylamido ligands can be readily modified by introduction of various R and R′ substituents (Chart 1–5). The first *N*,*N*′-chelating pyridylamido complex, $[Ru\{NPh(Py)\}_2(PPh_3)_2]$, was reported by Cotton and co-workers in 1984.[16b] To date, there are a number of reports on metal pyridylamides focusing on various issues.[16–21]

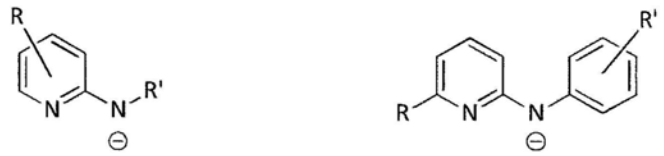

R = H, Me–4, Me–6
R' = H, Me, Ad, $SiMe_3$, $SiBu^tMe_2$, $SiBu^tPh_2$

R = H, Me, $C_6H_3Me_2$–2,6, $C_6H_2Pr^i_3$–2,4,6
R' = H, Bu^t_2–3,5, Pr^i–2, Pr^i_2–2,6, Me_2–2,4, Me_2–3,5, Me_3–2,4,6, Pr^i_2–2,6, Me_3–2,4,6

Chart 1–5

The coordination chemistry of the bulky $[N(SiBu^tMe_2)(2\text{–}C_5H_3N\text{–}6\text{–}Me)]^-$ ligand has been studied by our research group. A series of main-group, transition metal and lanthanide complexes was prepared and characterized (Chart 1–6).[18] In most of the cases, this ligand coordinated to metal ions in a *N*,*N*′-chelating manner. Nevertheless, they could also act as bridging ligands as in heterobimetallic Mn(II) and Co(II) complexes.[18e]

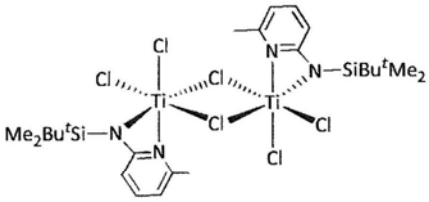

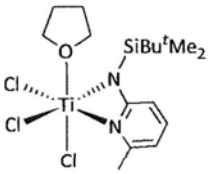

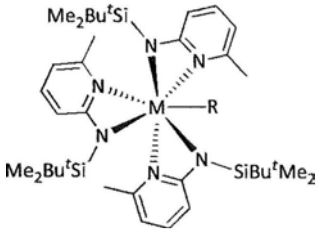

M = Zr, Hf; R = Cl, H, Me

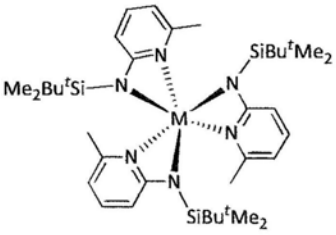

M = Y, Cr, In, Ce, Nd, Sm, Eu, Gd, Dy, Er, Yb

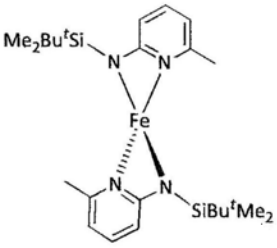

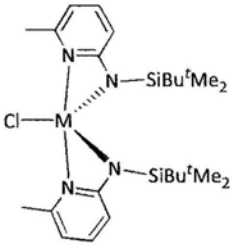

M = Al, Ga

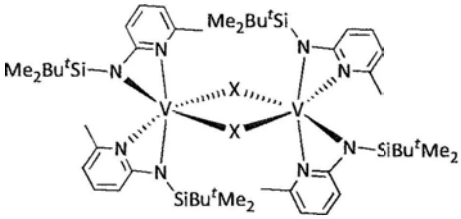

X = Cl, H

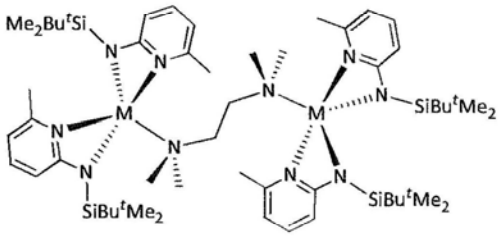

M = Fe, Co

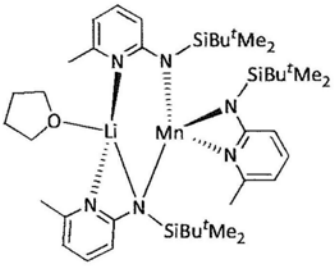

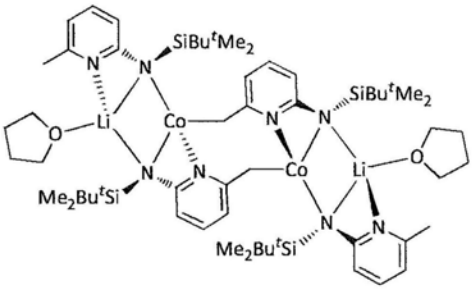

Lee *et al.*[18]

Chart 1–6

Group 4 metal complexes supported by 2-pyridylamido ligands have been examined because of their potential applications in alkene polymerization.[19] For instance, a Ti(IV) complex of the $[N(SiMe_3)(2\text{–}C_5H_3N\text{–}4\text{–}Me)]^-$ ligand has been

shown to be active catalyst for polymerization of propene and 1-butene.[19b] Controlled polymerization activity of a Zr(IV) complex derived from the $[N(Ar)(2–C_5H_3N–6–Ar')]^-$ (Ar = $C_6H_3Pr^i_2$–2,6, Ar' = $C_6H_2Pr^i_3$–2,4,6) ligand was also reported recently.[19l]

A number of transition metal complexes with interesting structures have been prepared by using the tridentate di(pyridyl)amido ligand (dpa). For example, metal ion chains of the type $M_3(dpa)_4X_2$ [M = Cr,[20a–d] Co,[20e–g] Ni,[20h] Ru,[20i] Rh,[20i] Cu;[20j,k] L= $N(2–C_5H_3N)_2$; X = uninegative anions] feature short metal-to-metal distances. A short Cr–Cr distance was also observed in a di(chromium) complex derived from the bidentate $[N(Ar)(2–C_5H_3N–6–Ar')]^-$ (Ar = $C_6H_2Me_3$–2,4,6, Ar' = $C_6H_2Pr^i_3$–2,4,6) ligand.[20p]

Synthesis and reactivity of late transition metal complexes have also been reported.[20e–x] Examples of these complexes include Ni(II) and Pd(II) derivatives of the $[N(SiMe_3)\ (2–C_5H_3N–4–Me)]^-$ ligand, which were shown to be active catalysts for Suzuki reaction and hydrosilane polymerization.[20t] On the other hand, late transition metal complexes supported by the $[N(SiMe_3)(2–C_5H_3N)]^-$ and $[NR(2–C_5H_3N–6–Me)]^-$ (R = $SiMe_3$, $SiBu^tMe_2$, CH_2Bu^t) ligands have also been synthesized by our research group (Chart 1–6).[18]

Stabilization of the large di- and trivalent lanthanide ions using pyridylamido ligands has been reported.[21] Heterobimetallic complexes featuring *d–f* interactions have been reported by Kempe's group, by virtue of the bridging coordination mode of pyridylamido ligands. (Chart 1–7).[1e,21b] Moreover, a series of homoleptic lanthanide(III) complexes derived from the bulky

$[N(SiBu^tMe_2)(2–C_5H_3N–6–Me)]^-$ ligand have been prepared in our laboratory (Chart 1–7).[18g–h] More recently, a few lanthanide(II) complexes supported by the sterically very demanding $[N(Ar)(2–C_6H_5N–6–Ar')]^-$ (Ar = $C_6H_3Pr^i_2$–2,6, $C_6H_2Me_3$–2,4,6, 2–C_5H_3N–6–Me; Ar' = $C_6H_2Pr^i_3$–2,4,6, $C_6H_3Me_2$–2,6) ligands have been reported.[21j–n]

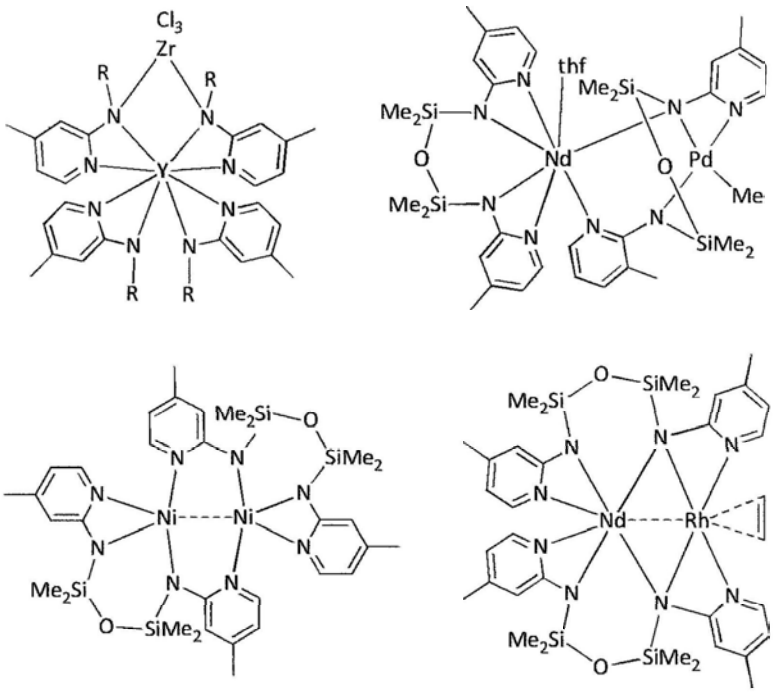

R = $SiMe_3$
Kemp *et al.*[1e,21b]

Chart 1–7

E. Fluorine-containing Amido Ligands

Incorporation of fluorine-containing substituents to amido ligands is a recent trend of ligand modification.[9g,10b,12l,13d,15d–e] Fluoro-substituted ligands have the following potential advantages. First of all, the electronic property of the ligand is

tuned by the highly electronegative fluorine atoms, thus offering the possibility of activity modification. Secondly, fluorine atoms are weakly coordinating, thus providing an additional coordination to the metal center. The labile M–F bond can stabilize and activate the metal centers via bond association and dissociation, respectively (Scheme 1–1). In order to facilitate the additional coordination, fluorine groups are usually located at the ortho positions of the phenyl rings attached to the amido nitrogen, which are close to metal centers upon complexation of the ligand.

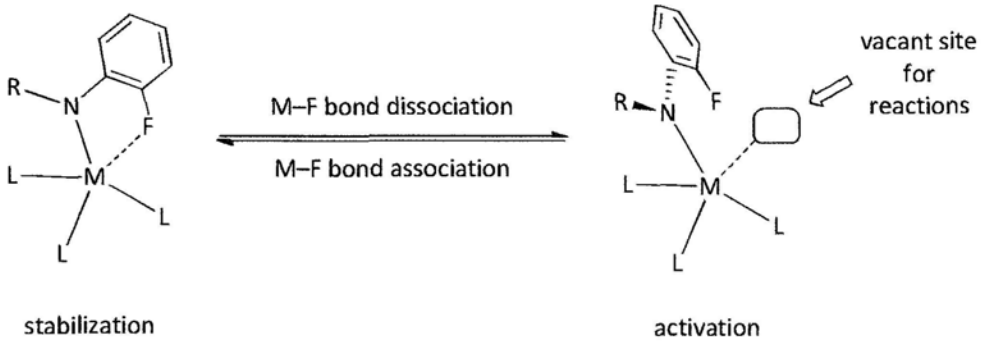

Scheme 1–1

Recently, the coordination chemistry of the $[N(C_6F_5)(SiMe_3)]^-$[13c] and $[N(C_6H_3Pr^i_2)(C_6F_5)]^-$[13d] ligands has been studied by our research group. Weak metal–fluorine interactions were observed in the complexes $[Co\{N(C_6H_3Pr^i_2)(C_6F_5)\}_2(Cl)Li(thf)_3]$ and $[Co\{N(C_6H_3Pr^i_2)(C_6F_5)\}_2(OMe)Li(tmeda)]$.[13d] A few examples of complexes containing metal–fluorine interactions are shown in Chart 1–8.

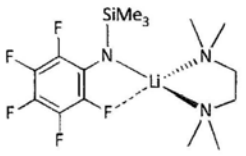

Eisen *et al.*[22a]

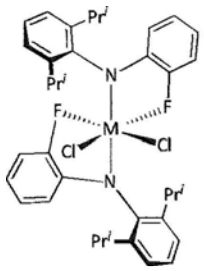

M = Zr, Hf Liang *et al.*[10b]

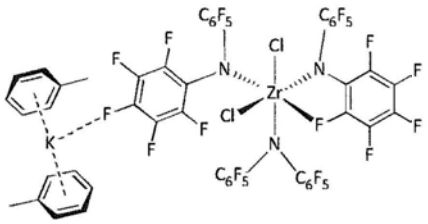

Watkin *et al.*[15d]

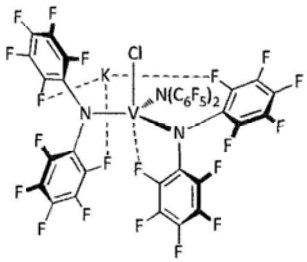

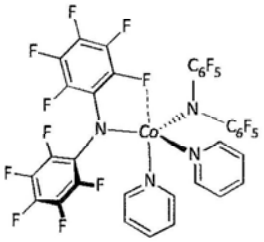

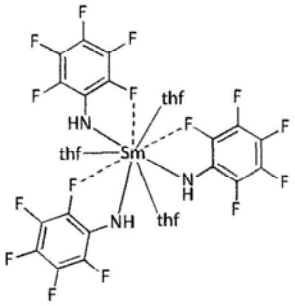

Watkin *et al.*[15d–e]

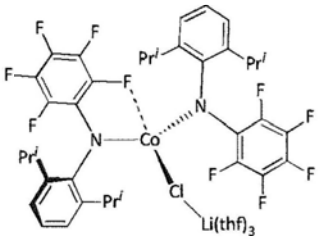

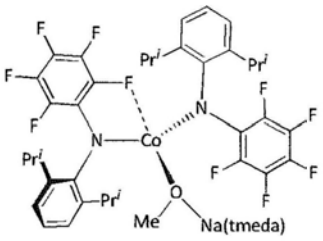

Lee *et al.*[13d]

Chart 1–8

Amidinate Ligands

A. General Features

Amidinates, with the general formula of $[RC(NR')(NR'')]^-$ (R, R', R'' = H, alkyl, aryl, silyl), are nitrogen analogues of carboxylate anions.[1i,j] Closely related are guanidinates, with an amino group attached to the central carbon atom of the NCN moiety (Chart 1–9).

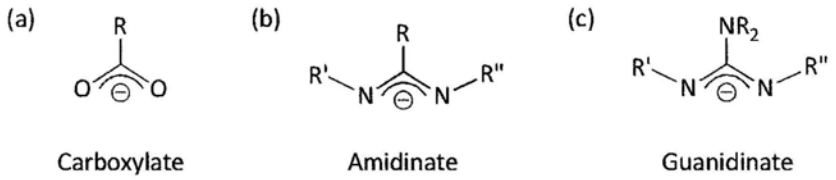

Chart 1–9

Amidinate ligands exhibit a rich coordination chemistry due to their flexible coordination modes (Chart 1–10).

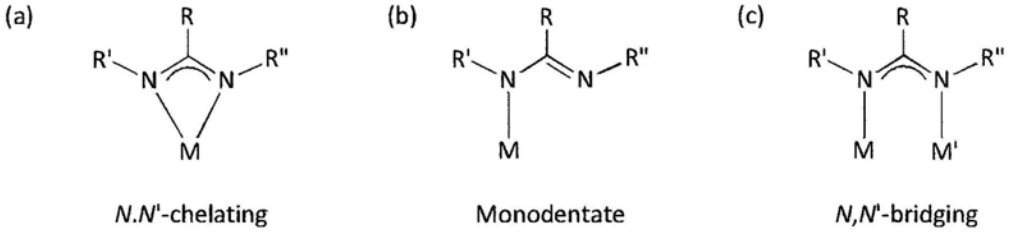

Chart 1–10

It has been suggested that adoption of different binding modes of amidinate ligands may depend on the orientation of the lone pairs on the nitrogen donors, which is influenced by the steric bulkiness of the substituents on the nitrogen and

carbons atoms (Chart 1–11).[22–23]

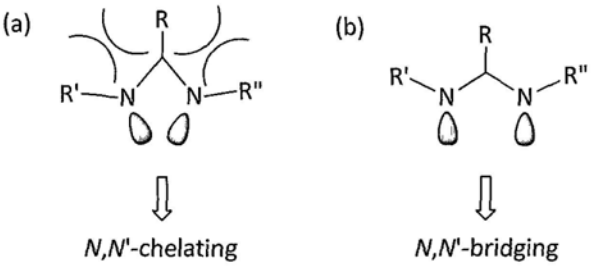

Chart 1–11

Amidinate ligands have been employed to stabilize a wide range of metal ions.[22–29] An efficient steric protection to the metal center can be provided by incorporation of bulky substituents to the nitrogen and/or carbon atoms on the amidinate backbone.

B. Amidinate Ligands with Bulky N-substituents

Sterically demanding alkyl, aryl or silyl substituents are usually incorporated to the nitrogen atoms of the NCN amidinate backbone in order to provide steric protection to the corresponding metal complexes (Chart 1–12).[1g–j,22–28]

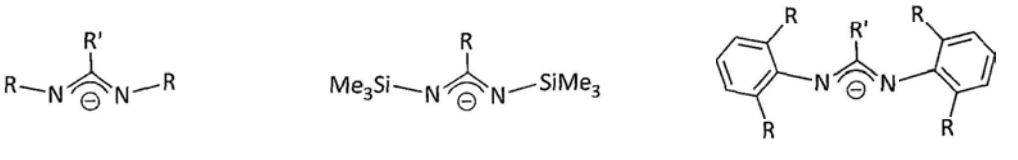

R = Pr^i; R' = Me, Et, Pr^i, Bu^t, Ph
R = Bu^t; R' = Me, Et, Ph
R = Cy; R' = H, Me, Bu^n, Bu^t, Fc, Ph, $C_6H_2(CF_3)_3$–2,4,6

R = Bu^t, Ph, C_6H_4OMe–4, $C_6H_4CF_3$–4

R = H; R' = H, Me
R = Me; R' = H, Ph
R = Pr^i; R' = H, Me, Bu^t, Ph, C_6H_4Me–2, C_6H_4Me–4,

Chart 1–12

Group 4 metal complexes supported by bulky amidinato ligands such as $[PhC\{N(SiMe_3)\}_2]^-$ and $[RC(NCy)_2]^-$ (R = Me, Bu^t) (Chart 1–14) have been reported.[24–25] Some of these complexes were shown to be active catalysts for alkene polymerizations and even dinitrogen activation. The chemistry of Group 4 metal amidinates will be discussed in more details in Chapter 3.

Bulky amidinate ligands have been proved to be capable of supporting metal complexes with unusual geometries. The four-coordinate metal centers in $[Cr\{MeC(NBu^t)_2\}_2]$[22a] and $[Fe\{PhC(NAr)_2\}_2]$ (Ar = $C_6H_3Pr^i_2$–2,6)[22b] were shown to be tetrahedral and square planar, respectively. Tetrahedral and square planar geometries are uncommon for high-spin Cr(II) and Fe(II) ions, respectively.

Recently, unsymmetrical amidinate ligands containing both trimethylsilyl and ortho-disubstituted aryl rings on the nitrogen atoms have been developed by our research group. Late transition metal complexes of the $[PhC(NSiMe_3)(NC_6H_3Me_2–2,6)]^-$ ligand were synthesized and characterized (Chart 1–13).[18d,26]

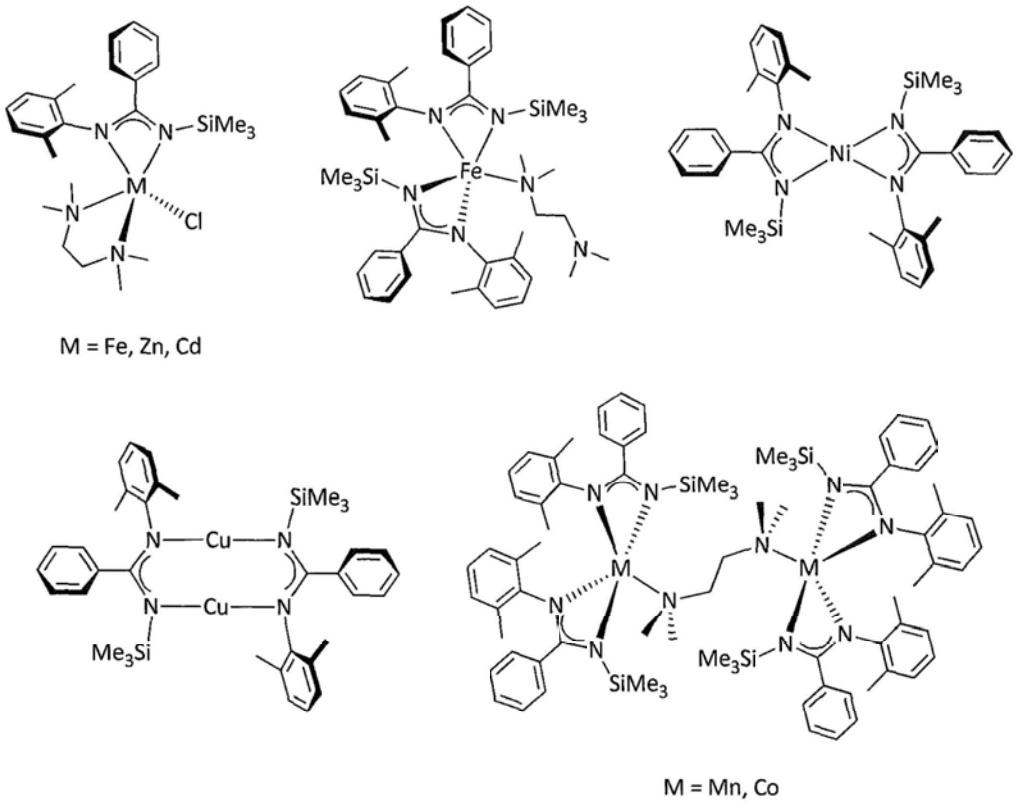

Lee *et al.*[18d,26]

Chart 1–13

In recent years, the chemistry of lanthanide(III) tris(amidinate) complexes has attracted much attention because of their high activity towards ring-opening polymerization of ε-caprolactone and trimethylene carbonate.[1j,27] On the other hand, reports on lanthanide(II) amidinates are still rare.[27f,h–j,28] By using the $[PhC(NSiMe_3)(NC_6H_3Pr^i_2\text{–}2,6)]^-$ ligand, a series of di- and trivalent lanthanide derivatives have been synthesized and structurally characterized by our research group (Chart 1–14).[13d,28] The catalytic properties of the lanthanide(III) amidinates towards the ring-opening polymerization of ε-caprolactone have also been investigated.[13d]

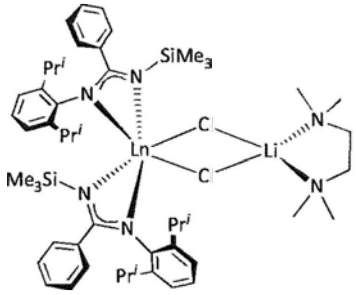

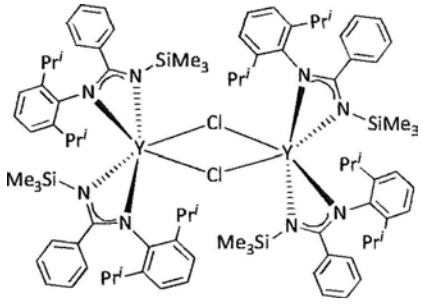

Ln = Y, Eu, Er, Lu

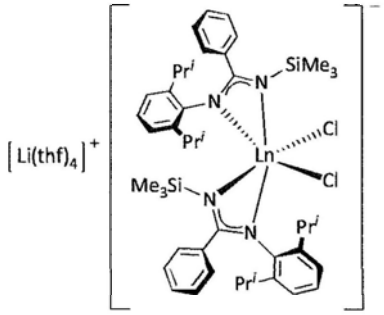

Ln = Ce, Nd, Sm

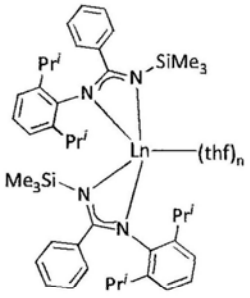

Ln = Sm, Eu; n = 2
Ln = Yb; n = 1

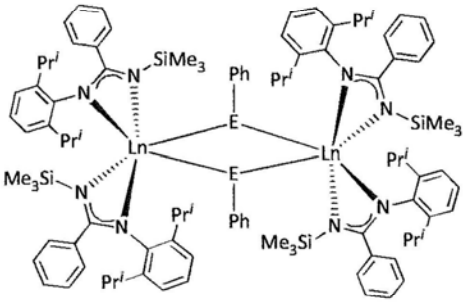

Ln = Sm; E = Te
Ln = Eu; E = Se

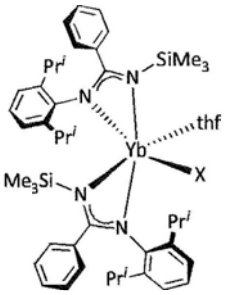

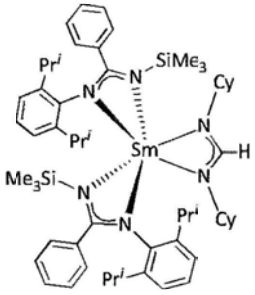

X = SePh, I

Lee *et al.*[13d,28]

Chart 1–14

C. Terphenyl Amidinates

Incorporation of a bulky terphenyl group on the central amidinate carbon atom is another approach to offer sufficient steric protection to the metal

center.[1h,29] Unusual three-coordinate Li complexes derived from sterically very bulky terphenyl substituted amidinate ligands have been reported (Chart 1–15).[29d] One noteworthy feature of these complexes is the uncommon monodentate coordination mode of the ligands.[23e,30]

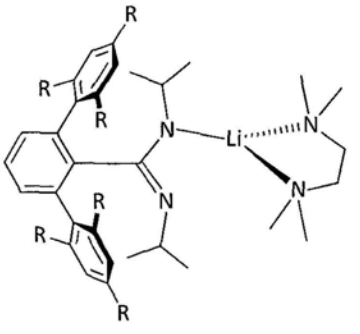

R = Me, Pr^{i}
Arnold *et al.*[29d]

Chart 1–15

Objectives of This Work

As described in the earlier sections of this chapter, the chemistry of Group 4 metal amides was dominated by complexes derived from silylated amido ligands. Group 4 metal complexes supported by monodentate *N*-alkylated amido ligands have received relatively less attention. One objective of our research work was focused on synthetic and structural studies of Group 4 metal complexes supported by *N*-alkylated arylamido ligands $[N(C_6H_3R_2–2,6)(CH_2Bu^t)]^-$ (R = Me, Pr^i) (Chapter 2). The catalytic properties of Group 4 metal amides towards alkene polymerization have been extensively studied. On the other hand, studies of their reaction chemistry with various alkyl or amide reagents are relatively rare. Therefore, the reaction chemistry of the Group 4 metal amides prepared in this work was examined. In addition, the chemistry of Group 4 metal complexes derived from the related amidinato ligand $[Ph(NC_6H_3Pr^i_2–2,6)(NSiMe_3)]^-$ was also studied (Chapter 3). Results of our studies may give some insights to the reactivity of Group 4 metal complexes supported by these monodentate and bidentate ligands.

The chemistry of lanthanide complexes is an active area in organometallic. The majority of the work reported in the literature has been focused on trivalent lanthanide complexes. Recently, lanthanide(II) chemistry has been a very topical area and a lot of related chemistry has been reported. Accordingly, the coordination chemistry of a bulky 2-pyridylamido ligand, $[N(C_6H_3Pr^i_2–2,6)(2–C_5H_3N–6–Me)]^-$, towards divalent lanthanide ions was studied in this work (Chapter 4). The reaction chemistry of these lanthanide(II) complexes was also examined.

References for Chapter 1

1. (a) Bradley, D. C.; Chisholm, M. H. *Acc. Chem. Res.* **1976**, *9*, 273–280.
   (b) Lappert, M. F.; Power, P. P.; Sanger, A. R.; Srivastava, R. C. *Metal and Metalloid Amides*, Horwood-Wiley, Chichester, **1980**.
   (c) Lappert, M. F.; Power, P. P.; Protchenko, A. V.; Seeber, A. L. *Metal Amide Chemistry*, John Wiley and Sons Ltd, **2009**.
   (d) Awander, R. *Top. Curr. Chem.* **1996**, *179*, 33–112.
   (e) Kempe, R. *Angew. Chem. Int. Ed.* **2000**, *39*, 468–493.
   (f) Kempe, R. *Eur. J. Inorg. Chem.* **2003**, 791–803.
   (g) Edelmann, F. T. *Top. Curr. Chem.* **1996**, *179*, 113–148.
   (h) Edelmann, F. T. *Adv. Organomet. Chem.* **2008**, *57*, 183–352.
   (i) Smolensky, E.; Eisen, M. S. *Dalton Trans.* **2007**, 5623–5650.
   (j) Edelmann, F. T. *Chem. Soc. Rev.* **2009**, *38*, 2253–2268.
   (k) Bailey, P. J.; Pace, S. *Coord. Chem. Rev.* **2001**, *214*, 91–141.
   (l) Gibson, V. C.; Spitzmesser, S. K. *Chem. Rev.* **2003**, *103*, 283–315.
2. Frankland, E. *Proc. Roy. Soc.* **1856–7**, *8*, 502–506.
3. Power, P. Xu, X. *J. Chem. Soc., Chem. Commun.* **1984**, 358–359.
4. (a) Bradley, D. C.; Ghotra, J. S.; Hart, A. *J. Chem. Soc., Dalton Trans.* **1973**, 1021–1023.
   (b) Ghotra, J. S.; Hursthouse, M. B.; Welch, A. J. *J. Chem. Soc., Chem. Commun.* **1973**, 669–670.
   (c) Aspinall, H. C.; Bradley, D. C.; Hursthouse, M. B.; Sales, K. D.; Walker, N. P. C.; Hussain, B. *J. Chem. Soc., Dalton, Trans.* **1989**, 623–626.
   (d) Edelmann, F. T.; Steiner, A.; Stalke, D. Gilje, J. W., Jagner, S.; Hakansson, M. *Polyhedron* **1994**, *13*, 539–546.
   (e) Zhou, S. –L.; Wang, S. –W.; Yang, G. –S.; Liu, X. –Y.; Sheng, E. –H.; Zhang, K. –H.; Cheng, L.; Huang, Z. –X. *Polyhedron* **2003**, *22*, 1019–1024.
   (f) Evans, W. J.; Lee, D. S.; Ziller, J. W. *J. Am. Chem. Soc.* **2004**, *126*, 454–455.
5. (a) Tilley, T. D.; Zalkin, A.; Andersen, R. A.; Templeton, D. H. *Inorg. Chem.* **1981**, *20*, 551–554.
   (b) Tilley, T. D.; Andersen, R. A.; Zalkin, A. *J. Am. Chem. Soc.* **1982**, *104*, 3725–3727.
   (c) Tilley, T. D.; Andersen, R. A.; Zalkin, A. *Inorg. Chem.* **1984**, *13*, 2271–2276.
   (d) Evans, W. J.; Drummond, D. K.; Zhang, H.; Atwood, J. L. *Inorg. Chem.* **1988**, *27*, 575–579.
6. Andersen, R. A. *Inorg. Chem.* **1979**, *18*, 1724–1725.
7. (a) Ellison, J. J.; Power, P. P.; Shoner, S. C. *J. Am. Chem. Soc.* **1989**, *111*, 8044–8046.
   (b) Bradley, D. C.; Hursthouse, M. B.; Malik, K. M. A.; Moseler, R. *Transition Met. Chem.* **1978**, *3*, 253–254.
   (c) Murray, B. D.; Power, P. P. *Inorg. Chem.* **1984**, *23*, 4584–4588.
   (d) Bartlett, R. A.; Power, P. P. *J. Am. Chem. Soc.* **1987**, *109*, 7563–7564.

(e) Chen, H.; Barlett, R. A.; Rasika, D. H. V.; Olmstead, M. M.; Power, P. P. *J. Am. Chem. Soc.* **1989**, *111*, 4338–4345.

8. (a) Dermer, O. C.; Fernelius, W. C. *Z. Anorg. Allg. Chem.* **1934**, *221*, 83–96.

9. (a) Cetinkaya, B.; Hitchcock, P. B.; Lappert, M. F.; Misra, M. C.; Thorne, A. J. *J. Chem. Soc., Chem. Commun.* **1984**, 148–149.

(b) Fjeldberg, T.; Hitchcock, P. B.; Lappert, M. L.; Thorne, A. J. *J. Chem. Soc., Chem. Commun.* **1984**, 822–824.

(c) Barr, D.; Clegg, W.; Mulvey, R. E.; Snaith, R.; Wright, D. S.; *J. Chem. Soc., Chem. Commun.* **1987**, 716–718.

(d) Bülow, R. v.; Gornitzka, H.; Kottke, T.; Stalke, D. *Chem. Commun.* **1996**, 1639–1640.

(e) Clegg, W.; Horsburgh, L.; Liddle, S. T.; Mackenzie, F. M.; Mulvey, R. E.; Robertson, A. *J. Chem. Soc., Dalton Trans.* **2000**, 1225–1231.

(f) Bezombes, J. P.; Hitchcock, P. B.; Lappert, M. L.; Merle, P. G. *J. Chem. Soc., Dalton Trans.* **2001**, 816–821.

(g) Aharonovich, S.; Botoshanski, M.; Eisen, M. S. *Inorg. Chem.* **2009**, *48*, 5269–5278.

10. (a) Johnson, A. R.; Wanandi, P. W.; Cummins, C. C.; Davis, W. M. *Organometallics* **1994**, *13*, 2907–2909.

(b) Johnson, A. R.; Davis, W. M.; Cummins, C. C. *Organometallics* **1996**, *15*, 3825–3835.

(a) Mokuolu, Q. F.; Duckmanton, P. A.; Blake, A. J.; Wilson, C.; Love, J. B. *Organometallics* **2003**, *22*, 4387–4389.

11. (a) Kasani, A.; Gambarotta, S.; Bensimon, C. *Can. J. Chem.* **1997**, *75*, 1494–1499.

(b) Lee, W. –Y.; Liang, L. –C. *Inorg. Chem.* **2008**, *47*, 3298–3306.

(c) Shah, S. A. A.; Dorn, H.; Voigt, A.; Roesky, H. W.; Parisini, E.; Schmidt, H. –G.; Noltemeyer, M. *Organometallics* **1996**, *15*, 3176–3181.

(d) Shah, S. A. A.; Dorn, H.; Roesky, H. W.; Parisini, E.; Schmidt, H. –D.; Noltemeyer, M. *Dalton Trans.* **1996**, 4143–4146.

(e) Nomura, K.; Fujii, K. *Organometallics* **2002**, *21*, 3042–3049.

12. (e) Wanandi, P. W.; Davis, W. M.; Cummins, C. C. *J. Am. Chem. Soc.* **1995**, *117*, 2110–2111.

(f) Peters, J. C.; Johnson, A. R.; Odom, A. L.; Wanandi, P. W.; Davis, W. M.; Cummins, C. C. *J. Am. Chem. Soc.* **1996**, *118*, 10175–10188.

(g) Peters, J. C.; Cherry, J. –P.; F.; Thomas, J. C.; Baraldo, L.; Mindiola, D. J.; Davis, W. M.; Cummins, C. C. *J. Am. Chem. Soc.* **1999**, *121*, 10053–10067.

(h) Mendiratta, A.; Cummins, C. C.; Cotton, F. A.; Ibragimov, S. A.; Murillo, C. A.; Villagrán, D. *Inorg. Chem.* **2006**, *45*, 4328–4330.

(i) Mendiratta, A.; Cummins, C. C. *Inorg. Chem.* **2005**, *44*, 7319–7321.

(j) Agapie, T.; Diaconescu, P. L.; Mindiola, D. J.; Cummins, C. C. *Organometallics* **2002**, *21*, 1329–1340.

(k) Mendiratta, A.; Figueroa, J. S.; Cummins, C. C. *Chem. Commun.* **2005**, 3403–3405.

(l) Giesbrecht, G. R.; Gordon, J. C.; Clark, D. L.; Hijar, C. A.; Scott, B.; L.; Watkin, J. G. *Polyhedron* **2003**, *22*, 153–163.

13. (a) Au-Yeung, H. Y.; Lam, C. H.; Lam, C. -K.; Wong, W. -Y.; Lee, H. K. *Inorg. Chem.* **2007**, *46*, 769–7697.
    (b) Au-Yeung, H. Y. *M. Phil. Thesis*, The Chinese University of Hong Kong, 2006.
    (c) Wong, G. F. *M. Phil. Thesis*, The Chinese University of Hong Kong, 2008.
    (d) Yao, S. *PhD. Thesis*, The Chinese University of Hong Kong, 2009.
14. (a) Ni, C.; Rekken, B.; Fettinger, J. C.; Long, G. J.; Power, P. P. *Dalton Trans.* **2009**, 8349–8355.
    (b) Merrill, W. A.; Stich, T. A.; Brynda, M.; Yeagle, G. J.; Fettinger, J. C.; Hont, R. D.; Reiff, W. M.; Schulz, C. E.; Britt, R. D.; Power, P. P. *J. Am. Chem. Soc.* **2009**, *131*, 12693–12702.
    (c) Wright, R. J.; Brynda, M.; Power, P. P. *Inorg. Chem.* **2005**, *44*, 3368–3370.
15. (a) Evans, W. J.; Ansari, M. A.; Ziller, J. W. Khan, S. I. *Inorg. Chem.* **1996**, *35*, 5435–5444.
    (b) Wong, W. –K.; Zhang, L.; Xue, F.; Mak, T. C. W. *Polyhedron*, **1997**, *16*, 345–347.
    (c) Wong, W. –K.; Zhang, L.; Xue, F.; Mak, T. C. W. *Polyhedron*, **1997**, *16*, 2013–2020.
    (d) Kraut, S.; Magull, J.; Schaller, U. *Z. Anorg. Allg. Chem.* **1998**, *624*, 1193–1201.
    (e) Click, D. R.; Scott, B. L.; Watkin, J. G. *Chem. Commun.* **1999**, 633–634.
    (f) Click, D. R.; Scott, B. L.; Watkin, J. G. *Acta Cryst.* **2000**, *C56*, 1095–1096.
    (g) Chan, H. –S.; Li, H. –W.; Zie, Z. *Chem. Commun.* **2002**, 652–653.
    (h) Deacon, G. B.; Fallon, G. D.; Forsyth, C. M.; Schumann, H. Weimann, R. *Chem. Ber./Recueil* **1997**, *130*, 409–415.
    (i) Zhou, L.; Wang, J.; Zhang, Y.; Yao, M.; Shen, Q. *Inorg. Chem.* **2007**, *46*, 5763–5772.
16. (a) Deeken, S.; Motz, G.; Kempe, R. *Z. Anorg. Allg. Chem.* **2007**, *633*, 320–325.
    (b) Chakravarty, A. R.; Cotton, F. A.; Shamshoum, E. S. *Inorg. Chim. Acta* **1984**, *86*, 5–11.
17. (a) Barr, D.; Clegg, W.; Mulvey, R. E.; Snaith, R. *J. Chem. Soc., Chem. Commun.* **1984**, 469–470.
    (b) Barr, D.; Clegg, W.; Mulvey, R. E.; Snaith, R. *J. Chem. Soc., Chem. Commun.* **1984**, 700–701.
    (c) Engelhardt, L. M.; Jacobsen, G. E.; Junk, P. C.; Raston, C. L.; Skelton, B. W.; White, A. H. *J. Chem. Soc., Dalton Trans.* **1988**, 1011–1020.
    (d) Raston, C. L.; Skelton, B. W.; Tolhurst, V. –A.; White, A. H. *Polyhedron* **1998**, *17*, 935–942.
    (e) Jones, C.; Junk, P. C.; Leary, S. G.; Smithies, N. A.; Steed, J. W. *Inorg. Chem. Commun.* **2002**, *5*, 533–536.
    (f) Scott, N. M.; Schareina, T.; Tok, O.; Kempe, R. *Eur. J. Inorg. Chem.* **2004**, 3297–3304.
18. (a) Cheng, P. S. *M. Phil. Thesis*, The Chinese University of Hong Kong, 2004.
    (b) Lee, H. K.; Wong, Y. –L.; Zhou, Z. –Y.; Zhang, Z. –Y.; Ng, D. K. P.; Mak, T. C. W. *J. Chem. Soc., Dalton Trans.* **2000**, 539–544.
    (c) Lee, H. K.; Lam, C. H.; Li, S. –L.; Zhang, Z. –Y.; Mak, T. C. W. *Inorg. Chem.* **2001**, *40*, 4691–4695.
    (d) Lam, C. H. *M. Phil. Thesis*, The Chinese University of Hong Kong, 2001.
    (e) Lam, T. S. *M. Phil. Thesis*, The Chinese University of Hong Kong, 2002.

(f) Lam, P. C. *M. Phil. Thesis*, The Chinese University of Hong Kong, 2006.

(g) Kui, S. C. F.; Li, H. –W.; Lee, H. K. *Inorg. Chem.* **2003**, *42*, 2824–2826.

(h) Kui, S. C. F. *M. Phil. Thesis*, The Chinese University of Hong Kong, 2001.

19. (a) Kempe, R.; Arndt, P. *Inorg. Chem.* **1996**, *35*, 2644–2649.

(b) Fuhrmann, H.; Brenner, S.; Arndt, P.; Kempe, R. *Inorg. Chem.* **1996**, *35*, 6742–6745.

(c) Polamo, M.; Leskelä, M. *J. Chem. Soc., Dalton Trans.* **1996**, 4345–4349.

(d) Spannenberg, A.; Tillack, A.; Arndt, P.; Kirmse, R.; Kempe, R. *Polyhedron* **1998**, *17*, 5–6.

(e) Morton, C.; O'Shaughnessy, P.; Scott, P. *Chem. Commun.* **2000**, 2099–2100.

(f) Jones, C.; Junk, P. C.; Leary, S. G.; Smithies, N. A. *Inorg. Chem. Commun.* **2003**, *6*, 1126–1128.

(g) Hillebrand, G.; Kempe, R. *Z. Kristallogr. NCS* **2003**, *218*, 467–468.

(h) Crust, E. J.; Clarke, A. J.; Deeth, R. J.; Morton, C.; Scott, P. *Dalton Trans.* **2004**, 2257–2266.

(i) Crust, E. J.; Clarke, A. J.; Deeth, R. J.; Morton, C.; Scott, P. *Dalton Trans.* **2004**, 4050–4058.

(j) Talja, M.; Klinga, M.; Polamo, M.; Aitola, E.; Leskelä, M. *Inorg. Chim. Acta* **2005**, *358*, 1061–1067.

(k) Noor, A.; Irrgang, T.; Kempe, R. *Z. Kristallogr. NCS* **2006**, *221*, 415–418.

(l) Kretschmer, W.; Hessen, B.; Noor, A.; Scott, N. M.; Kempe, R. *J. Organomet. Chem.* **2007**, *692*, 4569–4579.

(m) Noor, A.; Kempe, R. *Eur. J. Inorg. Chem.* **2008**, 2377–2381.

20. (a) Clérac, R.; Cotton, F. A.; Daniels, L. M.; Dunbar, K. R.; Murillo, C. A.; Pascual, I. *Inorg. Chem.* **2000**, *39*, 748–751.

(b) Clérac, R.; Cotton, F. A.; Daniels, L. M.; Dunbar, K. R.; Murillo, C. A.; Pascual, I. *Inorg. Chem.* **2000**, *39*, 748–751.

(c) Cotton, F. A.; Daniels, L. M.; Murillo, C. A.; Pascual, I. *J. Am. Chem. Soc.* **1997**, *119*, 10233–10224.

(d) Cotton, F. A.; Daniels, L. M.; Murillo, C. A.; Pascual, I. *Inorg. Chem. Commun.* **1998**, *1*, 1–.

(e) Yang, E.-C.; Cheng, M. C.; Tsai, M.-S.; Peng, S.-M. *J. Chem. Soc., Chem. Commun.* **1994**, 2377–2378.

(f) Cotton, F. A.; Daniels, L. M.; Jordan, G. T., IV. *Chem. Commun.* **1997**, 421–422.

(g) Cotton, F. A.; Daniels, L. M.; Jordan, G. T., IV. *J. Am. Chem. Soc.* **1997**, *119*, 10377–10381.

(h) Aduldecha, S.; Hathaway, B. *J. Chem. Soc., Dalton Trans.* **1991**, 993–998.

(i) Sheu, J.-T.; Lin, C.-C.; Chao, I.; Wang, C.-C.; Peng, S.-M. *Chem. Commun.* **1997**, 315–316.

(j) Wu, L.-P.; Field, P.; Morissey, T.; Murphey, C.; Nagle, P.; Hathaway, B.; Simmons, C.; Thornton, P. *J. Chem. Soc., Dalton Trans.* **1990**, 3835–3840.

(k) Pyrka, G. J.; El-Mekki, M.; Pinkerton, A. A. *J. Chem. Soc., Chem. Commun.* **1991**, 84–85.

(l) Calhorda, M. J.; Carrondo, M. D. C.; Costa, R. G. D.; Dias, A. R.; Duarte, M.; Hursthouse, M. B. *J. Organomet. Chem.* **1987**, *320*, 53–62.

(m) Engelhardt, L. M.; Jacobsen, G. E.; Patalinghug, W. C.; Skelton, B. W.; Raston, C. L.; White,

A. H. *J. Chem. Soc., Dalton Trans.* **1991**, 2859–2868.

(n) Edema, J. J. H.; Gambarotta, S.; Meetsma, A.; Spek, A. L.; Veldman, N. *Inorg. Chem.* **1992**, *30*, 2062–2066.

(o) Spannenberg, A.; Fuhrmann, H.; Arndt, P.; Baumann, W.; Kempe, R. *Angew. Chem. Int. Ed.* **1998**, *37*, 3363–3365.

(p) Noor, A.; Wagner, F. R.; Kempe, R. *Angew. Chem. Int. Ed.* **2008**, *47*, 7246–7249.

(q) Schareina, T.; Hillebrand, G.; Fuhrmann, H.; Kempe, R. *Eur. J. Inorg. Chem.* **2001**, 2421–2426.

(r) Davies, R. P.; Linton, D. J.; Schooler, L. P.; Snaith, R.; Wheatley, A. E. H. *Chem. Eur. J.* **2001**, 3696–3704.

(s) Ancker, T. R. v. d.; Engelhardt, L. M.; Henderson, M. J.; Jacobsen, G. E.; Raston, C. L.; Skelton, B. W.; White, A. H. *J. Organomet. Chem.* **2004**, *689*, 1991–1999.

(t) Deeken, S.; Proch, S.; Casini, E.; Braun, H. F.; Mechtler, C.; Marschner, C.; Motz, G.; Kempe, R. *Inorg. Chem.* **2006**, *45*, 1871–1878.

(u) Noor, A.; Kretschmer, W.; Kempe, R. *Eur. J. Inorg. Chem.* **2006**, 2683–2689.

(v) Deeken, S.; Irrgang, T.; Kempe, R. *Z. Kristallogr. NCS* **2006**, *221*, 93–94.

(w) Glatz, G.; Motz, G.; Kempe, R. *Z. Anorg. Allg. Chem.* **2008**, *643*, 2897–2902.

(x) Glatz, G.; Demeshko, S.; Motz, G.; Kempe, R. *Eur. J. Inorg. Chem.* **2009**, 1385–1392.

21. (a) Noss, H.; Oberthür, M.; Fischer, C.; Kretschmer, W. P.; Kempe, R. *Eur. J. Inorg. Chem.* **1999**, 2283–2288.

(b) Kempe, R.; Noss, H.; Irrgang, T. *J. Organomet. Chem.* **2002**, *647*, 12–20.

(c) Baldamus, J.; Cole, M. L.; Helmstedt, U.; Hey–Hawkins, E. –M.; Jones, C.; Junk, P. C.; Lange, F.; Smithies, N. A. *J. Organomet. Chem.* **2003**, *665*, 33–42.

(d) Quitmann, C. C.; Müller–Buschbaum, K. *Angew. Chem. Int. Ed.* **2004**, *43*, 5994–5996.

(e) Kretschmer, W. P.; Meetsma, A.; Hessen, B.; Schmalz, T.; Qayyum, S.; Kempe, R. *Chem. Eur. J.* **2006**, 8969–8978.

(f) Skvortsov, G. G.; Fukin, G. K.; Trifonov, A. A.; Noor, A.; Döring, C.; Kempe, R. *Organometallics* **2007**, *26*, 5770–5773.

(g) Lyubov, D. M.; Döring, C.; Fukin, G. K.; Cherkasov, A. V.; Shavyrin, A. S.; Kempe, R.; Trifonov, A. A. *Organometallics* **2008**, *27*, 2905–2907.

(h) Döring, C.; Kempe, R. *Eur. J. Inorg. Chem.* **2009**, 412–418.

(i) Sun, Y.; Zhang, Z.; Wang, X.; Li, X.; Weng, L.; Zhou, X. *Dalton Trans.* **2010**, *39*, 221–226.

(j) Scott, N. M.; Kempe, R. *Eur. J. Inorg. Chem.* **2005**, 1319–1324.

(k) Guillaume, S. M.; Schappacher, M.; Scott, N. M.; Kempe, R. *J. Polym. Sci. Part A: Polym. Chem.* **2007**, *45*, 3611–3619.

(l) Kietel, A. M.; Tok, P.; Kempe, R. *Eur. J. Inorg. Chem.* **2007**, 4583–4586.

(m) Qayyum, S.; Haberland, K.; Forsyth, C. M.; Junk, P. C.; Deason, G. B.; Kempe, R. *Eur. J. Inorg. Chem.* **2008**, 557–562.

(n) Dietel, A. M.; Döring, C.; Glatz, G.; Butovskii, M. V.; Tok, O.; Schappacher, F. M.; Pöttgen, R.; Kempe, R. *Eur. J. Inorg. Chem.* **2009**, 1051–1059.

(o) Cole, M. L.; Junk, P. C. *New. J. Chem.* **2003**, *27*, 1032–1037.

22. (a) Sadique, A. R.; Heeg, M. J.; Winter, C. H. *J. Am. Chem. Soc.* **2003**, *125*, 7774–7775.

(b) Nijhuis, C. A.; Jellema, E.; Sciarone, T. J. J.; Meetsma, A.; Budzelaar, P. H. M.; Hesen, B. *Eur. J. Inorg. Chem.* **2005**, 2089–2099.

23. (a) Coles, M. P.; Swenson, D. C.; Jordan, R. F. *Organometallics* **1997**, *16*, 5183–5194.

(b) Coles, M. P.; Swenson, D. C.; Jordan, R. F. *Organometallics* **1998**, *17*, 4042–4048.

(c) Schmidt, J. A. R; Arnold, J. *Dalton Trans.* **2002**, 2890–2899.

(d) Cotton, F. A.; Haefner, S. C.; Matonic, J. H.; Wang, X.; Murillo, C. A. *Polyhedron* **1997**, *16*, 541–550.

(e) Junk, P. C.; Cole, M. L. *Chem. Commun.* **2007**, 1579–1590.

(f) Cole, M. L.; Junk, P. C. *Dalton Trans.* **2003**, 2109–2111.

(g) Cole, M. L.; Deacon, G. B.; Forsyth, C. M.; Konstas, K.; Junk, P. C. *Dalton Trans.* **2006**, 3360–3367.

(h) Cole, M. L.; Evans, D. J.; Junk, P. C.; Louis, L. M. *New J. Chem.* **2002**, *26*, 1015–1024.

(h) Cole, M. L.; Jones, C.; Junk, P. C.; Kloth, M.; Stasch, A. *Chem. Eur. J.* **2005**, *11*, 4482–4491.

24. (a) Zhang, Y.; Sita, L. R. *Chem. Commun.* **2003**, 2358–2359.

(b) Kissounko, D. A.; Fettinger, J. C.; Sita, L. R. *Inorg. Chim. Acta* **2003**, *345*, 121–129.

(c) Zhang, Y.; Reeder, E. K.; Keaton, R.; Sita, L. R. *Organometallics* **2004**, *23*, 3512–3520.

(d) Kissounko, D.; Epshteyn, A.; Fettinger, J. C.; Sita, L. R. *Organometallics* **2004**, *23*, 531–535.

(e) Kissounko, D.; Epshteyn, A.; Fettinger, J. C.; Sita, L. R. *Organometallics* **2006**, *25*, 1076–1078.

(f) Fontaine, P. P.; Epshteyn, A.; Zavalij, P. Y.; Sita, L. R. *J. Organomet. Chem.* **2007**, *692*, 4683–4689.

(g) Hirotsu, M.; Fontaine, P. P.; Zavalij, P. Y.; Sita, L. R. *J. Am. Chem. Soc.* **2007**, *129*, 12690–12692.

25. (a) Herskovics–Korine, D.; Eisen, M. S. *J. Organomet. Chem.* **1995**, *503*, 307–314.

(b) Flores, J. C.; Chien, J. C. W.; Rausch, M. D. *Organometallics* **1995**, *14*, 1827–1833.

(c) Flores, J. C.; Chien, J. C. W.; Rausch, M. D. *Organometallics* **1995**, *14*, 2106–2108.

(d) Walther, D.; Fischer, R.; Görls, H.; Koch, J.; Schweder, B. *J. Organomet. Chem.* **1996**, *508*, 13–22.

(e) Hagadorn, J. R.; Arnold, J. *J. Am. Chem. Soc.* **1996**, *118*, 893–894.

(f) Hagadorn, J. R.; Arnold, J. *J. Chem. Soc., Dalton Trans.* **1997**, 3087–3096.

(g) Littke, A.; Sleiman, N.; Bensimon, C.; Richeson, D. S. *Organometallics* **1998**, *17*, 446–451.

(h) Zhang, Y.; Xie, J. –R.; Guo, J. –P.; Wei, X. –H.; Huang, S. –P.; Liu, D. –S. *Inorg. Chim. Acta* **2009**, *362*, 583–586.

26. Lee, H. K.; Lam, T. S.; Lam, C. –K.; Li, H. –W.; Fung, S. M. *New J. Chem.* **2003**, *27*, 1310–1318.

27. (a) Zhou, Y; Yap, G. P. A.; Richeson, D. S.; *Organometallics* **1998**, *17*, 4387–4391.

(b) Bambirra, S.; B, M. W.; Meetsma, A.; Hessen, B. *J. Am. Chem. Soc.* **2004**, *126*, 9182–9183.

(c) Bambirra, S.; Perazzolo, F.; Boot, S. J.; Sciarone, T. J. J. Meetsma, A.; Hessen, B. *Organometallics* **2008**, *27*, 704–712.

(d) Ge, S.; Meetsma, Hessen, B. *Organometallics* **2008**, *27*, 3131–3135.

(e) Cole, M. L.; Deason, G. B.; Junk, P. C. Konstas, K. *Chem. Commun.* **2005**, 1581–1583.

(f) Cole, M. L.; Junk, P. C. *Chem. Commun.* **2005**, 2695–2697.

(g) Cole, M. L.; Deacon, G. B.; Forsyth, C. M.; Junk, P. C. Konstas, K.; Wang, J. *Chem. Eur. J.* **2007**, *13*, 8092–8110.

(h) Wedler, M.; Noltemeyer, M.; Pieper, U.; Schmidt, H. –G.; Stalke, D. Edelmann. F. T. *Angew. Chem. Int. Ed. Engl.* **1990**, *29*, 894–896.

(i) Wedler, M.; Recknagel, A.; Gilje, J. W.; Noltemeyer, M.; Edelmann. F. T. J. Organomet. Chem. **1992**, *462*, 295–306.

(j) Heitmann, D.; Jones, C.; Junk, P. C.; Lippert, K. –A.; Stasch, A. *Dalton Trans.* **2007**, 187–189.

(k) Heitmann, D.; Jones, C.; Milla, D. P.; Stasch, A. *Dalton Trans.* **2010**, *39*, 1877–1882.

28. Yao, S.; Chan, H. –S.; Lam, C. –K.; Lee, H. K. *Inorg. Chem.* **2009**, *48*, 9936–9946.

29. (a) Baker, R. J.; Jones, C. *J. Organomet. Chem.* **2006**, *691*, 65–71.

(b) Schmidt, J. A. R; Arnold, J. *Chem. Commun.* **1999**, 2149–2150.

(c) Schmidt, J. A. R; Arnold, J. *Organometallics* **2002**, *21*, 2306–2313.

(d) Schmidt, J. A. R; Arnold, J. *Dalton Trans.* **2002**, 3454–3461.

(e) Jenkins, H. A.; Abeysekera, D.; Dickie, D. A.; Clyburne, J. A. C. *Dalton Trans.* **2002**, 3919–3922.

(f) Green, S. P.; Jones, C.; Stasch, A. *Science* **2007**, *318*, 1754–1757.

30. Another example of rare monodentate binding mode of amidinate ligand: Foley, S. R.; Bensimon, C.; Richeson, D. S. *J. Am. Chem. Soc.* **1997**, *119*, 10359–10363.

Chapter 2

Group 4 Metal Complexes Supported by *N*-alkylated Arylamido Ligands

The first part of this chapter gives a brief review on the chemistry of Group 4 metal complexes derived from arylamido ligands. The second part of this chapter covers the results of our work on synthesis and structures of Group 4 metal complexes supported by the bulky $[N(C_6H_3R_2\text{–}2,6)(CH_2Bu^t)]^-$ *[R = Me (L^1), Pr^i (L^2)] ligands. In addition, ligand substitution reactions of our current Group 4 metal amide complexes are also reported.*

Introduction

An Overview on Group 4 Metal Arylamido Complexes

A. Common Preparation Methods for Metal Amides

Over the past decades, various synthetic methods have been developed for the preparation of metal amides. The most commonly used synthetic routes include alkane elimination, hydrogen elimination, ammonium halide elimination, transamination, and transmetallation.[1]

Alkane elimination involves the reaction of a metal alkyl with an amine. Therefore, its applications are limited to metal ions with readily available alkyl derivatives. For example, $Zn(NEt_2)_2$, the first metal amide, was prepared by the reaction of $ZnEt_2$ with $HNEt_2$, in which ethane was eliminated (Scheme 2–1).[2]

$$ZnEt_2 + 2\,HNEt_2 \longrightarrow Zr(NEt)_2 + 2\,C_2H_6$$

Scheme 2–1

Hydrogen elimination is another method using amines as starting materials (Scheme 2–2). This method involves the reaction of a metal hydride with an amine. This is a clean reaction as hydrogen is the only by-product. Nevertheless, it is less widely applied than other synthetic methods as many metal hydrides are not readily available.

$$L_nMH + HNR_2 \longrightarrow L_nMNR_2 + H_2$$

Scheme 2–2

The ammonium halide elimination method involves the nucleophilic attack on a metal halide by an appropriate amine, yielding the corresponding metal amide with elimination of an ammonium halide salt (Scheme 2–3). As metal halides are more easily accessible than metal alkyls, this method has been widely used in amidometal chemistry. Ammonium halide elimination works particularly well with metal halides with a higher covalent character, rendering these metal halides more susceptible to necleophilic attack. However, this synthetic method cannot be extended to the heavier *p*-block or transition elements because of a relatively high ionic character of the metal–halide bonds in the latter halide complexes. Moreover, halide complexes of the heavier *p*-block and transition elements readily form stable adducts with amines.

$$L_nMX + 2\,HNR_2 \longrightarrow L_nMNR_2 + [R_2NH_2]^+[X]^-$$

Scheme 2–3

Transamination involves the reaction of a metal amide with an amine (Scheme 2–4). This type of reaction is usually controlled by volatility. The more volatile amine is eliminated from the reaction.

$$L_nMNR_2 + HN(R')_2 \longrightarrow L_nMN(R')_2 + HNR_2$$

Scheme 2–4

Transmetallation, otherwise named salt metathesis, involves the reaction of a metal halide with a ligand-transfer reagent, the latter is usually a Group 1 metal amide (Scheme 2–5). It is applicable to a wide range of elements and is therefore a commonly employed synthetic method.

$$L_nMX + M'NRR' \longrightarrow L_nMNRR' + M'X$$

Scheme 2–5

B. Group 4 Metal Arylamides Reported in the Literature

The first Group 4 metal arylamide, $[Ti(NPh_2)_4]$, was reported in 1934.[3a] It was until 1990s that the molecular structures of this Ti(IV) complex[3b] and its Zr(IV)[4a] and Hf(IV) counterparts[4b] were reported. These complexes display a similar molecular structure in which four $[NPh_2]^-$ ligands coordinate to the metal(IV) center, forming a tetrahedral geometry around the metal ion.

The catalytic properties of Group 4 metal amides towards olefin polymerization have been extensively studied. For example, Ti(IV), Zr(IV) and Hf(IV) complexes supported by the *N*-silylated arylamido ligands $[N(C_6H_3R_2\text{–}2,6)(SiMe_3)]^-$ (R = Me, Pr^i) (Chart 2–1) were shown to be active catalysts for ethylene polymerization.[5]

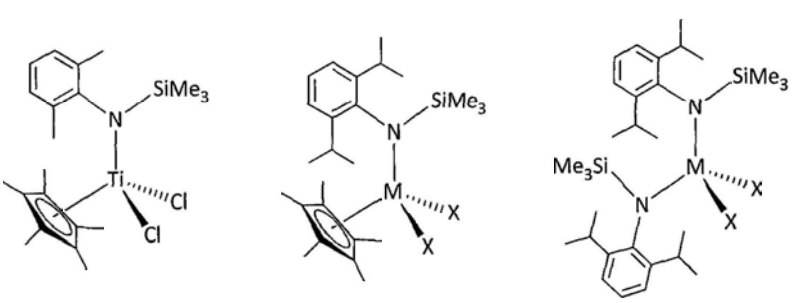

Nomura *et al.*[5a]

M = Zr, Hf; X = F, Cl, Me
Roesky *et al.*[5b,c]

Chart 2–1

Besides, the chemistry of Group 4 metal complexes supported by the related

N-alkylated arylamido ligands $[NRAr]^-$ (R = $C(CD_3)_2Me$, Bu^t, $CHBu^t_2$, Ad; Ar = Ph, $C_6H_3Me_2$–3,5, $C_6H_4PPh_2$–3) has also been studied. A series of Ti(III), Ti(IV) and Zr(IV) complexes have been reported (Chart 2–2).[6–8] It is noteworthy that π-stacking of aryl rings and H···Cl hydrogen bonding were observed in $[Ti\{N(CHBu^t_2)Ar'\}_2Cl_2]$.[7]

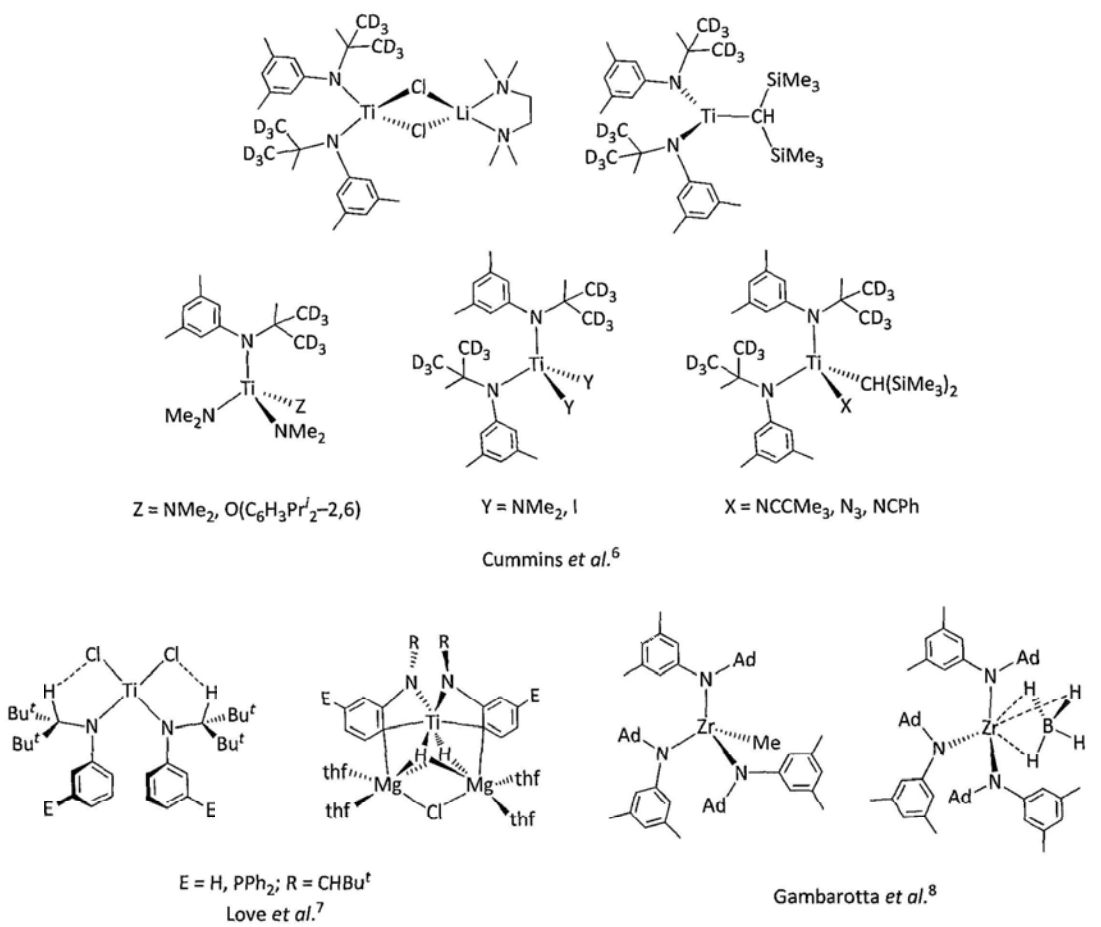

Chart 2–2

The reaction chemistry of the Ti(III) complexes $[Ti(NBu^tAr)_3]$ (Ar = Ph, $C_6H_3Me_2$–3,5) has been examined by Cummins and co-workers.[9] Treatment of $[Ti(NBu^tAr)_3]$ (Ar = Ph, $C_6H_3Me_2$–3,5) with CO_2 led to the di-titanium(III) complexes $[Ti(NBu^tAr)(\mu_2\text{–}O_2CNBu^tAr)_2]_2$ (Chart 2–3).[9a] Activation of dinitrogen was

demonstrated by [Ti(NBu^{t}Ph)$_3$] together with [Mo(NRAr)$_3$], from which a heterobinuclear dinitrogen complex was obtained.[9b] One-electron reduction reactions of [Ti(NRAr)$_3$] (R = C(CD$_3$)$_2$Me, Ar = C$_3$H$_6$Me$_2$–3,5) with [V(O)(OPr^i)$_3$] and [Mo(N)(OBu^t)$_3$] afforded the heterobimetallic μ–oxo complexes [(Pr^{i}O)$_3$V–O–Ti(NRAr)$_3$][9c] and [(Bu^{t}O)$_2$(N)Mo–O–Ti(NRAr)$_3$],[9d] respectively.

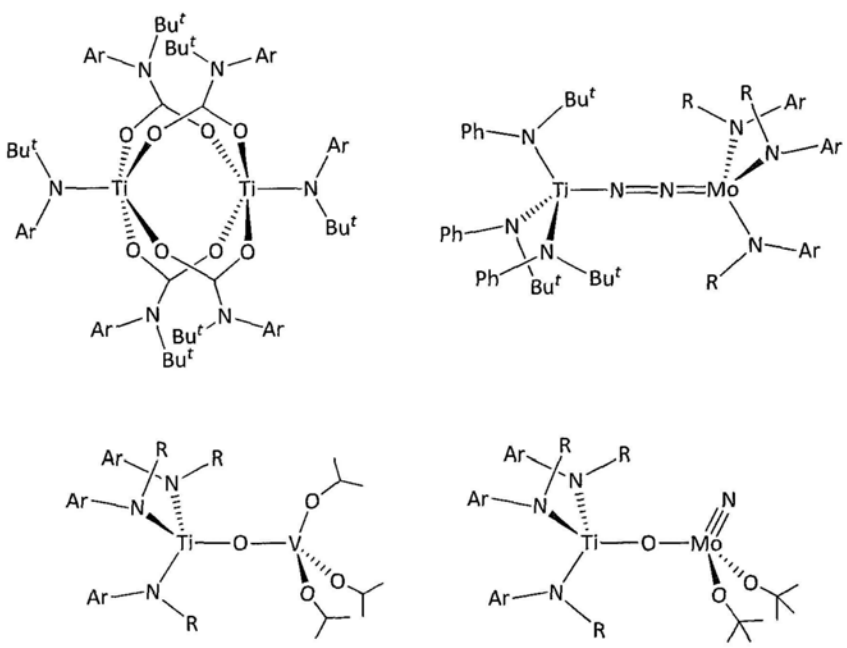

R = C(CD$_3$)$_2$Me, Ar = C$_6$H$_3$Me$_2$-3,5
Cummins *et al.*[9]

Chart 2–3

Results and Discussion

Group 4 Metal Complexes Derived from the $[N(C_6H_3R_2\text{–}2,6)(CH_2Bu^t)]^-$ (R = Me, Pr^i) Ligands

A. Preparation of Ligand Precursors and the Corresponding Lithium Derivatives

The precursor amines $[HN(C_6H_3R_2\text{–}2,6)(CH_2Bu^t)]$ $[HL^n$: n = 1, R = Me (**3**); n = 2, R = Pr^i (**4**)] were prepared according to procedures previously developed in our laboratory with minor modifications (Scheme 2–6).[10]

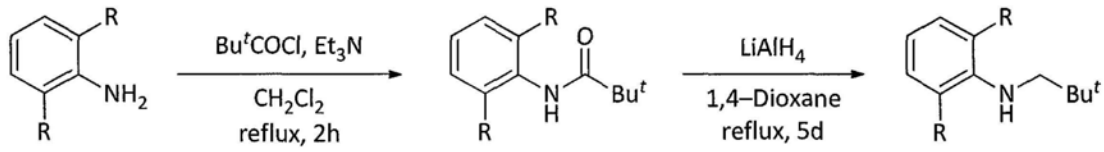

1: R = Me
2: R = Pr^i

3: R = Me 58%
4: R = Pr^i 66%

Scheme 2–6

Treatment of $H_2N(C_6H_3R_2\text{–}2,6)$ (R = Me, Pr^i) with trimethylacetyl chloride and triethylamine gave compounds **1** and **2**. Reduction of compounds **1** and **2** by $LiAlH_4$ in 1,4–dioxane under reflux for 5 d yielded the *N*-alkylated arylamines **3** and **4** in overall yields of 58% and 66%, respectively.

Lithiation of ligand precursors **3** and **4** with $LiBu^n$ in the presence of tmeda afforded $[LiL^n(tmeda)]$ [n = 1 (**5**), n = 2 (**6**)] in excellent yields of 99% and 98%, respectively (Scheme 2–7). In the absence of tmeda, lithiation of compound **4** in

thf gave the thf-adduct $LiL^2(thf)_2$ (**7**) in 99% yield. Lithium reagents **5–7** were used as ligand-transfer reagents in the following complexation reactions.

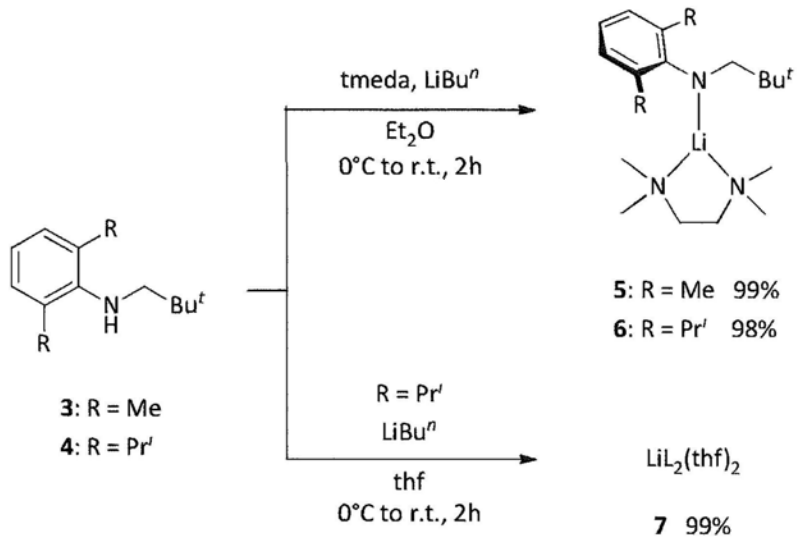

Scheme 2–7

B. Synthesis of Ti(IV), Zr(IV) and Hf(IV) Amido Complexes

Salt metathesis reactions of an appropriate anhydrous MCl_4 (M = Zr, Hf) with two molar equivalents of lithium reagents **5** and **6** in toluene yielded the heterobimetallic *ate*-complexes $[M(L^n)_2Cl(\mu\text{–}Cl)_2Li(tmeda)]$ [M = Zr, n = 1 (**8**), n = 2 (**9**); M = Hf, n = 1 (**10**), n = 2 (**11**)] (Scheme 2–8). The Zr(IV) (**8** and **9**) and Hf(IV) (**10** and **11**) complexes were isolated as pale yellow and colorless crystals, respectively. Complexes **8–11** are readily soluble in commonly organic solvents except hexane.

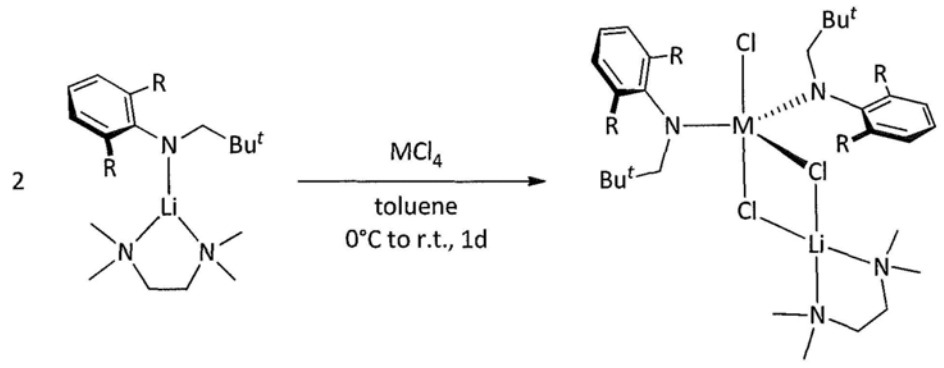

5: R = Me
6: R = Pr^i

8: R = Me, M = Zr 40%
9: R = Pr^i, M = Zr 35%
10: R = Me, M = Hf 33%
11: R = Pr^i, M = Hf 28%

Scheme 2–8

It is believed that the tmeda ligand helps to stabilize complexes **8–11** as LiCl-adducts. In order to prevent the formation of the LiCl-adducts, we have also employed the tmeda-free lithium complex $LiL^2(thf)_2$ (**7**) as a ligand-transfer reagent. Treatment of the appropriate $MCl_4(thf)_x$ (M = Ti, x = 2; M = Zr, Hf, x = 0) with two equivalents of compound **7** gave the neutral, four-coordinate metal(IV) bis(amide) complexes $[M(L^2)_2Cl_2]$ [M = Ti (**12**), Zr (**13**), Hf (**14**)] (Scheme 2–9).

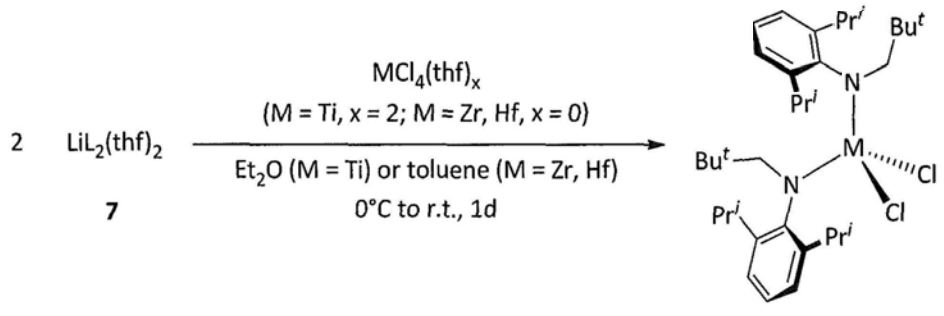

12: M = Ti 36%
13: M = Zr 61%
14: M = Hf 44%

Scheme 2–9

Interestingly, the Zr(IV) *ate*-complex $[Zr(L^2)_2Cl(\mu\text{–}Cl)_2Li(thf)_2]$ (**13a**) was observed in the crude product but was absent after recrystallization of the crude product from toluene.* Conceivably, complex **13a** was an initial product of the reaction. When the crude product was dried under vacuum during work-up, the coordinated thf molecules were removed leading to the detachment of the "$LiCl(thf)_2$" moiety and the isolation of **13** as a final product (Scheme 2–10).

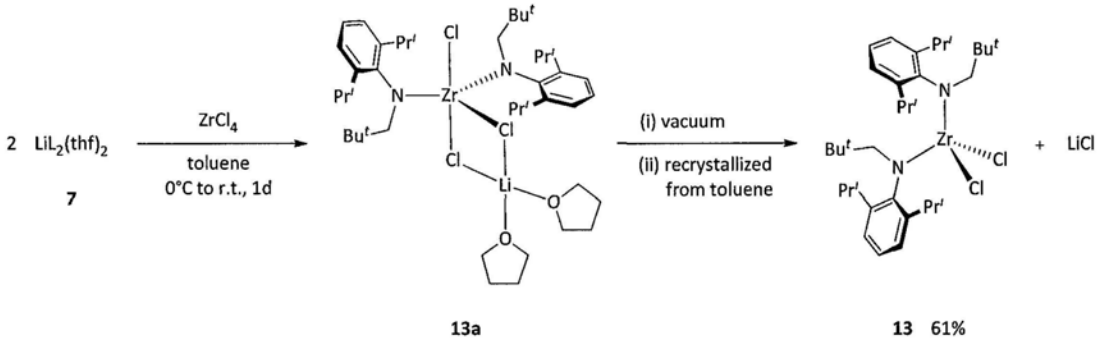

Scheme 2–10

We envisaged that the neutral, four-coordinate complexes **13** and **14** are more reactive than the *ate*-complexes **8–11**. Therefore, subsequent reactions of **13** and **14** with alkyl, amide and alkoxide reagents, as well as reducing agents, were studied in this work (*vide infra*).

Physical Characterization of Complexes 8–14

The formulation of complexes **8–14** has been confirmed by elemental analysis, NMR spectroscopy, and single-crystal X-ray diffraction analysis. Table 2–1 summarizes some of the physical properties of compounds **8–14**.

---

* The presence of **13a** in the crude product was confirmed by a single-crystal X-ray diffraction study.

Table 2–1 Some physical properties of compounds **8–14**.

Compound	Appearance	M.p. (°C)
$[Zr(L^1)_2Cl(\mu\text{–}Cl)_2Li(tmeda)]$ (**8**)	Pale yellow crystals	169–174
$[Zr(L^2)_2Cl(\mu\text{–}Cl)_2Li(tmeda)]$ (**9**)	Pale yellow crystals	190–193 (dec.)
$[Hf(L^1)_2Cl(\mu\text{–}Cl)_2Li(tmeda)]$ (**10**)	Colorless crystals	176–178
$[Hf(L^2)_2Cl(\mu\text{–}Cl)_2Li(tmeda)]$ (**11**)	Colorless crystals	319–324 (dec.)
$[Ti(L^2)_2Cl_2]$ (**12**)	Red crystals	241–245
$[Zr(L^2)_2Cl_2]$ (**13**)	Pale yellow crystals	214–219
$[Hf(L^2)_2Cl_2]$ (**14**)	Colorless crystals	222–227

NMR Spectra of Complexes **8–14**

1. $[M(L^n)_2Cl(\mu\text{–}Cl)_2Li(tmeda)]$ [M = Zr, n = 1 (**8**), n = 2 (**9**); M = Hf, n = 1 (**10**), n = 2 (**11**)]

NMR spectra of complexes **8–11** are shown in Figures A3–1 to A3–8 (see Appendix 3). The ^1H and ^{13}C NMR spectra of these complexes showed resonance signals assignable to a pair of L^1 ligands and one coordinated tmeda molecule. Only one set of resonance signals assignable to the L^1 ligand were observed, indicating that the two L^1 ligands in each complex are equivalent with a plane of symmetry containing the three chloride ligands present in the molecule (Figure 2–9). The methylene protons of the L^1 ligand appear as one singlet (at 3.84 ppm for **8** and 3.80 ppm for **10**). The two methyl substituents of the aryl ring are isochronous, as indicated by the occurrence of only one singlet (at 2.80 ppm for **8** and 2.81 ppm for **10**) assignable to the methyl protons.

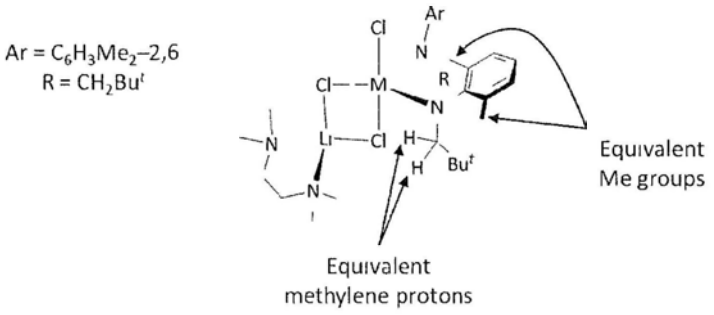

Figure 2–9

The ^{1}H and ^{13}C NMR spectra of complexes **9** and **11** showed one set of resonance signals assignable to the L^2 ligands and tmeda molecule in a ratio of 2:1. The two L^2 ligands in each complex are equivalent (occurring as one set of resonance signals), suggesting the presence of a symmetry plane in the molecule (Figure 2–10). The isopropyl methine protons appear as a broad signal (at 4.29 ppm for **9** and 4.11 ppm for **11**), presumably as a result of overlapping of two septets, and the isopropyl methyl protons occur as two doublets (at 1.47 and 1.64 ppm for **9,** and 1.51 and 1.62 ppm for **11**). These indicate that the two isopropyl substituents of the L^2 ligand are chemically nonequivalent. Apparently, a restricted rotation about the N–C_{ipso} bond locks the aryl ring at a position that the isopropyl substituents are not interchangeable.

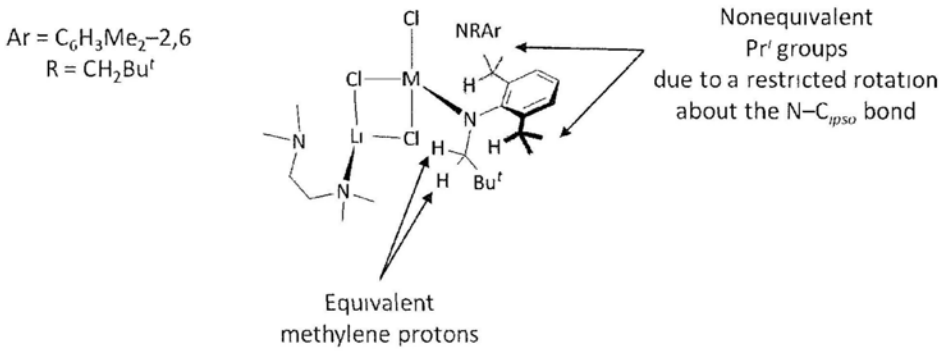

Figure 2–10

The ^{7}Li NMR spectra of the complexes **9** and **11** showed one singlet at –1.68 and –1.92 ppm, respectively.

2. $[M(L^2)_2Cl_2]$ [M = Ti (**12**), Zr (**13**), Hf (**14**)]

The ^{1}H and ^{13}C NMR spectra of complexes **12–14** (Figures A2–9 to A2–14) showed one set of resonance signals assignable to the L^2 ligand, indicating that the two L^2 ligands in each complex are equivalent. The isopropyl substituents in each complex are equivalent, as only one septet (at 3.91 ppm for **12**, 3.88 ppm for **13** and 3.92 for **14**) assignable to the methine protons is observed in their ^{1}H NMR spectra. Despite the equivalence of the two isopropyl substituents of the L^2 ligand, the isopropyl methyl protons occur as two doublets (at 1.42 and 1.60 ppm for **12**, 1.43 and 1.56 ppm for **13**, and 1.45 and 1.54 ppm for **14**) in the ^{1}H NMR spectra. It is inferred that the geminal methyl groups of the isopropyl substituent are diastereotopic (Figure 2–11).[13]

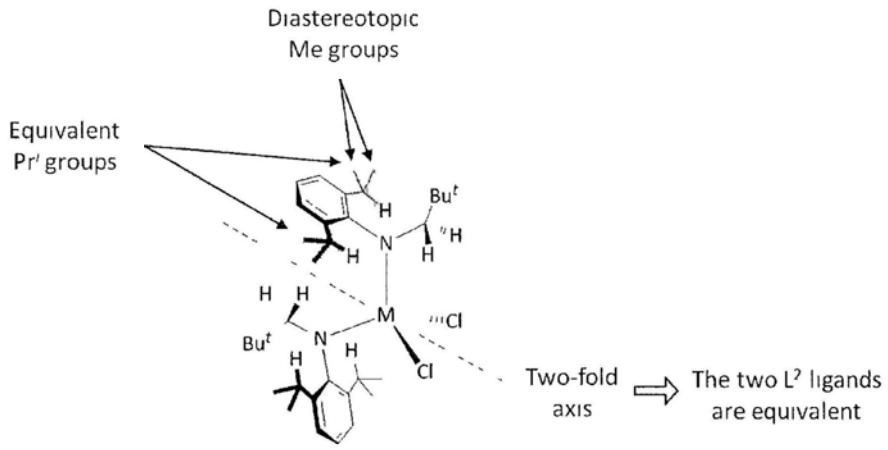

Figure 2–11

Crystal Structures of Complexes **8–14**

Single crystals of **8**•0.5PhMe, **9**, **10**•PhMe, **11**, **13**, **13a** and **14** were obtained from toluene, whereas those of **12** were obtained from hexane. The solid-state structures of these complexes were elucidated by X-ray crystallography. Selected crystallographic data are listed in Appendix 2.

1. $[M(L^n)_2Cl(\mu\text{–}Cl)_2Li(tmeda)]$ [M = Zr, n = 1 (**8**), n = 2 (**9**); M = Hf, n = 1 (**10**), n = 2 (**11**)] and $[Zr(L^2)_2Cl(\mu\text{–}Cl)_2Li(thf)_2]$ (**13a**)

Figures 2–12 to 2–16 show the molecular structures of the heterobimetallic complexes **8–11** and **13a**, respectively. Selected bond lengths and angles are presented in Tables 2–2 to 2–6.

Crystals of **8**•0.5PhMe and **10**•PhMe belongs to the triclinic space group $P\bar{1}$, whereas complexes **9** and **11** crystallize in the monoclinic space group $P2_1/n$. The related **13a** crystallizes in the monoclinic space group *Cc*. The Group 4 metal center in each complex is coordinated by two amido ligands L^n, one terminal chloride ligand, and two bridging chloride ligands. The latters act as bridging ligands, connecting the Group 4 metal ion to the lithium ion. The geometry around the metal(IV) center is best described as distorted trigonal bipyramidal, with the terminal chloride ligand [Cl(1)] and one of the bridging chloride ligands [Cl(2)] occupying the axial positions. The sum of angles around the metal(IV) center on the N(1)–N(2)–Cl(3) plane is close to 360°.

The Zr(IV) complexes **8**, **9** and **13a** have similar structural parameters. The observed Zr–N distances in **8**, **9** and **13a** are 2.022(6)–2.024(6), 2.041(2)–2.061(2)

and 2.046(4)–2.060(4) Å, respectively. The slightly longer Zr–N distances in **9** and **13a** can be attributed to the sterically more demanding L^2 ligand. The Zr–N bond lengths in complexes **8**, **9** and **13a** are comparable to those of 2.0393(3)–2.063(5) Å in $[\{Li(thf)_4\}\{Zr(NMe_2)_3(SiBu^tPh_2)_2\}]$[11b] and 2.040(2)–2.010(3) Å in $[Zr\{N(SiHMe_2)_2\}_2(Cl)(\mu\text{–}Cl)]_2$.[11c] They are shorter than those of 2.102(2)–2.179(2) Å in $[\{K(C_7H_8)_2\}\{Zr[N(C_6F_5)_2]_3Cl_2\}]$, where the Zr(IV) center has a five-coordinate ligand environment.[11a] The terminal Zr–Cl distances in **8** [2.469(1) Å], **9** [2.469(9) Å] and **13a** [2.435(1) Å] are similar to those of 2.4468(8)–2.4882(8) Å in $[\{K(C_7H_8)_2\}\{Zr[N(C_6F_5)_2]_3Cl_2\}]$,[11a] but slightly longer than that of 2.392(1) Å in $[Zr\{N(SiHMe_2)_2\}_2(Cl)(\mu\text{–}Cl)]_2$.[11c] The bridging Zr–Cl bond lengths of 2.541(1) and 2.578(1) Å in **8**, 2.529(9) and 2.566(9) Å in **9**, and 2.523(1) and 2.533(1) Å in **13a** are shorter than the corresponding distances of 2.599(1)–2.628(1) Å reported for $[Zr\{N(SiHMe_2)_2\}_2(Cl)(\mu\text{–}Cl)]_2$.[11c]

The Hf(IV) complexes **10** and **11** have similar structural parameters. The Hf–N bond lengths in **10** are 2.014(4) and 2.024(5) Å, whereas the corresponding distances in **11** are 2.037(3) and 2.042(3) Å. The marginally longer Hf–N distances in **11** can be attributed to the larger steric requirement of the L^2 ligand. The Hf–N distances in complex **10** and **11** are slightly shorter than those of 2.04(1)–2.063(5) Å reported for the five-coordinate $[\{Li(thf)_4\}\{Hf(NMe_2)_3(SiBu^tPh_2)_2\}]$.[11d] The terminal Hf–Cl distances of 2.439(1) Å in complex **10** and 2.416(1) Å in **11** are slightly longer than those in the four-coordinate $[Hf\{N(C_6H_3Pr^i_2\text{–}2,6)(SiMe_3)\}_2Cl_2]$ [2.344(1) and 2.383(1) Å].[5a]

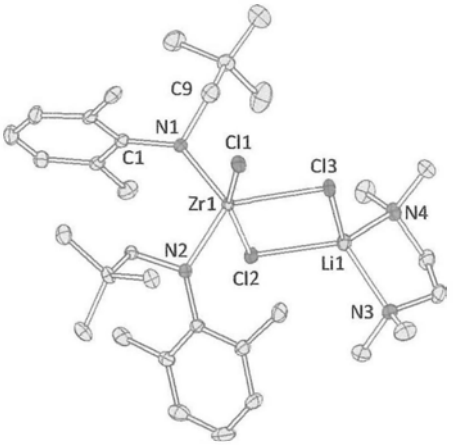

Figure 2–12 Molecular structure of $[Zr(L^1)_2Cl(\mu\text{–}Cl)_2Li(tmeda)]\cdot0.5PhMe$ (**8**•0.5PhMe). The solvated PhMe molecule is omitted for clarity.

Table 2–2 Selected bond lengths (Å) and angles (deg.) for compound **8**•0.5PhMe.

$[Zr(L^1)_2Cl(\mu\text{–}Cl)_2Li(tmeda)]\cdot0.5PhMe$ (**8**•0.5PhMe)			
Zr(1)–N(1)	2.022(6)	Li(1)–N(3)	2.054(1)
Zr(1)–N(2)	2.024(6)	Li(1)–N(4)	2.058(1)
Zr(1)–Cl(1)	2.469(1)	Li(1)–Cl(2)	2.335(1)
Zr(1)–Cl(2)	2.578(1)	Li(1)–Cl(3)	2.342(1)
Zr(1)–Cl(3)	2.541(1)	N(1)–C(1)	1.451(9)
		N(1)–C(9)	1.51(1)
N(1)–Zr(1)–N(2)	112.6(2)	Cl(1)–Zr(1)–Cl(2)	159.9(7)
N(2)–Zr(1)–Cl(3)	130.4(1)	C(1)–N(1)–Zr(1)	132.3(5)
N(1)–Zr(1)–Cl(3)	116.4(1)	C(9)–N(1)–Zr(1)	107.9(5)
Cl(2)–Li(1)–Cl(3)	88.7(4)	C(1)–N(1)–C(9)	115.0(6)
N(3)–Li(1)–N(4)	89.6(6)		

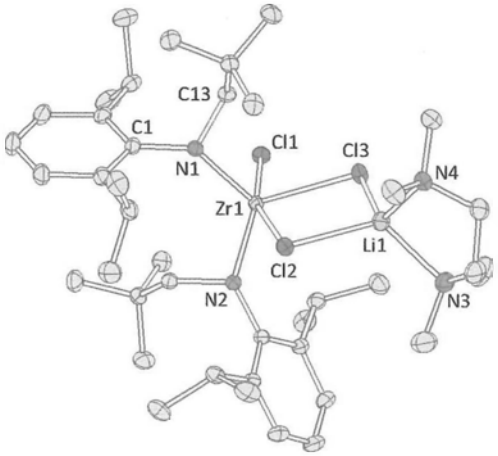

Figure 2–13 Molecular structure of $[Zr(L^2)_2Cl(\mu\text{–}Cl)_2Li(tmeda)]$ (**9**).

Table 2–3 Selected bond lengths (Å) and angles (deg.) for compound **9**.

$[Zr(L^2)_2Cl(\mu\text{–}Cl)_2Li(tmeda)]$ (**9**)			
Zr(1)–N(1)	2.061(2)	Li(1)–N(3)	2.068(7)
Zr(1)–N(2)	2.041(2)	Li(1)–N(4)	2.062(7)
Zr(1)–Cl(1)	2.469(9)	Li(1)–Cl(2)	2.331(6)
Zr(1)–Cl(2)	2.566(9)	Li(1)–Cl(3)	2.302(6)
Zr(1)–Cl(3)	2.529(9)	N(1)–C(1)	1.447(4)
		N(1)–C(13)	1.490(4)
N(1)–Zr(1)–N(2)	112.5(1)	Cl(1)–Zr(1)–Cl(2)	161.5(3)
N(2)–Zr(1)–Cl(3)	120.6(7)	C(1)–N(1)–Zr(1)	135.5(1)
N(1)–Zr(1)–Cl(3)	118.7(7)	C(13)–N(1)–Zr(1)	103.7(1)
Cl(2)–Li(1)–Cl(3)	89.7(2)	C(1)–N(1)–C(13)	117.8(3)
N(3)–Li(1)–N(4)	90.2(3)		

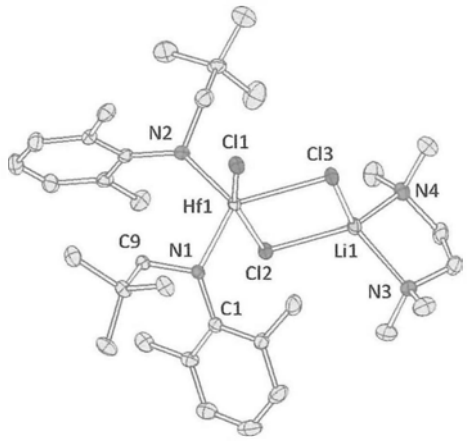

Figure 2–14 Molecular structure of $[Hf(L^1)_2Cl(\mu\text{–}Cl)_2Li(tmeda)]\cdot PhMe$ (**10**•PhMe). The solvated PhMe molecule is omitted for clarity.

Table 2–4 Selected bond lengths (Å) and angles (deg.) for compound **10**•PhMe.

$[Hf(L^1)_2Cl(\mu\text{–}Cl)_2Li(tmeda)]\cdot PhMe$ (**10**•PhMe)			
Hf(1)–N(1)	2.014(4)	Li(1)–N(3)	2.07(1)
Hf(1)–N(2)	2.024(5)	Li(1)–N(4)	2.08(1)
Hf(1)–Cl(1)	2.439(1)	Li(1)–Cl(2)	2.33(1)
Hf(1)–Cl(2)	2.541(1)	Li(1)–Cl(3)	2.32(1)
Hf(1)–Cl(3)	2.526(1)	N(1)–C(1)	1.422(7)
		N(1)–C(9)	1.482(7)
N(1)–Hf(1)–N(2)	110.5(1)	Cl(1)–Hf(1)–Cl(2)	159.8(6)
N(2)–Hf(1)–Cl(3)	116.6(1)	C(1)–N(1)–Hf(1)	129.1(3)
N(1)–Hf(1)–Cl(3)	132.4(1)	C(9)–N(1)–Hf(1)	111.9(3)
Cl(2)–Li(1)–Cl(3)	115.1(5)	C(1)–N(1)–C(9)	118.8(4)
N(3)–Li(1)–N(4)	88.2(4)		

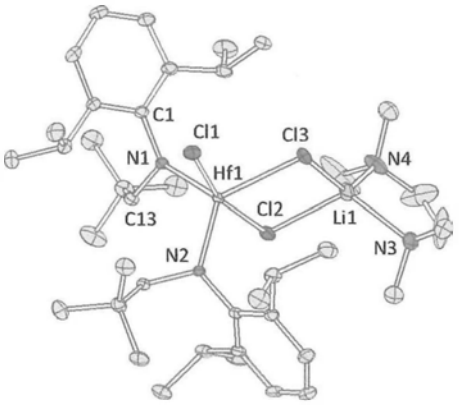

Figure 2–15 Molecular structure of $[Hf(L^2)_2Cl(\mu\text{–}Cl)_2Li(tmeda)]$ (**11**).

Table 2–5 Selected bond lengths (Å) and angles (deg.) for compound **11**.

$[Hf(L^2)_2Cl(\mu\text{–}Cl)_2Li(tmeda)]$ (**11**)			
Hf(1)–N(1)	2.037(3)	Li(1)–N(3)	2.05(1)
Hf(1)–N(2)	2.042(3)	Li(1)–N(4)	2.07(1)
Hf(1)–Cl(1)	2.416(1)	Li(1)–Cl(2)	2.345(9)
Hf(1)–Cl(2)	2.493(1)	Li(1)–Cl(3)	2.360(9)
Hf(1)–Cl(3)	2.488(1)	N(1)–C(1)	1.444(5)
		N(1)–C(13)	1.475(5)
N(1)–Hf(1)–N(2)	113.3(1)	Cl(1)–Hf(1)–Cl(2)	165.3(1)
N(2)–Hf(1)–Cl(3)	124.7(1)	C(1)–N(1)–Hf(1)	126.7(2)
N(1)–Hf(1)–Cl(3)	121.9(1)	C(13)–N(1)–Hf(1)	114.9(2)
Cl(2)–Li(1)–Cl(3)	86.8(3)	C(1)–N(1)–C(13)	116.5(3)
N(3)–Li(1)–N(4)	90.9(4)		

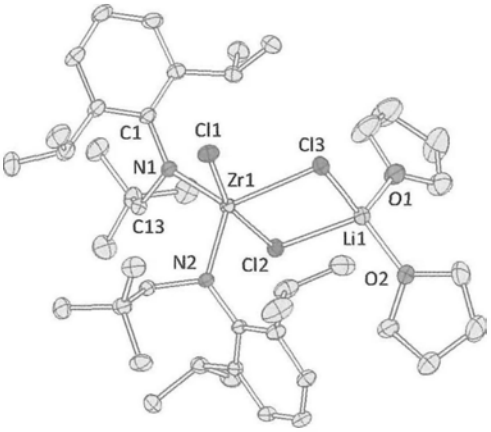

Figure 2–16 Molecular structure of $[Zr(L^2)_2Cl(\mu\text{–}Cl)_2Li(thf)_2]$ (**13a**).

Table 2–6 Selected bond lengths (Å) and angles (deg.) for compound **13a**.

$[Zr(L^2)_2Cl(\mu\text{–}Cl)_2Li(thf)_2]$ (**13a**)			
Zr(1)–N(1)	2.046(4)	Li(1)–O(1)	1.87(1)
Zr(1)–N(2)	2.060(4)	Li(1)–O(2)	1.88(1)
Zr(1)–Cl(1)	2.435(1)	Li(1)–Cl(2)	2.39(1)
Zr(1)–Cl(2)	2.533(1)	Li(1)–Cl(3)	2.36(1)
Zr(1)–Cl(3)	2.523(1)	N(1)–C(1)	1.443(6)
		N(1)–C(13)	1.465(7)
N(1)–Zr(1)–N(2)	113.5(1)	Cl(1)–Zr(1)–Cl(2)	163.0(1)
N(2)–Zr(1)–Cl(3)	124.4(1)	C(1)–N(1)–Zr(1)	129.4(3)
N(1)–Zr(1)–Cl(3)	121.9(1)	C(13)–N(1)–Zr(1)	112.4(3)
Cl(3)–Li(1)–Cl(3)	89.7(2)	C(1)–N(1)–C(13)	117.1(4)
N(3)–Li(1)–N(4)	90.2(3)		

2. $[M(L^2)_2Cl_2]$ [M = Ti (**12**), Zr (**13**), Hf (**14**)]

Molecular structures of the neutral bis(amido) M(IV) dichloride complexes **12–14** are shown in Figures 2–17 to 2–19. Selected bond distances and angles are summarized in Tables 2–7 to 2–9.

Complexes **12–14** are isostructural. They crystallize in the orthorhombic space group $P2_12_12_1$. The Group 4 metal ion is coordinated by two arylamido ligands and two chloride ligands, with a C_2-axis passing through the metal center. The coordination geometry around the metal center can be described as pseudo tetrahedral.

The Ti–N distances in **12** [1.889(1) and 1.891(2) Å] are comparable to the corresponding distances reported for Ti(IV) bis(amido) complexes $[Ti\{NBu^tPh\}_2Cl_2]$ [1.888(1) and 1.894(1) Å][7] and $[Ti\{N(SiMe_3)_2\}_2Cl_2]$ [1.877(2) and 1.882(2) Å],[12a] tris(amido) complex $[Ti\{NBu^t(C_6H_3Me_2\text{–}3,5)\}_3Cl]$ [1.922(4)–1.929(4) Å],[6a] as well as tetra(amido) complexes $[Ti(NPh_2)_4]$ [1.926(3)–1.948(3) Å][3a] and $[Ti(NMe_2)_4]$ [1.897(2)–1.924(2) Å].[12b] The Ti–Cl bond distances in **12** [2.2396(9) and 2.2451(8) Å] are comparable to those observed in $[Ti\{NBu^tPh\}_2Cl_2]$ [2.2493(6) and 2.2530(6) Å],[7] $[Ti\{N(SiMe_3)_2\}_2Cl_2]$ [2.231(1) and 2.239(9) Å],[12a] and $[Ti\{NBu^t(C_6H_3Me_2\text{–}3,5)\}_3Cl]$ [2.281(2)].[6a]

The Zr–N bonds of 2.020(3) and 2.025(3) Å in complex **13** are similar to those of 2.029(2) and 2.030(2) Å reported for the four-coordinate $[Zr\{N(C_6H_3Pr^i_2\text{–}2,6)(SiMe_3)\}_2Cl_2]$.[5a] However, they are marginally shorter than those reported for the five-coordinate $[Zr\{N(SiMe_3)_2\}_2Cl_2(thf)]$ [2.040(3) and 2.051(3) Å],[12a] and shorter than those reported for the six-coordinate $[Zr\{N(C_6H_3Pr^i_2\text{–}2,6)(C_6H_4F\text{–}2)\}_2Cl_2]$ [2.116(1)

and 2.130(1) Å].[12c] The Zr–Cl distances in compound **13** [2.371(1) and 2.379(1) Å] are shorter than those in [Zr{N(SiMe$_3$)$_2$}$_2$Cl$_2$(thf)] [2.460(1) and 2.482(1) Å].[12a] They are similar to that of 2.380(1) in [Zr{N(C$_6$H$_3$Pr$^i_2$–2,6)(SiMe$_3$)}$_2$Cl$_2$],[4a] but marginally longer than those of 2.3491(7) and 2.3648(7) Å reported for [Zr{N(C$_6$H$_3$Pr$^i_2$–2,6)(C$_6$H$_4$F–2)}$_2$Cl$_2$].[12c]

The Hf–N distances of 2.003(3) and 2.006(3) Å in **14** are slightly shorter than the corresponding distances reported for the four-coordinate [Hf{N(C$_6$H$_3$Pr$^i_2$–2,6)(SiMe$_3$)}$_2$Cl$_2$] [2.018(3) and 2.028(3) Å][4a] and the five-coordinate [Hf{N(SiMe$_3$)$_2$}$_2$Cl$_2$(thf)] [2.042(5) and 2.033(6) Å],[12a] and much shorter than those reported for the six-coordinate [Hf{N(C$_6$H$_3$Pr$^i_2$–2,6)(C$_6$H$_4$F–2)}$_2$Cl$_2$] [2.114(3) and 2.117(3) Å].[12c] The Hf–Cl bond lengths in **14** [2.345(1) and 2.353(1) Å] are comparable to those in [Hf{N(SiMe$_3$)$_2$}$_2$Cl$_2$(thf)] [2.439(1) and 2.449(1) Å],[12a] [Hf{N(C$_6$H$_3$Pr$^i_2$–2,6)(SiMe3)}Cl$_2$] [2.344(1) and 2.350(1) Å][5a] and [Hf{N(C$_6$H$_3$Pr$^i_2$–2,6)(C$_6$H$_4$F–2)}$_2$Cl$_2$] [2.334(1) and 2.336(1) Å].[12c]

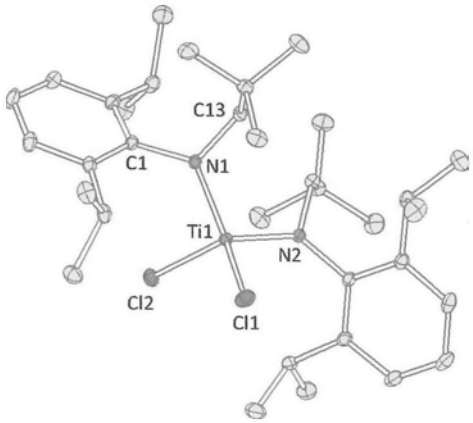

Figure 2–17 Molecular structure of $[Ti(L^2)_2Cl_2]$ (**12**).

Table 2–7 Selected bond lengths (Å) and angles (deg.) for compound **12**.

$[Ti(L^2)_2Cl_2]$ (**12**)			
Ti(1)–N(1)	1.889(1)	Ti(1)–Cl(1)	2.245(1)
Ti(1)–N(2)	1.891(2)	Ti(1)–Cl(2)	2.240(1)
N(1)–C(1)	1.447(3)	N(1)–C(13)	1.485(3)
N(1)–Ti(1)–N(2)	114.42(8)	C(1)–N(1)–Ti(1)	125.8(1)
N(1)–Ti(1)–Cl(1)	111.35(6)	C(13)–N(1)–Ti(1)	116.8(1)
Cl(1)–Ti(1)–Cl(2)	111.78(4)	C(1)–N(1)–C(13)	116.8(1)

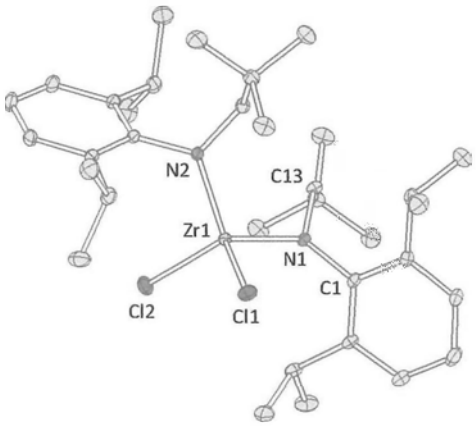

Figure 2–18 Molecular structure of $[Zr(L^2)_2Cl_2]$ (**13**).

Table 2–8 Selected bond lengths (Å) and angles (deg.) for compound **13**.

$[Zr(L^2)_2Cl_2]$ (**13**)			
Zr(1)–N(1)	2.020(3)	Zr(1)–Cl(1)	2.371(1)
Zr(1)–N(2)	2.025(3)	Zr(1)–Cl(2)	2.379(1)
N(1)–C(1)	1.440(4)	N(1)–C(13)	1.489(4)
N(1)–Zr(1)–N(2)	112.9(1)	C(1)–N(1)–Zr(1)	125.9(2)
N(1)–Zr(1)–Cl(1)	103.4(8)	C(13)–N(1)–Zr(1)	115.8(2)
Cl(1)–Zr(1)–Cl(2)	112.2(4)	C(1)–N(1)–C(13)	117.6(3)

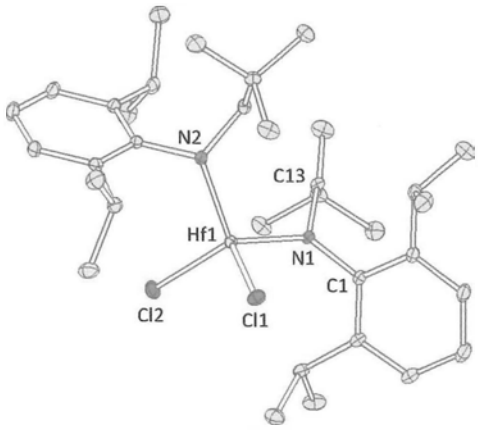

Figure 2–19 Molecular structure of $[Hf(L^2)_2Cl_2]$ (**14**).

Table 2–9 Selected bond lengths (Å) and angles (deg.) for compound **14**.

$[Hf(L^2)_2Cl_2]$ (**14**)			
Hf(1)–N(1)	2.006(3)	Hf(1)–Cl(1)	2.345(1)
Hf(1)–N(2)	2.003(3)	Hf(1)–Cl(2)	2.353(1)
N(1)–C(1)	1.441(4)	N(1)–C(13)	1.486(4)
N(1)–Hf(1)–N(2)	111.3(1)	C(1)–N(1)–Hf(1)	124.5(2)
N(1)–Hf(1)–Cl(1)	104.2(7)	C(13)–N(1)–Hf(1)	118.4(2)
Cl(1)–Hf(1)–Cl(2)	112.52(4)	C(1)–N(1)–C(13)	116.5(3)

C. Synthesis of Mixed-amido Zr(IV) and Hf(IV) Complexes

As depicted in Scheme 2–11, mixed-ligand tetra(amido) complexes **15** and **16** were obtained as colorless crystals by reacting complexes **13** and **14**, respectively, with two equivalents of $LiNMe_2$ in toluene. Complexes **15** and **16** are readily soluble in toluene but only sparingly soluble in hexane.

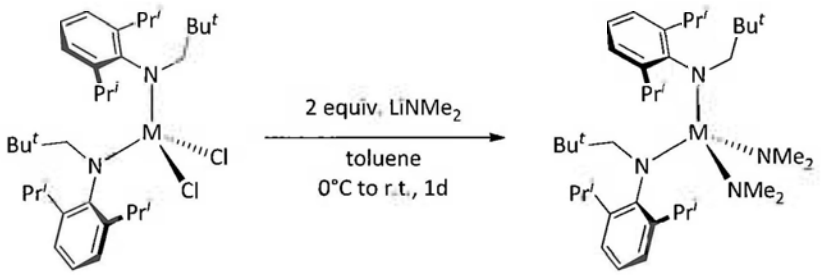

13: M = Zr
14: M = Hf

15: M = Zr 74%
16: M = Hf 47%

Scheme 2–11

Reactions of **15** and **16** with excess methyl iodide were studied in this work. Two products were isolated in each case, which were identified to be the corresponding monoiodide (**17** and **19**) and diiodide complexes (**18** and **20**) (Scheme 2–12). The monoiodide complexes **17** and **19** were isolated as colorless crystals, whereas the diiodide complexes **18** and **20** were obtained as yellow crystals. In the case of zirconium, the diiodide complex **18** was found to be the major product, whereas the monoiodide compound **19** was the major product in the case of hafnium. The two products in each reaction could be separated by fractional crystallization from hexane, in which the major product was obtained in the first fraction.

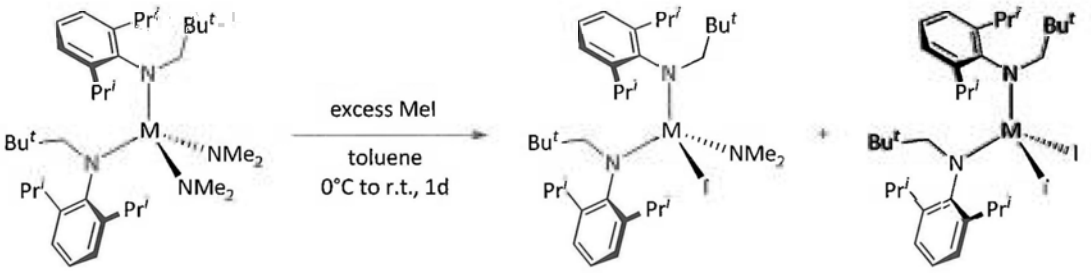

15: M = Zr
16: M = Hf

17: M = Zr 5%
19: M = Hf 44%

18: M = Zr 54%
20: M = Hf 5%

Scheme 2–12

Physical Characterization of Complexes **15–20**

Complexes **15–20** have been characterized by elemental analysis, melting point determination, NMR spectroscopy, and X-ray crystallography. Table 2–2 shows some of the physical properties of complexes **15–20**.

Table 2–10 Some physical properties of compounds **15–20**.

Compound	Appearance	M.p. (°C)
$[Zr(L^2)_2(NMe_2)_2]$ (**15**)	Colorless crystals	238–240 (dec.)
$[Zr(L^2)_2(NMe_2)(I)]$ (**17**)	Colorless crystals	210–211 (dec.)
$[Zr(L^2)_2I_2]$ (**18**)	Yellow crystals	228–230
$[Hf(L^2)_2(NMe_2)(I)]$ (**19**)	Colorless crystals	200–205

NMR Spectra of Complexes **15–20**

1. $[M(L^2)_2(NMe_2)_2]$ [M = Zr (**15**), Hf (**16**)]

The ^1H and ^{13}C NMR spectra of complexes **15** and **16** are shown in Figures A2–15 to A2–18. Only one set of resonance signals assignable to the L^2 ligand

were observed in their NMR spectra, indicating that the two L^2 ligands in each complex are equivalent. The two NMe_2 ligands in the complex are also equivalent as only one resonance signal (at 2.69 ppm for **15** and 2.67 ppm for **16** in the ^1H NMR spectra) assignable to the NMe_2 ligand was observed in each spectrum. In the ^1H NMR spectrum, the occurrence of only one septet signal assignable to the isopropyl methine protons suggests that the two isopropyl substituents of the L^2 ligand are equivalent (Figure 2–20). There are two doublets assignable to the isopropyl methyl protons in the ^1H NMR spectrum, showing that the geminal methyl groups of the isopropyl substituent are diastereotopic.

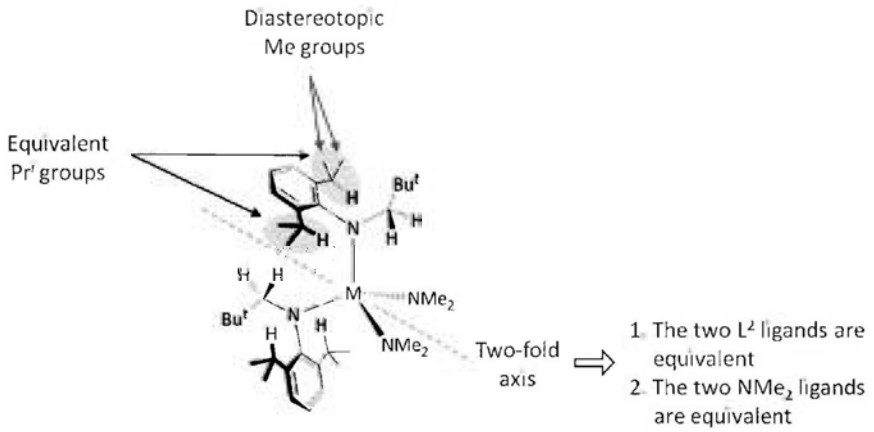

Figure 2–20

2. $[M(L^2)_2(NMe_2)(I)]$ [M = Zr (**17**), Hf (**19**)]

The ^1H and ^{13}C NMR spectra of **17** (Figure A2–19 and A2–20) and **19** (Figures A2–23 and A2–24) showed resonance signals assignable to the L^2 ligand and the NMe_2 ligands in a ratio of 1:1. The occurrence of two septets (at 3.62 and 4.42 ppm for **17**, and 3.72 and 4.34 ppm for **19**) assignable to the isopropyl methine

protons of the L^2 ligand indicates that the two isopropyl substituents of the L^2 ligand are nonequivalent. This is probably due to a restricted rotation about the N–C_{ipso} bond so that the aryl ring is locked at a position that the two isopropyl substituents are not interchangeable. This also leads to the nonequivalence of (i) the two *o*–aromatic carbons, and (ii) the two *m*–aromatic carbons, which are reflected by a total of six resonance signals assignable to the aromatic carbons in the ^{13}C NMR spectrum. The diastereotopic isopropyl methyl groups occur as four doublets in the ^1H NMR spectrum. Moreover, the methylene protons of the neopentyl substituent occur as two doublets (at 4.08 and 4.19 ppm for **17**, and 3.97 and 4.11 ppm for **19**), indicating that they are diastereotopic (Figure 2–21).

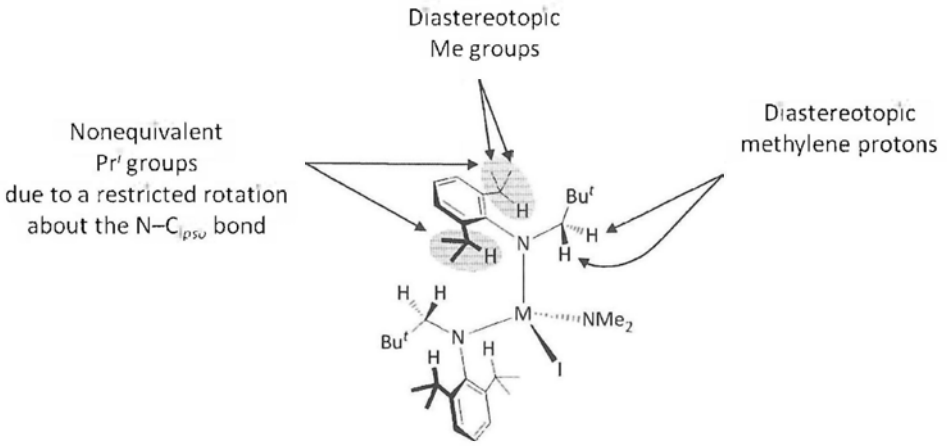

Figure 2–21

3. $[M(L^2)_2I_2]$ [M = Zr (**18**), Hf (**20**)]

The ^1H and ^{13}C NMR spectra of **18** and **20** are shown in Figures A2–22 and A2–22, and A2–25 and A2–26. Each spectrum showed one set of resonance signals assignable to the L^2 ligand, indicating the equivalence of the two L^2 ligands in each complex. In the ^1H NMR spectrum, only one septet assignable to the

isopropyl methine protons is observed, showing that the two isopropyl substituents of the L^2 ligand are equivalent. Two doublets assignable to the isopropyl methyl protons are observed. This indicates that the geminal methyl groups of the isopropyl substituent are diastereotopic (Figure 2–22).

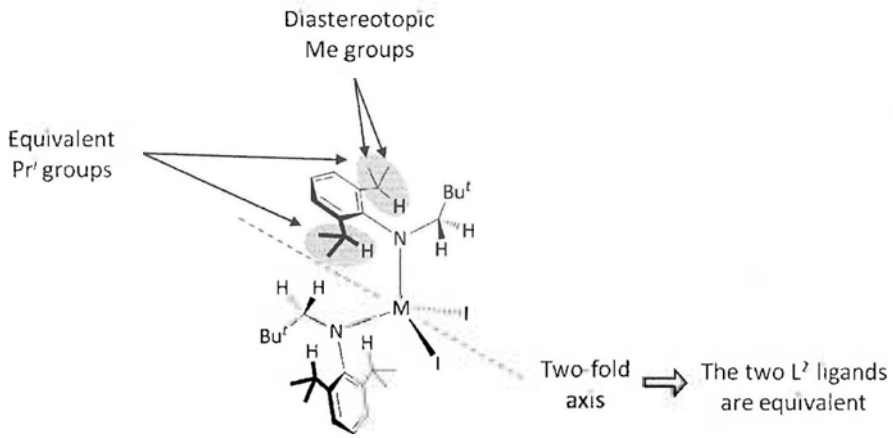

Figure 2–22

Crystal Structures of Complexes **15–20**

1. $[M(L^2)_2(NMe_2)_2]$ [M = Zr (**15**), Hf (**16**)]

The solid-state structures of complexes **15** and **16** are shown in Figures 2–23 and 2–24, respectively. Selected bond distances and angles of the complexes are summarized in Tables 2–11 and 2–12.

Complexes **15** and **16** are isostructural. They crystallize in the monoclinic space group $P2_1/c$. The metal center in each complex is coordinated by two L^2 ligands and two NMe_2 ligands. The coordination geometry around the metal center can be described as distorted tetrahedral.

The observed Zr–N_{aryl} distances in **15** are 2.080(3) and 2.102(2) Å. They are slightly longer than those of 2.020(3) and 2.025(3) Å in the dichloride precursor complex **13**. This can be attributed to the more bulky ligand environment of complex **15** as compared to that of **13**. The Zr–N_{NMe_2} distances of 2.024(3) and 2.039(3) Å in **15** are close to the corresponding distances reported for the four-coordinate $[Zr\{N(SiMe_3)_2\}_2(NMe_2)(Cl)]$ [2.024(3) Å][12d] and the binuclear $[Zr\{N(SiMe_3)_2\}(NMe_2)_2(Cl)]_2$ [2.030(1) and 2.036(1) Å].[12a]

The Hf–N_{aryl} distances of 2.059(3) and 2.082(3) Å in **16** are slightly longer than the corresponding distances in the dichloride precursor complex **14** [2.003(3) and 2.006(3) Å]. The Hf–N_{NMe_2} distances in **16** are 2.011(4) and 2.019(4) Å. They are slightly shorter than those of 2.019(3) and 2.036(3) Å in the binuclear $[Hf\{N(SiMe_3)_2\}(NMe_2)_2(\mu\text{–}Cl)]_2$.[12a]

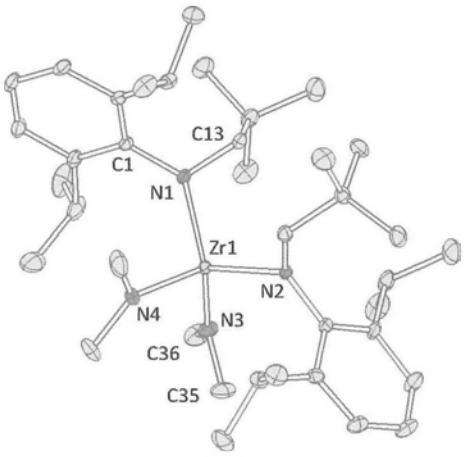

Figure 2–23 Molecular structure of $[Zr(L^2)_2(NMe_2)_2]$ (**15**).

Table 2–11 Selected bond lengths (Å) and angles (deg.) for compound **15**.

$[Zr(L^2)_2(NMe_2)_2]$ (**15**)			
Zr(1)–N(1)	2.080(3)	Zr(1)–N(3)	2.024(3)
Zr(1)–N(2)	2.102(2)	Zr(1)–N(4)	2.039(3)
N(1)–C(1)	1.439(4)	N(3)–C(35)	1.462(5)
N(1)–C(13)	1.469(4)	N(3)–C(36)	1.460(5)
N(1)–Zr(1)–N(2)	112.8(1)	C(1)–N(1)–Zr(1)	127.8(2)
N(1)–Zr(1)–N(3)	114.1(1)	C(13)–N(1)–Zr(1)	112.1(1)
N(3)–Zr(1)–N(4)	104.5(1)	C(1)–N(1)–C(13)	118.5(3)
Zr(1)–N(3)–C(35)	107.6(2)	C(35)–N(3)–C(36)	110.4(3)
Zr(1)–N(3)–C(36)	141.8(3)		

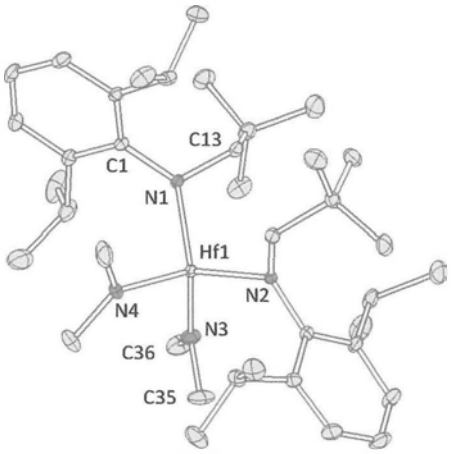

Figure 2–24 Molecular structure of $[Hf(L^2)_2(NMe_2)_2]$ (**16**).

Table 2–12 Selected bond lengths (Å) and angles (deg.) for compound **16**.

$[Hf(L^2)_2(NMe_2)_2]$ (**16**)			
Hf(1)–N(1)	2.059(3)	Hf(1)–N(3)	2.011(4)
Hf(1)–N(2)	2.082(3)	Hf(1)–N(4)	2.019(4)
N(1)–C(1)	1.442(4)	N(3)–C(35)	1.462(6)
N(1)–C(13)	1.489(5)	N(3)–C(36)	1.459(6)
N(1)–Hf(1)–N(2)	112.3(1)	C(1)–N(1)–Hf(1)	127.4(2)
N(1)–Hf(1)–N(3)	113.9(1)	C(13)–N(1)–Hf(1)	113.5(2)
N(3)–Hf(1)–N(4)	105.1(1)	C(1)–N(1)–C(13)	117.5(3)
Hf(1)–N(3)–C(35)	108.4(3)	C(35)–N(3)–C(36)	110.3(4)
Hf(1)–N(3)–C(36)	141.1(3)		

2. $[M(L^2)_2(NMe_2)(I)]$ [M = Zr (**17**), Hf (**19**)]

The molecular structures of complexes **17** and **19** are shown in Figures 2–25 and 2–26. Selected bond lengths and angles of these complexes are listed in Tables 2–13 and 2–14.

Crystals of **17** and **19** belong to the monoclinic space group $P2_1/n$. These two complexes are isostructural. The metal center in each complex is coordinated by a pair of L^2 ligands, one NMe_2 ligand and one iodide ligand. The coordination geometry around the metal center can be described as distorted tetrahedral.

The observed Zr–N distances in **17** are 2.046(2) and 2.053(2) Å ($Zr–N_{aryl}$), and 2.009(3) Å ($Zr–N_{NMe_2}$). The $Zr–N_{aryl}$ distances are shorter than those of 2.080(3) and 2.102(2) Å in $[Zr(L^2)_2(NMe_2)_2]$ (**15**). The Zr–I distance of 2.8221(4) Å in complex **17** is slightly shorter than the corresponding distances in $[Zr(Cp^{tt})_2I_2]$ [2.8258(8) and 2.8454(8) Å],[14a] and the terminal Zr–I distance in the binuclear $[Zr(NEt_2)_2I(\mu\text{-}I)]_2$ [2.8544(9)].[14b]

The observed Hf–N distances in **19** are 2.032(3) and 2.043(2) Å ($Hf–N_{aryl}$), and 1.996(3) Å ($Hf–N_{NMe_2}$). The $Hf–N_{aryl}$ distances are only slightly shorter than the corresponding distances in $[Hf(L^2)_2(NMe_2)_2]$ (**16**) [2.059(3) and 2.082(3) Å]. The Hf–I distance of 2.7837(4) Å in complex **19** is comparable to the Hf–I distance in $[Hf(Cp^{tt})_2I_2]$ [2.7890(8) Å],[14a] but shorter than those of 2.884(1) in $[(Cp^{Me})_2Hf(I)(\mu–N_2)(Me)Hf(Cp^{Me})_2]$.[14c]

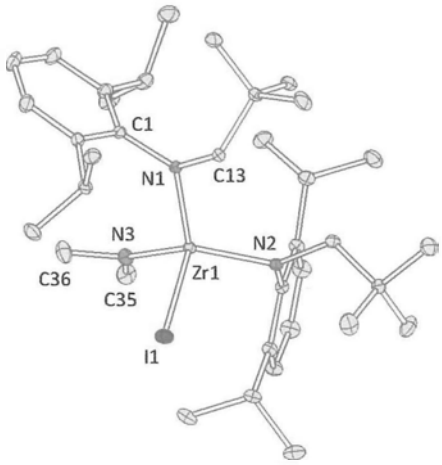

Figure 2–25 Molecular structure of $[Zr(L^2)_2(NMe_2)I]$ (**17**).

Table 2–13 Selected bond lengths (Å) and angles (deg.) for compound **17**.

$[Zr(L^2)_2(NMe_2)I]$ (**17**)			
Zr(1)–N(1)	2.053(2)	Zr(1)–N(3)	2.009(3)
Zr(1)–N(2)	2.046(2)	Zr(1)–I(1)	2.8221(4)
N(1)–C(1)	1.453(4)	N(3)–C(35)	1.460(5)
N(1)–C(13)	1.471(4)	N(3)–C(36)	1.453(5)
N(1)–Zr(1)–N(2)	112.42(9)	C(1)–N(1)–Zr(1)	126.7(1)
N(1)–Zr(1)–N(3)	109.0(1)	C(13)–N(1)–Zr(1)	114.3(1)
N(1)–Zr(1)–I(1)	102.87(6)	C(1)–N(1)–C(13)	116.3(2)
N(3)–Zr(1)–I(1)	105.96(9)	Zr(1)–N(3)–C(35)	134.5(3)
Zr(1)–N(3)–C(36)	114.0(2)	C(35)–N(3)–C(36)	111.2(3)

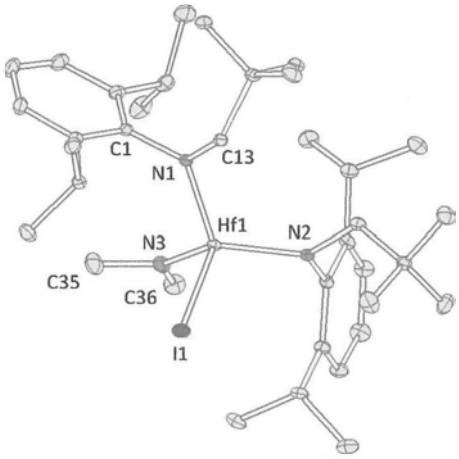

Figure 2–26 Molecular structure of $[Hf(L^2)_2(NMe_2)I]$ (**19**).

Table 2–14 Selected bond lengths (Å) and angles (deg.) for compound **19**.

$[Hf(L^2)_2(NMe_2)I]$ (**19**)			
Hf(1)–N(1)	2.043(2)	Hf(1)–N(3)	1.996(3)
Hf(1)–N(2)	2.032(3)	Hf(1)–I(1)	2.7837(4)
N(1)–C(1)	1.446(4)	N(3)–C(35)	1.459(5)
N(1)–C(13)	1.470(4)	N(3)–C(36)	1.451(5)
N(1)–Hf(1)–N(2)	116.2(1)	C(1)–N(1)–Hf(1)	126.4(1)
N(1)–Hf(1)–N(3)	109.1(1)	C(13)–N(1)–Hf(1)	114.8(2)
N(1)–Hf(1)–I(1)	103.65(7)	C(1)–N(1)–C(13)	116.1(3)
N(3)–Hf(1)–I(1)	106.62(9)	Hf(1)–N(3)–C(35)	113.8(3)
Hf(1)–N(3)–C(36)	134.8(3)	C(35)–N(3)–C(36)	111.1(3)

3. $[Zr(L^2)_2I_2]$ (**18**)

The solid-state structure of complex **18** is shown in Figure 2–27, with selected bond distances and angles summarized in Table 2–15. Complex **18** crystallizes in the orthorhombic space group $P2_12_12_1$. The tetrahedral Zr(IV) center is coordinated by two L^2 ligands and two iodide ligands. The complex contains a C_2-axis passing through the metal center.

The observed Zr–N distances in **18** are 2.003(4) and 2.009(4) Å, which are shorter than those of 2.020(3) and 2.025(3) Å in the dichloride derivative $[Zr(L^2)_2Cl_2]$ (**13**), though iodide ligands are more bulky than chloride ligands. This may be attributed to a difference in electronic properties of chloride and iodide anions. As iodide ligands are less basic than chloride ligands, the Zr(IV) center in **18** receive less electron density from the iodide ligands and thus form stronger bonds with the L^2 ligands. The Zr–I distances of 2.7256(7) and 2.7587(7) Å in complex **18** are shorter than those of 2.8221(4) Å in the monoiodide complex **17**. This may be due to the sterically less congested ligand environment in complex **18**. The Zr–I distances in **18** are shorter than those in $[Zr(Cp^{tt})_2I_2]$ (Cp^{tt} = η^5–1,3–di–tert–butyl cyclopentadienyl) [2.8258(8) and 2.8454(8) Å],[14a] and the terminal Zr–I distance in the binuclear $[Zr(NEt_2)_2I(\mu\text{-}I)]_2$ [2.8544(9)].[14b]

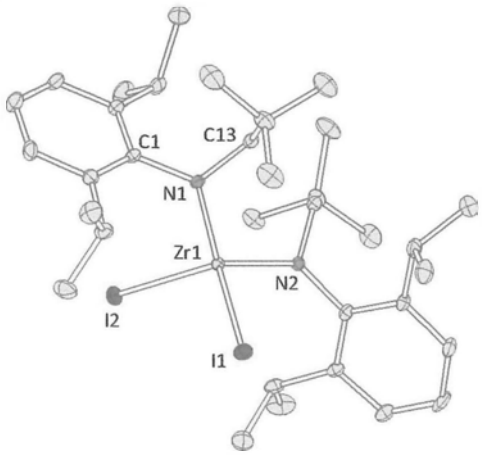

Figure 2–27 Molecular structure of $[Zr(L^2)_2I_2]$ (**18**).

Table 2–15 Selected bond lengths (Å) and angles (deg.) for compound **18**.

$[Zr(L^2)_2I_2]$ (**18**)			
Zr(1)–N(1)	2.003(4)	Zr(1)–I(1)	2.7256(7)
Zr(1)–N(2)	2.009(4)	Zr(1)–I(2)	2.7587(7)
N(1)–C(1)	1.469(7)	N(1)–C(13)	1.459(7)
N(1)–Zr(1)–N(2)	114.5(1)	C(1)–N(1)–Zr(1)	123.2(3)
N(1)–Zr(1)–I(1)	109.2(1)	C(13)–N(1)–Zr(1)	117.1(3)
I(1)–Zr(1)–I(2)	112.46(2)	C(1)–N(1)–C(13)	118.6(4)

D. Synthesis of Bis(amido) Zr(IV) and Hf(IV) Dimethyl Complexes

Synthesis of metal–alkyl complexes have attracted much attention because they are believed to be highly reactive pre-catalysts and key intermediates in polymerization reactions.[15]

As depicted in Scheme 2–13, treatment of **13** and **14** in toluene with two equivalents of LiMe led to $[M(L^2)_2Me_2]$ [M = Zr (**21**), Hf (**22**)]. Complexes **21** and **22** were isolated as colorless crystals from hexane. They are highly soluble in common organic solvents. Being extremely sensitive to air and moisture, the crystalline complexes turned quickly to a sticky brown solid upon exposure to air.

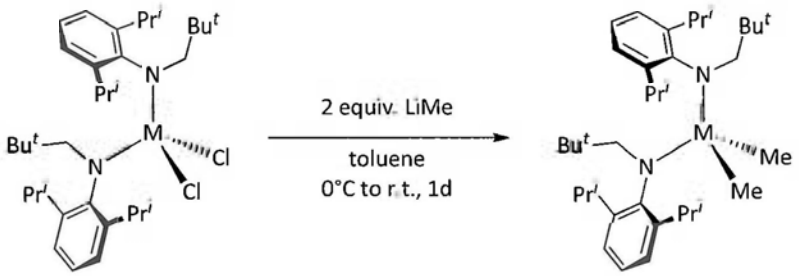

13: M = Zr
14: M = Hf

21: M = Zr 66%
22: M = Hf 65%

Scheme 2–13

The successful isolation of the dimethyl complexes **21** and **22** prompted us to prepare other alkyl derivatives. Unfortunately, attempts to isolate other alkyl derivatives of **13** and **14** have been unsuccessful. Reaction of **13** with EtMgBr only led to a yellow intractable oil. Treatment of **13** with $LiBu^n$ and gave an orange intractable oil. Moreover, reaction of **13** with $LiC{\equiv}CSiMe_3$ resulted in a pale brown solid, whose ^1H NMR spectrum showed resonance signals assignable to the ligand

precursor HL^2. Attempts to prepare a Hf(IV) alkyl complex by treatment of **14** with $LiCH_2SiMe_3$ have also been unsuccessful. Only a pale yellow intractable oil was obtained after the reaction. During the course of these reactions, the reaction mixtures darkened when they were allowed to warm from 0 °C to room temperature. An unidentified white powder was isolated after the reactions. Conceivably, the desired metal species were formed at low temperatures, but they readily decomposed when the reaction mixtures were brought to ambient conditions.

Physical Characterization of Complexes **21** and **22**

Complexes **21** and **22** have been characterized by elemental analysis, melting point determination, NMR spectroscopy, and X-ray crystallography. Results of elemental analysis were consistent with the formulation of the two complexes as shown in Scheme 2–13. Some of the physical properties of compounds **21** and **22** are listed in Table 2–16.

Table 2–16 Some physical properties of compounds **21** and **22**.

Compound	Appearance	M.p. (°C)
$[Zr(L^2)_2Me_2]$ (**21**)	Colorless crystals	160–164
$[Hf(L^2)_2Me_2]$ (**22**)	Colorless crystals	182–183

NMR Spectra of Complexes **21** and **22**

The ^1H and ^{13}C NMR spectra of complexes **21** and **22** are shown in Figures A3–27 to A3–30. The NMR spectra showed one set of resonance signals assignable

to the L^2 and methyl ligands. This indicates that the two L^2 ligands are equivalent and the two methyl ligands are also identical to each other, suggesting the existence of a C_2-axis bisecting the N–M–N and Cl–M–Cl angles in the molecule.

The two isopropyl substituents of the L^2 ligand in **21** are chemically equivalent, and the geminal methyl groups of the isopropyl substituents are isochronous, as indicated by the occurrence of one septet at 3.90 ppm and one doublet at 1.40 ppm in the ^{1}H NMR spectrum.

On the other hand, the isopropyl substituents of the L^2 ligands in **22** occur as one septet at 3.95 ppm and two doublets at 1.39 and 1.43 ppm in the ^{1}H NMR spectrum. This spectroscopic behavior indicates that the two isopropyl substituents of the L^2 ligand are equivalent, but the geminal methyl groups of each isopropyl substituent are diastereotopic (Figure 2–28).

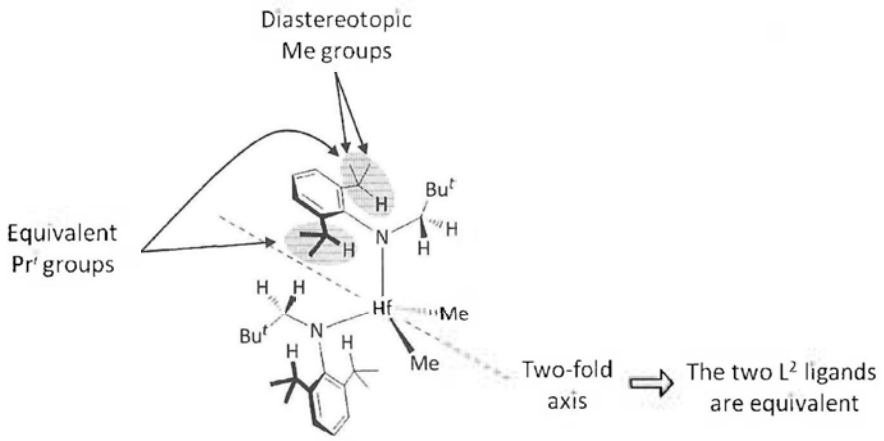

Figure 2–28

Crystal Structures of **21** and **22**

Molecular structures of complexes **21** and **22** are shown in Figures 2–29 and 2–30, respectively. Selected bond lengths and angles are listed in Tables 2–17 and 2–18.

Complexes **21** and **22** crystallize in the orthorhombic space groups $P2_12_12_1$ and *Pnma*, respectively. These two complexes have similar molecular structures with the metal center being coordinated by two L^2 ligands and two methyl ligands. Both complexes contain a C_2-axis passing through the metal center.

The observed Zr–N bond distances of 2.046(2) Å and 2.048(3) in **21** are slightly longer than those of 2.020(3) and 2.025(3) Å in the dichloride precursor complex **13**, though methyl ligands are less bulky than chloride ligands. This may be attributed to a difference in the basicity of the methyl and chloride ligands. Because the methyl ligand is more nucleophilic as compared to the chloride anion, it binds strongly to the Zr(IV) center and, thus, weakening the Zr–N bonds.

The Zr–N distances in complex **21** are shorter than the corresponding distances reported for $[Zr\{N(C_6H_3Pr^i_2\text{–}2,6)(SiMe_3)\}_2Me_2]$ [2.056(3) and 2.066 Å][5b] and $[Zr\{N(C_6H_3Pr^i_2\text{–}2,6)(C_6H_4F\text{–}2)\}_2Cl_2]$ [2.143(3) and 2.151(3) Å].[12c] The Zr–Me bond lengths of 2.217 and 2.243 Å in **21** are slightly shorter than those in $[Zr\{N(C_6H_3Pr^i_2\text{–}2,6)(SiMe_3)\}_2Me_2]$ [2.224(4) and 2.327(3) Å],[5b] but marginally longer than those reported for $[Zr\{N(C_6H_3Pr^i_2\text{–}2,6)(C_6H_4F\text{–}2)\}_2Me_2]$ [2.216(5) and 2.228(5) Å].[12c]

The L^2 and methyl ligands around the Hf(IV) center in complex **22** are two-fold disordered. The Hf–N distances [2.015 and 2.03(1)Å] in complex **22** are slightly longer than the corresponding distances [2.003(3) Å and 2.006(3)] in the dichloride precursor complex **14**. Compared with other Hf(IV) methyl complexes, the Hf–N distances in **22** are shorter than those of 2.147(3) and 2.149(3) Å in the six-coordinate amidophosphine complex $[Hf(N_2P_2)Me_2]$ $[N_2P_2 = PhP(CH_2SiMe_2NSiMe_2CH_2)_2PPh]$.[176a] On the other hand, the Hf–Me distances in **22** [2.20(1) and 2.22(1) Å] are slightly shorter than those of 2.263(1) and 2.277(1) Å in $[Hf(N_2P_2)Me_2]$,[16a] and 2.237 Å in $[Hf(Cp)_2\{NH_2B(C_6F_5)_3\}(Me)]$.[16b]

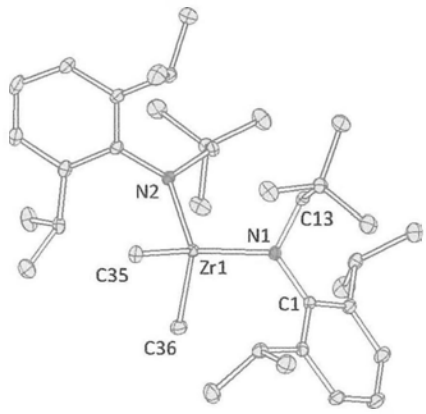

Figure 2–29 Molecular structure of $[Zr(L^2)_2Me_2]$ (**21**).

Table 2–17 Selected bond lengths (Å) and angles (deg.) for compound **21**.

$[Zr(L^2)_2Me_2]$ (**21**)			
Zr(1)–N(1)	2.048(3)	Zr(1)–C(35)	2.217(3)
Zr(1)–N(2)	2.046(2)	Zr(1)–C(36)	2.243(4)
N(1)–C(1)	1.437(4)	N(1)–C(13)	1.470(4)
N(1)–Zr(1)–N(2)	116.8(1)	C(1)–N(1)–Zr(1)	121.8(2)
N(1)–Zr(1)–C(35)	108.5(1)	C(13)–N(1)–Zr(1)	118.1(1)
C(35)–Zr(1)–C(36)	109.3(1)	C(1)–N(1)–C(13)	118.2(2)

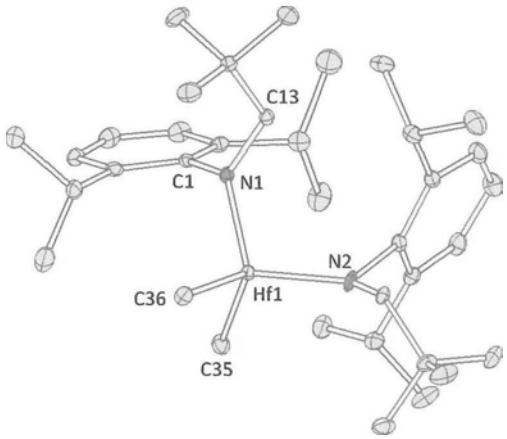

Figure 2–30 Molecular structure of $[Hf(L^2)_2Me_2]$ (**22**).

The L^2 and methyl ligands are two-fold disordered. Only one set of ligand orientation is shown.

Table 2–18 Selected bond lengths (Å) and angles (deg.) for compound **22**.

$[Hf(L^2)_2Me_2]$ (**22**)			
Hf(1)–N(1)	2.03(1)	Hf(1)–C(35)	2.20(1)
Hf(1)–N(2)	2.015(8)	Hf(1)–C(36)	2.22(1)
N(1)–C(1)	1.44(1)	N(1)–C(13)	1.48(1)
N(1)–Hf(1)–N(2)	109.4(3)	C(1)–N(1)–Hf(1)	122.7(8)
N(1)–Hf(1)–C(35)	107.8(5)	C(13)–N(1)–Hf(1)	118.3(8)
C(35)–Hf(1)–C(36)	109.5(6)	C(1)–N(1)–C(13)	117(1)

*E. Other Attempted Reactions of Complex **13***

1. Attempted Reactions of **13** with NaOR (R = Me, Bu^t) and NaN_3

Compound **13** was found to be unreactive towards NaOMe, $NaOBu^t$ and NaN_3 at room temperature. Moreover, no reaction of **13** with NaOMe was observed even at an elevated temperature of 40 °C. Complex **13** was recovered after the reactions, as concluded from NMR spectroscopic analysis.

2. Attempted Reactions of Complex **13** with Reducing Agents

Reactions of complex **13** with various reducing agents such as KC_8, K, Na and $LiAlH_4$ were examined in this work. Unfortunately, complex product mixtures were obtained after these reactions, and characterization of the product mixtures was difficult to carry out.

3. Catalytic Properties of Complexes **13**, **21** and **22**

Attempted study on the catalytic properties of complex **13** and **21** have also been carried out. Unfortunately, both complexes **13** and **21** [with $B(C_6F_5)_3$ as a co-catalyst] were found to be inactive towards polymerization of styrene or 1-hexene (monomer to initiator ratio = 200:1). Complexes **13** and **22** were also found to be inactive towards the ring-opening polymerization of ε-caprolactone (monomer to initiator ratio = 200:1).

F. Synthesis of Ti(III) Amido Complexes

Transmetallation reactions of $TiCl_3(thf)_3$ with lithium amides **5** and **6** in thf yielded yellowish-green, crystalline Ti(III) complexes $[Ti(L^1)_2(\mu\text{–}Cl)_2Li(tmeda)]$ **(23)**

and $[Li(tmeda)_2]^+[Ti(L^2)_2Cl_2]^-$ (**24**), respectively (Scheme 2–14). Complexes **23** and **24** are readily soluble in thf and toluene, but only sparingly soluble in diethyl ether and hexane. They are extremely sensitive to air and moisture, turning quickly to black solids.

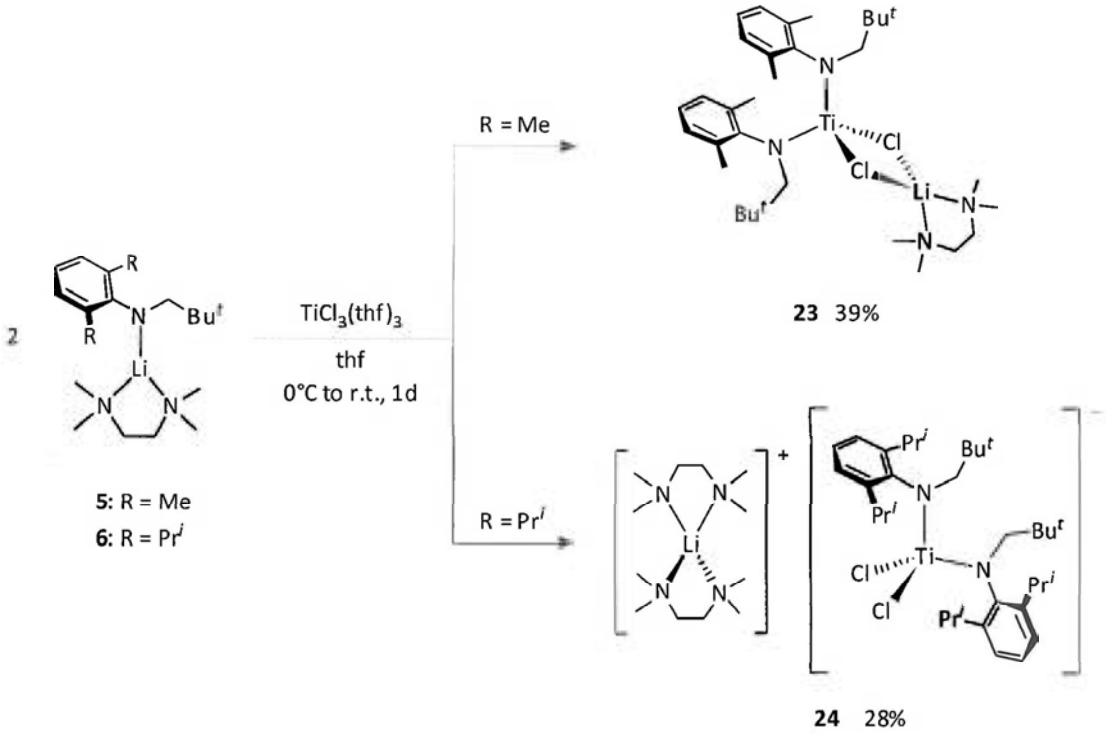

Scheme 2–14

Physical Characterization of Complexes **23** and **24**

Complexes **23** and **24** have been characterized by elemental analysis, melting-point measurement, and single-crystal X-ray crystallography. Table 2–19 summarizes some of the physical properties of compounds **23** and **24**. Results of elemental analysis were consistent with the formulation of these complexes as shown in the Scheme 2–3. No assignable signals were observed in the ^{1}H NMR spectra of the paramagnetic complexes **23** and **24**. On the other hand, a

solid-state EPR spectrum of **24** was obtained at 60 K, which showed a nearly isotropic signal at g = 1.94.

Table 2–19 Some physical properties of compounds **23** and **24**.

Compound	Appearance	M.p. (°C)
$[Ti(L^1)_2(\mu\text{–}Cl)_2Li(tmeda)]$ (**23**)	Yellowish-green crystals	186–189
$[Li(tmeda)_2][Ti(L^2)_2Cl_2]$ (**24**)	Yellowish-green crystals	184–185 (dec.)

Crystal Structures of **23** and **24**

The molecular structures of the Ti(III) complexes $[Ti(L^1)_2(\mu\text{–}Cl)_2Li(tmeda)]$ (**23**) and $[Li(tmeda)_2]^+[Ti(L^2)_2Cl_2]^-$ (**24**) are shown in Figures 2–31 and 2–32, respectively. Selected bond distances and angles are summarized in Tables 2–20 and 2–21.

Complex **23** crystallizes in the monoclinic space group $P2_1/n$. The pseudo tetrahedral Ti(III) center is bonded to two L^1 ligands and two bridging chloride ligands. The observed Ti–N distances are 1.929(3) and 1.933(3) Å, whereas the Ti–Cl distances are 2.386(1) Å. The two bridging chloride ligands link up the Ti(III) ion and the Li ion. Coordination of a tmeda ligand to the Li ion completes a distorted tetrahedral geometry around the alkali metal center with Li–N distances of 2.078(6) Å and Li–Cl distances of 2.371(6) and 2.372(6) Å.

Cummins and co-workers have reported a three-coordinate Ti(III) complex, $[Ti\{N(C_6H_3Me_2\text{–}3,5)(C(CD_3)_2Me)\}_3]$ [Ti–N distances = 1.933(3)–2.005(3) Å].[9c] Using a highly electronegative $[N(C_6F_5)_2]^-$ ligand, Watkin and co-workers have also prepared the $[Na(thf)_2]^+[Ti\{N(C_6F_5)_2\}_4]^-$ complex [Ti–N distances = 2.039(3) Å].[11a] Compared with these complexes, the observed Ti–N distances in complex **23** are

slightly shorter, probably due to a less congested ligand environment around the Ti(III) center in **23**.

Complex **24** crystallizes in the monoclinic space group *Cc*. The crystal structure of the complex consists of an ion pair. The Ti(III) ion is bound by two L^2 ligands and two chloride ligands, whereas the Li ion is coordinated by two chelating tmeda ligands. Both metal ions adopt a distorted tetrahedral geometry. The observed Ti–N distances in **24** are 1.949(5) and 1.960(4) Å. They are slightly shorter than those of 1.933(3)–2.005(3) Å reported for $[Ti\{N(C_6H_3Me_2\text{–}3,5)(C(CD_3)_2Me)\}_3]$[9c] and 2.039(3) Å in $[Na(thf)_2]^+[Ti\{N(C_6F_5)_2\}_4]^-$.[11a] The observed Ti–Cl distances in **24** are 2.334(1) and 2.342(1) Å.

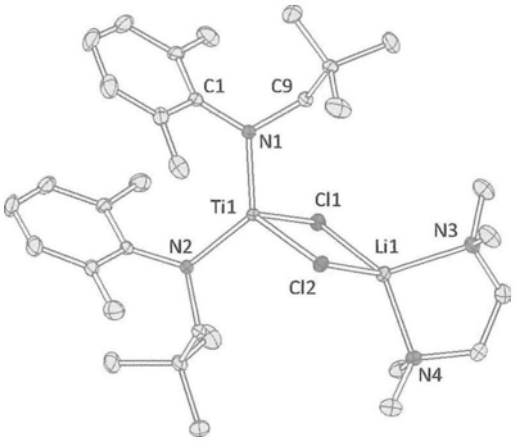

Figure 2–31 Molecular structure of $[Ti(L^1)_2(\mu\text{–}Cl)_2Li(tmeda)]$ (**23**).

Table 2–20 Selected bond lengths (Å) and angles (deg.) for compound **23**.

$[Ti(L^1)_2(\mu\text{–}Cl)_2Li(tmeda)]$ (**23**)			
Ti(1)–N(1)	1.929(3)	Li(1)–N(3)	2.078(6)
Ti(1)–N(2)	1.933(3)	Li(1)–N(4)	2.078(6)
Ti(1)–Cl(1)	2.386(1)	Li(1)–Cl(1)	2.371(6)
Ti(1)–Cl(2)	2.386(1)	Li(1)–Cl(2)	2.372(6)
N(1)–C(1)	1.429(4)	N(1)–C(9)	1.476(4)
N(1)–Ti(1)–N(2)	126.1(1)	C(1)–N(1)–Ti(1)	125.9(2)
N(1)–Ti(1)–Cl(1)	108.3(1)	C(9)–N(1)–Ti(1)	114.5(2)
Cl(1)–Ti(1)–Cl(2)	93.4(1)	C(1)–N(1)–C(9)	118.9(3)
Cl(1)–Li(1)–Cl(2)	94.1(1)	N(3)–Li(1)–N(4)	89.2(2)

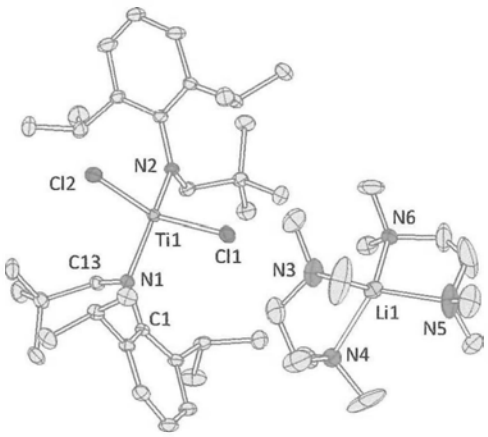

Figure 2–32 Molecular structure of $[Li(tmeda)]^+[Ti(L^2)_2Cl_2]^-$ (**24**).

Table 2–21 Selected bond lengths (Å) and angles (deg.) for compound **24**.

$[Li(tmeda)]^+[Ti(L^2)_2Cl_2]^-$ (**24**)			
Ti(1)–N(1)	1.949(5)	Li(1)–N(3)	2.28(1)
Ti(1)–N(2)	1.960(4)	Li(1)–N(4)	2.19(1)
Ti(1)–Cl(1)	2.334(1)	Li(1)–N(5)	2.08(1)
Ti(1)–Cl(2)	2.342(1)	Li(1)–N(6)	2.13(1)
N(1)–C(1)	1.444(7)	N(1)–C(13)	1.46(7)
N(1)–Ti(1)–N(2)	116.1(1)	C(1)–N(1)–Ti(1)	126.1(4)
N(1)–Ti(1)–Cl(1)	104.8(1)	C(13)–N(1)–Ti(1)	117.1(3)
Cl(1)–Ti(1)–Cl(2)	111.4(1)	C(1)–N(1)–C(13)	115.6(4)
N(3)–Li(1)–N(4)	82.1(6)	N(5)–Li(1)–N(6)	92.3(7)

Summary

A series of Group 4 metal complexes supported by the *N*-alkylated arylamido ligands $[N(C_6H_3R_2\text{–}2,6)(CH_2Bu^t)]^-$ (L^1: R = Me, L^2: R = Pr^i) have been synthesized and structurally characterized. Metathetical reactions of MCl_4 (M = Zr, Hf) with two molar equivalents of $[LiL^n(tmeda)]$ [*n* = 1 (**5**), n = 2 (**6**)] gave the heterobimetallic complexes $[M(L^n)_2Cl(\mu\text{–}Cl)_2Li(tmeda)]$ [M = Zr, *n* = 1 (**8**), *n* = 2 (**9**); M = Hf, *n* = 1 (**10**), *n* = 2 (**11**)]. Neutral complexes $[M(L^2)_2Cl_2]$ [M = Ti (**12**), Zr (**13**), Hf (**14**)] were isolated by the reactions of $MCl_4(thf)_x$ (M = Ti, x = 2; M = Zr, Hf, x = 0) with the tmeda-free lithium reagent $[LiL^2(thf)_2]$ (**7**).

The $[M(L^2)_2Cl_2]$ [M = Zr (**13**), Hf (**14**)] complexes underwent ligand substitution reactions, leading to a series of alkyl, amido and iodo derivatives. Reactions of complexes **13** and **14** with $LiNMe_2$ afforded the corresponding tetra(amido) complexes $[M(L^2)_2(NMe_2)_2]$ [M = Zr (**15**), Hf (**16**)]. Subsequent reactions of complexes **15** and **16** with methyl iodide led to a mixture of the corresponding monoiodide (**17** and **19**) and diiodide (**18** and **20**) complexes. In the case of zirconium, the diiodide complex $[Zr(L^2)_2I_2]$ (**18**) was found to be the major product, whereas the monoiodide compound $[Hf(L^2)_2(NMe_2)(I)]$ (**19**) was the major product in the case of hafnium. The bis(amido) dimethyl complexes $[M(L^2)_2Me_2]$ [M = Zr (**21**), Hf (**22**)] were prepared by the reactions of the corresponding dichloride complexes **13** and **14** with two equivalents of LiMe.

Ti(III) amide-chloride complexes $[Ti(L^1)_2(\mu\text{–}Cl)_2Li(tmeda)]$ (**23**) and $[Li(tmeda)_2]^+[Ti(L^2)_2Cl_2]^-$ (**24**) have also been synthesized by the reactions of $TiCl_3(thf)_3$ with the lithium reagents **5** and **6**, respectively.

Results of our studies have demonstrated that the *N*-alkylated arylamido ligands L^1 and L^2 are suitable supporting ligands for a series of Ti(III), Ti(IV), Zr(IV) and Hf(IV) complexes. The bis(amido) M(IV) dichloride complexes [M = Zr (**13**), Hf (**14**)] were also shown to be good starting materials for mixed-amido, -iodo and -methyl complexes.

Experimental for Chapter 2

Materials

Anhydrous $TiCl_3$, $TiCl_4(thf)_2$, $ZrCl_4$ and $HfCl_4$ (Strem), LiMe (1.6 M in Et_2O) (Acros), $LiNMe_2$ (Alfa Aesar) and MeI (Acros) were used as received. The ligand precursors HL^n [n = 1, R = Me (**3**); n = 2, R = Pr^i (**4**)], and the lithium reagents [LiL^n(tmeda)] [n = 1 (**5**), n = 2 (**6**)] and $LiL^2(thf)_2$ (**7**), were prepared according to published procedures.[10]

General procedure for the synthesis of [$M(L^n)_2Cl(\mu\text{–}Cl)_2Li$(tmeda)] [M = Zr, n = 1 (8), n = 2 (9); M = Hf, n = 1 (10), n = 2 (11)].

To a Schlenk flask charged with MCl_4 and toluene (15 ml) at 0 °C was added dropwise a solution of [LiL^n(tmeda)] in toluene (20 ml). The reaction mixture was stirred at room temperature for 1 d, filtered and concentrated to *ca.* 5 ml. Standing the solution at room temperature for 1 d gave the desired product as a crystalline solid.

Synthesis of [$Zr(L^1)_2Cl(\mu\text{–}Cl)_2Li$(tmeda)] (8).

$ZrCl_4$: 0.62 g, 2.67 mmol; [LiL^1(tmeda)]: 1.62 g, 5.15 mmol. Product: pale yellow, block-shaped crystals. Yield: 0.77 g, 1.03 mmol, 40%. M.p.: 169–174 °C. ^{1}H NMR (300.13 MHz, C_6D_6): δ 7.01 (d, J = 6.0 Hz, 4H, *m*–Ar*H*), 6.90 (t, J = 6.0 Hz, 2H, *p*–Ar*H*), 3.84 (s, 4H, CH_2CMe_3), 2.80 (s, 12H, ArMe_2), 1.82 (s, 12H, NMe_2), 1.68 (s, 4H, NCH_2), 0.98 (s, 18H, CMe_3). ^{13}C NMR (75.47 MHz, C_6D_6): δ 150.5, 133.5, 129.5, 124.4, 57.0, 56.0, 45.2, 36.2, 29.1, 21.5. Anal.: Calc. for $C_{35.5}H_{60}Cl_3LiN_4Zr$: C, 57.05; H, 8.09; N, 7.50%. Found: C, 57.47; H, 8.31; N, 7.44%.

Synthesis of [Zr(L^2)$_2$Cl(μ–Cl)$_2$Li(tmeda)] (9).

$ZrCl_4$: 0.77 g, 3.28 mmol; [LiL^2(tmeda)]: 2.38 g, 6.44 mmol. Product: pale yellow, block-shaped crystals. Yield: 0.93 g, 1.15 mmol, 35%. M.p.: 190–195 °C (dec.). ^{1}H NMR (300.13 MHz, C_6D_6): δ 7.18–7.08 (m, 10H, Ar*H*), 4.29 (br. sept, 4H, C*H*Me$_2$), 4.19 (s, 4H, C*H*$_2$CMe$_3$), 1.72 (s, 12H, N*Me*$_2$), 1.64 (d, *J* = 6.5 Hz, 12H, CH*Me*$_2$), 1.58 (s, 4H, NC*H*$_2$), 1.47 (d, *J* = 6.5 Hz, 12H, CH*Me*$_2$), 1.01 (s, 18H, C*Me*$_3$). ^{13}C NMR (75.47 MHz, C_6D_6): δ 148.5, 144.6, 125.6, 125.3, 58.6, 56.3, 45.3, 37.2, 29.5, 28.2, 26.9, 26.0. ^{7}Li NMR (155.44 MHz, C_6D_6): δ -1.68 (s). Anal.: Calc. for $C_{40}H_{72}Cl_3LiN_4Zr$: C, 59.05; H, 8.92; N, 6.88%. Found: C, 58.95; H, 9.04; N, 7.05%.

Synthesis of [Hf(L^1)$_2$Cl(μ–Cl)$_2$Li(tmeda)] (10).

$HfCl_4$: 0.99 g, 3.03 mmol; [LiL^1(tmeda)]: 2.23 g, 6.05 mmol. Product: colorless, block-shaped crystals. Yield: 0.67 g, 0.76 mmol, 33%. M.p.: 176–178 °C. ^{1}H NMR (400.13 MHz, C_6D_6): δ 7.04 (d, *J* = 6.0 Hz, 2H, *m*–Ar*H*), 6.90 (t, *J* = 6.0 Hz, 2H, *p*–Ar*H*), 3.79 (s, 4H, C*H*$_2$CMe$_3$), 2.81 (s, 12H, Ar*Me*$_2$), 1.75 (s, 12H, N*Me*$_2$), 1.55 (s, 4H, NC*H*$_2$), 0.98 (s, 18H, C*Me*$_3$). ^{13}C NMR (100.64 MHz, C_6D_6): δ 150.7, 134.4, 129.4, 124.1, 57.5, 56.0, 45.1, 36.3, 29.2, 21.5. Anal.: Calc. for $C_{32}H_{56}Cl_3LiN_4Hf$: C, 48.74; H, 7.16; N, 7.10%. Found: C, 46.73; H, 7.25; N, 7.17%.*

Synthesis of [Hf(L^2)$_2$Cl(μ–Cl)$_2$Li(tmeda)] (11).

$HfCl_4$: 0.99 g, 3.03 mmol; [LiL^2(tmeda)]: 2.23 g, 6.05 mmol. Product: colorless, block-shaped crystals. Yield: 0.78 g, 0.87 mmol, 28%. M.p.: 319–324 °C (dec.). ^{1}H NMR (300.13 MHz, C_6D_6): δ 7.18–7.07 (m, 6H, Ar*H*), 4.29 (s, 4H, C*H*$_2$CMe$_3$), 4.11 (br, 4H, C*H*Me$_2$), 1.70 (s, 12H, N*Me*$_2$), 1.62 (d, *J* = 6.3 Hz, 12H, CH*Me*$_2$), 1.58 (s, 4H,

* Satisfactory elemental analysis data for this compound could not be obtained.

NCH_2), 1.51 (d, J = 6.3 Hz, 12H, CHMe_2), 1.04 (s, 18H, CMe_3). ^{13}C NMR (75.47 MHz, C_6D_6): δ 149.3, 145.1, 125.1, 124.0, 60.0, 56.4, 45.3, 37.3, 29.5, 28.7, 27.1, 26.0. ^{7}Li NMR (116.64 MHz, C_6D_6): δ -1.92 (s). Anal.: Calc. for $C_{40}H_{72}Cl_3LiN_4Hf$: C, 53.33; H, 8.06; N, 6.22%. Found: C, 53.02; H, 8.24; N, 6.26%.

Synthesis of [Ti(L^2)$_2$Cl$_2$] (12)

To a slurry of $TiCl_4(thf)_2$ (0.77 g, 2.30 mmol) in diethyl ether (10 ml) at 0 °C was added dropwise a solution of LiL^2(thf)$_2$ (1.70 g, 4.28 mmol) in the same solvent (10 ml). After stirring for 1 d at room temperature, the brown reaction mixture was filtered. All the volatiles were removed in *vacuo* and the residue was extracted with hexane (20 ml). The solution was filtered and concentrated to *ca.* 5 ml. Standing the solution at room temperature gave red, block-shaped crystals of **12**. Yield: 0.49 g, 0.81 mmol, 36%. M.p.: 241–245 °C. ^{1}H NMR (300.13 MHz, C_6D_6): δ 7.24–7.20 (m, 2H, *p*–Ar*H*), 7.17–7.13 (m, 4H, *m*–Ar*H*), 4.54 (s, 4H, CH_2CMe$_3$), 3.91 (sept, J = 6.7 Hz, 4H, C*H*Me$_2$), 1.60 (d, J = 6.7 Hz, 12H, CHMe_2), 1.42 (d, J = 6.7 Hz, 12H, CHMe_2), 0.93 (s, 18H, CMe_3). ^{13}C NMR (75.47 MHz, C_6D_6): δ 151.9, 141.4, 125.5, 124.0, 67.3, 36.3, 29.0, 28.9, 26.5, 24.7. Anal.: Calc. for $C_{34}H_{56}Cl_2N_2Ti$: C, 66.77; H, 9.23; N, 4.58%. Found: C, 66.69; H, 9.40; N, 4.84%.

General procedure for the synthesis of [M(L^2)$_2$Cl$_2$] [M = Zr (13), Hf (14)].

A solution of LiL^2(thf)$_2$ in toluene (20 ml) was added to a slurry of MCl_4 in the same solvent (15 ml) at 0 °C. The reaction mixture was stirred at room temperature for 1 d. All the volatiles were removed *in vacuo*. The resulting residue was redissolved toluene, filtered and then concentrated to *ca.* 5 ml. The desired products were obtained as a crystalline solid at room temperature.

Synthesis of $[Zr(L^2)_2Cl_2]$ (13).

$ZrCl_4$: 0.49 g, 2.09 mmol; $LiL^2(thf)_2$: 1.66 g, 4.18 mmol. Product: pale yellow, block-shaped crystals. Yield: 0.83 g, 1.27 mmol, 61%. M.p.: 214–219 °C. ^1H NMR (300.13 MHz, C_6D_6): δ 7.25–7.22 (m, 2H, *p*–Ar*H*), 7.17–7.15 (m, 4H, *m*–Ar*H*), 4.00 (s, 4H, CH_2CMe_3), 3.88 (sept, *J* = 6.8 Hz, 4H, $CHMe_2$), 1.56 (d, *J* = 6.8 Hz, 12H, $CHMe_2$), 1.43 (d, *J* = 6.8 Hz, 12H, $CHMe_2$), 0.93 (s, 18H, CMe_3). ^{13}C NMR (75.47 MHz, C_6D_6): δ 144.6, 143.9, 127.3, 125.5, 63.6, 35.7, 28.9, 28.7, 26.7, 24.9. Anal.: Calc. for $C_{34}H_{56}Cl_2N_2Zr$: C, 62.35; H, 8.62; N, 4.28%. Found: C, 61.87; H, 8.79; N, 4.42%.

Synthesis of $[Hf(L^2)_2Cl_2]$ (14).

$HfCl_4$: 0.64 g, 2.0 mmol; $LiL^2(thf)_2$: 1.59 g, 4.0 mmol. Product: colorless, block-shaped crystals. Yield: 0.65 g, 0.88 mmol, 44%. M.p.: 222–227 °C. ^1H NMR (300.13 MHz, C_6D_6): δ 7.24-7.21 (m, 2H, *p*–Ar*H*), 7.20–7.16 (m, 4H, *m*–Ar*H*), 3.99 (s, 4H, CH_2CMe_3), 3.92 (sept, *J* = 6.8 Hz, 4H, $CHMe_2$), 1.54 (d, *J* = 6.8 Hz, 12H, $CHMe_2$), 1.45 (d, *J* = 6.8 Hz, 12H, $CHMe_2$), 0.94 (s, 18H, CMe_3). ^{13}C NMR (75.47 MHz, C_6D_6): δ 144.6, 144.4, 127.1, 125.5, 63.8, 36.0, 28.9, 28.8, 26.8, 24.8. Anal.: Calc. for $C_{34}H_{56}Cl_2N_2Hf$: C, 55.05; H, 7.60; N, 3.77%. Found: C, 54.39; H, 7.70; N, 3.80%.

General procedure for the synthesis of $[M(L^2)_2(NMe_2)_2]$ [M = Zr (15), Hf (16)].

To a slurry of $LiNMe_2$ in toluene (10 ml) at 0 °C was added a solution of $[M(L^2)_2Cl_2]$ in toluene (20 ml). The reaction mixture was stirred at room temperature for 1 d, filtered and then concentrated to *ca*. 5ml. Standing the solution at room temperature yielded the desired products as colorless, block-shaped crystals.

Synthesis of $[Zr(L^2)_2(NMe_2)_2]$ (15).

$[Zr(L^2)_2Cl_2]$: 1.44 g, 2.19 mmol; $LiNMe_2$: 0.23 g, 4.51 mmol. Yield: 1.09 g, 1.62 mmol, 74%. M.p.: 238–240 °C (dec.). ^{1}H NMR (300.13 MHz, C_6D_6): δ 7.21-7.10 (m, 6H, Ar), 3.88 (s, 4H, CH_2CMe_3), 3.85 (sept, J = 6.8 Hz, 8H, $CHMe_2$), 2.69 (s, 12H, NMe_2), 1.51 (d, J = 6.8 Hz, 12H, $CHMe_2$), 1.33 (d, J = 6.8 Hz, 12H, $CHMe_2$), 0.99 (s, 18H, CMe_3). ^{13}C NMR (75.47 MHz, C_6D_6): δ 148.7, 144.0, 124.6, 124.3, 64.0, 42.1, 35.2, 29.2, 28.5, 25.7, 25.3. Anal.: Calc. for $C_{38}H_{68}N_4Zr$: C, 67.90; H, 10.20; N, 8.33%. Found: C, 67.84; H, 10.44; N, 8.61%.

Synthesis of $[Hf(L^2)_2(NMe_2)_2]$ (16).

$[Hf(L^2)_2Cl_2]$ (**6**): 1.25 g, 1.69 mmol; $LiNMe_2$: 0.17 g, 3.38 mmol. Yield: 0.60 g, 0.79 mmol, 47%. ^{1}H NMR (300.13 MHz, C_6D_6): δ 7.16-7.05 (m, 6H, Ar), 3.83 (sept, J = 6.8 Hz, 8H, $CHMe_2$), 3.80 (s, 8H, CH_2CMe_3), 2.67 (s, 12H, NMe_2), 1.46 (d, J = 6.8 Hz, 12H, $CHMe_2$), 1.29 (d, J = 6.8 Hz, 12H, $CHMe_2$), 0.93 (s, 18H, CMe_3). ^{13}C NMR (75.47 MHz, C_6D_6): δ 148.8, 144.5, 124.6, 124.5, 63.5, 41.8, 35.3, 29.2, 28.4, 25.8, 25.4. Anal.: Calc. for $C_{38}H_{68}N_4Hf$: C, 60.10; H, 9.02; N, 7.37%. Found: C, 60.01; H, 9.25; N, 7.48%.

General procedure for the synthesis of $[M(L^2)_2(NMe_2)(I)]$ [M = Zr (17), Hf (19)] and $[M(L^2)_2I_2]$ [M = Zr (18), Hf (20)].

Methyl iodide was slowly added to a solution of $[M(L^2)_2(NMe_2)_2]$ in toluene (35 ml) at 0 °C. The reaction mixture was stirred at room temperature for 1 d to give a pale yellow suspension. All the volatiles were removed *in vacuo* and the residue was extracted with hexane, filtered, and concentrated to *ca.* 5 ml. A crystalline solid was obtained upon standing the solution at room temperature.

Synthesis of $[Zr(L^2)_2(NMe_2)(I)]$ (17) and $[Zr(L^2)_2I_2]$ (18).

$[Zr(L^2)_2(NMe_2)_2]$ (**15**): 1.18 g, 1.76 mmol; MeI: 0.85 ml, 13.7 mmol. Yellow, block-shaped crystals of **18** were isolated as the major product. Yield: 0.80 g, 0.95 mmol, 54%. M.p.: 228–230 °C. ^{1}H NMR (300.13 MHz, C_6D_6): δ 7.14–7.06 (m, 6H, *m*–Ar*H*), 3.95 (s, 4H, C*H*$_2$CMe$_3$), 3.91 (sept, *J* = 6.8, 4H, C*H*Me$_2$), 1.52 (d, *J* = 6.8 Hz, 12H, CH*Me*$_2$), 1.36 (d, 12H, *J* = 6.8 Hz, CH*Me*$_2$), 0.86 (s, 18H, C*Me*$_3$). ^{13}C NMR (75.47 MHz, C_6D_6K): δ 145.3, 143.1, 127.5, 125.7, 61.4, 35.7, 29.1, 28.9, 26.7, 25.3. Anal.: Calc. for $C_{34}H_{56}I_2N_2Zr$: C, 48.74; H, 6.74; N, 3.34%. Found: C, 48.59; H, 6.83; N, 4.25%.* Complex **17** was isolated as colorless crystals from the second batch of the crystalline product. Yield: 0.06 g, 0.08 mmol, 5%. M.p.: 210–211 °C (dec.). ^{1}H NMR (300.13 MHz, C_6D_6): δ 7.26-7.14 (m, 6H, Ar), 4.42 (sept, *J* = 6.6 Hz, 2H, C*H*Me$_2$), 4.19 (d, *J* = 12 Hz, 2H, C*H*$_2$CMe$_3$), 4.08 (d, *J* = 12 Hz, 2H, C*H*$_2$CMe$_3$), 3.63 (sept, *J* = 6.0 Hz, 2H, C*H*Me$_2$), 2.29 (s, 6H, N*Me*$_2$), 1.54 (d, *J* = 6.0 Hz, 6H, CH*Me*$_2$), 1.52 (d, *J* = 6.0 Hz, 6H, CH*Me*$_2$), 1.45 (d, *J* = 6.0 Hz, 6H, CH*Me*$_2$), 1.24 (d, *J* = 6.0 Hz, 6H, CH*Me*$_2$), 1.05 (s, 18H, C*Me*$_3$). ^{13}C NMR (75.47 MHz, C_6D_6): δ 144.8, 144.6, 144.4, 126.5, 126.1, 125.0, 66.5, 41.4, 35.7, 29.0, 28.8, 28.6, 27.4, 26.1, 25.7, 25.3 (CH*Me*$_2$).

Synthesis of $[Hf(L^2)_2(NMe_2)(I)]$ (19) and $Hf(L^2)_2I_2$ (20).

$[Hf(L^2)_2(NMe_2)_2]$ (**16**): 0.99 g, 1.31 mmol; MeI: 0.85 ml, 13.65 mmol. The first batch of the crystals obtained was found to be complex **19** (colorless crystals). Yield: 0.487 g, 0.58 mmol, 44%. M.p.: 200–205 °C. ^{1}H NMR (300.13 MHz, C_6D_6): δ 7.24-7.14 (m, 6H, Ar), 4.34 (sept, *J* = 6.8 Hz, 2H, C*H*Me$_2$), 4.11 (d, *J* = 14.3 Hz, 2H, C*H*$_2$CMe$_3$), 3.97 (d, *J* = 14.3 Hz, 2H, C*H*$_2$CMe$_3$), 3.74 (sept, *J* = 6.8 Hz, 2H, C*H*Me$_2$), 2.36 (s, 6H, N*Me*$_2$), 1.52 (d, *J* = 6.8 Hz, 6H, CH*Me*$_2$), 1.48 (d, *J* = 6.8 Hz, 6H, CH*Me*$_2$),

* Attempts to obtain better analytical data for this compound were not successful.

1.45 (d, J = 6.8 Hz, 6H, CHMe_2), 1.27 (d, J = 6.8 Hz, 6H, CHMe_2), 1.02 (s, 18H, CMe_3). ^{13}C NMR (75.47 MHz, C_6D_6): δ 145.0, 144.8, 128.6, 126.3, 126.0, 124.9, 65.4, 40.4, 35.8, 29.1, 28.7, 28.6, 27.1, 26.3, 25.7, 25.4. Anal.: Calc. for $C_{36}H_{62}IN_3Hf$: C, 51.34; H, 7.42; N, 4.99%. Found: C, 50.77; H, 7.54; N, 5.05%. The second batch of the product contained yellow crystals, which were confirmed to be **20**. Yield: 0.062 g, 0.07 mmol, 5%. ^{1}H NMR (300.13 MHz, C_6D_6): δ 7.16–7.09 (m, 6H, Ar), 3.99–3.90 (s and sept, 8H, CH_2CMe$_3$ and CHMe$_2$), 1.53 (d, J = 6.8 Hz, 12H, CHMe_2), 1.38 (d, 12H, J = 6.8 Hz, CHMe_2), 0.88 (s, 18H, CMe_3). ^{13}C NMR (75.47 MHz, C_6D_6K): δ 144.1, 128.6, 127.3, 125.7, 62.2, 35.6, 29.13, 29.07, 26.8, 25.3.

General procedure for the synthesis of [M(L^2)$_2$Me$_2$] [M = Zr (21), Hf (22)].

A solution of LiMe in diethyl ether (1.6 M) was added to a solution of [M(L^2)$_2$Cl$_2$] in toluene (35 ml) at 0 °C. The reaction mixture turned immediately to a pale yellow suspension. Stirring was continued at room temperature for 1 d, yielding a dark green solution. All the volatiles were removed *in vacuo* and the resulting dark green solid residue was extracted with hexane (20 ml x1). The solution was filtered and then concentrated to *ca.* 5 ml to give the *title* compound as colorless crystals.

Synthesis of [Zr(L^2)$_2$Me$_2$] (21).

[Zr(L^2)$_2$Cl$_2$] (13): 1.50 g, 2.29 mmol; LiMe: 1.6 M in Et_2O, 2.9 ml, 4.64 mmol. Yield: 0.93 g, 1.51 mmol, 66%. M.p.: 160–164 °C. ^{1}H NMR (300.13 MHz, C_6D_6): δ 7.19 (br, 2H, *p*–Ar*H*), 7.17–7.15 (m, 4H, *m*–Ar*H*), 3.90 (sept, J = 6.8 Hz, 4H, CHMe$_2$), 3.72 (s 4H, CH_2CMe$_3$), 1.40 (d, J = 6.8 Hz, 24H, CHMe_2), 0.91 (s, 18H, CMe_3), 0.63 (s, 6H, Me). ^{13}C NMR (75.47 MHz, C_6D_6): δ 145.4, 144.6, 126.3, 125.3, 62.7, 43.9, 35.3, 28.9, 28.3, 26.2, 25.6. Anal.: Calc. for $C_{36}H_{62}N_2Zr$: C, 70.41; H, 10.18; N, 4.56%. Found: C, 69.96; H, 10.36; N, 4.92%.

Synthesis of $[Hf(L^2)_2Me_2]$ (22).

$[Hf(L^2)_2Cl_2]$ (**14**): 1.56 g, 2.10 mmol; LiMe: 1.6 M in Et_2O, 2.7 ml, 4.32 mmol. Yield: 0.959 g, 1.37 mmol, 65%. M.p.: 182–183 °C. ^1H NMR (300.13 MHz, C_6D_6): δ 7.19-7.16 (m, 6H, Ar), 3.95 (sept, *J* = 6.9 Hz, 4H, C*H*Me_2), 3.66 (s 4H, C*H*$_2$CMe_3), 1.43 (d, *J* = 6.9 Hz, 12H, CH*Me*$_2$), 1.39 (d, *J* = 6.9 Hz, 12H, CH*Me*$_2$), 0.90 (s, 18H, C*Me*$_3$), 0.48 (s, 6H, *Me*). ^{13}C NMR (75.47 MHz, C_6D_6): δ 145.3, 145.1, 126.0, 125.2, 62.1, 56.2, 35.6, 28.9, 28.4, 26.7, 25.2. Anal.: Calc. for $C_{36}H_{62}N_2Hf$: C, 61.65; H, 8.91; N, 3.99%. Found: C, 60.59; H, 9.11; N, 4.36%.*

Synthesis of $[Ti(L^1)_2(\mu\text{–}Cl)_2Li(tmeda)]$ (23).

A solution of $TiCl_3(thf)_3$ in thf was freshly prepared by stirring $TiCl_3$ (0.38 g, 2.52 mmol) in thf (15 ml) for 0.5 h. A thf solution of $[LiL^1(tmeda)]$ (1.48 g, 4.71 mmol) was slowly added at 0 °C and the reaction mixture was stirred at room temperature for 1 d, yielding a clear olive brown solution was obtained. All the volatiles were removed by vacuum. The solid residue was then extracted with toluene (20 ml x1). The toluene solution was filtered and concentrated to *ca.* 5 ml. The *title* compound was obtained as yellowish-green crystals upon standing the solution at room temperature overnight. Yield: 0.57 g, 0.92 mmol, 39%. M.p.: 186–189 °C. Anal.: Calc. for $C_{32}H_{56}Cl_2LiN_4Ti$: C, 61.74; H, 9.07; N, 9.00%. Found: C, 61.31; H, 9.62; N, 9.27%.

Synthesis of $[Li(tmeda)_2]^+[Ti(L^2)_2Cl_2]^-$ (24).

$TiCl_3$ (0.48 g, 3.09 mmol) was dissolved in thf (15 ml) to give a bright blue solution of $TiCl_3(thf)_3$. A solution of $[LiL^2(tmeda)]$ (2.21 g, 5.98 mmol) in thf (10 ml)

---

* Attempts to obtain better analytical data for this compound were not successful.

was added. The reaction mixture was stirred at room temperature for 1 d. All the volatiles were removed in *vacuo* and the residue was extracted with toluene (20 ml x1). The toluene solution was then filtered and concentrated to *ca.* 5 ml. Standing the solution at room temperature overnight yielded complex **24** as yellowish-green crystals. Yield: 0.72 g, 0.85 mmol, 28%. M.p.: 184–185 (dec.). Anal.: Calc. for $C_{46}H_{88}Cl_2LiN_6Ti$: C, 64.93; H, 10.42; N, 9.87%. Found: C, 64.12; H, 10.55; N, 9.77%.

References for Chapter 2

1. Lappert, M. F.; Power, P. P.; Sanger, A. R.; Srivastava, R. C. *Metal and Metalloid Amides*, Horwood-Wiley, Chichester, **1980**.
2. Frankland, E. *Proc. Roy. Soc.* **1856–7**, *8*, 502–506.
3. (a) Putzer, M. A.; Neumüller, B.; Dehnicke, K. *Z. Anorg. Allg. Chem.* **1998**, *624*, 929–930.
   (b) Dermer, O. C.; Fernelius, W. C. K. *Z. Anorg. Allg. Chem.* **1934**, *221*, 83–96.
4. (a) Polamo, M.; Mutikainen, I.; Leskelä, M. *Z. Kristallogr.* **1996**, *211*, 641–642.
   (b) Polamo, M.; Mutikainen, I.; Leskelä, M. *Acta Cryst.* **1996**, *C52*, 1348–1350.
5. (a) Nomura, K.; Fujii, K. *Organometallics* **2002**, *21*, 3042–3049.
   (b) Shah, S. A. A.; Dorn, H.; Voigt, A.; Roesky, H. W.; Parisini, E.; Schmidt, H. –G.; Noltemeyer, M. *Organometallics* **1996**, *15*, 3176–3181.
   (c) Shah, S. A. A.; Dorn, H.; Roesky, H. W.; Parisini, E.; Schmidt, H. –G.; Noltemeyer, M. *J. Chem. Soc., Dalton Trans.* **1996**, 4143–4146.
6. (a) Johnson, A. R.; Wanandi, P. W.; Cummins, C. C.; Davis, W. M. *Organometallics* **1994**, *13*, 2907–2909.
   (b) Johnson, A. R.; Davis, W. M.; Cummins, C. C. *Organometallics* **1996**, *15*, 3825–3835.
7. Mokuolu, Q. F.; Duckmanton, P. A.; Blake, A. J.; Wilson, C.; Love, J. B. *Organometallics* **2003**, *22*, 4387–4389.
8. Kasani, A.; Gambarotta, S.; Bensimon, C. *Can. J. Chem.* **1997**, *75*, 1494–1499.
9. (a) Mendiratta, A.; Cummins, C. C.; Cotton, F. A.; Ibragimov, S. A.; Murillo, C. A.; Villagrán, D. *Inorg. Chem.* **2006**, *45*, 4328–4330.
   (b) Peters, J. C.; Cherry, J. –P.; F.; Thomas, J. C.; Baraldo, L.; Mindiola, D. J.; Davis, W. M.; Cummins, C. C. *J. Am. Chem. Soc.* **1999**, *121*, 10053–10067.
   (c) Wanandi, P. W.; Davis, W. M.; Cummins, C. C. *J. Am. Chem. Soc.* **1995**, *117*, 2110–2111.
   (d) Peters, J. C.; Johnson, A. R.; Odom, A. L.; Wanandi, P. W.; Davis, W. M.; Cummins, C. C. *J. Am. Chem. Soc.* **1996**, *118*, 10175–10188.
10. (a) Au–Yeung, H. Y.; Lam, C. H.; Lam, C. –K.; Wong, W. –Y.; Lee, H. K. *Inorg. Chem.* **2007**, *46*, 7695–7697.
    (b) Au-Yeung, H. Y. *M. Phil. Thesis*, The Chinese University of Hong Kong, 2006.
11. (a) Giesbrecht, G. R.; Gordon, J. C.; Clark, D. L.; Hijar, C. A.; Scott, B. L.; Watkin, J. G. *Polyhedron* **2003**, *22*, 153–163.
    (b) Wu, Z.; Diminnie, J. B.; Xue, Z. –L. *J. Am. Chem. Soc.* **1999**, *121*, 4300–4301.
    (c) Herrmann, W. A.; Huber, N. W.; Behm, J. *Chem. Ber.* **1992**, *125*, 1405–1407.
    (d) Qiu, H. Q.; Cai, H.; Woods, J. B.; Wu, Z.; Chen, T.; Tu, X.; Xue, Z. –L. *Organometallics* **2005**, *24*, 4190–4197.
12. (a) Yu, X.; Chen, S. –J.; Wang, X.; Chen, X. –T.; Xue, Z. –L. *Organometallics* **2009**, *28*, 4269–4275.

(b) Davie, M. E.; Foerster, T.; Parsons, S.; Pulham, C.; Rankin, D. W. H.; Smart, B. A. *Polyhedron* **2006**, *25*, 923–929.

(c) Lee, W. –Y.; Liang, L. –C. *Inorg. Chem.* **2008**, *47*, 3298–3306.

(d) Yu, X.; Bi, S.; Guzei, L. A.; Lin, Z.; Xue, Z. –L. *Inorg. Chem.* **2004**, *43*, 7111–7119.

13. (a) Scollard, J. D.; McConville, D. H.; Vittal, J. J. *Organometallics* **1995**, *14*, 5478-5480.

(b) Scollard, J. D.; McConville, D. H.; Vittal, J. J. *Organometallics* **1997**, *16*, 4415-4420.

(c) Hill, M. S.; Hitchcock, P. B.; *Organometallics* **2002**, *21*, 3258-3262.

14. (a) King, W. A.; Bella, S. D.; Gulino, A.; Lanza, G.; Fragalà, I. L.; Stern, C. L.; Marks, T. J. *J. Am. Chem. Soc.* **1999**, *121*, 355–366.

(b) Lehn, J. –S. M.; Hoffmann, D. M. *Inorg. Chem.* **2002**, *41*, 4063–4067.

(c) Benito–Garagorri, D.; Bernskoetter, W. H.; Lobkovsky, E.; Chirik, P. J. *Organometallics* **2009**, *28*, 4807–4813.

15. Moss, J. R. *J. Mol. Catal. A: Chem.* **1996**, *107*, 169–174.

16. (a) Fryzuk, M. D.; Corkin, J. R.; Patrick, B. O. *Can. J. Chem.* **2003**, *81*, 1376–1387.

(b) Mountford, A. J.; Clegg, W.; Coles, S. J.; Harrington, R. W.; Horton, P. N.; Humphrey, S. M.; Hursthouse, M. B.; Wright, J. A.; Lancaster, S. J. *Chem. Eur. J.* **2007**, *13*, 4535–4547.

Chapter 3

Group 4 Metal Complexes Supported by an Unsymmetrical Benzamidinate Ligand

The first part of this chapter gives an overview on Group 4 metal amidinate complexes. The second part of this chapter covers the results of our work on Group 4 metal amidinates derived from the $[PhC(NC_6H_3Pr^i_2\text{–}2,6)(NSiMe_3)]^-$ *(*L^3*) ligand. Ligand substitution reactions of complex* $[Zr(L^3)_2Cl_2]$ *with LiMe and* $PhCH_2MgCl$ *are also reported.*

Introduction

An Overview on Group 4 Metal Amidinates

The recent development in the chemistry of Group 4 metal amidinate complexes has been motivated mainly by a search for new ligand systems as alternatives for cyclopentadienyl anions.[1] The majority of work on Group 4 metal amidinates has been focused on their potential applications in catalysis. Ti(IV), Zr(IV) and Hf(IV) complexes supported by the $[MeC(NCy)_2]^-$ and $[PhC(NSiMe_3)_2]^-$ ligands (Chart 3–1) were found to be active catalysts for ethylene polymerization.[2,3a–c] In a study on polymerization of styrene, the use of Ti(IV) mono(amidinate) complexes supported by the $[PhC(NSiMe_3)_2]^-$ ligand (Chart 3–2) has led to syndiotactic polystyrene.[3a]

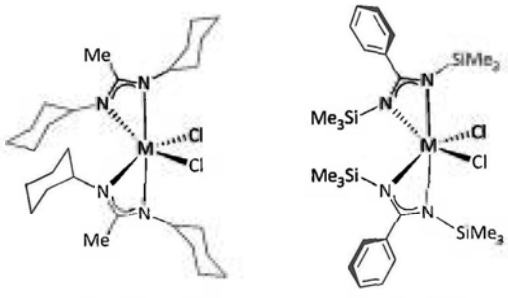

M = Ti, Zr, Hf
Richeson *et al.*[2]

M = Ti, Zr
Rausch *et al.*[3a]

Chart 3–1

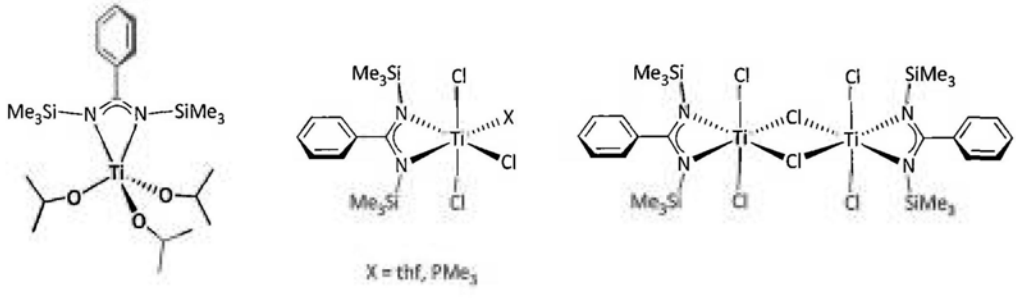

Rausch *et al.*[3a]

Chart 3–2

A rich reduction chemistry has also been demonstrated by Ti(IV) complexes derived from the $[PhC(NSiMe_3)_2]^-$ ligand (Scheme 3–1). Reduction of $[Ti\{PhC(NSiMe_3)_2\}_2Cl_2]$ with lithium metal in the presence of tmeda led to the heterobimetallic Ti(III) complex $[Ti\{PhC(NSiMe_3)_2\}_2(\mu\text{–}Cl)_2Li(tmeda)]$.[4] On the other hand, reduction of $[Ti\{PhC(NSiMe_3)_2\}_2Cl_2]$ with sodium amalgam in toluene gave the mononuclear Ti(III) complex $[Ti\{PhC(NSiMe_3)_2\}_2Cl]$.[5] Further reduction of $[Ti\{PhC(NSiMe_3)_2\}_2Cl_2]$ with sodium amalgam lead to the N_2 activated product $[Ti\{PhC(NSiMe_3)_2\}_2]_2(\mu\text{–}N_2)$.[5] The same reaction under a CO atmosphere for two days gave the CO activated product $[Ti\{PhC(NSiMe_3)_2\}_2]_2(\mu\text{–}O)$.[5]

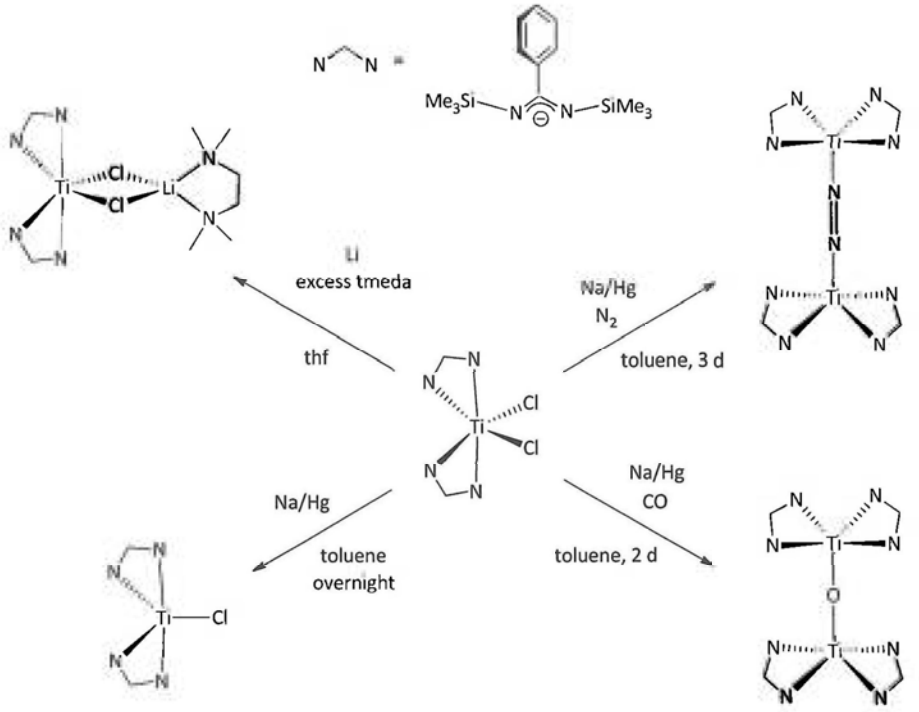

Scheme 3–1

The Zr(IV) complex $[Zr\{PhC(NSiMe_3)_2\}_2Cl_2]$ has been proven to be an excellent starting material for the preparation of a wide range of alkyl, amide and

chalcogenide derivatives (Scheme 3–2).[3c,d]

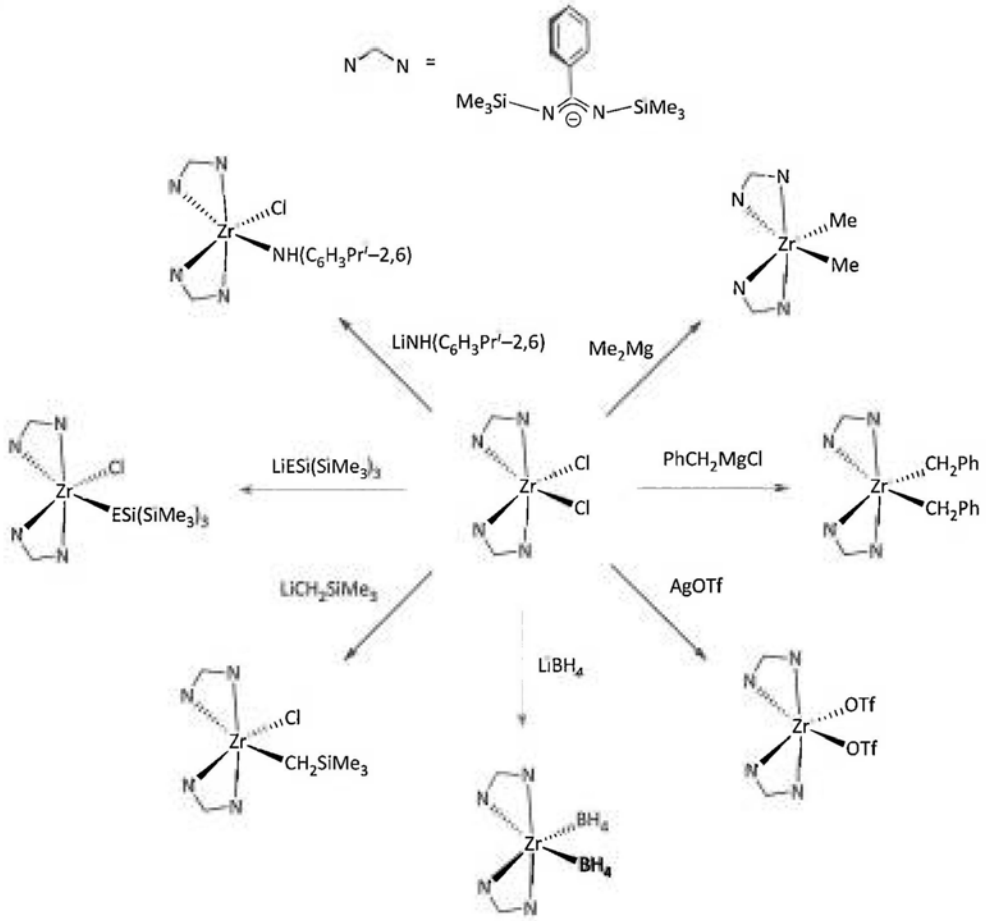

Scheme 3–2

Structural variation as a result of ligand modification has also been reported in Zr(IV) bis(amidinate) complexes of the type $[ZrL_2Cl_2]$ (L = $[PhC(NC_6H_3Me_2–2,6)(NC_6H_3Pr^i_2–2,6)]^-$, $[PhC(NC_6H_3Pr^i_2–2,6)_2]^-$). The two amidinate ligands in $[Zr\{PhC(NC_6H_3Me_2–2,6)(NC_6H_3Pr^i_2–2,6)\}_2Cl_2]$ coordinated to the Zr(IV) center in a *cis* manner, whereas those in the closely related $[Zr\{PhC(NC_6H_3Pr^i_2–2,6)_2\}_2Cl_2]$ are *trans* to each other (Chart 3–5).[6] The

unprecedented *trans* geometry in the latter complex was attributed to a larger steric bulkiness of the $[PhC(NC_6H_3Pr^i_2{-}2,6)_2]^-$ ligand.

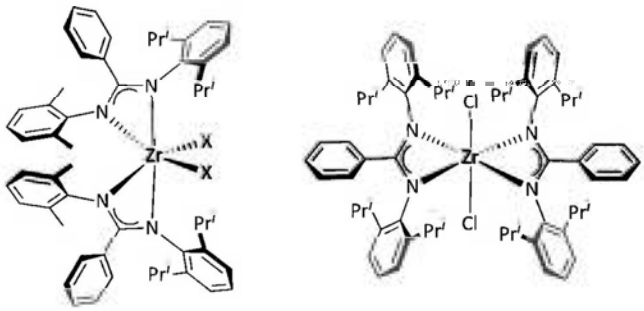

Hessen *et al.*[4]

Chart 3–3

Results and Discussion

Group 4 Metal Complexes of the $[PhC(NC_6H_3Pr^i_2\text{–}2,6)(NSiMe_3)]^-$ Ligand

A. Lithium and Potassium Derivatives of the $[PhC(NC_6H_3Pr^i_2\text{–}2,6)(NSiMe_3)]^-$ (L^3) Ligand

Lithium salt (**28**) and potassium salt (**30**) of the $[PhC(NC_6H_3Pr^i_2\text{–}2,6)(NSiMe_3)]^-$ (L^3) ligand were prepared according to procedures developed previously by our group with minor modifications.[7] As outlined in Scheme 3–3, lithiation of $H_2N(C_6H_3Pr^i_2\text{–}2,6)$ followed by quenching of the reaction mixture with Me_3SiCl gave the *N*-silylated aniline $HN(C_6H_3Pr^i_2\text{–}2,6)(SiMe_3)$ (**25**) in 78% yield.[8]

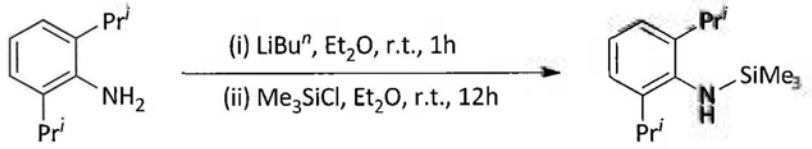

25 78%

Scheme 3–3

The synthesis of lithium salts **28** and **29** is summarized in Scheme 3–4. Treatment of compound **25** with $LiBu^n$ in the presence of tmeda gave lithium amide **26**. Subsequent reaction of compound **26** with PhCN afforded $[LiL^3(tmeda)]$ (**28**) as colorless crystals in 86% yield.[7] The reaction of compound **26** with PhCN involves an insertion of the *N*-silylated amide $[N(C_6H_3Pr^i_2\text{–}2,6)(SiMe_3)]^-$ into the C≡N functionality, followed by a 1,3–silyl migration.

On the other hand, lithiation of **25** with $LiBu^n$ in thf, followed by addition of

PhCN yielded the new lithium amidinate, $LiL^3(thf)_2$ (**29**), as colorless crystals in 68% yield (Scheme 3–4). Complex **29** is readily soluble in thf. It is sensitive to air and moisture. It decomposed to a brown intractable oil upon exposure to air.

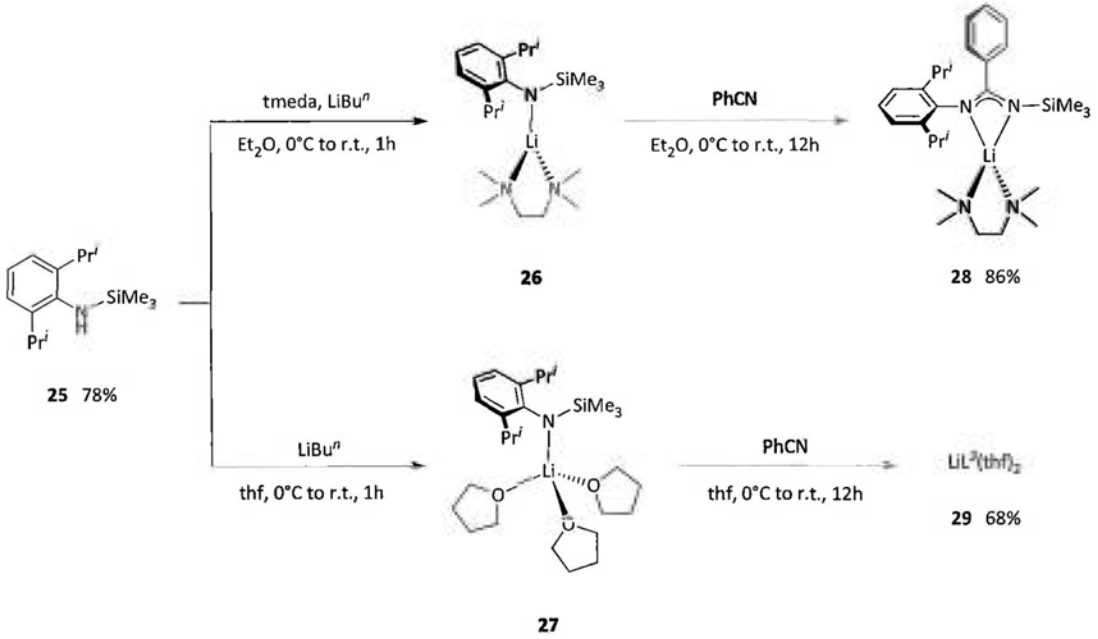

Scheme 3–4

Subsequent reaction of complex **28** with an equal molar amount of $KOBu^t$ afforded the corresponding potassium salt $[KL^3]_\infty$ (**30**),[7] which was isolated as colorless crystals in 65% yield (Scheme 3–5).

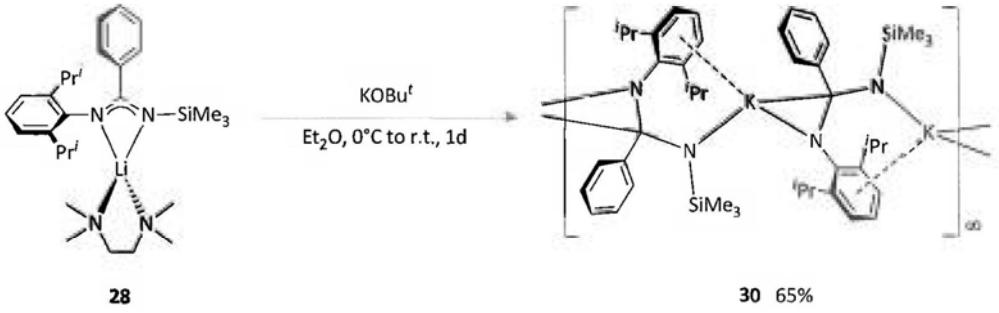

Scheme 3–5

Physical Characterization of $LiL^3(thf)_2$ (**29**)

Complex **29** melted under nitrogen at 146–151 °C. Results of elemental analysis were consistent with its empirical formula. The ^1H and ^{13}C NMR spectra of compound **29** are shown in Figures A2–31 and A2–32 (Appendix 2), respectively. The spectra showed one set of resonance signals assignable to one L^3 ligand and two thf molecules.

B. Bis(amidinato) Ti(III) Chloride and Methyl Complexes

Treatment of two equivalents of lithium amidinate **29** with a solution of freshly prepared $TiCl_3(thf)_3$ in thf gave the red crystalline Ti(III) bis(amidinate) chloride complex $[Ti(L^3)_2Cl]$ (**31**) in 51% yield (Scheme 3–6). Complex **31** is readily soluble in hexane and thf. In addition, it is highly sensitive to air and moisture. It turned quickly to a white solid upon exposure to air.

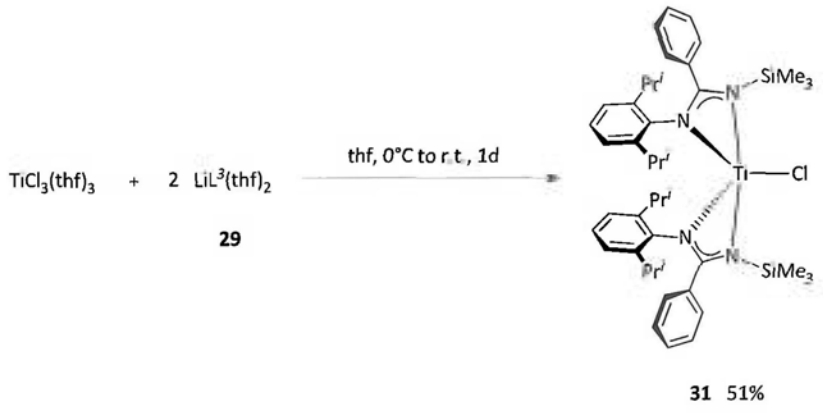

Scheme 3–6

The presence of a chloride ligand in complex **31** allows further functionalization of the compound by metathetical reactions. The Ti(III) bis(amidinate) methyl complex $[Ti(L^3)_2Me]$ (**32**) was synthesized by alkylation of **31** with LiMe in hexane

(Scheme 3–7).

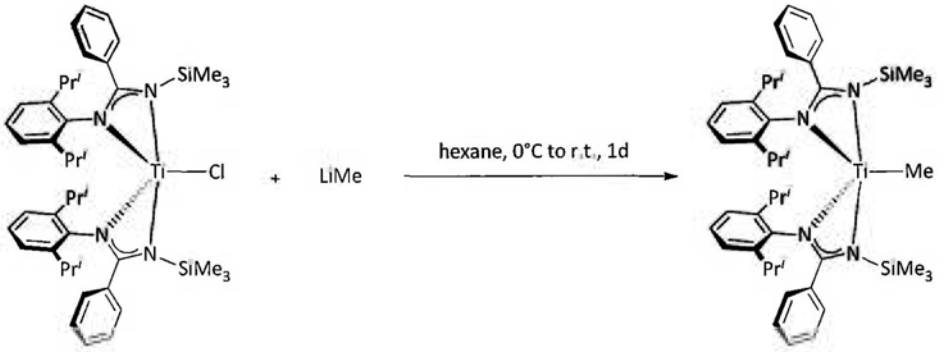

31 **32** 69%

Scheme 3–7

Compound **32** was isolated as deep red crystals in a satisfactory yield of 69%. It is highly soluble in hexane and very sensitive to air and moisture. The methyl complex turned immediately to a white powder when exposed to air.

Physical Characterization of Complexes **31** and **32**

Table 3–1 summarizes some of the physical properties of complexes **31** and **32**. Results of elemental analysis obtained for the two complexes were consistent with their formulation as shown in Schemes 3–6 and 3–7. The molecular structures of complexes **31** and **32** were elucidated by X-ray crystallography (*vide infra*).

Table 3–1 Some physical properties of compounds **31** and **32**.

Compound	Appearance	M.p. (°C)
$[Ti(L^3)_2Cl]$ (**31**)	Red crystals	190–195 (dec.)
$[Ti(L^3)_2Me]$ (**32**)	Deep red crystals	198–201

Crystal Structures of Complexes **31** and **32**

Single crystals of complexes **31** and **32** were obtained from hexane and their solid-state structures were determined by X-ray diffraction studies. Selected crystallographic data are summarized in Appendix 3.

1. $[Ti(L^3)_2Cl]$ (**31**)

The molecular structure of complex **31** is shown in Figure 3–1. Selected bond lengths and angles of **31** are listed in Table 3–2. Complex **31** crystallizes in the monoclinic space group $P2_1/c$. There are two independent molecules in the asymmetric unit. The Ti(III) center is coordinated by two κ^2-bound L^3 ligands and one chloride ligand. The coordination geometry around the Ti(III) center can be described as distorted trigonal bipyramidal. The equatorial plane consists of N(1), N(3) and Cl(1), and N(1′), N(3′) and Cl(1′) (sum of bond angles = 360.1°), respectively, whereas the two axial positions are occupied by N(2) and N(4) [N(2)–Ti(1)–N(4) = 144.7(1)°], and N(2′) and N(4′) [N(2′)–Ti(1′)–N(4′) = 146.1(2)°].

The L^3 ligands in complex **31** bind to the Ti(III) center in an unsymmetrical manner. The Ti–N_{aryl} distances [2.045(5)–2.076(5) Å] are shorter than the corresponding Ti–N_{silyl} distances [2.137(5)–2.158(5) Å]. The unsymmetrical coordination mode of this type of ligands has been reported previously.[7,9] A delocalization of the anionic charge over the N–C–N moiety is observed, as indicated by the nearly identical C–N distances, which are shorter than the C–N single bond length (1.47 Å), but longer than the C=N double bond (1.29 Å).

The Ti–N distances of 2.045(5)–2.158(5) Å in complex **31** are comparable to

those of 2.051(3)–2.164(3) Å in the monomeric [Ti{PhC(NSiMe$_3$)$_2$}$_2$Cl].[5b] On the other hand, the Ti–Cl distances of 2.256(2) and 2.260(2) Å in **31** are shorter than that of 2.328(1) Å in [Ti{PhC(NSiMe$_3$)$_2$}$_2$Cl].[5b] The N_{aryl}–Ti–N_{silyl} bite angles in **31** fall within the range of 63.2(2)–64.3(1)°, which are close to those of 64.3(1)–65.4(1) Å in [Ti{PhC(NSiMe$_3$)$_2$}$_2$Cl].[5b]

2. [Ti(L^3)$_2$Me] (**32**)

The molecular structure of the methyl derivative **32** is shown in Figure 3–2 with selected bond lengths and angles listed in Table 3–3. Complex **32** crystallizes in the triclinic space group $P\bar{1}$. The molecular structure of **32** is similar to that of complex **31**. The observed Ti–N distances of 2.03(2)–2.20(1) Å in **32** are close to those of 2.045(5)–2.158(5) Å in **31**. They are also comparable to those in the five-coordinate [Ti{PhC(NSiMe$_3$)$_2$}$_2$Me] [2.095(3)–2.164(3) Å][5a] and [Ti{PhC(NSiMe$_3$)$_2$}$_2$Cl] [2.051(3)–2.164(3) Å].[5b] The Ti–Me distances of 2.11(4) and 2.13(3) Å in **32** are similar to that of 2.120(5) Å in [Ti{PhC(NSiMe$_3$)$_2$}$_2$Me].[5a] The N_{aryl}–Ti–N_{silyl} bite angles in complex **32** [62.6(5)–65.9(5)°] are close to those reported for [Ti{PhC(NSiMe$_3$)$_2$}$_2$Cl] [64.3(1)–65.4(1)°].[5b]

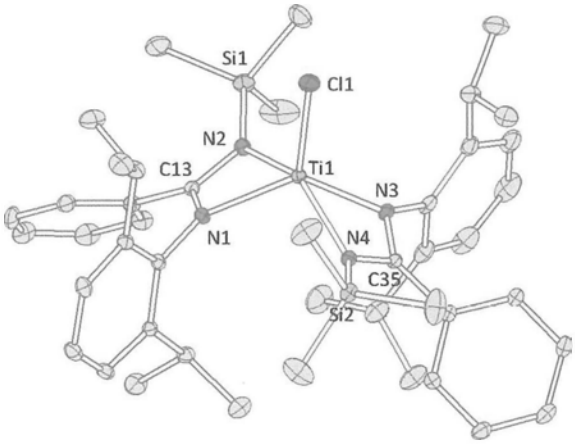

Figure 3–1 Molecular structure of $[Ti(L^3)_2Cl]$ (**31**).

Only one of the two independent molecules in the asymmetric unit is shown.

Table 3–2 Selected bond lengths (Å) and angles (deg.) for compound **31**.

$[Ti(L^3)_2Cl]$ (**31**)			
Ti(1)–N(1)	2.065(5)	Ti(1)–N(2)	2.137(5)
Ti(1)–N(3)	2.075(5)	Ti(1)–N(4)	2.152(5)
Ti(1)–Cl(1)	2.260(2)	N(1)–C(13)	1.349(7)
N(2)–C(13)	1.343(8)	N(3)–C(35)	1.346(7)
N(4)–C(35)	1.336(7)		
Ti(1')–N(1')	2.045(5)	Ti(1')–N(2')	2.158(5)
Ti(1')–N(3')	2.076(5)	Ti(1')–N(4')	2.152(6)
Ti(1')–Cl(1')	2.256(2)	N(1')–C(13')	1.334(8)
N(2')–C(13')	1.326(7)	N(3')–C(35')	1.320(8)
N(4')–C(35')	1.337(8)		
N(1)–Ti(1)–N(2)	64.3(1)	N(3)–Ti(1)–N(4)	63.7(2)
Cl(1)–Ti(1)–N(1)	115.7(1)	Cl(1)–Ti(1)–N(2)	107.3(1)
Cl(1)–Ti(1)–N(3)	116.8(1)	Cl(1)–Ti(1)–N(4)	108.0(1)
N(1)–Ti(1)–N(3)	127.6(2)	N(2)–Ti(1)–N(4)	144.7(1)
N(1')–Ti(1')–N(2')	63.9(2)	N(3')–Ti(1')–N(4')	63.2(2)
Cl(1')–Ti(1')–N(1')	113.9(1)	Cl(1')–Ti(1')–N(2')	107.7(1)
Cl(1')–Ti(1')–N(3')	118.0(1)	Cl(1')–Ti(1')–N(4')	106.2(1)
N(1')–Ti(1')–N(3')	128.2(2)	N(2')–Ti(1')–N(4')	146.1(2)

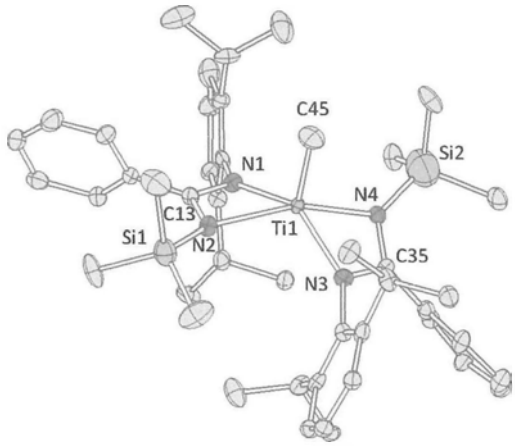

Figure 3–2 Molecular structure of [Ti(L^3)$_2$Me] (**32**).

Table 3–3 Selected bond lengths (Å) and angles (deg.) for compound **32**.

[Ti(L^3)$_2$Me] (**32**)			
Ti(1)–N(1)	2.18(1)	Ti(1)–N(2)	2.20(1)
Ti(1)–N(3)	2.03(2)	Ti(1)–N(4)	2.17(1)
Ti(1)–C(45)	2.13(3)	N(1)–C(13)	1.35(1)
N(2)–C(13)	1.38(1)	N(3)–C(35)	1.41(3)
N(4)–C(35)	1.35(1)		
Ti(1')–N(1')	2.06(1)	Ti(1')–N(2')	2.07(1)
Ti(1')–N(3')	2.13(1)	Ti(1')–N(4')	2.14(3)
Ti(1')–C(45')	2.11(4)	N(1')–C(13')	1.33(2)
N(2')–C(13')	1.34(1)	N(3')–C(35')	1.28(2)
N(4')–C(35')	1.41(2)		
N(1)–Ti(1)–N(2)	64(1)	N(3)–Ti(1)–N(4)	65(1)
C(45)–Ti(1)–N(1)	112(1)	C(45)–Ti(1)–N(2)	99(1)
C(45)–Ti(1)–N(3)	112(1)	C(45)–Ti(1)–N(4)	107(1)
N(1)–Ti(1)–N(3)	135(1)	N(2)–Ti(1)–N(4)	155(1)
N(1')–Ti(1')–N(2')	66(1)	N(3')–Ti(1')–N(4')	63(1)
C(45')–Ti(1')–N(1')	114(1)	C(45')–Ti(1')–N(2')	98(1)
C(45')–Ti(1')–N(3')	110(1)	C(45')–Ti(1')–N(4')	99(1)
N(1')–Ti(1')–N(3')	136(1)	N(2')–Ti(1')–N(4')	163(1)

C. Ti(IV) Complex Derived from the L^3 Ligand

Attempts to prepare a Ti(IV) bis(amidinate) dichloride complex of the type $[Ti(L^3)_2Cl_2]$ by the reaction of $TiCl_4(thf)_2$ with two equivalents of $[LiL^3(tmeda)]$ (**28**) have led to a dark brown, very air sensitive crystalline product (**33**) (Scheme 3–8).

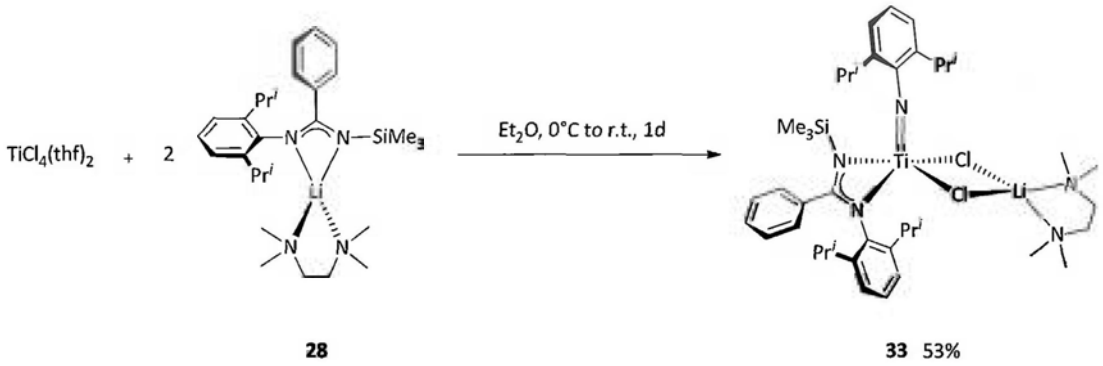

Scheme 3–8

A further investigation was carried out by reacting $TiCl_4(thf)_2$ with $[LiL^3(thf)_2]$ (**29**) (Scheme 3–9). It was anticipated that the absence of tmeda would lead to a product other than **33**. In our hands, an orange crystalline product was isolated in the latter reaction. NMR spectroscopic analysis of the crude product suggested that the product has a formulation similar to that of complex **33**, except the presence of a tmeda ligand. Unfortunately, further attempts to characterize the orange crystalline product have been unsuccessful as the crude product was found to be insoluble in common organic solvents such as hexane, diethyl ether and toluene.

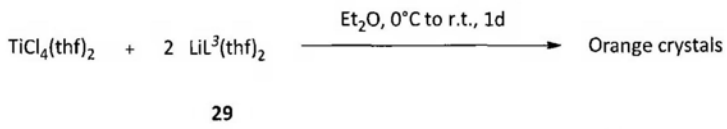

Scheme 3–9

Physical Characterization of Complex **33**

Complex **33** has been characterized by X-ray crystallography, elemental analysis, and NMR spectroscopy. Complex **33** was isolated as dark brown crystals which melted at 219–224 °C. Results of elemental analysis were consistent with the empirical formula of **33** as shown in Scheme 3–8.

NMR Spectra of Complex **33**

The ^{1}H and ^{13}C NMR spectra of complex **33** (Figures A2–33 and A2–34) showed resonance signals corresponding to one imido $[NC_6H_3Pr^{i}_2–2,6)]^{2-}$ ligand, one L^3 ligand, and one tmeda molecule. The isopropyl substituents of the imido $[NC_6H_3Pr^{i}_2–2,6)]^{2-}$ ligand occur as a septet at 4.87 ppm and a doublet at 1.52 ppm. The isopropyl substituents of the L^3 ligand are apparently chemically equivalent with the methine proton resonance at 3.78 ppm and the diastereotopic methyl group resonance at 1.12 and 1.29 ppm.

Crystal Structure of Complex **33**·$0.5C_6H_{14}$

The solid-state structure of the solvated complex **33**·$0.5C_6H_{14}$ is shown in Figure 3–3. Selected bond distances and angles are listed in Table 3–4. The solvated **33**·$0.5C_6H_{14}$ complex crystallizes in the triclinic space group $P\bar{1}$. The Ti(IV) center is coordinated by one κ^2-bound L^3 ligand, one terminal imido $[NC_6H_3Pr^{i}_2–2,6]^{2-}$ ligand and two chloride ligands. The two chloride ligands further coordinate to a lithium ion, which is, in turn, chelated by a tmeda molecule. The Ti(IV) center adopts a distorted trigonal bipyramidal geometry, with N(1), N(2) and Cl(2) forming the equatorial plane (sum of bond angles around Ti(IV) center =

358.3°), whereas N(3) and Cl(1) occupying the axial coordination positions [N(3)–Ti(1)–Cl(1) = 142.1(1)°].

Compared with other Ti(IV) imido complexes supported by amidinate ligands, the Ti–$N_{amidinate}$ distances of 2.116(3) and 2.123(3) Å in **33** are marginally shorter than those of 2.148(8)–2.156(8) Å in [Ti{PhC($NSiMe_3$)$_2$}$_2$($NCMe_3$)],[5b] and 2.114(4) and 2.288(4) Å in [Ti{PhC($NSiMe_3$)$_2$}($NC_6H_3Me_2$–2,6)Cl(py)$_2$].[10] The observed Ti–N_{imido} distance of 1.690(4) Å in **33** is slightly longer than that of 1.656(9) Å in [Ti{PhC($NSiMe_3$)$_2$}$_2$($NCMe_3$)][5b] but slightly shorter than that of 1.727(4) in [Ti{PhC($NSiMe_3$)$_2$}($NC_6H_3Me_2$–2,6)Cl(py)$_2$].[10] The differences in the Ti–N_{imido} distances in these complexes may be attributed to the steric environment around the metal centers. The imido ligand in **33** is bent, with a C(1)–N(1)–Ti(1) angle of 169.3(3)°. Similar bent structures have also been reported for [Ti{PhC($NSiMe_3$)$_2$}$_2$ ($NCMe_3$)] [C(1A)–N(5)–Ti = 166(1)°][5b] and [Ti{PhC($NSiMe_3$)$_2$}($NC_6H_3Me_2$–2,6)Cl(py)$_2$] [C(1)–N(1)–Ti(1) = 170.4(4)°],[10] respectively.

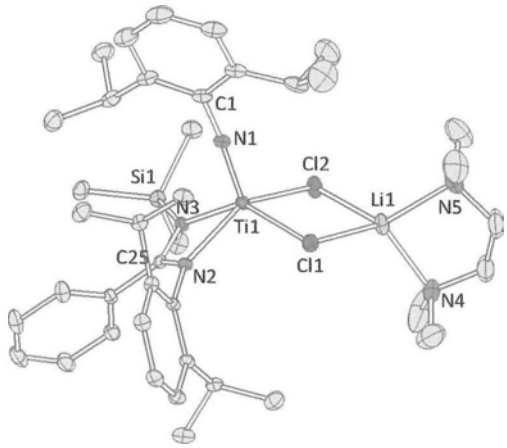

Figure 3–3 Molecular structure of $[Ti(L^3)(NC_6H_3Pr^i_2\text{–}2,6)(\mu\text{–}Cl)_2Li(tmeda)]\cdot 0.5C_6H_{14}$ (**33**$\cdot 0.5C_6H_{14}$). The solvated C_6H_{14} molecule is omitted for clarity.

Table 3–4 Selected bond lengths (Å) and angles (deg.) for compound **33**$\bullet 0.5C_6H_{14}$.

$[Ti(L^3)(NC_6H_3Pr^i_2\text{–}2,6)(\mu\text{–}Cl)_2Li(tmeda)]\bullet 0.5C_6H_{14}$ (**33**$\bullet 0.5C_6H_{14}$)			
Ti(1)–N(1)	1.690(4)	Li(1)–N(4)	2.07(1)
Ti(1)–N(2)	2.116(3)	Li(1)–N(5)	2.06(1)
Ti(1)–N(3)	2.123(3)	Li(1)–Cl(1)	2.367(9)
Ti(1)–Cl(1)	2.406(1)	Li(1)–Cl(2)	2.386(8)
Ti(1)–Cl(2)	2.396(1)	N(2)–C(25)	1.339(5)
		N(3)–C(25)	1.325(5)
N(2)–Ti(1)–N(3)	63.6(1)	Cl(1)–Ti(1)–Cl(2)	89.8(1)
N(4)–Li(1)–N(5)	87.3(4)	Cl(1)–Li(1)–Cl(2)	90.9(3)
N(1)–Ti(1)–N(2)	107.1(1)	N(1)–Ti(1)–N(3)	105.9(1)
N(1)–Ti(1)–Cl(1)	107.5(1)	N(1)–Ti(1)–Cl(2)	110.5(1)
N(2)–Ti(1)–Cl(2)	140.7(1)	N(3)–Ti(1)–Cl(1)	142.1(1)
C(1)–N(1)–Ti(1)	169.3(3)		

D. Bis(amidinato) Zr(IV) and Hf(IV) Dichloride Complexes

Reactions of MCl_4 (M = Zr, Hf) with **28** have led to the neutral amidinate complexes $[M(L^3)_2Cl_2]$ [M = Zr (**34**), Hf (**35**)] (Scheme 3–10). Complexes **34** and **35** were isolated as colorless crystals from diethyl ether in 77% and 47% yield, respectively. They are readily soluble in thf, toluene and diethyl ether, but only sparingly soluble in hexane.

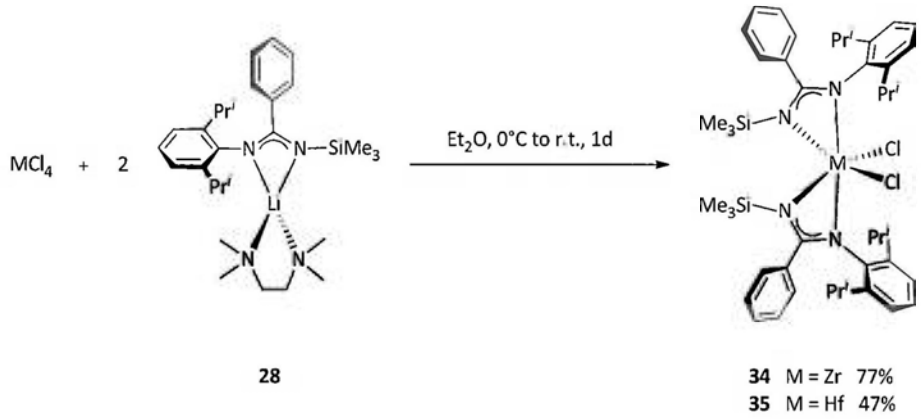

Scheme 3–10

Physical Characterization of Complexes **34** and **35**

Melting points of **34** and **35** have been determined and listed in Table 3–5. Results of elemental analysis were consistent with the formulation of these two complexes as shown in Schemes 3–8. Single-crystal X-ray diffraction studies and NMR spectroscopic analysis of **34** and **35** were also performed (*vide infra*).

Table 3–5 Some physical properties of compounds **34** and **35**.

Compound	Appearance	M.p. (°C)
$[Zr(L^3)_2Cl_2]$ (**34**)	Colorless crystals	Dec.at 239–240 °C without melting
$[Hf(L^3)_2Cl_2]$ (**35**)	Colorless crystals	138–141

NMR Spectra of Complexes **34** and **35**

^{1}H and ^{13}C NMR spectra of complexes **34** and **35** are shown in Figures A3–35 to A3–38 (in Appendix 3). The NMR spectra of each complex showed one set of resonance signals assignable to the L^3 ligand. The ^{1}H NMR spectra of these two complexes showed two resonances for the isopropyl methine protons (3.66 and 3.83 ppm for **34**, and 3.51 and 3.90 ppm for **35**), and four resonance signals for the isopropyl methyl groups (at 0.77, 1.31, 1.36 and 1.63 ppm for **34**, and 0.70, 1.30, 1.34, 1.65 ppm for **35**). These spectroscopic behaviors suggest that the two methyl groups on the isopropyl substituents are prochiral due to the presence of a chiral metal center, and a restricted rotation about the N–C_{ipso} bond.

Crystal Structures of Complexes **34** and **35**

Single crystals of **34** and **35** were obtained from diethyl ether. The molecular structures of the two complexes are shown in Figures 3–5 and 3–6 with selected bond distances and angles listed in Tables 3–6 and 3–7. Complexes **34** and **35** are isostructural. Both complexes crystallize in the monoclinic space group $P2_1/n$. The Zr(IV) and Hf(IV) centers are six-coordinate, with the metal ions surrounded by two κ^2-bound L^3 ligands and two chloride ligands. The two L^3 ligands are *cis* to each other, resulting in a C_2-axis bisecting the Cl–M–Cl angle. The molecule has no symmetry plane and is therefore chiral.

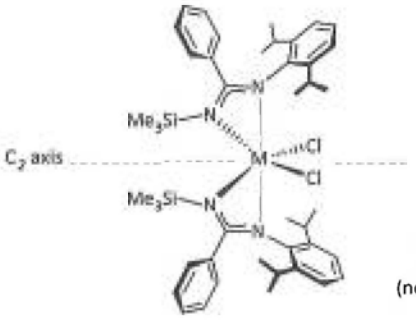

Chiral molecule
(no symmetry plane)

The L^3 ligand in complexes **34** and **35** bind to the metal center in an unsymmetrical manner. The M–N_{aryl} distances [M = Zr (**34**), Zr(1)–N(1) = 2.267(3) Å and Zr(1)–N(3) = 2.260(3) Å; M = Hf (**35**), Hf(1)–N(1) = 2.246(2) Å and Hf(1)–N(3) = 2.238(2) Å] are longer than the corresponding M–N_{silyl} distances [M = Zr (**34**), Zr(1)–N(2) = 2.208(3) Å and Zr(1)–N(4) = 2.205(3) Å; M = Hf (**35**), Hf(1)–N(2) = Hf(1)–N(4) = 2.197(2) Å].

The observed Zr–N distances of 2.205(3)–2.267(3) Å in complex **34** are comparable to the corresponding distances reported for [Zr{MeC(NCy)$_2$}$_2$Cl$_2$] [2.186(8)–2.234(8) Å],[2] [Zr{PhC(NSiMe$_3$)$_2$}$_2$Cl$_2$] [2.204(5)–2.251(4) Å],[3b–d] [Zr{PhC(NC$_6$H$_3$Me$_2$–2,6)(NC$_6$H$_3$Pr$^i_2$–2,6)}$_2$Cl$_2$] [2.180(2) and 2.309(2) Å][6] and [Zr{PhC(NC$_6$H$_3$Pr$^i_2$–2,6)$_2$}$_2$Cl$_2$] [2.207(2)–2.217(2) Å].[6] The observed Zr–Cl distances of 2.401(1) and 2.403(1) Å in **34** are close to those reported for [Zr{PhC(NSiMe$_3$)$_2$}$_2$Cl$_2$] [2.4002(9)–2.403(1) Å][3b–d] and [Zr{PhC(NC$_6$H$_3$Me$_2$–2,6)(NC$_6$H$_3$Pr$^i_2$–2,6)}$_2$Cl$_2$] [2.3997(8) Å],[6] but slightly shorter than the Zr–Cl distances in [Zr{MeC(NCy)$_2$}$_2$Cl$_2$] [2.426(3) and 2.436(3) Å][2] and [Zr{PhC(NC$_6$H$_3$Pr$^i_2$–2,6)$_2$}$_2$Cl$_2$] [2.437(1) Å].[6] The observed Hf–N distances in complex **35** are 2.197(2)–2.246(2) Å. The observed Hf–Cl distances are 2.3839(8) and 2.3875(8) Å. Complex **35** represents a rare example of structurally characterized bis(amidinato) Hf(IV) complexes.

The N–M–N bite angles subtended by the L^3 ligand are 59.6(1)° and 60.0(1)° in **34**, and 60.09(8)° and 60.52(8)° in **35**. The N–Zr–N bite angles in **34** are similar to those of other Zr(IV) amidinate complexes reported in the literature.[2,3b–d,6]

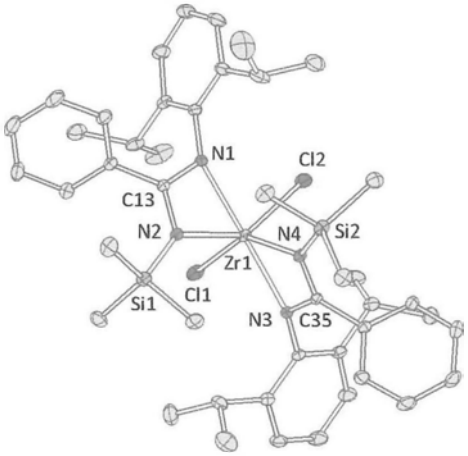

Figure 3–4 Molecular structure of $[Zr(L^3)_2Cl_2]$ (**34**).

Table 3–6 Selected bond lengths (Å) and angles (deg.) for compound **34**.

$[Zr(L^3)_2Cl_2]$ (**34**)			
Zr(1)–N(1)	2.267(3)	Zr(1)–N(2)	2.208(3)
Zr(1)–N(3)	2.260(3)	Zr(1)–N(4)	2.205(3)
Zr(1)–Cl(1)	2.403(1)	Zr(1)–Cl(2)	2.401(1)
N(1)–C(13)	1.322(4)	N(2)–C(13)	1.345(4)
N(3)–C(35)	1.324(4)	N(4)–C(35)	1.350(4)
N(1)–Zr(1)–N(2)	59.6(1)	N(3)–Zr(1)–N(4)	60.0(1)
N(1)–Zr(1)–N(3)	170.9(1)	N(2)–Zr(1)–N(4)	94.1(1)
Cl(1)–Zr(1)–Cl(2)	101.2(1)		

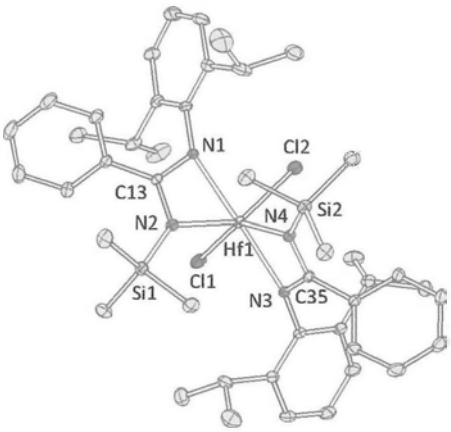

Figure 3–5 Molecular structure of $[Hf(L^3)_2Cl_2]$ (**35**).

Table 3–7 Selected bond lengths (Å) and angles (deg.) for compound **35**.

$[Hf(L^3)_2Cl_2]$ (**35**)			
Hf(1)–N(1)	2.246(2)	Hf(1)–N(2)	2.197(2)
Hf(1)–N(3)	2.238(2)	Hf(1)–N(4)	2.197(2)
Hf(1)–Cl(1)	2.388(1)	Hf(1)–Cl(2)	2.384(1)
N(1)–C(13)	1.323(3)	N(2)–C(13)	1.350(3)
N(3)–C(35)	1.327(3)	N(4)–C(35)	1.346(3)
N(1)–Hf(1)–N(2)	60.5(1)	N(3)–Hf(1)–N(4)	60.1(1)
N(1)–Hf(1)–N(3)	171.5(1)	N(2)–Hf(1)–N(4)	93.8(1)
Cl(1)–Hf(1)–Cl(2)	101.0(1)		

E. Bis(amidinato) Zr(IV) Alkyl Complexes

The two chloride ligands in complex **34** could be replaced by alkyl ligands. Treatment of **34** with two equivalents of LiMe afforded the colorless, crystalline dimethyl complex $[Zr(L^3)_2Me_2]$ (**36**) in 45% yield (Scheme 3–11). It is very sensitive to air and moisture, turning into a brown solid upon exposure to air.

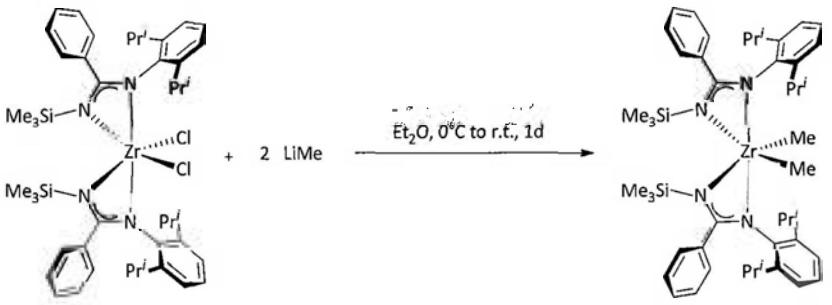

34 **36** 45%

Scheme 3–11

It is believed that the $[Zr(L^3)_2Me_2]$ complex (**36**) is highly reactive due to the presence of two labile methyl ligands. Accordingly, the reactions of **36** with MeI and $AlMe_3$ were examined. Surprisingly, no reaction was observed by reacting complex **36** with two equivalents of MeI. Only the starting complex was recovered after the reaction, as confirmed by ^1H NMR spectroscopy. Complex **36** was also inert towards $AlMe_3$ (two equivalents). The unexpected inertness of **36** may be attributed to the sterically crowded ligand environment around the Zr(IV) center.

Alkylation of complex **34** with two equivalents of $PhCH_2MgCl$ led to the mono(benzyl) complex $[Zr(L^3)_2(CH_2Ph)Cl]$ (**37**) in 19% yield (Scheme 3–12). Complex **37** is readily soluble in diethyl ether and hexane.

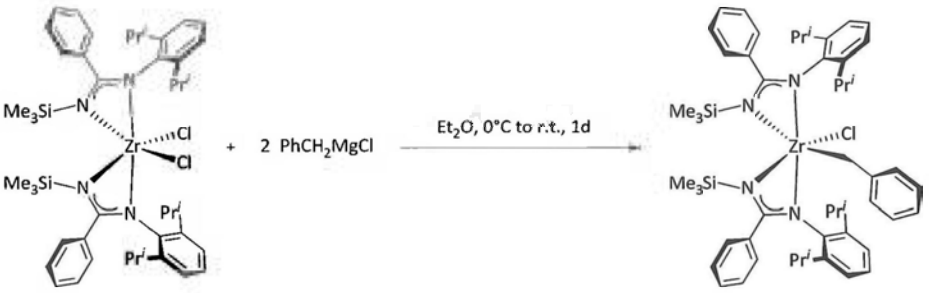

34 **37** 19%

Scheme 3–12

Zr(IV) dibenzyl complexes supported by the $[PhC(NSiMe_3)_2]^-$ ligand has been reported by other research groups.[3c,d] The successful isolation of mono(benzyl) complex **37** but not the expected bis(benzyl) derivative in this work may be attributed to the steric saturation generated by two bulky L^3 ligands in **37**.

Attempts to prepare a Zr(IV) *n*-propyl complex by the reaction of complex **34** with Pr^nMgBr have been unsuccessful (Scheme 3–13). A colorless crystalline product was isolated. Surprisingly, a Mg(II) salt of the L^3 ligand, $[Mg(L^3)_2]$ (**38**), was found to be the only isolable product of the reaction. The structure of **38** was determined by X-ray crystallography. NMR spectroscopic and elemental analysis suggested the presence of **38** together with some unidentified species.

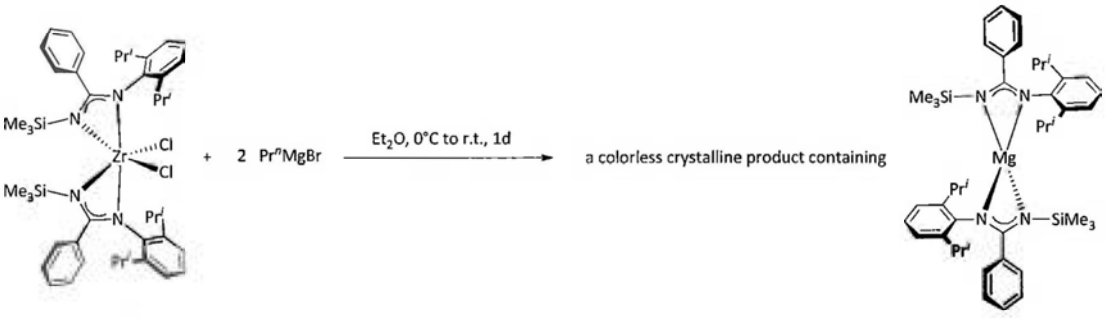

34 **38**

Scheme 3–13

Physical Characterization of Complexes **36** and **37**

Table 3–8 lists some of the physical properties of complexes **36** and **37**. Complexes **36** and **37** have been characterized by melting-point measurement, elemental analysis, NMR spectroscopy and X-ray crystallography. Results of elemental analysis were consistent with their formulation as shown in Schemes 3–11 and 3–12.

Table 3–8 Some physical properties of compounds **36** and **37**.

Compound	Appearance	M.p. (°C)
$[Zr(L^3)_2Me_2]$ (**36**)	Colorless crystals	Dec.at 216–218 °C without melting
$[Zr(L^3)_2(CH_2Ph)Cl]$ (**37**)	Yellow crystals	239–240

NMR Spectra of Complexes **36** and **37**

1. $[Zr(L^3)_2Me_2]$ (**36**)

The ^1H and ^{13}C NMR spectra of complex **36** are shown in Figures A3–39 and A3–40. Each spectrum showed one set of resonance signals assignable to the L^3 ligand, indicating that the two L^3 ligands in **36** are chemically equivalent. The methyl ligands in **36** occur as one singlet resonance signal in both spectra (at 0.89 ppm in the ^1H NMR spectrum and 49.9 ppm in the ^{13}C NMR spectrum). In the ^1H NMR spectrum, two nonequivalent isopropyl substituents were observed, with the methine protons resonance at 3.61 and 4.09 ppm, and diastereotopic methyl groups resonance at 0.94, 1.15 and 1.41 ppm in an integral ratio of 1:1:2. These spectroscopic behaviors suggest that the two methyl groups on the isopropyl substituents are prochiral due to the presence of a chiral metal center and a

restricted rotation about the N–C_{ipso} bond.

2. $[Zr(L^3)_2(CH_2Ph)Cl]$ (**37**)

The ^1H and ^{13}C NMR spectra of complex **37** are shown in Figures A3–41 and A3–42. In the ^1H NMR spectrum, two nonequivalent trimethylsilyl groups (at 0.23 and 0.26 ppm), suggesting the two L^3 ligands are nonequivalent. Four nonequivalent isopropyl substituents (the methine protons resonance at 3.34, 3.62, and 3.77 ppm in an integral ratio of 1:1:2, and methyl protons resonance at 0.40, 0.80, 1.03, 1.11, 1.23, 1.26, 1.32, 1.54 ppm) were observed. These spectroscopic behaviors suggest that the two methyl groups on the isopropyl substituents are prochiral due to the presence of a chiral center and a restricted rotation of the N–C_{ipso} bond. Moreover, the diastereotopic methylene protons of the benzyl ligand occur as two doublets at 2.93 and 3.25 ppm.

Crystal Structures of Complexes **36** and **37**

Single crystals of **36** and **37** were obtained from hexane.

1. $[Zr(L^3)_2Me_2]$ (**36**)

The crystal structure of complex **36** is shown in Figure 3–6. Selected bond lengths and angles are listed in Table 3–9. Complex **36** crystallizes in the monoclinic space group $P2_1/n$. The molecular structure of **36** is similar to that of **34**, with the six-coordinate Zr(IV) center bound by two κ^2-bound L^3 ligands in a *cis* fashion and two methyl ligands. The molecule contains a C_2-axis, which bisects the

Me–Zr–Me angle. The molecule does not have any symmetry plane and is thus chiral.

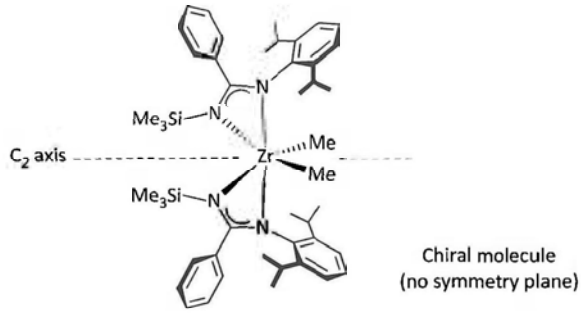

The Zr–N distances of 2.232(2)–2.327(2) Å in **36** are similar to those reported for $[Zr\{MeC(NCy)_2\}_2Me_2]$ [2.225(4)– 2.291(4) Å],[2] $[Zr\{PhC(NSiMe_3)_2\}_2Me_2]$ [2.237(2)–2.319(2) Å],[3b,d] $[Zr\{PhC(NC_6H_3Me_2\text{–}2,6)(NC_6H_3Pr^i_2\text{–}2,6)\}_2Me_2]$ [2.224(3)–2.341(3) Å],[6] and $[Zr\{PhC(NC_6H_3Pr^i_2\text{–}2,6)_2\}_2Me_2]$ [2.263(5)–2.337(5) Å].[6] The observed Zr–Me distances in **36** are 2.241(3) and 2.250(3) Å. They are similar to those reported for $[Zr\{MeC(NCy)_2\}_2Me_2]$ [2.244(6) and 2.245(8) Å],[2] $[Zr\{PhC(NSiMe_3)_2\}_2Me_2]$ [2.241(4) and 2.248(2) Å],[3b–d] $[Zr\{PhC(NC_6H_3Me_2\text{–}2,6)(NC_6H_3Pr^i_2\text{–}2,6)\}_2Me_2]$ [2.226(5) Å][6] and $[Zr\{PhC(NC_6H_3Pr^i_2\text{–}2,6)_2\}_2Me_2]$ [2.243(6) and 2.247(7) Å].[6]

2. $[Zr(L^3)_2(CH_2Ph)Cl]$ (**37**)

The solid-state structure of complex **37** is shown in Figure 3–7 with selected bond lengths and angles listed in Table 3–10. Complex **37** crystallizes in the monoclinic space group $P2_1/c$. The coordination sphere of the six-coordinate Zr(IV) ion consists of two κ^2-bound L^3 ligands, one benzyl ligand and one chloride ligand. The two chelating L^3 ligands are *cis* to each other. The chiral molecule of **37** belongs to the C_1 point group. Similar to the dichloride precursor **34** and dimethyl complex **36**, the two L^3 ligands in complex **37** bind to the Zr(IV) centers in an unsymmetrical manner. The Zr–N_{aryl} distances [Zr(1)–N(1) = 2.290(2) and Zr(1)–N(3)

= 2.325(2) Å] are slightly longer than the corresponding Zr–N_{silyl} distances [Zr(1)–N(2) = 2.207(3) and Zr(1)–N(4) = 2.209(2) Å].

The observed Zr–N distances of 2.207(3)–2.325(2) Å in **37** are comparable to those reported for [Zr{PhC($NSiMe_3$)$_2$}$_2$$Cl_2$] [2.204(5)–2.251(4) Å][3b,d] and [Zr{PhC($NSiMe_3$)$_2$}$_2$(CH_2Ph)$_2$] [2.225(3)–2.283(3) Å].[3c] The Zr–C_{benzyl} distance in **37** of 2.250(3) Å is shorter than those of 2.315(4)–2.301(3) Å in [Zr{PhC($NSiMe_3$)$_2$}$_2$ (CH_2Ph)$_2$].[3c] The Zr–Cl distance of 2.432(1) Å in **37** is longer than those of 2.4002(9)–2.403(1) Å and 2.3997(8) Å in [Zr{PhC($NSiMe_3$)$_2$}$_2$$Cl_2$][5b–d] and [Zr{PhC($NC_6H_3Me_2$–2,6)($NC_6H_3Pr^i_2$–2,6)}$_2$$Cl_2$],[4] respectively. It is also comparable to those of 2.426(3) and 2.436(3) Å in [Zr{MeC(NCy)$_2$}$_2$$Cl_2$],[2] and 2.437(1) Å in [Zr{PhC($NC_6H_3Pr^i_2$–2,6)$_2$}$_2$$Cl_2$].[4]

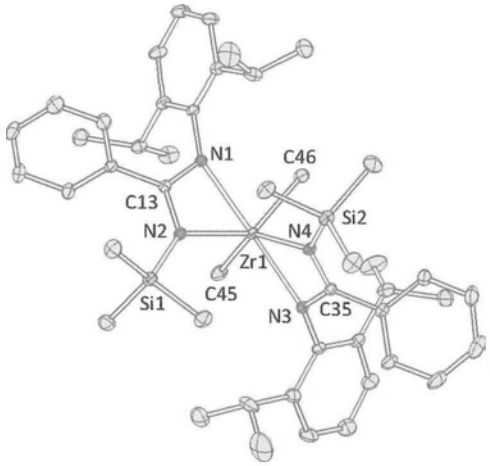

Figure 3–6 Molecular structure of $[Zr(L^3)_2Me_2]$ (**36**).

Table 3–9 Selected bond lengths (Å) and angles (deg.) for compound **36**.

$[Zr(L^3)_2Me_2]$ (**36**)			
Zr(1)–N(1)	2.316(2)	Zr(1)–N(2)	2.239(2)
Zr(1)–N(3)	2.327(2)	Zr(1)–N(4)	2.232(2)
Zr(1)–C(45)	2.250(3)	Zr(1)–C(46)	2.241(3)
N(1)–C(13)	1.311(3)	N(2)–C(13)	1.349(3)
N(3)–C(35)	1.311(3)	N(4)–C(35)	1.339(3)
N(1)–Zr(1)–N(2)	58.4(1)	N(3)–Zr(1)–N(4)	58.2(1)
N(1)–Zr(1)–N(3)	174.6(1)	N(2)–Zr(1)–N(4)	99.1(1)
C(45)–Zr(1)–C(46)	98.2(1)		

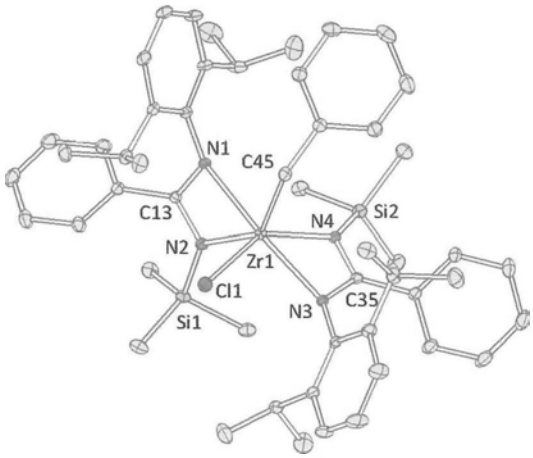

Figure 3–7 Molecular structure of $[Zr(L^3)_2(CH_2Ph)(Cl)]$ (**37**).

Table 3–10 Selected bond lengths (Å) and angles (deg.) for compound **37**.

$[Zr(L^3)_2(CH_2Ph)(Cl)]$ (**37**)			
Zr(1)–N(1)	2.325(2)	Zr(1)–N(2)	2.207(3)
Zr(1)–N(3)	2.290(2)	Zr(1)–N(4)	2.209(2)
Zr(1)–Cl(1)	2.432(1)	Zr(1)–C(45)	2.250(3)
N(1)–C(13)	1.313(4)	N(2)–C(13)	1.356(4)
N(3)–C(35)	1.326(4)	N(4)–C(35)	1.360(4)
N(1)–Zr(1)–N(2)	58.9(1)	N(3)–Zr(1)–N(4)	59.9(1)
N(1)–Zr(1)–N(3)	172.3(1)	N(2)–Zr(1)–N(4)	98.8(1)
N(1)–Zr(1)–C(45)	81.9(1)	N(2)–Zr(1)–C(45)	140.5(1)
N(3)–Zr(1)–C(45)	100.2(1)	N(4)–Zr(1)–C(45)	100.3(1)
N(1)–Zr(1)–Cl(1)	102.7(1)	N(2)–Zr(1)–Cl(1)	92.0(1)
N(3)–Zr(1)–Cl(1)	84.6(1)	N(4)–Zr(1)–Cl(1)	143.8(1)
C(45)–Zr(1)–Cl(1)	92.5(9)		

*F. Other Attempted Reactions of Complex **34***

1. Attempted Reactions of **34** with $LiNMe_2$ and NaOMe

Complex **34** was found to be unreactive towards NaOMe. Only the unreacted starting material **34** was recovered after the reaction, as indicated by ^1H NMR spectroscopic analysis. On the other hand, treatment of complex **34** with $LiNMe_2$ only resulted in the isolation of a pale yellow intractable oil.

2. Attempted Reactions of Complex **34** with Reducing Agents

The reaction chemistry of **34** towards reducing agents such as K and KC_8 has been briefly examined. Unfortunately, no reaction between complex **34** and potassium metal was observed. The ^1H NMR spectrum of the colorless crystals obtained after treatment of complex **34** with excess K showed only the presence of unreacted complex **34**. Reaction of complex **34** with one equivalent of KC_8 gave an orange crystalline product, which was found to be a mixture of unreacted complex **34** together with some unidentified impurities based on its ^1H NMR spectrum.

G. Bis(amidinato) Mg(II) and Ca(II) Complexes

The isolation of $[Mg(L^3)_2]$ (**38**) (see Section E2) revealed the capability of the L^3 ligand to stabilize Group 2 metal ions. In our studies, direct reaction of the lithium salt **29** with one or two equivalents of Pr^nMgBr in hexane afforded the colorless, crystalline thf-adduct $[Mg(L^3)_2(thf)]$ (**39**) (Scheme 3–14).

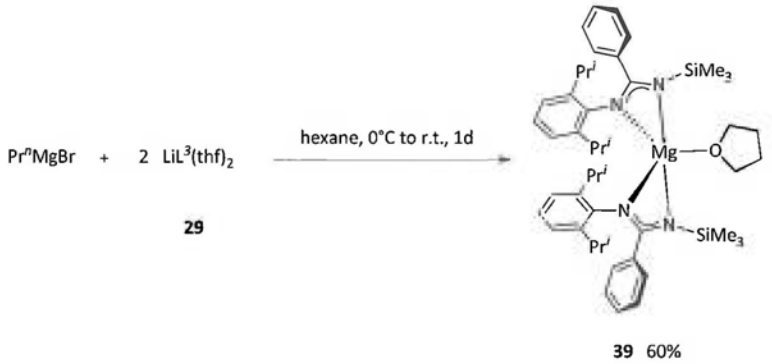

Scheme 3–14

Most of the magnesium amidinates reported in the literature were synthesized by insertion of carbodiimides into an appropriate Mg–C bond.[11] Scheme 3–14 represents an alternative synthetic route for Mg(II) amidinato complexes.

The Ca(II) counterpart [Ca(L^3)$_2$(thf)] (**40**) was also prepared by the reaction of two molar equivalents of potassium amidinate **30** with anhydrous CaI$_2$ in thf (Scheme 3–15).

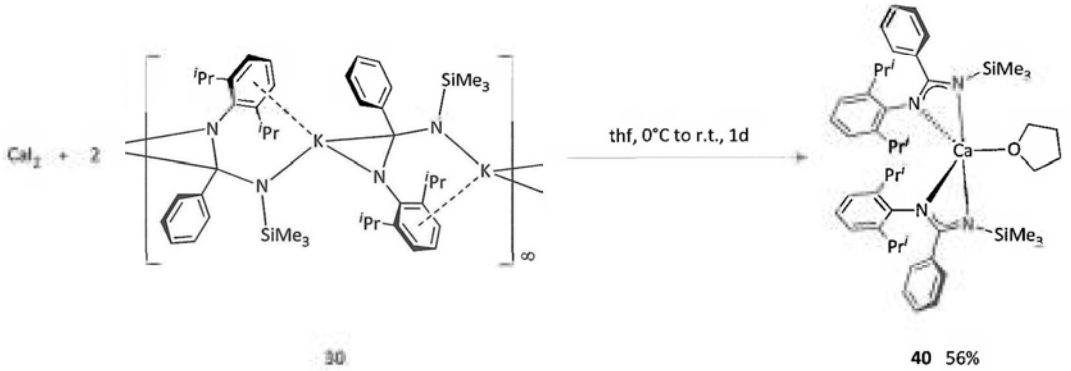

Scheme 3–15

The Mg(II) bis(amidinate) complex **39** was found to be unreactive towards KC$_8$ (one equivalent). Only the unreacted complex **39** was isolated after the reaction,

as confirmed by ^{1}H NMR spectroscopy and X-ray crystallography.

Physical Characterization of Complexes **39** and **40**

Complexes **39** and **40** were characterized by NMR spectroscopy, elemental analysis, in addition to X-ray crystallography. Table 3–11 shows some of the physical properties of the two complexes. Results of elemental analysis were consistent with their empirical formula shown in Schemes 3–14 and 3–15.

Table 3–11 Some physical properties of compounds **39** and **40**.

Compound	Appearance	M.p. (°C)
[Mg(L^3)$_2$(thf)] (**39**)	Colorless crystals	250–254
[Ca(L^3)$_2$(thf)] (**40**)	Colorless crystals	216–221

NMR Spectra of Complexes **39** and **40**

1. [Mg(L^3)$_2$(thf)] (**39**)

The ^{1}H and ^{13}C NMR spectra of complex **39** are shown in Figures A2–43 and A2–44. The two L^3 ligands in **39** were shown to be identical as only one set of resonance signals assignable to the L^3 ligand are observed in the NMR spectra. In the ^{1}H NMR spectrum, two chemically nonequivalent isopropyl substituents are shown, with the methine protons resonance at 3.32 and 3.93 ppm, and diastereotopic methyl groups resonance at 0.98, 1.28, 1.52 and 1.65 ppm. These spectroscopic behaviors suggest that the two methyl groups on the isopropyl substituents are prochiral due to the presence of a chiral center and a restricted rotation of the N–C_{ipso} bond.

2. $[Ca(L^3)_2(thf)]$ (**40**)

The ^1H and ^{13}C NMR spectra of complex **40** (Figures A2–45 and A2–46) showed one set of resonance signals assignable to the L^3 ligand and thf molecule in a ratio of 2:1. The two isopropyl substituents of the L^3 ligand in the complex are shown to be chemically equivalent, with the methine proton resonance occurring at 3.59 ppm and the diastereotopic methyl groups resonance at 1.32 and 1.42 ppm.

Crystal Structures of Complexes **39** and **40**

The molecular structures of the Mg(II) amidinate complex **39** and the Ca(II) derivative **40** were also determined in this work. Figures 3–8 and 3–9 show the crystal structures of **39** and **40**, respectively. Selected bond lengths and angles are listed in Tables 3–12 and 3–13.

Complex **39** crystallizes in the monoclinic space group $P2_1/n$, whereas crystals of complex **40** belong to the triclinic space group $P\bar{1}$. The two complexes are isotypic. The alkali-earth metal ion is coordinated by two κ^2-bound L^3 ligands. Coordination by one thf molecule completes a distorted trigonal bipyramidal geometry around the metal center. The N(1), N(3) and O(1) atoms occupy the equatorial plane [sum of bond angles = 360.1° in **39** and **40**], whereas the N(2) and N(4) atoms occupy the axial positions [N(2)–Mg(1)–N(4) = 167.0(1)°, N(2)–Ca(1)–N(4) = 163.0(1)°]. A C_2-axis axis passes through the M–O bond. The Mg–N distances [2.103(3)–2.174(3) Å] in complex **39** are comparable to the corresponding distances in the six-coordinate $[Mg\{PhC(NPr^i)\}_2\}_2(thf)_2]$ [2.161(6) and 2.168(6) Å],[12a] $[Mg\{HC(NC_6H_4Me\text{–}4)_2\}_2(thf)_2]$ [2.149(2)–2.172(3) Å][12b] and $[Mg\{HC(NC_6H_4Me\text{–}2)_2\}_2(thf)_2]$ [2.158(3) and 2.172(3) Å].[12b] The observed Mg–O

distance in **39** is 2.064(3) Å. It is shorter than those reported for other six-coordinate Mg(II) amidinate complexes: $[Mg\{PhC(NPr^i)_2\}_2(thf)_2]$ [2.226(9) and 2.331(9) Å],[12a] $[Mg\{HC(NC_6H_4Me–4)_2\}_2(thf)_2]$[12b] [2.149(2) and 2.151(1) Å], and $[Mg\{HC(NC_6H_4Me–2)_2\}_2(thf)_2]$ [2.134(2) Å].[12b]

The Ca–N distances in complex **40** fall within the range of 2.360(4)–2.411(4) Å. They are comparable to those of 2.361(3) and 2.406(3) Å in $[Ca\{HC(NC_6H_3Pr^i_2–2,6)_2\}_2(thf)]$.[13] The Ca–O distance of 2.328(4) Å in **40** is comparable to that of 2.323(3) Å in $[Ca\{HC(NC_6H_3Pr^i_2–2,6)_2\}_2(thf)]$.[13]

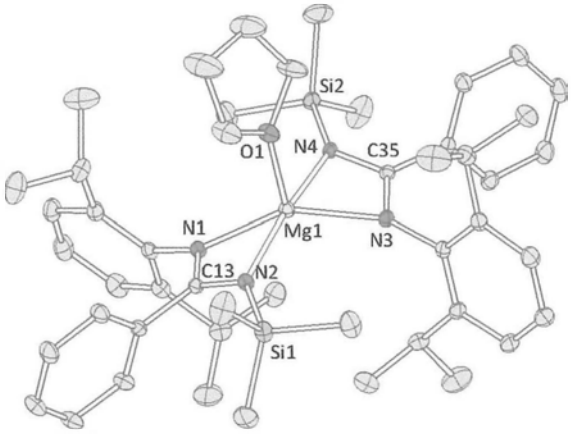

Figure 3–8 Molecular structure of $[Mg(L^3)_2(thf)]$ (**39**).

Table 3–12 Selected bond lengths (Å) and angles (deg.) for compound **39**.

$[Mg(L^3)_2(thf)]$ (**39**)			
Mg(1)–N(1)	2.107(3)	Mg(1)–N(2)	2.169(3)
Mg(1)–N(3)	2.103(3)	Mg(1)–N(4)	2.174(3)
Mg(1)–O(1)	2.064(3)	N(1)–C(13)	1.326(4)
N(2)–C(13)	1.328(4)	N(3)–C(35)	1.323(4)
N(4)–C(35)	1.338(4)		
N(1)–Mg(1)–N(2)	63.7(1)	N(3)–Mg(1)–N(4)	63.7(1)
O(1)–Mg(1)–N(1)	109.2(1)	O(1)–Mg(1)–N(2)	95.9(1)
O(1)–Mg(1)–N(3)	108.4(1)	O(1)–Mg(1)–N(4)	94.1(1)
N(1)–Mg(1)–N(3)	142.5(1)	N(2)–Mg(1)–N(4)	167.0(1)

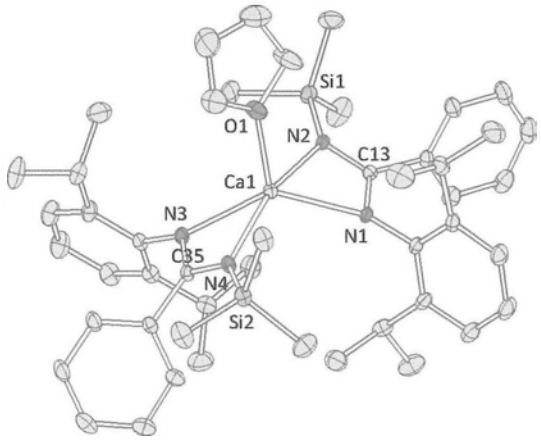

Figure 3–9 Molecular structure of $[Ca(L^3)_2(thf)]$ (**40**).

Table 3–13 Selected bond lengths (Å) and angles (deg.) for compound **40**.

$[Ca(L^3)_2(thf)]$ (**40**)			
Ca(1)–N(1)	2.375(4)	Ca(1)–N(2)	2.401(4)
Ca(1)–N(3)	2.360(4)	Ca(1)–N(4)	2.411(4)
Ca(1)–O(1)	2.328(4)	N(1)–C(13)	1.324(5)
N(2)–C(13)	1.327(5)	N(3)–C(35)	1.337(6)
N(4)–C(35)	1.325(6)		
N(1)–Ca(1)–N(2)	57.0(1)	N(3)–Ca(1)–N(4)	57.4(1)
O(1)–Ca(1)–N(1)	117.4(1)	O(1)–Ca(1)–N(2)	95.5(1)
O(1)–Ca(1)–N(3)	111.6(1)	O(1)–Ca(1)–N(4)	101.0(1)
N(1)–Ca(1)–N(3)	131.1(1)	N(2)–Ca(1)–N(4)	163.0(1)

Summary

A series of Group 4 metal complexes supported by the unsymmetrical $[PhC(NC_6H_3Pr^i_2\text{–}2,6)(NSiMe_3)]^-$ (L^3) ligand was synthesized and structurally characterized in this work. The reaction of $TiCl_3(thf)_3$ with two molar equivalents of $[LiL^3(thf)_2]$ (**29**) gave $[Ti(L^3)_2Cl]$ (**31**). Furthermore, treatment of complex **31** with LiMe led to the corresponding methyl derivative $[Ti(L^3)_2Me]$ (**32**). Ti(IV), Zr(IV) and Hf(IV) chloride complexes of the L^3 ligand were also prepared in this work. The reaction of $TiCl_4(thf)_2$ with $[LiL^3(tmeda)]$ (**28**) led to the isolation of $[Ti(L^3)(NC_6H_3Pr^i_2\text{–}2,6)(\mu\text{–}Cl)_2Li(tmeda)]$ (**33**). Treatment of MCl_4 (M = Zr, Hf) with complex **28** yielded the corresponding neutral complexes $[M(L^3)_2Cl_2]$ [M = Zr (**34**), Hf (**35**)]. In addition, ligand substitution reactions of complex **34** have been studied. Treatment of **34** with LiMe gave the bis(methyl) complex $[Zr(L^3)_2Me_2]$ (**36**). The mono(benzyl) complex $[Zr(L^3)_2(CH_2Ph)Cl]$ (**37**) was obtained via reaction of **34** with $PhCH_2MgCl$.

The L^3 ligand was proved to be a good supporting ligand for stabilization of a range of Ti(III), Ti(IV), Zr(IV) and Hf(IV) complexes. The bis(amidinate) Zr(IV) dichloride complex **34** acted as a good starting material for the corresponding methyl and benzyl derivatives.

Mg(II) and Ca(II) complexes supported by the L^3 ligand were also isolated in this work. Direct reaction of $[LiL^3(thf)_2]$ (**29**) with one or two equivalents of Pr^nMgBr afforded the Mg(II) amidinate $[Mg(L^3)_2(thf)]$ (**39**). The analogous Ca(II) derivative, $[Ca(L^3)_2(thf)]$ (**40**), was synthesized by metathesis reaction of two equivalents of $[KL^3]_\infty$ (**30**) with CaI_2.

Experimental for Chapter 3

Materials

Anhydrous $TiCl_3$, $TiCl_4(thf)_2$, $ZrCl_4$ and $HfCl_4$ (Strem), CaI_2 (Aldrich), LiMe (1.6 M in Et_2O), $LiBu^n$ (1.6 M in hexanes) (Acros), Pr^nMgBr (2.0 M in Et_2O) and $PhCH_2MgCl$ (1.0 M in Et_2O) (Aldrich) were used as received. The lithium amidinate $[LiL^3(tmeda)]$ (**28**) and potassium amidinate $[KL^3]_\infty$ (**30**) were prepared according to published procedures.[7,8]

Synthesis of $LiL^3(thf)_2$ (29).

To a solution of $HN(C_6H_3Pr^i_2\text{–}2,6)(SiMe_3)$ (**25**)[8] (2.67 g, 10.73 mmol) in thf (30 ml) at 0 °C was slowly added a solution of $LiBu^n$ in hexanes (1.6 M, 6.7 ml, 10.7 mmol) using a syringe. After stirring at room temperature for 1 h, PhCN (1.1 ml, 10.8 mmol) was added and the resulting mixture was stirred at room temperature for another 8 h. Concentration of the resultant solution to *ca.* 10 ml gave complex **29** as colorless crystals. Yield: 3.68 g, 7.32 mmol, 68%. M.p.: 146–151 °C. ^1H NMR (300.13 MHz, C_6D_6): δ 7.26 (br., 2H, *m*–ArH), 6.98–6.87 (m, 6H, *p*–Ar*H* and C_6H_5), 3.52 (m, 10H, C*H*Me_2 and thf), 1.39 (m, 8H, thf), 1.18 (d, *J* = 6.5 Hz, 12H, CH*Me*$_2$), 0.22 (s, 9H, Si*Me*$_3$). ^{13}C NMR (75.47 MHz, C_6D_6): δ 175.8, 146.5, 141.9, 129.1, 128.8, 128.2, 127.9, 127.4, 123.1, 68.2, 28.4, 25.6, 23.2, 3.39. Anal.: Calc. for $C_{30}H_{47}LiN_2O_2Si$: C, 71.67; H, 9.42; N, 5.57%. Found: C, 71.10; H, 9.61; N, 6.12%.

Synthesis of $[Ti(L^3)_2Cl]$ (31).

A slurry of $TiCl_3$ (0.39 g, 2.55 mmol) in thf (15 ml) was stirred at room temperature for 30 min, yielding a bright blue solution of $TiCl_3(thf)_3$ in thf.[14] The solution was cooled to 0 °C , followed by addition of a solution of $[LiL^3(thf)_2]$ (2.58 g,

5.14 mmol) in thf. The reaction mixture was stirred at room temperature for 1 d to give a red solution. All the volatiles were removed in *vacuo* and the solid residue was extracted with hexane. After filtration, the solution was concentrated to *ca.* 5 ml, affording complex **31** as red crystals. Yield: 1.03 g, 1.31 mmol, 52%. M.p.: 190–195 °C. Anal.: Calc. for $C_{44}H_{62}ClN_4Si_2Ti$: C, 67.19; H, 7.95; N, 7.12%. Found: C, 66.87; H, 8.21; N, 7.31%.

Synthesis of [Ti(L^3)$_2$Me] (32).

To a solution of [Ti(L^3)$_2$Cl] (**31**) (0.69 g, 0.87 mmol) in hexane (20 ml) at 0 °C was slowly added LiMe (1.6 M in Et_2O, 0.7 ml, 1.12 mmol). The resulting solution was stirred at room temperature for 1 d, filtered and concentrated to *ca.* 5 ml. Standing the solution at room temperature overnight gave compound **32** as deep red crystals. Yield: 0.46 g, 0.60 mmol, 69%. M.p.: 198–201 °C. Anal.: Calc. for $C_{45}H_{65}N_4Si_2Ti$: C, 70.55; H, 8.55; N, 7.31%. Found: C, 70.13; H, 8.94; N, 7.58%.

Synthesis of [Ti(L^3)(NC$_6$H$_3$Pr$^i_2$–2,6)(μ–Cl)$_2$Li(tmeda)] (33).

A solution of [LiL^3(tmeda)](2.65 g, 5.57 mmol) in Et_2O (15 ml) was added to a slurry of $TiCl_4(thf)_2$ (1.05 g, 3.15 mmol) in Et_2O (10 ml) at 0 °C. The reaction mixture was brought to room temperature and stirred for 1 d. All the volatiles were removed in *vacuo* and the solid residue was extracted with hexane. The solution was filtered and concentrated to *ca.* 5 ml to give the *title* compound as dark brown crystals. The product was recrystallized from toluene. Yield: 1.14 g, 1.49 mmol, 53%. M.p.: 219–224 °C. ^{1}H NMR (400.19 MHz, C_6D_6): δ 7.47 (d, *J* = 7.0 Hz, 2H, *m*–Ar*H*), 7.13–7.09 (m, 3H, *m*–*Ph*Me and Ar*H*), 7.07–6.84 (m, 8.5H, *o*–*Ph*Me, *p*–*Ph*Me, Ar*H* and C_6H_5), 4.87 (sept, *J* = 6.8 Hz, 2H, C*H*Me$_2$), 3.78 (br, 2H, C*H*Me$_2$), 2.11 (s, 1.5H, Ph*Me*), 1.93 (s, 12H, N*Me*$_2$), 1.62 (s, 4H, NC*H*$_2$), 1.52 (d, *J* = 6.8 Hz, 12H,

CH*Me*$_2$), 1.29 (d, *J* = 6.8 Hz, 6H, CH*Me*$_2$), 1.12 (d, *J* = 6.8 Hz, 6H, CH*Me*$_2$), 0.47 (s, 9H, Si*Me*$_3$). ^{13}C NMR (75.47 MHz, C_6D_6): δ 173.8, 159.4, 143.8, 143.5, 142.4, 137.9, 136.1, 129.5, 129.3, 128.6, 128.2, 127.9, 125.7, 125.6, 123.5, 122.4, 121.9, 56.9, 45.5, 28.4, 27.7, 26.2, 25.1, 24.0, 21.4, 3.2. Anal.: Calc. for $C_{40}H_{64}Cl_2LiN_5SiTi\cdot 0.5C_7H_8$: C, 64.12; H, 8.41; N, 8.59%. Found: C, 64.17; H, 8.81; N, 8.69%.

A General procedure for the synthesis of [M(L^3)$_2$Cl$_2$] [M = Zr (34), Hf (35)].

To a slurry of MCl_4 in Et_2O (10 ml) at 0 °C was added a solution of [LiL^3(tmeda)] in the same solvent (20 ml). The reaction mixture was stirred at room temperature for 1 d and then filtered. Concentration of the filtrate to *ca.* 5 ml yielded the *title* complexes as colorless crystals.

Synthesis of [Zr(L^3)$_2$Cl$_2$] (34).

$ZrCl_4$: 0.50 g, 2.13 mmol; [LiL^3(tmeda)]: 2.00 g, 4.21 mmol. Yield: 1.40 g, 1.62 mmol, 77%. M.p.: Decomposed at 239–240 °C without melting. ^{1}H NMR (300.13 MHz, C_6D_6): δ 7.32–7.31 (m, 4H, Ar*H*), 7.03–6.98 (m, 6H, Ar*H* and C_6H_5), 6.84–6.80 (m, 6H, Ar*H* and C_6H_5), 3.83 (br, 2H, C*H*Me$_2$), 3.67 (br, 2H, C*H*Me$_2$), 1.62 (br, 6H, CH*Me*$_2$), 1.36 (br, 6H, CH*Me*$_2$), 1.31 (br, 6H, CH*Me*$_2$), 0.77 (br, 6H, CH*Me*$_2$), 0.28 (s, 18H, Si*Me*$_3$). ^{13}C NMR (100.62 MHz, C_6D_6): δ 182.2, 143.5, 140.7, 135.3, 130.4, 126.7, 124.2, 124.0, 28.7, 27.5, 26.1, 25.0, 23.2, 2.5. Anal.: Calc. for $C_{44}H_{62}Cl_2N_4Si_2Zr$: C, 61.08; H, 7.22; N, 6.47%. Found: C, 61.11; H, 7.25; N, 6.70%.

Synthesis of [Hf(L^3)$_2$Cl$_2$] (35).

$HfCl_4$: 0.72 g, 2.25 mmol; [LiL^3(tmeda)]: 2.04 g, 4.30 mmol. Yield: 0.96 g, 1.00 mmol, 47%. M.p.: 138–141 °C. ^{1}H NMR (300.13 MHz, C_6D_6): δ7.32–7.25 (m, 4H, Ar*H*), 7.13–7.06 (m, 2H, C_6H_5), 7.00 (t, *J* = 7.5 Hz, 2H, p–Ar*H*), 6.89–6.85 (m, 2H,

C_6H_5), 6.84–6.80 (m, 6H, C_6H_5), 3.90 (br, 2H, C*H*Me$_2$), 3.51 (br, 2H, C*H*Me$_2$), 1.65 (br, 6H, CH*Me*$_2$), 1.34 (br, 6H, CH*Me*$_2$), 1.31 (br, 6H, CH*Me*$_2$), 0.70 (br, 6H, CH*Me*$_2$), 0.28 (s, 18H, Si*Me*$_3$). ^{13}C NMR (100.62 MHz, C_6D_6): δ 182.4, 143.8, 140.2, 135.8, 130.4, 127.0, 126.8, 124.4, 123.9, 28.6, 27.7, 26.1, 25.3, 23.3, 2.7. Anal.: Calc. for $C_{44}H_{62}Cl_2N_4Si_2Hf$: C, 55.48; H, 6.56; N, 5.88%. Found: C, 55.77; H, 6.64; N, 6.02%.

Synthesis of [Zr(L^3)$_2$Me$_2$] (36).

To a solution of [Zr(L^3)$_2$Cl$_2$] (2.18 g, 2.52 mmol) in Et_2O at 0 °C was slowly added a solution of LiMe in Et_2O (1.6 M, 3.0 ml, 4.8 mmol). The reaction mixture was then brought to room temperature, stirred for 1 d, filtered and concentrated to *ca.* 5 ml. A brown solid was obtained and isolated. Recrystallization of the brown solid from hexane yielded complex **36** as colorless crystals. Yield: 0.90 g, 1.09 mmol, 45%. M.p.: Decomposed at 216–218 °C without melting. ^{1}H NMR (400.13 MHz, C_6D_6): δ 7.40–7.37 (m, 4H, Ar*H*), 7.08–7.02 (m, 6H, Ar*H* and C_6H_5), 6.92–6.85 (m, 6H, Ar*H* and C_6H_5), 4.09 (sept, *J* = 6.7 Hz, 2H, C*H*Me$_2$), 3.61 (sept, *J* = 6.7 Hz, 2H, C*H*Me$_2$), 1.41 (d, *J* = 6.7 Hz, 12H, CH*Me*$_2$), 1.15 (d, *J* = 6.7 Hz, 6H, CH*Me*$_2$), 0.94 (d, *J* = 6.7 Hz, 6H, CH*Me*$_2$), 0.89 (s, 6H, Me), 0.24 (s, 18H, Si*Me*$_3$). ^{13}C NMR (100.62 MHz, C_6D_6): δ 180.7, 143.4, 142.7, 141.8, 136.7, 129.9, 125.9, 124.1, 124.1, 49.9, 28.4, 28.3, 26.5, 26.3, 24.7, 23.8, 2.5. Anal.: Calc. for $C_{46}H_{68}N_4Si_2Zr$: C, 67.01; H, 8.31; N, 6.79%. Found: C, 67.44; H, 8.96; N, 7.06%.

Synthesis of [Zr(L^3)$_2$(CH$_2$Ph)Cl] (37).

A solution of $PhCH_2MgCl$ in Et_2O (1.0 M, 3.2 ml, 2.3 mmol) was slowly added to a solution of [Zr(L^3)$_2$Cl$_2$] (1.42 g, 1.64 mmol) in Et_2O at 0 °C. After stirring at room temperature for 1 d, the reaction mixture was filtered and concentrated to *ca.* 5 ml. A brown solid was obtained, which was recrystallized from hexane to yield

the *title* compound as bright yellow crystals. Yield: 0.28 g, 0.31 mmol, 19%. M.p.: 239–240 °C. ^{1}H NMR (300.13 MHz, C_6D_6): δ 7.46–7.44 (br, 4H, Ar*H*), 7.15–7.00 (m, 5H, Ar*H*, C_6H_5 and benzyl C_6H_5), 6.96–6.84 (m, 12H, Ar*H*, C_6H_5 and benzyl C_6H_5), 3.77 (sept, *J* = 6.6 Hz, 2H, C*H*Me$_2$), 3.62 (sept, *J* = 6.6 Hz, 1H, C*H*Me$_2$), 3.34 (sept, *J* = 6.6 Hz, 1H, C*H*Me$_2$), 3.23 (d, *J* = 10.9 Hz, 1H, C*H*$_2$Ph), 2.93 (d, *J* = 10.9 Hz, 1H, C*H*$_2$Ph), 1.54 (d, *J* = 6.6 Hz, 3H, CH*Me*$_2$), 1.32 (d, *J* = 6.6 Hz, 3H, CH*Me*$_2$), 1.26 (d, *J* = 6.6 Hz, 3H, CH*Me*$_2$), 1.23 (d, *J* = 6.6 Hz, 3H, CH*Me*$_2$), 1.11 (d, *J* = 6.6 Hz, 3H, CH*Me*$_2$), 1.03 (d, *J* = 6.6 Hz, 3H, CH*Me*$_2$), 0.80 (d, *J* = 6.6 Hz, 3H, CH*Me*$_2$), 0.40 (d, *J* = 6.6 Hz, 3H, CH*Me*$_2$), 0.26 (s, 9H, Si*Me*$_3$), 0.23 (s, 9H, Si*Me*$_3$). ^{13}C NMR (75.47 MHz, C_6D_6): δ 182.8, 180.8, 148.7, 144.0, 143.5, 143.0, 142.6, 141.4, 141.1, 136.0, 130.3, 130.2, 128.6, 128.2, 127.3, 126.5, 126.4, 125.7, 124.7, 124.2, 123.9, 122.1, 82.7, 28.8, 28.7, 28.5, 28.3, 26.5, 26.1, 26.0, 25.8, 25.5, 25.1, 24.7, 24.1, 3.2, 3.0. Anal.: Calc. for $C_{51}H_{69}ClN_4Si_2Zr$: C, 66.51; H, 7.55; N, 6.08%. Found: C, 66.14; H, 7.71; N, 6.28%.

Synthesis of [Mg(L^3)$_2$(thf)] (39).

To a solution of [LiL^3(thf)$_2$] (2.10 g, 4.18 mmol) in Et_2O at 0°C was added Pr^{n}MgBr (2.0 M in Et_2O, 1.0 ml, 2.0 mmol). The reaction mixture was stirred at room temperature for 1 d. All of the volatiles were removed in *vacuo* and the resulting residue was extracted with hexane. The solution was filtered and then concentrated to *ca.* 5 ml to give complex **39** as colorless crystals. Yield: 0.96 g, 1.20 mmol, 60%. M.p.: 250–254 °C. ^{1}H NMR (300.13 MHz, C_6D_6): δ 7.26 (d, *J* = 7.2 Hz, 4H, *m*–Ar*H*), 7.16–7.10 (br, 2H, Ph), 7.03–6.93 (m, 8H, Ph), 6.84 (t, *J* = 7.2 Hz, 2H, *p*–Ar*H*), 4.18 (br, 4H, thf), 3.93 (br, 2H, C*H*Me$_2$), 3.33 (br, 2H, C*H*Me$_2$), 1.65 (br, 6H, C*H*Me$_2$), 1.55 (br, 10H, thf and CH*Me*$_2$), 1.28 (br, 6H, CH*Me*$_2$), 0.98 (br, 6H, CH*Me*$_2$), –0.22 (s, 18H, Si*Me*$_3$). ^{13}C NMR (75.47 MHz, C_6D_6): δ 177.1, 144.2, 143.2, 141.4, 140.0, 127.4, 127.5, 124.3, 123.3, 70.4, 28.9, 28.3, 26.4, 25.5, 25.2, 24.1, 23.8,

3.0. Anal.: Calc. for $C_{48}H_{70}MgN_4OSi_2$: C, 72.10; H, 8.82; N, 7.00%. Found: C, 71.73; H, 9.31; N, 7.36%.

Synthesis of $[Ca(L^3)_2(thf)]$ (40).

A solution of $[KL^3]_\infty$ (1.93 g, 4.93 mmol) in thf (20 ml) was added dropwise to a slurry of CaI_2 (0.71 g, 2.43 mmol) in the same solvent (10 ml) at 0 °C. After stirring at room temperature for 1 d, the reaction mixture was pumped to dryness. The residue was extracted with hexane and filtered. Concentration of the filtrate afforded complex **40** as colorless crystals. Yield: 1.10 g, 1.35 mmol, 56%. M.p.: 216–221 °C. ^{1}H NMR (400.13 MHz, C_6D_6): δ 7.23 (d, *J* = 7.4 Hz, 4H, *m*–Ar*H*), 7.02 (d, *J* = 7.0 Hz, 4H, *m*–Ph), 6.98–6.94 (m, 6H, Ph), 6.84 (t, *J* = 7.4 Hz, 2H, *p*–Ar*H*), 3.92 (br, 4H, thf), 3.59 (br, 2H, C*H*Me$_2$), 1.44–1.41 (m, 16H, thf and CH*Me*$_2$), 1.32 (br, 12H, CH*Me*$_2$), –0.10 (s, 18H, Si*Me*$_3$). ^{13}C NMR (75.47 MHz, C_6D_6): δ 176.1, 145.6, 141.2, 129.1, 127.6, 127.4, 127.1, 123.6, 123.0, 69.3, 28.8, 25.8, 25.3, 22.9, 3.1. Anal.: Calc. for $C_{48}H_{70}CaN_4OSi_2$: C, 70.71; H, 8.65; N, 6.87%. Found: C, 70.23; H, 9.43; N, 7.19%.

References for Chapter 3

1. Edelmann, F. T. *Adv. Organomet. Chem.* **2008**, *57*, 183–352.
2. Littke, A. Sleiman, N.; Bensimon, C.; Richeson, D. S. *Organometallics* **1998**, *17*, 446–451.
3. (a) Flores, J. C.; Chien, J. C. W.; Rausch, M. D. *Organometallics* **1995**, *14*, 1827–1833.
   (b) Herskovics–Korine, D.; Eisen, M. S. *J. Organomet. Chem.* **1995**, *503*, 307–314.
   (c) Walther, D.; Fischer, R.; Görls, H.; Koch, J.; Schweder, B. *J. Organomet. Chem.* **1996**, *508*, 13–22.
   (d) Hagadorn, J. R.; Arnold, J. *K. J. Chem. Soc., Dalton Trans.* **1997**, 3087–3096.
4. Dick, D. G.; Duchateau, R.; Edema, J. J. H.; Gambarotta, S. *Inorg. Chem.* **1993**, *32*, 1959–1962.
5. (a) Hagadorn, J. R.; Arnold, J. *J. Am. Chem. Soc.* **1996**, *118*, 893–894.
   (b) Hagadorn, J. R.; Arnold, J. *Organometallics* **1998**, *17*, 1355–1368.
6. Otten, E.; Kijkstra, P.; Visser, C.; Meetsma, A.; Hessen, B. *Organometallics* **2005**, *24*, 4374–4386.
7. Yao, S.; Chan, H. –S.; Lam, C. –K.; Lee, H. K. *Inorg. Chem.* **2009**, *48*, 9936–9946.
8. Chao, Y. –W.; Wexler, P. A.; Wigley, D. E. *Inorg. Chem.* **1989**, *28*, 3860–3868.
9. Lee, H. K.; Lam, T. S.; Lam, C. –K.; Li, H. –W.; Fung, S. M. *New J. Chem.* **2003**, *27*, 1310–1318.
10. Stewart, P. J.; Blake, A. J.; Mountford, P. *Inorg. Chem.* **1997**, *36*, 3616–3622.
11. Edelmann, F. T. *Adv. Organomet. Chem.* **2008**, *57*, 183–352.
12. (a) Srinivas, B.; Chang, C. –C.; Chen, C. –H.; Chiang, M. Y.; Chen, I. –T.; Wang, Y.; Lee, G. –H. *J. Chem. Soc., Dalton Trans.* **1997**, 957–963.
    (b) Cole, M. L.; Evans, D. J.; Junk, P. C.; Louis, L. M. *New J. Chem.* **2002**, *26*, 1015–1024.
13. Cole, M. L.; Junk, P. C. *New J. Chem.* **2005**, *29*, 135–140.
14. Johnson, A. R.; Davis, W. M.; Cummins, C. C. *Organometallics* **1996**, *15*, 3825–3835.

Chapter 4

Divalent Lanthanide Complexes Derived from a 2-Pyridylamido ligand

The first part of this chapter covers a brief account on divalent lanthanide complexes and their reaction chemistry. The second part of this chapter focuses on our work on the coordination chemistry of the $[N(C_6H_3Pr^i_2\text{–}2,6)(2\text{–}C_5H_3N\text{–}6\text{–}Me)]^-$ *(*L^4*) ligand with divalent lanthanide ions [Sm(II), Eu(II) and Yb(II)]. Results of our studies on reactions of divalent lanthanide complexes of* L^4 *are also presented.*

Introduction

An Overview on Divalent Lanthanide Complexes

Divalent lanthanide compounds have attracted much attention due to their strong reducing properties. For instance, SmI_2 has proven to be an excellent one-electron reductant in organic synthesis.[1–3] Lanthanide(II) cyclopentadienyl (Cp) complexes have also been shown to be reactive in small-molecule transformations,[1,4,5] dinitrogen activation,[1] olefin polymerizations[1,6] and electron-transfer reactions (Scheme 4–1).[1,7–9]

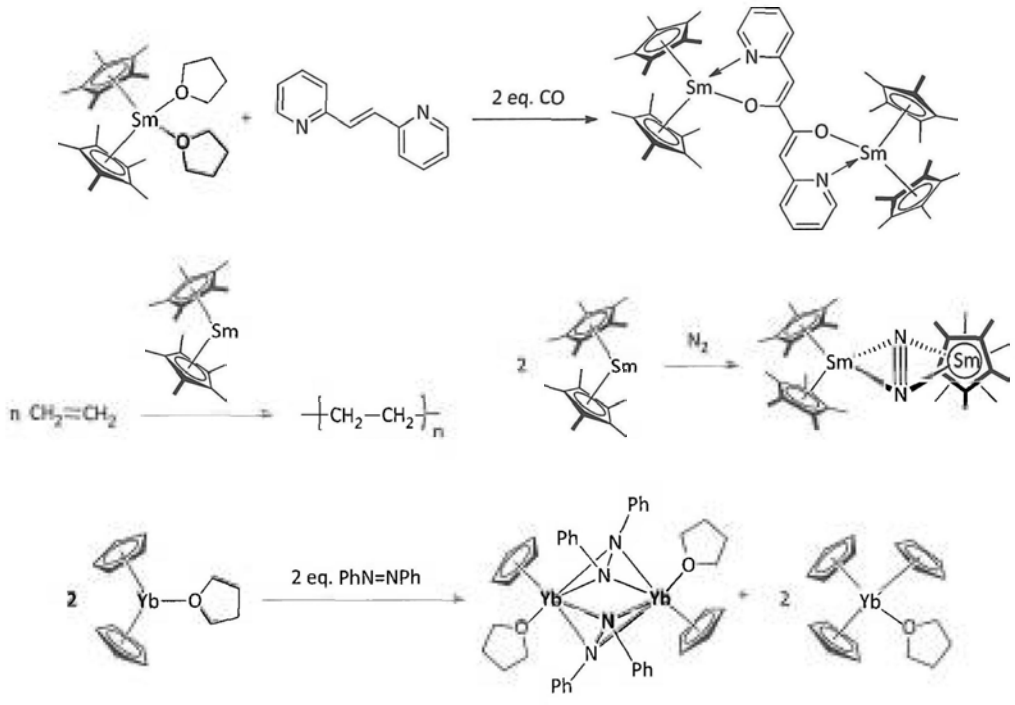

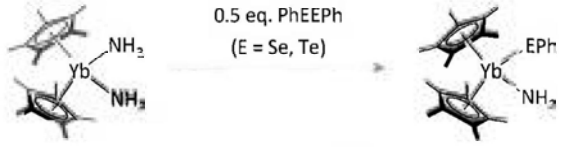

Scheme 4–1

Over the past decades, studies of lanthanide(II) complexes supported by anionic nitrogen-based ligands have attracted considerable attention. These studies were motivated by the development of alternative ligands as substitute for cyclopentadienyl anions. Using the bulky $[N(SiMe_3)_2]^-$ ligand, mononuclear bis(amido) Ln(II) complexes of the type $[Ln\{N(SiMe_3)_2\}_2(thf)_2]$ (Ln = Sm, Eu, Yb) were synthesized. The Eu(II) derivative $[Eu\{N(SiMe_3)_2\}_2(thf)_2]$ was prepared by reduction of its trivalent precursor $[Eu\{N(SiMe_3)_2\}_3/EuCl_3$ (2:1) mixture] with sodium naphthalene in thf.[10] The Sm(II) and Yb(II) analogues were prepared by treatment of the appropriate LnI_2 (Ln = Sm, Yb) with two equivalents of $MN(SiMe_3)_2$ (Ln = Sm, M = Na;[11] Ln = Yb, M = K[12]). The Yb(II) derivatives $[Yb\{N(SiMe_3)_2\}_2(L)_2]$ (L = OEt_2, dmpe, $AlMe_3$) were also prepared by Andersen and co-workers.[13] In addition, heterobimetallic Ln(II) complexes $[NaLn\{N(SiMe_3)_2\}_3]$ (Ln = Yb, Eu) were synthesized by the reaction of the appropriate $LnI_2(thf)_2$ with two equivalents of $NaN(SiMe_3)_2$ (Chart 4–1).[14] Monosubstituted Sm(II) complex $[\{Sm\{N(SiMe_3)_2\}(\mu\text{–}I)(dme)(thf)\}_2]$ was also prepared by reaction of $[Sm\{N(SiMe_3)_2\}_2(thf)_2]$ with one equivalent of $SmI_2(thf)_2$.[11]

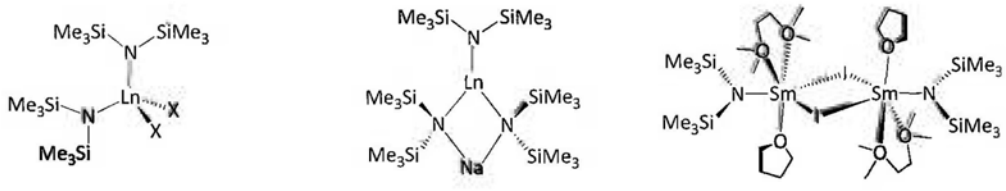

Ln = Eu, X = thf, dme Zalkin *et al.*[10]
Ln= Sm, X = thf Evans *et al.*[11]
Ln = Yb, X = thf Lappert *et al.*[12]
Ln = Yb, X = Et_2O, dmpe, $AlMe_3$ Andersen *et al.*[13]

Ln = Yb, Eu Andersen *et al.*[13]

Evans *et al.*[11]

Chart 4–1

Beside the bis(trimethylsilyl)amido ligand, arylamido ligands such as $[NPh_2]^-$,

$[NPh(SiMe_3)]^-$ and $[N(C_6H_3Pr^i_2\text{–}2,6)(SiMe_3)]^-$ were also shown to be versatile in supporting lanthanide(II) complexes. Neutral mononuclear Yb(II) complexes $Yb(NPh_2)_2(thf)_4$ and $Yb\{NPh(SiMe_3)\}_2(thf)_3$ were synthesized by salt elimination reactions of YbI_2 with an appropriate potassium amide (Scheme 4–2).[15] The dme-adduct $[Yb\{NPh(SiMe_3)\}_2(dme)_2]$ can be prepared by reduction of the trivalent precursor $[Yb\{NPh(SiMe_3)\}_2(thf)Cl]_2$ with Na/K alloy.[16] The lanthanide(II) complexes $[Ln\{N(C_6H_3Pr^i_2\text{–}2,6)(SiMe_3)\}_2(thf)_2]$ (Ln = Sm, Eu, Yb), were synthesized by redox transmetallation reactions of $Hg[N(C_6H_3Pr^i_2\text{–}2,6)(SiMe_3)]_2$ with elemental samarium, europium and ytterbium, respectively.[17]

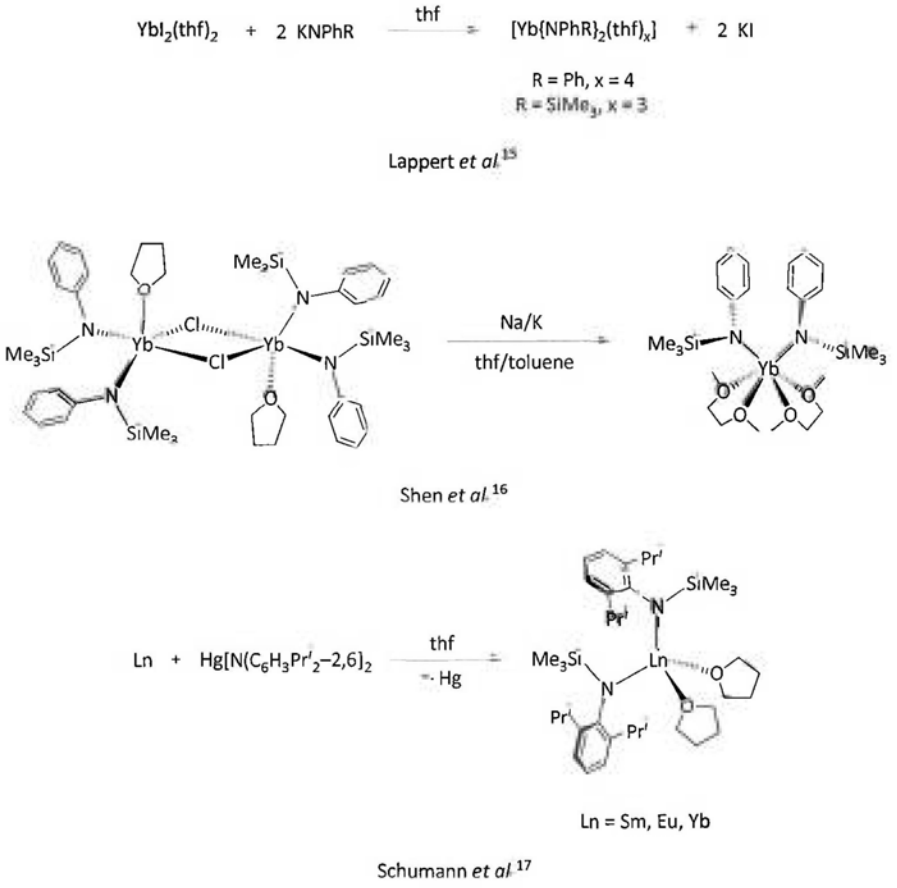

Scheme 4–2

Apart from the monodentate silyl- and arylamido ligands, bidentate

N-donating ligands such as β-diketiminates,[18–20] amidinates,[21–24] guanidinates,[25,26] and 2-pyridylamides[27–29] have also been employed in lanthanide(II) chemistry. Lappert and co-workers have reported the homoleptic $[Yb\{\{N(Ar)CPh\}_2CH\}_2]$ (Ar = $C_6H_3Pr^i_2$–2,6)], which were synthesized by reaction of $YbI_2(thf)_2$ with the corresponding sodium or potassium β-diketiminate. Alternatively, the compound could also be prepared by direct reaction of the ytterbium alkyl complex $[Yb\{CH(Ar)_2\}_2(OEt_2)_2]$ with PhCN (Scheme 4–3).[18] The heteroleptic $[\{Yb\{\{N(SiMe_3)CMe\}_2CH\}(I)(thf)\}_2]$ and $[\{Yb\{\{N(SiMe_3)CPh\}_2CH\}(I)(thf)\}_2]$ were also reported.[19] They were prepared by a salt elimination method from $YbI_2(thf)_2$ and the appropriate potassium salt, or ligand redistribution reactions of $YbI_2(thf)_2$ with the corresponding bis(β-diketiminate) complexes. In addition, the Eu(II) β-diketiminate complex $[Eu\{\{N(Ar')CMe\}_2CH\}_2(thf)]$ (Ar' = $C_6H_3Me_2$–2,6) was obtained unexpectedly in the reaction of $EuCl_3$ with $Na\{\{N(Ar')CMe\}_2CH\}$, in which oxidation-coupling of the β-diketiminate ligands occured.[20]

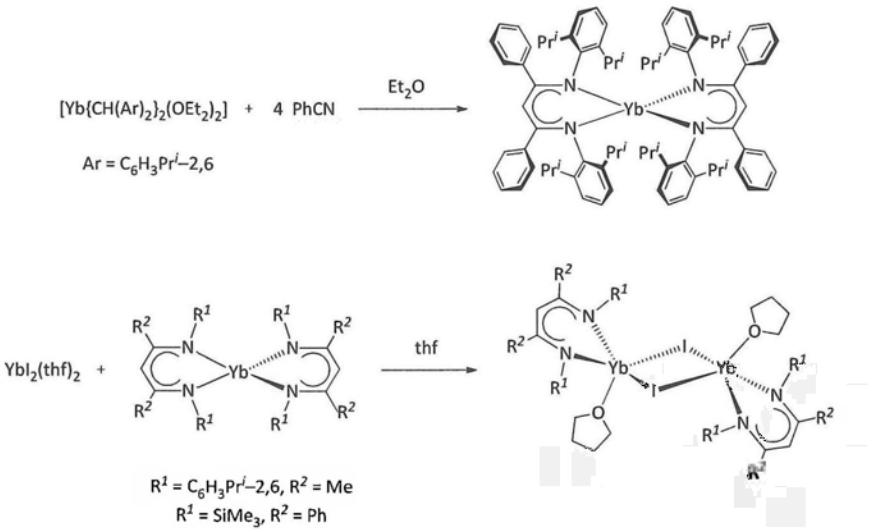

Lappert *et al.*[18,19]

Scheme 4–3

The heteroleptic Yb(II) complex $[\{Yb\{\{N(SiMe_3)CMe\}_2CH\}(I)(thf)\}_2]$ was shown

to be a good starting material for the preparation of other Yb(II) amide and hydrocarbyl complexes (Scheme 4–4).[19]

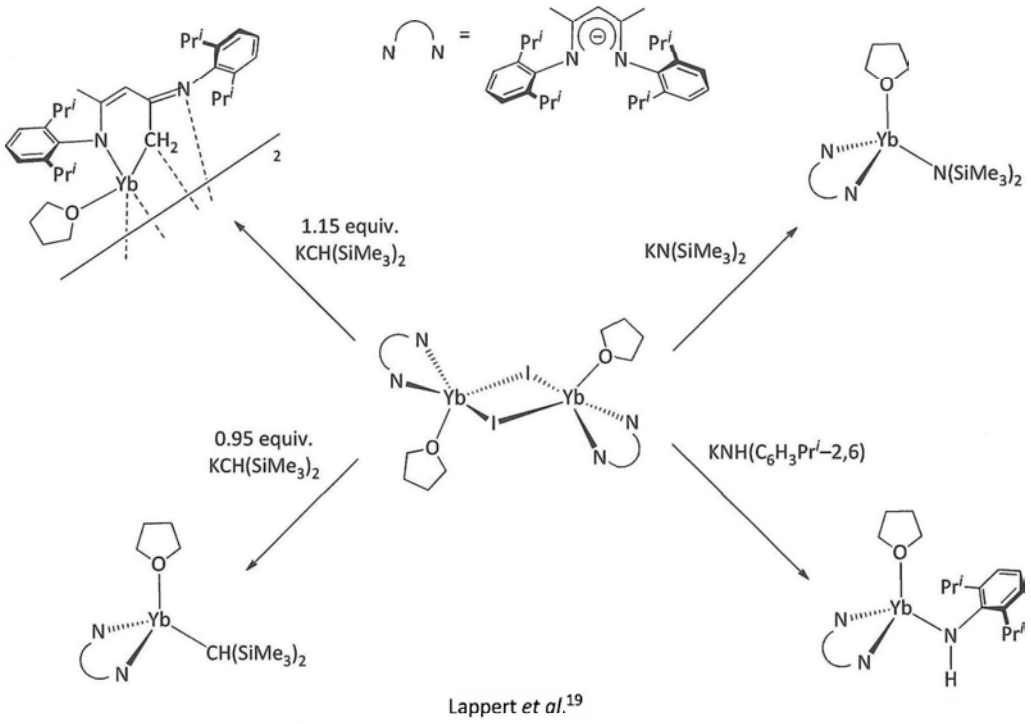

Scheme 4–4

The first Sm(II) formidinate complex $[Sm\{HC(NC_6H_3Pr^i_2\text{–}2,6)_2\}_2(thf)_2]$ was reported by Junk and co-workers.[21] It was synthesized by (i) a salt elimination reaction of $SmI_2(thf)_2$ with the corresponding sodium amidinate, (ii) transamination reaction of $[Sm\{N(SiMe_3)_2\}_2(thf)_2]$ with the ligand precursor $(C_6H_3Pr^i_2\text{–}2,6)NHCH{=}N(C_6H_3Pr^i_2\text{–}2,6)$, or (iii) redox transmetallation of excess samarium metal with bis(pentafluorophenyl)mercury and the precursor amidine $(C_6H_3Pr^i_2\text{–}2,6)NHCH{=}N(C_6H_3Pr^i_2\text{–}2,6)$. Using the *N*-silylated benzamidinate ligands $[(C_6H_4R\text{–}4)C(NSiMe_3)_2]^-$ (R = H, OMe, Ph), Edelmann and co-workers have successfully synthesized a series of Yb(II) complexes of the type

$[Yb\{(C_6H_4R–4)C(NSiMe_3)_2\}_2(thf)_x]$ (R = H, OMe, x = 2; R = Ph, x = 0).[22] Reactions of $[Yb\{PhC(NSiMe_3)_2\}_2(thf)_2]$ with $\{Me_2NCS_2\}_2$ gave the Yb(III) complex $[Yb\{PhC(NSiMe_3)_2\}_3(S_2CNMe_2)]$ (Scheme 4–5). Reactions of $[Yb\{(C_6H_4R–4)C(NSiMe_3)_2\}_2(thf)_2]$ (R = H, OMe) with diaryl diselenides and ditelluride led to the Yb(III) complexes $[Yb\{PhC(NSiMe_3)_2\}_2(SeR')(thf)]$ (R' = Ph, Mes) and $[Yb\{(C_6H_4OMe–4)C(NSiMe_3)_2\}_2(TeR')(thf)]$ (R' = Mes).[22,23] Recently, a series of Sm(II), Eu(II) and Yb(II) complexes supported by the unsymmetrical amidinate ligand $[PhC(NC_6H_3Pr^i_2–2,6)(NSiMe_3)]^-$ have been reported.[23] The reaction chemistry of these complexes has also been studied (Scheme 4–6).

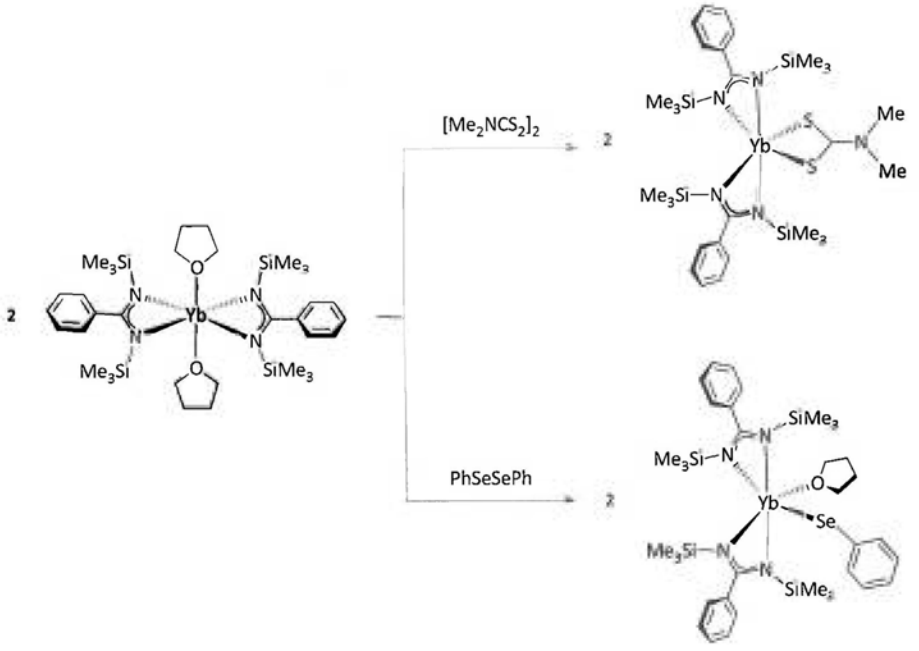

Edelmann *et al.*[22]

Scheme 4–5

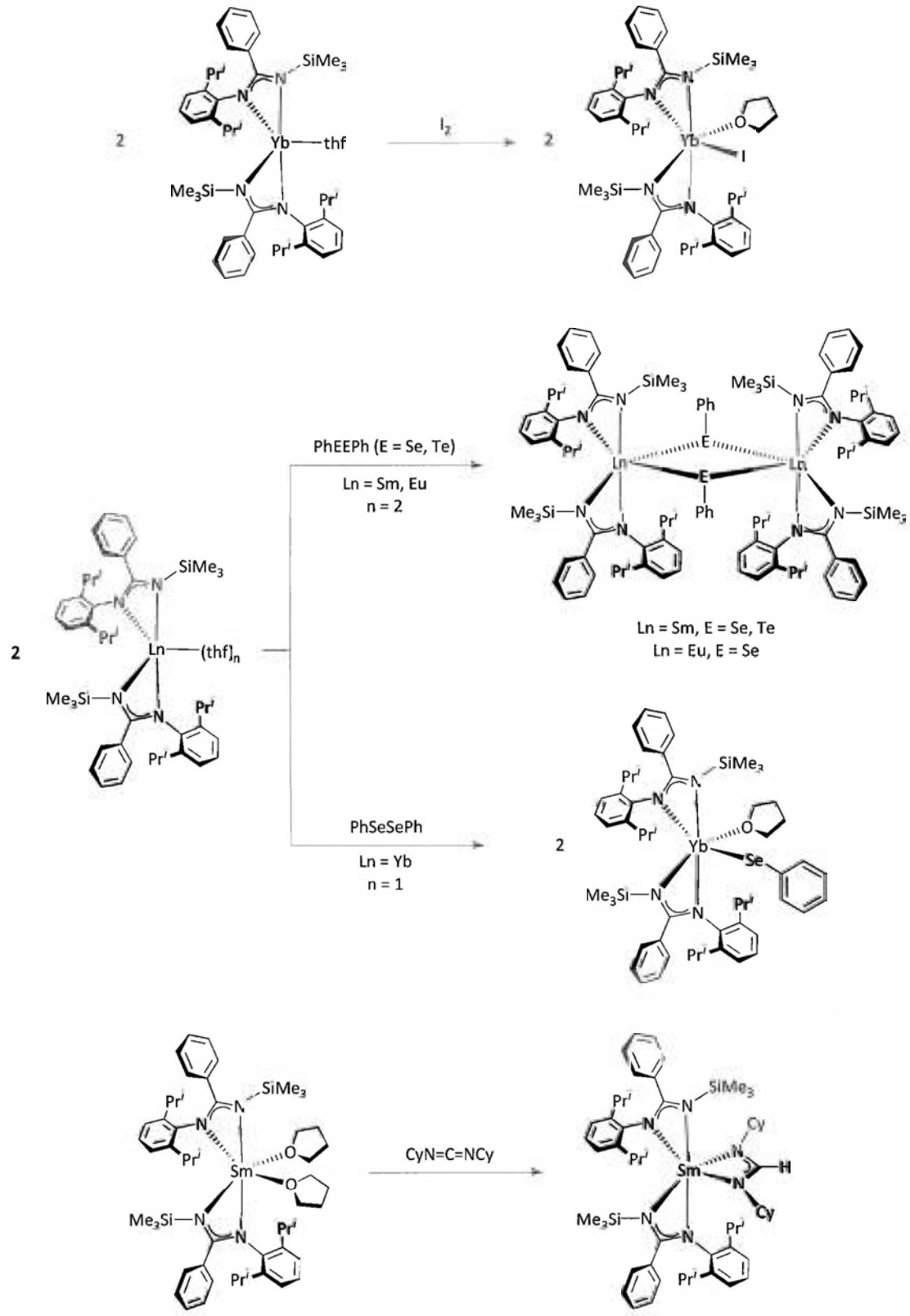

Lee *et al.*[24]

Scheme 4–6

Homoleptic guanidinate complexes $[Ln\{Cy_2NC(NC_6H_3Pr^i_2\text{–}2,6)_2\}_2]$ (Ln = Sm, Eu, Yb) have been reported by Jones and co-workers (Chart 4–2).[25] The Sm(II) and Eu(II) bis(guanidinates) were found to adopt a planar coordination geometry in the solid state, which is rarely observed for four-coordinate lanthanide(II) complexes derived from bidentate ligands. The related $[Ln\{Pr^i_2NC(NC_6H_3Pr^i_2\text{–}2,6)_2\}_2]$ (Ln = Sm, Eu, Yb) were also prepared.[26] Reaction of $[Sm\{Pr^i_2NC(NC_6H_3Pr^i_2\text{–}2,6)_2\}_2]$ with CS_2 led to reductive coupling of CS_2.

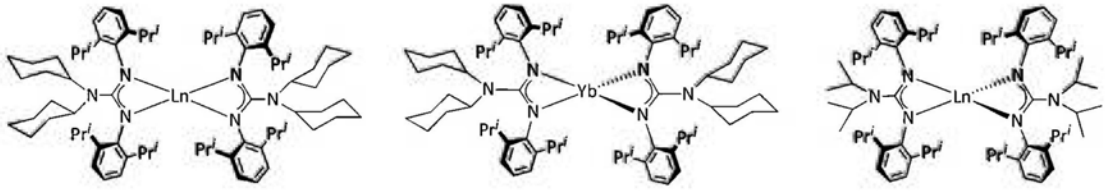

Jones *et al.*[25,26]

Chart 4–2

A few examples of divalent lanthanide complexes supported by very bulky 2-pyridylamido ligands have been reported (Chart 4–3). Heteroleptic complexes $[\{Ln(Ap^*)(I)(thf)_2\}_2]$ [Ln = Sm,[27] Eu,[28] Yb[27]; Ap* = $N(C_6H_3Pr^i_2\text{–}2,6)\{2\text{–}C_5H_3N\text{–}6\text{–}(C_6H_2Pr^i_3\text{–}2,4,6)\}$] were synthesized by reactions of $LnI_2(thf)_x$ (Ln = Sm, Yb, x = 3; Ln = Eu, x = 5) with KAp*. Reductions of $[\{Ln(Ap^*)(I)(thf)_2\}_2]$ (Ln = Eu, Yb) with KC_8 led to the neutral mononuclear $[Ln(Ap^*)_2(thf)_2]$.[28] The related mononuclear Yb(II) complexes $[Yb(Ap')_2(thf)]$ [Ap' = $N(C_6H_3Pr^i_2\text{–}2,6)\{2\text{–}C_5H_3N\text{–}6\text{–}(C_6H_3Me_2\text{–}2,6)\}$] and $[Yb(Ap^{Me})_2(thf)_2]$ [Ap^{Me} = $N(C_6H_2Me_3\text{–}2,4,6)\{2\text{–}C_5H_3N\text{–}6\text{–}(C_6H_2Me_3\text{–}2,4,6)\}$] were also prepared by reactions of $YbI_2(thf)_4$ with the corresponding potassium amides.[29] The unsolvated $[Yb(Ap')_2]$ was obtained by treatment of ytterbium metal with ligand

precursor Ap'H and metallic mercury.

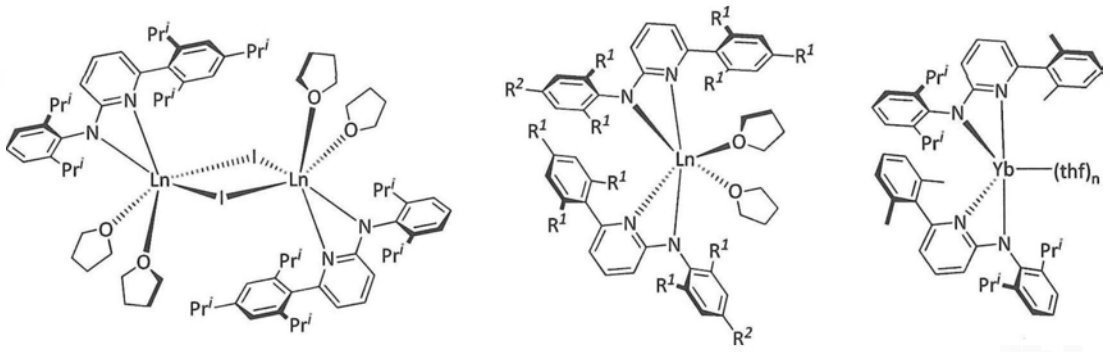

Ln = Sm, Eu, Yb

$R^1 = Pr^i$, $R^2 = H$; Ln = Eu, Yb
$R^1 = R^2 = Me$; Ln = Yb

n = 0 or 1

Kempe *et al.*[27-29]

Chart 4–3

Synthesis and structural studies of divalent lanthanide complexes supported by anionic *N*-donating ligands still remain an underdeveloped area. Moreover, the reaction chemistry of these complexes has been rarely reported. Accordingly, the coordination chemistry of the $[N(C_6H_3Pr^i_2\text{–}2,6)(2\text{–}C_5H_3N\text{–}6\text{–}Me)]^-$ (L^4) ligand towards lanthanide(II) ions and the reaction chemistry of our new divalent lanthanide complexes have been studied in this work.

Results and Discussion

Lanthanide Complexes of the $[N(C_6H_3Pr^i_2\text{–}2,6)(2\text{–}C_5H_3N\text{–}6\text{–}Me)]^-$ (L^4) Ligand

A. Synthesis of Ligand Precursor $[HN(C_6H_3Pr^i_2\text{–}2,6)(2\text{–}C_5H_3N\text{–}6\text{–}Me)]$ (HL^4) and the Corresponding Potassium Amides

The ligand precursor $[HN(C_6H_3Pr^i_2\text{–}2,6)(2\text{–}C_5H_3N\text{–}6\text{–}Me)]$ (HL^4) (**41**) was prepared by a palladium-catalyzed aryl amination method similar to the one reported by Buchwald and co-workers.[30] Treatment of $H_2N(C_6H_3Pr^i_2\text{–}2,6)$ with $2\text{–}BrC_5H_3N\text{–}6\text{–}Me$ in the presence of $NaOBu^t$, 1% tris(dibenzylideneacetone)-dipalladium(0) $[Pd_2(dba)_3]$, and 3% 1,3–bis(diphenylphosphanyl)propane (DPPP) in toluene under reflux for two days gave compound **41** as a pale yellow solid in 80% yield (Scheme 4–7).

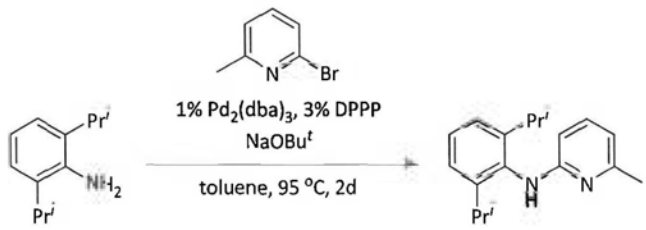

41 80 %

Scheme 4–7

Deprotonation of compound **41** with potassium hydride in diethyl ether led to the dimeric potassium amide $[\{KL^4(OEt_2)\}_2]$ (**42**) (Scheme 4–8). On the other hand, treatment of **41** with potassium hydride in thf yielded $KL^4(thf)_2$ (**43**).

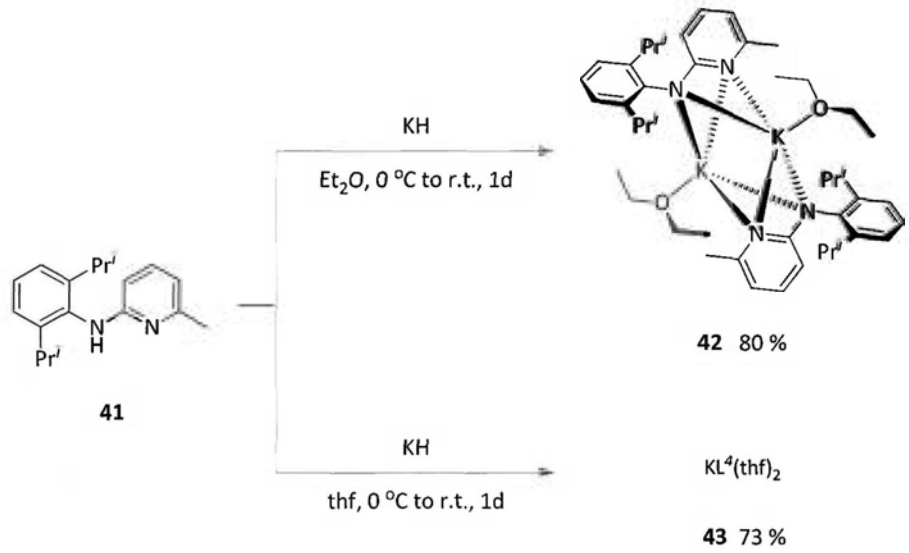

Scheme 4–8

Physical Characterization of Compounds **41–43**

Tables 4–1 listed some of the physical properties of compounds **41–43**. The formulation of these compounds was confirmed by NMR spectroscopy and elemental analysis. The solid-state structures of **41** and **42** were elucidated by X-ray crystallography.

Table 4–1 Some physical properties of compounds **41–43**.

Compound	Appearance	M.p. (°C)
$[HL^4]$ (**41**)	Pale yellow solid	127–130
$[\{KL^4(OEt_2)\}_2]$ (**42**)	Colorless crystals	261–266
$KL^4(thf)_2$ (**43**)	Colorless crystals	294–297

NMR Spectra of Compounds **41–43**

1. [HL^4] (**41**)

The ^1H and ^{13}C NMR spectra of compound **41** (Figures A2–47 and A2–48 in Appendix 2) showed well-resolved resonance signals corresponding to [HL^4].

2. [{$KL^4(OEt_2)$}$_2$] (**42**) and $KL^4(thf)_2$ (**43**)

The ^1H and ^{13}C NMR spectra of compounds **42** and **43** are shown in Figures A2–49 to A2–52 in Appendix 2. The NMR spectra showed one set of resonance signals assignable to the L^4 ligand, indicating that the two L^4 ligands in each complex are chemically equivalent. The ratio of L^4 : Et_2O as shown in the ^1H NMR spectrum of **42** is 1:1, whereas the L^4 : thf ratio in the ^1H NMR spectrum of **43** is 1:2. Only one septet assignable to the isopropyl methine protons (at 2.92 ppm for **42** and 3.03 ppm for **43**) was observed in each ^1H NMR spectrum, indicating that the two isopropyl substituents of the L^4 ligand are identical to each other. However, two nonequivalent methyl groups (with resonance signals at 0.93 and 1.18 ppm for **42**, and 1.00 and 1.23 ppm for **43**) were observed in each spectrum. This suggests that the geminal methyl groups of the isopropyl substituent are diastereotopic.

Crystal Structure of Complex **42**

The molecular structure of complex **42** is shown in Figure 4–1 with selected bond distances and angles summarized in Table 4–2. Selected crystallographic data of the complex are listed in Appendix 3. Single crystals of **42** were obtained from diethyl ether. Complex **42** crystallizes as a dimer in the triclinic space group

$P\bar{1}$. The crystal structure of **42** consists of two potassium ions and two bridging L^4 ligands. Each potassium ion is also bound by one diethyl ether molecule, which forms a distorted tetrahedral geometry around the alkali metal atom.

The observed K–N_{amido} distance of 2.785(1) Å in complex **42** is shorter than the corresponding distances reported for [{K{N(SiBu^{t}Me$_2$)(2–C$_5$H$_3$NMe–6)}(tmeda)}$_2$] [2.875(4) and 2.034(4) Å],[31] [{K{N(SiMe$_3$)(Py)}(12C4)}$_2$] [2.858(2) and 2.912(2) Å],[32] [{K{N(Ph)(Py)}(12C4)}$_2$] [2.798(4)–2.904(5) Å][33] and [(K{μ–N(Ph)(Py)})$_2$(μ'–thf)$_3$]$_\infty$ [2.836(2) and 2.924(2)].[34] The K–$N_{pyridyl}$ distance of 2.850(2) Å is also slightly shorter than the corresponding bond lengths reported for [{K{N(SiBu^{t}Me$_2$)(2–C$_5$H$_3$NMe–6)}(tmeda)}$_2$] [2.906(4) and 2.955(4) Å],[31] [{K{N(SiMe$_3$)(Py)}(12C4)}$_2$] [2.853(2) and 2.858(2) Å],[32] [{K{N(Ph)(Py)}(12C4)}$_2$] [2.911(5)–2.991(5) Å][33] and [(K{μ–N(Ph)(Py)})$_2$(μ'–thf)$_3$]$_\infty$ [2.870(2) and 2.908(2)].[34] The N_{amido}–K–$N_{pyridyl}$ bite angles in complex **42** [47.98(5)°] is acute.

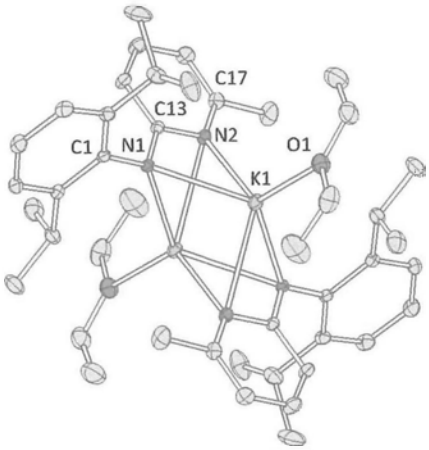

Figure 4–1 Molecular structure of $[K(L^4)(OEt_2)]_2$ (**42**).

Table 4–2 Selected bond lengths (Å) and angles (deg.) for compound **42**

$[K(L^4)(OEt_2)]_2$ (**42**)			
K(1)–N(1)	2.785(1)	K(1)–N(2)	2.850(2)
K(1)–O(1)	2.749(2)	N(1)–C(13)	1.336(3)
N(2)–C(13)	1.376(3)	N(1)–C(1)	1.418(3)
N(2)–C(17)	1.352(3)		
N(1)–K(1)–N(2)	47.98(5)	N(1)–K(1)–O(1)	121.56(6)
N(2)–K(1)–O(1)	126.96(7)		

B. Synthesis of Lanthanide(II) Amido Complexes

The coordination chemistry of the L^4 ligand towards divalent lanthanide ions [Yb(II), Eu(II) and Sm(II)] has been studied in this work. Metathetical reactions of $LnI_2(thf)_2$ with $[\{KL^4(OEt_2)\}_2]$ (**42**) yielded the corresponding lanthanide amido complexes **44–46** (Scheme 4–9).

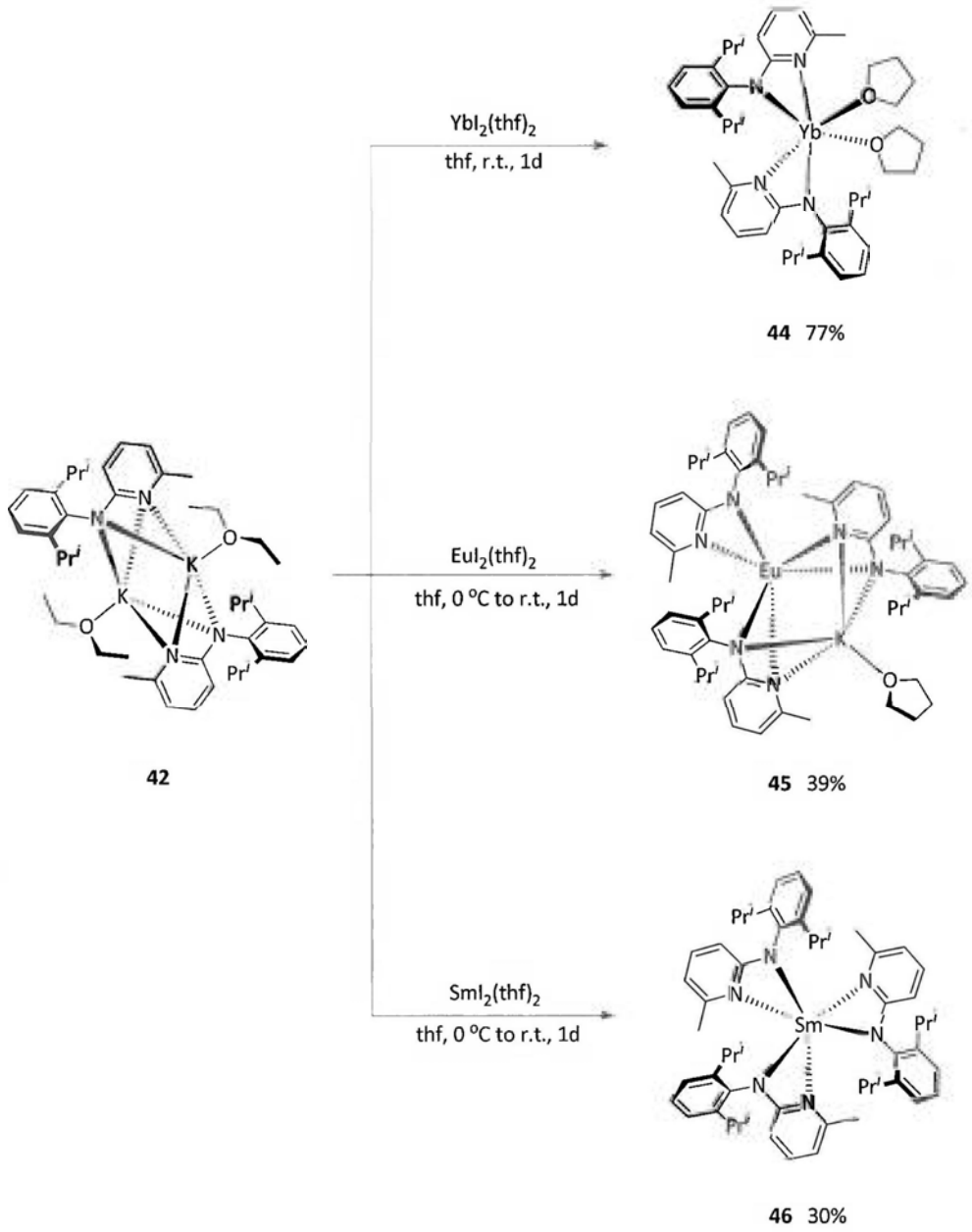

Scheme 4–9

Reaction of **42** with $YbI_2(thf)_2$ in thf afforded the neutral Yb(II) complex $[Yb(L^4)_2(thf)_2]$ (**44**) as dark purple crystals in 77% yield. Treatment of **42** with $EuI_2(thf)_2$ under a similar reaction condition gave the orange crystalline heterobimetallic complex $[Eu(L^4)(\mu\text{–}L^4)_2K(thf)]$ (**45**) in 39% yield. Both complexes **44** and **45** are sensitive to air and moisture, turning to a yellow and red solid, respectively, upon exposure to air.

A neutral Yb(II) complex of the L^4 ligand (**44**) was obtained in the present study. On the other hand, the Eu(II) derivative (**45**) was isolated as an *ate*-complex. This can be attributed to a larger ionic radius of Eu(II) ion as compared to that of Yb(II) ion.

On the other hand, reaction of **42** with $SmI_2(thf)_2$ led to the homoleptic Sm(III) derivative $[Sm(L^4)_3]$ (**46**), which was isolated as yellow crystals (30% yield). The same product could also be obtained (18% yield) a transamination reaction of **41** with $[Sm(N(SiMe_3)_2)_2(thf)_2]$. It is believed that the highly reducing property of the Sm(II) ion (more negative reduction potential of the Sm(III)/Sm(II) couple) favors the formation of **46** instead of a Sm(II) complex.

Physical Characterization of Complexes **44–46**

Tables 4–3 listed some of the physical properties of compounds **44–46**. The formulation of these complexes was confirmed by elemental analysis. ^1H and ^{13}C NMR spectra of **44** and **46** were also measured. The solid-state structures of **44–46** were elucidated by single-crystal X-ray diffraction study.

Table 4–3 Some physical properties of compounds **44–46**.

Compound	Appearance	M.p. (°C)
$[Yb(L^4)_2(thf)_2]$ (**44**)	Dark purple crystals	216–219 (dec)
$[Eu(L^4)(\mu\text{–}L^4)_2K(thf)]$ (**45**)	Orange crystals	190–193
$[Sm(L^4)_3]$ (**46**)	Yellow crystals	Dec. at 357–359 °C without melting

NMR Spectra of Complexes **44** and **46**

1. $[Yb(L^4)_2(thf)_2]$ (**44**)

The ^1H and ^{13}C NMR spectra of the diamagnetic Yb(II) complex **44** showed one set of resonance signals assignable to two L^4 ligands and two thf molecules (Figures A2–53 and A2–54). In the ^1H NMR spectrum, the isopropyl methine protons occur as one resonance signal at 3.49 ppm, indicating that the two isopropyl substituents of the L^4 ligand are equivalent. However, the isopropyl methyl groups appear as two doublets at 1.11 and 1.27 ppm. This indicates that the isopropyl methyl groups are diastereotopic.

2. $[Sm(L^4)_3]$ (**46**)

The ^1H NMR spectrum of the paramagnetic complex **46** showed one set of isotropically shifted signals, which are assignable to the L^4 ligand based on the integration of these signals (Figures A2–55).

Crystal Structures of Compounds **44–46**

The solid-state structures of complexes **44–46** were elucidated by

single-crystal X-ray diffraction analysis. Selected crystallographic data of these complexes are listed in Appendix 3.

1. $[Yb(L^4)_2(thf)_2]$ (**44**)

The molecular structure of complex **44** is shown in Figure 4–2. Selected bond lengths and angles are listed in Table 4–4. Crystals of complex **44** were obtained from a toluene solution. They belong to the triclinic space group $P\bar{1}$. The Yb(II) center in the mononuclear complex is bound by two L^4 ligands and two thf molecules. The coordination geometry around the metal center can be described as distorted octahedral.

The observed Yb–N_{amido} distances in complex **44** are 2.427(3) and 2.431(3) Å. Comparing with other neutral six-coordinate Yb(II) complexes, they are close to those in $[Yb(Ap^*)_2(thf)_2]$ [Ap* = $N(C_6H_3Pr^i_2–2,6)\{2–C_5H_3N–6–(C_6H_2Pr^i_3–2,4,6)\}$] [2.431(6) and 2.464(7) Å],[28] but longer than that in $[Yb(Ap^{Me})_2(thf)_2]$ [Ap^{Me} = $N(C_6H_2Me_3–2,4,6)\{2–C_5H_3N–6–(C_6H_2Me_3–2,4,6)\}$] [2.396(5) Å].[29] Apparently, the more bulky L^4 and Ap* ligands lead to longer Yb–N distances in **44** and $[Yb(Ap^*)_2(thf)_2]$ as compared with that of $[Yb(Ap^{Me})_2(thf)_2]$. The Yb–N_{amido} distances in complex **44** are also longer than the corresponding distances in the five-coordinate $[Yb(Ap')_2(thf)]$ [Ap' = $N(C_6H_3Pr^i_2–2,6)\{2–C_5H_3N–6–(C_6H_3Me_2–2,6)\}$] [2.380(4) and 2.384(3) Å] and the four-coordinate $[Yb(Ap')_2]$ [2.371(1) and 2.404(1) Å].[29] This may be ascribed to the more crowded six-coordinate environment around the Yb(II) ion in complex **44**.

The observed Yb–$N_{pyridyl}$ distances in complex **44** are 2.451(3) and 2.505(4) Å. They are slightly shorter than those of 2.511(5) and 2.511(6) Å in $[Yb(Ap^*)_2(thf)_2]$,[28] and 2.544(4) Å in $[Yb(Ap^{Me})_2(thf)_2]$,[29] but comparable to those reported for

[Yb(Ap')$_2$(thf)] [2.479(4) and 2.466(4) Å] and [Yb(Ap')$_2$] [2.432(1) and 2.449(1) Å].[29] The N_{amido}–Yb–$N_{pyridyl}$ bite angles in complex **44** are acute, namely 55.0(1)° and 55.5(1)°.

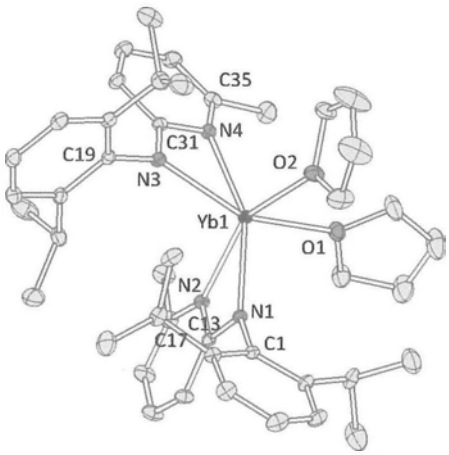

Figure 4–2 Molecular structure of $[Yb(L^4)_2(thf)_2]$ (**44**).

Table 4–4 Selected bond lengths (Å) and angles (deg.) for compound **44**.

$[Yb(L^4)_2(thf)_2]$ (**44**)			
Yb(1)–N(1)	2.431(3)	Yb(1)–N(2)	2.451(3)
Yb(1)–N(3)	2.427(3)	Yb(1)–N(4)	2.505(4)
Yb(1)–O(1)	2.488(3)	Yb(1)–O(2)	2.416(3)
N(1)–C(13)	1.338(5)	N(2)–C(13)	1.376(5)
N(1)–C(1)	1.425(5)	N(2)–C(17)	1.358(5)
N(3)–C(31)	1.327(5)	N(4)–C(31)	1.383(5)
N(3)–C(19)	1.430(5)	N(4)–C(35)	1.348(6)
N(1)–Yb(1)–N(2)	55.5(1)	N(3)–Yb(1)–N(4)	55.0(1)
N(1)–Yb(1)–N(3)	112.0(1)	N(1)–Yb(1)–N(4)	154.2(1)
N(2)–Yb(1)–N(3)	100.7(1)	N(2)–Yb(1)–N(4)	102.3(1)
O(1)–Yb(1)–O(2)	82.5(1)		

2. $[Eu(L^4)(\mu\text{–}L^4)_2K(thf)]$ (**45**)

The crystal structure of complex **45** is shown in Figure 4–3 with selected bond distances and angles listed in Table 4–5.

Complex **45** crystallizes in the triclinic space group $P\bar{1}$. In each molecule, the Eu(II) center is coordinated by one *N,N'*-chelating and two *N,N'*-bridging L^4 ligands. The latters are further coordinated to potassium ion K(1). Coordination of a thf molecule completes a distorted octahedral geometry around the potassium cation. The Eu(II) center adopts a distorted octahedral coordination geometry.

The observed Eu–N_{amido}(terminal) distance [Eu(1)–N(1)] [2.563(3) Å] in complex **45** is very close to the corresponding values in the $[Eu(Ap^*)_2(thf)_2]$ [2.526(6) and 2.547(6)],[28] but longer the Eu–N_{amido}(terminal) distances in $[Eu\{N(SiMe_3)_2\}\{\mu\text{–}N(SiMe_3)_2\}_2Na]$ [2.448(4) Å][14] and $[\{Eu(Ap^*)(I)(thf)_2\}_2]$ [Ap* = $N(C_6H_3Pr^i_2\text{–}2,6)\{2\text{–}C_5H_3N\text{–}6\text{–}(C_6H_2Pr^i_3\text{–}2,4,6)\}$] [2.481(3) Å].[28] The more crowded ligand environment in **45** and $[Eu(Ap^*)_2(thf)_2]$ leads to the longer Eu–N_{amido}(terminal) distances in these complexes as compared with that of $[\{Eu(Ap^*)(I)(thf)_2\}_2]$. The Eu–$N_{amido}$(bridging) distances in **45** are 2.582(3) and 2.718(3) Å. They are slightly longer than the Eu–N(bridging) distances in $[Eu\{N(SiMe_3)_2\}\{\mu\text{–}N(SiMe_3)_2\}_2Na]$ [2.539(4) and 2.554(4) Å].[14]

The observed Eu–$N_{pyridyl}$(terminal) distance in complex **45** [2.605(3) Å] is comparable to that of 2.583(3) Å in $[\{Eu(Ap^*)(I)(thf)_2\}_2]$, but slightly shorter than those of 2.671(6) and 2.691(6) Å in $[Eu(Ap^*)_2(thf)_2]$.[28] The bridging Eu–$N_{pyridyl}$ distances of in **45** are 2.610(3) and 2.682(3) Å. The N_{amido}–Eu–$N_{pyridyl}$ bite angle subtended by the terminal L^4 ligand in complex **45** [52.1(1)°] is acute.

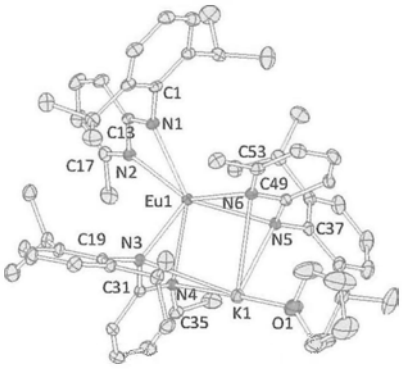

Figure 4–3 Molecular structure of [Eu(L^4)(μ–L^4)$_2$K(thf)] (**45**).

Table 4–5 Selected bond lengths (Å) and angles (deg.) for compound **45**.

[Eu(L^4)(μ–L^4)$_2$K(thf)] (**45**)			
Eu(1)–N(1)	2.563(3)	Eu(1)–N(2)	2.605(3)
Eu(1)–N(3)	2.582(3)	Eu(1)–N(4)	2.682(3)
Eu(1)–N(5)	2.718(3)	Eu(1)–N(6)	2.610(3)
K(1)–N(3)	3.11(4)	K(1)–N(4)	2.958(3)
K(1)–N(5)	2.928(3)	K(1)–N(6)	3.110(3)
K(1)–O(1)	2.666(4)	N(1)–C(13)	1.321(5)
N(2)–C(13)	1.370(5)	N(1)–C(1)	1.433(5)
N(2)–C(17)	1.343(5)	N(3)–C(31)	1.339(5)
N(4)–C(31)	1.376(5)	N(3)–C(19)	1.432(5)
N(4)–C(35)	1.347(5)	N(5)–C(49)	1.335(5)
N(6)–C(49)	1.371(5)	N(5)–C(37)	1.431(5)
N(6)–C(53)	1.345(5)		
N(1)–Eu(1)–N(2)	52.1(1)	N(3)–Eu(1)–N(4)	51.2(1)
N(5)–Eu(1)–N(6)	50.4(1)	N(1)–Eu(1)–N(3)	107.2(1)
N(1)–Eu(1)–N(4)	145.9(1)	N(1)–Eu(1)–N(5)	130.1(1)
N(1)–Eu(1)–N(6)	95.1(3)	N(2)–Eu(1)–N(3)	104.0(1)
N(2)–Eu(1)–N(4)	103.0(1)	N(2)–Eu(1)–N(5)	137.6(1)
N(2)–Eu(1)–N(6)	144.5(1)	N(3)–Eu(1)–N(5)	112.0(1)
N(3)–Eu(1)–N(6)	98.3(1)	N(5)–K(1)–N(6)	44.0(1)
N(3)–K(1)–N(4)	44.0(1)	N(3)–K(1)–N(5)	93.3(1)
N(3)–K(1)–N(6)	78.3(1)	O(1)–K(1)–N(3)	134.2(1)
O(1)–K(1)–N(4)	177.5(1)	O(1)–K(1)–N(5)	106.6(1)
O(1)–K(1)–N(6)	88.0(1)		

3. $[Sm(L^4)_3]$ (**46**)

The molecular structure of complex **46** is shown in Figure 4–5. Selected bond lengths and angles of the complex are summarized in Table 4–6. Complex **46** crystallizes in the hexagonal crystal system with space group *P*3. The solid-state structure consists of two independent molecules in the asymmetric unit. The Sm(III) ions in the complex is bounded by three *N,N'*-chelating L^4 ligands, with a crystallographic three-fold axis passing through the metal center.

The observed Sm–N_{amido} distances of 2.338(6) and 2.383(5) Å in **46** are comparable to those of 2.369(3)–2.378(3) Å in the related $[Sm\{N(SiBu^tMe_2)(2\text{–}C_5H_3N\text{–}6\text{–}Me)\}_3]$,[31] and 2.334(2) and 2.352(2) Å in the bis(amido) complex $[Sm(Ap')_2(Cl)(thf)]$.[35] The Sm–$N_{pyridyl}$ distances [2.489(7) and 2.511(6) Å] in **46** are longer than the corresponding Sm–N_{amido} distances, suggesting that L^4 binds as a pyridylamido ligand. The Sm–$N_{pyridyl}$ distances are comparable to the corresponding distances in other related Sm(II) amido complexes.[31,35] The N_{amido}–Sm–$N_{pyridyl}$ bite angles are acute, namely 55.0(1)° and 56.1(1)°.

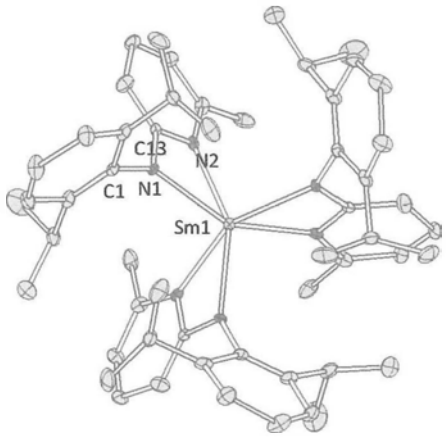

Figure 4–5 Molecular structure of $[Sm(L^4)_3]$ (**46**).

Only one of the two independent molecules in the asymmetric unit is shown.

Table 4–6 Selected bond lengths (Å) and angles (deg.) for compound **46**.

$[Sm(L^4)_3]$ (**46**)			
Sm(1)–N(1)	2.38(1)	Sm(1)–N(2)	2.49(1)
N(1)–C(13)	1.38(1)	N(2)–C(13)	1.38(1)
N(1)–C(1)	1.43(1)	N(2)–C(17)	1.40(1)
Sm(1')–N(1')	2.34(1)	Sm(1')–N(2')	2.51(1)
N(1')–C(13')	1.29(1)	N(2')–C(13')	1.36(1)
N(1')–C(1')	1.43(1)	N(2')–C(17')	1.29(1)
N(1)–Sm(1)–N(2)	56.1(1)	N(1)–Sm(1)–N(1)#3	112.3(1)
N(1)–Sm(1)–N(2)#3	98.0(1)	N(2)–Sm(1)–N(1)#3	149.5(1)
N(2)–Sm(1)–N(2)#3	95.5(1)		
N(1')–Sm(1')–N(2')	55.0(1)	N(1')–Sm(1')–N(1')#1	111.6(1)
N(1')–Sm(1')–N(2')#1	149.4(1)	N(2')–Sm(1')–N(1')#1	98.9(1)
N(2')–Sm(1')–N(2')#1	97.3(1)		

C. Reactivity Studies

1. Reactions of $[Yb(L^4)_2(thf)_2]$ (**44**) and $[Eu(L^4)(\mu\text{–}L^4)_2K(thf)]$ (**45**) with I_2

Complex **44** reacted readily with I_2 in thf to give the Yb(III) complex $[Yb(L^4)_2(I)(thf)]$ (**47**) (Scheme 4–10). It was isolated from a concentrated thf solution as orange-red crystals in 56% yield. Complex **47** is readily soluble in thf, but only sparingly soluble in toluene.

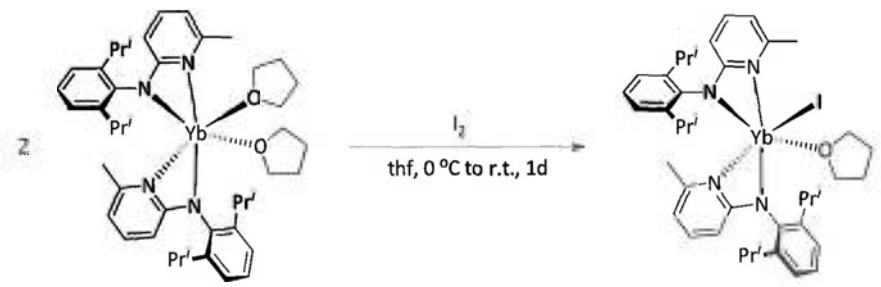

44 **47** 45%

Scheme 4–10

Treatment of complex **45** with I_2 under a similar reaction condition led to the homoleptic Eu(III) complex $[Eu(L^4)_3]$ (**48**) (Scheme 4–11). It is believed that the presence of three chelating L^4 ligands prevent the coordination of iodide ligand to the Eu(III) center. Complex **48** was isolated as purple crystals in 64% yield. It is readily soluble in thf and toluene.

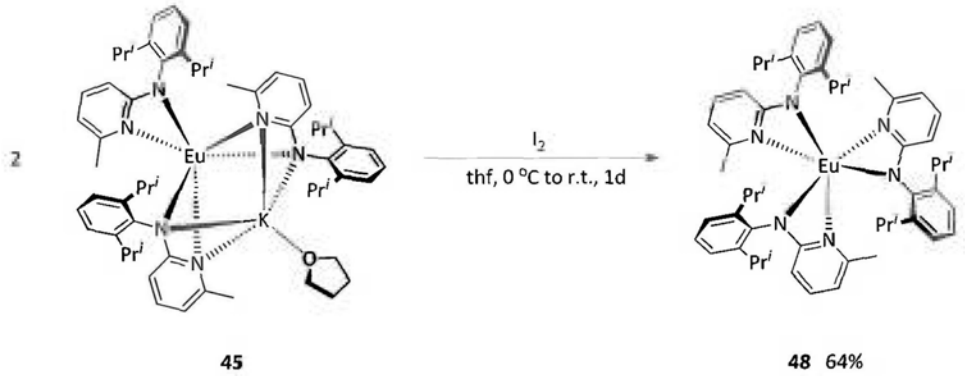

Scheme 4–11

2. Reaction of $[Yb(L^4)_2(thf)_2]$ (**44**) with CuI

Reaction of complex **44** with CuI gave the Yb(III) complex **47** (Scheme 4–12). The oxidation of Yb(II) to Yb(III) by Cu(I) led to deposition of a copper mirror on the reaction vessel.

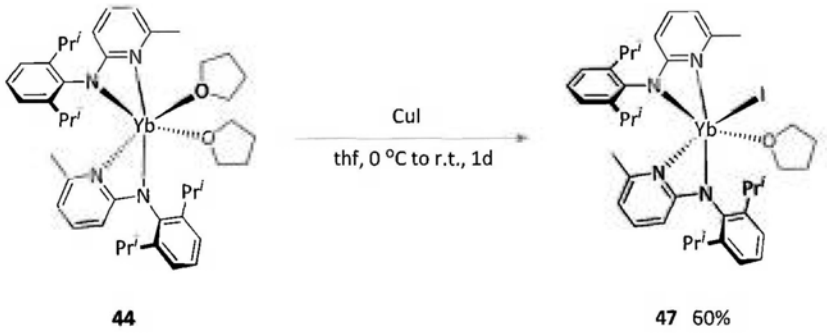

Scheme 4–12

3. Reactions of $[Yb(L^4)_2(thf)_2]$ (**44**) with PhEEPh (E = S, Se, Te)

The reactions of complex **44** with PhEEPh (E = S, Se, Te) were also examined. Interestingly, the homoleptic Yb(III) complex $[Yb(L^4)_3]$ (**49**) was the only isolable

product in these reactions (Scheme 4–13). Complex **49** is readily soluble in thf and toluene. It was isolated as yellow crystals from a toluene solution.

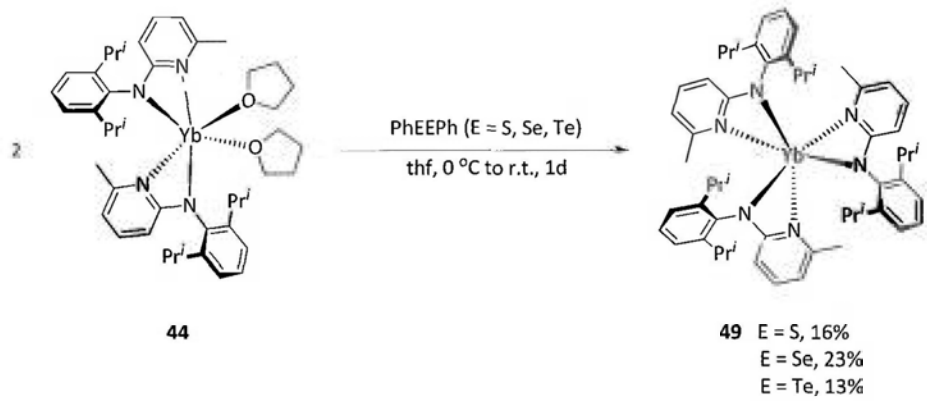

Scheme 4–13

3. Reaction of $[Yb(L^4)_2(I)(thf)]$ (**47**) with $KOBu^t$

We also attempted to prepare a Yb(III) alkoxide complex by reacting complex **47** with $KOBu^t$. However, only the homoleptic Yb(III) complex **49** was isolated after the reaction (Scheme 4–14).

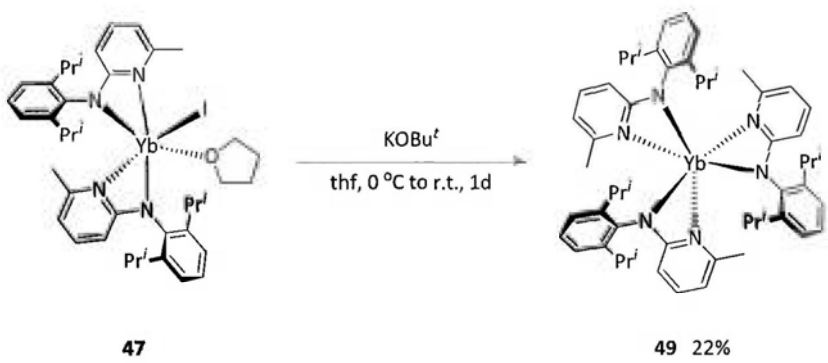

Scheme 4–14

Physical Characterization of Complexes **47–49**

Table 4–7 listed some of the physical properties of complexes **47–49**. Their

formulation was confirmed by elemental analysis. The ^{1}H NMR spectrum of the paramagnetic complex **49** was also recorded, which showed one set of isotropically shifted signals that are assignable to the L^4 ligand (Figures A2–56).

Table 4–7 Some physical properties of compounds **47–49**.

Compound	Appearance	M.p. (°C)
$[Yb(L^4)_2(I)(thf)]$ (**47**)	Orange-red crystals	241–243 (dec.)
$[Eu(L^4)_3]$ (**48**)	Purple crystals	378–380 (dec.)
$[Yb(L^4)_3]$ (**49**)	Yellow crystals	219–220 (dec.)

Crystal Structures of Complexes **47–49**

Solid-state structures of complexes **47–49** were elucidated by single-crystal X-ray diffraction analysis. Selected crystallographic data of these complexes are listed in Appendix 3.

1. $[Yb(L^4)_2(I)(thf)]$ (**47**)

The solid-state structure of complex **47** is shown in Figure 4–6 with selected bond distances and angles presented in Table 4–8.

Single crystals of complex **47** were obtained from a thf solution. The complex crystallizes in the monoclinic space group $P2_1/c$. The Yb(III) center is coordinated by two *N,N'*-chelating L^4 ligands, one iodide ligand and one thf molecule, which result in a distorted octahedral geometry around the metal ion.

The observed Yb–N_{amido} distances of 2.241(2) and 2.265(2) Å in complex **47** are comparable to the corresponding distances in the homoleptic Yb(III) complex [Yb(Ap^{Me})$_3$] [2.263(7)–2.299(7) Å],[29] but slightly shorter than those in the heteroleptic Yb(III) complex [Yb(Ap*Py)(I)(μ–Ap*Py)$_2$YbI$_2$] [Ap*Py = N(2–C_5H_3N–6–Ar")(2–C_5H_3N–6–Me)] [2.294(6)–2.482(6) Å].[36] The observed Yb–$N_{pyridyl}$ distances in complex **47** are 2.363(3) and 2.366(2) Å. They are comparable to those of 2.357(8)–2.543(7) Å and 2.383(6)–2.437(6) Å in [Yb(Ap^{Me})$_3$][29] and [Yb(Ap*Py)(I)(μ–Ap*Py)$_2$YbI$_2$], respectively.[36] The Yb–I distance of 2.9204(3) Å in **47** is comparable to those in [Yb(Ap*Py)(I)(μ–Ap*Py)$_2$YbI$_2$] [2.8462(7)–2.9511(6) Å].[36] The N_{amido}–Yb–$N_{pyridyl}$ bite angles in complex **47** are acute, namely 58.42(8)° and 58.50(9)°.

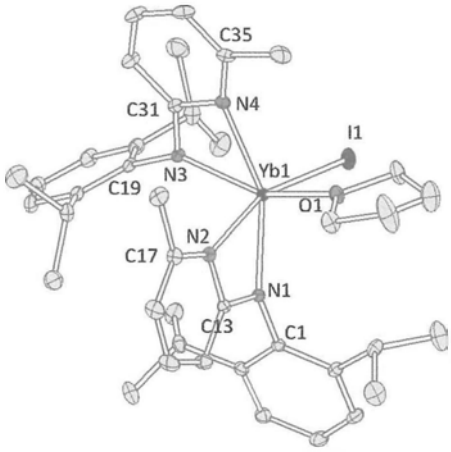

Figure 4–6 Molecular structure of $[Yb(L^4)_2(I)(thf)]$ (**47**).

Table 4–8 Selected bond lengths (Å) and angles (deg.) for compound **47**.

$[Yb(L^4)_2(I)(thf)]$ (**47**)			
Yb(1)–N(1)	2.241(2)	Yb(1)–N(2)	2.363(3)
Yb(1)–N(3)	2.265(2)	Yb(1)–N(4)	2.366(2)
Yb(1)–I(1)	2.920(1)	Yb(1)–O(1)	2.362(2)
N(1)–C(13)	1.347(4)	N(2)–C(13)	1.365(4)
N(1)–C(1)	1.435(4)	N(2)–C(17)	1.342(4)
N(3)–C(31)	1.352(4)	N(4)–C(31)	1.370(4)
N(3)–C(19)	1.440(4)	N(4)–C(35)	1.356(4)
N(1)–Yb(1)–N(2)	58.50(9)	N(3)–Yb(1)–N(4)	58.42(8)
N(1)–Yb(1)–N(3)	108.34(8)	N(1)–Yb(1)–N(4)	151.38(9)
N(2)–Yb(1)–N(3)	93.06(9)	N(2)–Yb(1)–N(4)	95.10(9)
N(1)–Yb(1)–I(1)	103.70(6)	N(2)–Yb(1)–I(1)	161.04(6)
N(3)–Yb(1)–I(1)	99.42(6)	N(4)–Yb(1)–I(1)	103.58(6)
I(1)–Yb(1)–O(1)	92.46(6)	O(1)–Yb(1)–N(1)	95.19(8)
O(1)–Yb(1)–N(2)	83.49(8)	O(1)–Yb(1)–N(3)	150.06(9)
O(1)–Yb(1)–N(4)	92.15(9)		

2. $[Ln(L^4)_3]$ [Ln = Eu (**48**), Yb(**49**)]

The molecular structures of complexes **48** and **49** are shown in Figures 4–7 and 4–8. Selected bond lengths and angles of these complexes are summarized in Tables 4–9 and 4–10. The molecular structures of the homoleptic Eu(III) and Yb(III) complexes **48** and **49** are similar to that of the Sm(III) derivative **46**. The Ln(III) ions in each complex is bounded by three *N,N'*-chelating L^4 ligands, with a crystallographic three-fold axis passing through the metal center.

Complex **48** crystallizes in the hexagonal crystal system with space group *P*3. The complex contains two independent molecules in the asymmetric unit. The observed Eu–N_{amido} distances in complex **48** [Eu(1)–N(1) = 2.346(3) Å, Eu(1')–N(1') = 2.354(3) Å] are marginally shorter than the corresponding distances reported for $[Eu\{N(SiBu^tMe_2)(2\text{–}C_5H_3N\text{–}6\text{–}Me)\}_3]$ [2.361(4)–2.367(3) Å],[31] but much longer than that of 2.259 Å in the three-coordinate $[Eu\{N(SiMe_3)_2\}_3]$.[37] The observed Eu–$N_{pyridyl}$ distances of 2.462(3) and 2.520(3) Å are comparable to those in $[Eu\{N(SiBu^tMe_2)(2\text{–}C_5H_3N\text{–}6\text{–}Me)\}_3]$ [2.461(5)–2.490(4) Å].[31] The N_{amido}–Eu–$N_{pyridyl}$ bite angles are acute, namely 55.7(1)° and 55.82(9)°.

The Yb(III) derivative **49** crystallizes in the hexagonal space group $P\bar{1}$. The Yb–N_{amido} bond lengths in **49** [2.279(5) Å] are similar to those of 2.263(7)–2.299(7) Å and 2.257(4)–2.300(4) Å in $[Yb(Ap^{Me})_3]$[29] and $[Yb\{N(SiBu^tMe_2)(2\text{–}C_5H_3N\text{–}6\text{–}Me)\}_3]$,[31] respectively. The Yb–$N_{pyridyl}$ distance of 2.382(5) Å is comparable to those of 2.357(8)–2.543(7) Å in $[Yb(Ap^{Me})_3]$[29] and 2.349(4)–2.375(4) Å in $[Yb\{N(SiBu^tMe_2)(2\text{–}C_5H_3N\text{–}6\text{–}Me)\}_3]$.[31] The N_{amido}–Yb–$N_{pyridyl}$ bite angle is also acute, namely 58.1(1)°.

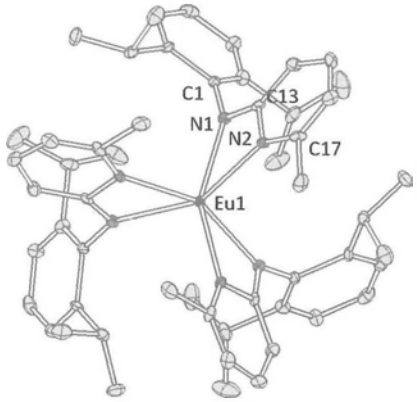

Figure 4–7 Molecular structure of $[Eu(L^4)_3]$ (**48**).

Only one of the two independent molecules in the asymmetric unit is shown.

Table 4–9 Selected bond lengths (Å) and angles (deg.) for compound **48**

$[Eu(L^4)_3]$ (**48**)			
Eu(1)–N(1)	2.354(3)	Eu(1)–N(2)	2.520(3)
N(1)–C(13)	1.287(5)	N(2)–C(13)	1.440(4)
N(1)–C(1)	1.398(5)	N(2)–C(17)	1.291(6)
Eu(1')–N(1')	2.346(3)	Eu(1')–N(2')	2.462(3)
N(1')–C(13')	1.408(4)	N(2')–C(13')	1.295(4)
N(1')–C(1')	1.459(4)	N(2')–C(17')	1.407(5)
N(1)–Eu(1)–N(2)	55.8(1)	N(1)–Eu(1)–N(1)#3	111.6(1)
N(1)–Eu(1)–N(2)#3	149.3(1)	N(2)–Eu(1)–N(1)#3	98.9(1)
N(2)–Eu(1)–N(2)#3	96.2(1)		
N(1')–Eu(1')–N(2')	55.7(1)	N(1')–Eu(1')–N(1')#1	111.9(1)
N(1')–Eu(1')–N(2')#1	98.2(1)	N(2')–Eu(1')–N(1')#1	149.8(1)
N(2')–Eu(1')–N(2')#1	96.6(1)		

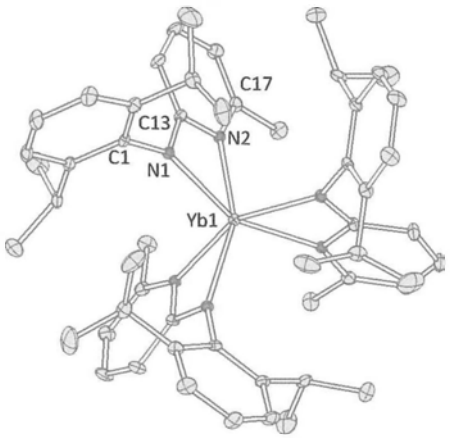

Figure 4–8 Molecular structure of $[Yb(L^4)_3]$ (**49**).

Table 4–10 Selected bond lengths (Å) and angles (deg.) for compound **49**.

$[Yb(L^4)_3]$ (**49**)			
Yb(1)–N(1)	2.279(5)	Yb(1)–N(2)	2.382(5)
N(1)–C(13)	1.348(8)	N(2)–C(13)	1.375(8)
N(1)–C(1)	1.430(7)	N(2)–C(17)	1.351(8)
N(1)–Yb(1)–N(2)	58.1(1)	N(1)–Yb(1)–N(1)#1	109.9(1)
N(1)–Yb(1)–N(2)#1	98.5(1)	N(2)–Yb(1)–N(1)#1	151.7(1)
N(2)–Yb(1)–N(2)#1	96.3(1)		

Summary

The coordination chemistry of the bulky 2-pyridylamido ligand $[N(C_6H_3Pr^i_2\text{–}2,6)(2\text{–}C_5H_3N\text{–}6\text{–}Me)]^-$ (L^4) with Yb(II), Eu(II) and Sm(II) ions has been studied. Divalent lanthanide complexes $[Yb(L^4)_2(thf)_2]$ (**44**) and $[Eu(L^4)(\mu\text{–}L^4)_2K(thf)]$ (**45**) were synthesized by metathetical reactions of $LnI_2(thf)_2$ (Ln = Yb, Eu) with potassium amide $[\{KL^4(OEt_2)\}_2]$ (**42**). On the other hand, treatment of $SmI_2(thf)_2$ with **42** led to the homoleptic Sm(III) derivative $[Sm(L^4)_3]$ (**46**).

The reaction chemistry of the Ln(II) complexes **44** and **45** has also been examined in this work. Oxidation of complexes **44** and **45** with iodine yielded Ln(III) complexes $[Yb(L^4)_2(I)(thf)]$ (**47**) and $[Eu(L^4)_3]$ (**48**), respectively. Complex **47** could also be prepared by the reaction of complex **44** with CuI. Reactions of complex **44** with PhEEPh (E = S, Se, Te) resulted only in the isolation of the Yb(III) tris(amido) complex $[Yb(L^4)_3]$ (**49**). Attempts to react complex **47** with $KOBu^t$ gave $[Yb(L^4)_3]$ (**49**) as the only isolable product.

The present study has demonstrated that the sterically very bulky L^4 ligand was capable of supporting the corresponding Eu(II) and Yb(II) complexes. The Eu(II) complex **45** was obtained as an "*ate*-complex", whereas the Yb(II) derivative **44** was isolated as a neutral mononuclear bis(amido) complex. The difference in the structures of **44** and **45** may be attributed to the different ionic radii of Eu(II) and Yb(II). Unfortunately, attempts to prepare a Sm(II) derivative have been unsuccessful. Only the corresponding Sm(III) complex was obtained in this work. The reducing properties of complexes **44** and **45** were also examined. To our knowledge, a systematic investigation on the reducing properties of Eu(II) and Yb(II) amido complexes was rare in the literature.

Experimental for Chapter 4

Materials

Sodium *tert*-butoxide, potassium *tert*-butoxide, tris(dibenzylideneacetone)-dipalladium(0) (Aldrich), 1,3–bis(diphenylphosphanyl)propane, potassium hydride (Acros) and 2–BrC_5H_3N–6–Me (Alfa Aesar) were used as received. $H_2N(C_6H_3Pr^i_2$–2,6) was distilled over KOH before use. $LnI_2(thf)_2$ (Ln = Sm, Eu, Yb)[38–40] and $Sm[N(SiMe_3)_2]_2(thf)_2$[41] were prepared according to literature procedures.

Synthesis of [$HN(C_6H_3Pr^i_2$–2,6)(2–C_5H_3N–6–Me)] (HL^4) (41)

To a slurry of sodium *tert*-butoxide (2.56 g, 26.64 mmol), tris(dibenzylideneacetone)dipalladium(0) (0.25 g, 0.27 mmol) and 1,3–bis(diphenylphosphanyl)propane (0.34 g, 0.81 mmol) in toluene (20 ml) was added a solution of $H_2N(C_6H_3Pr^i_2$–2,6) (4.78 g, 26.96 mmol) and 2–BrC_5H_3N–6–Me (4.53 g, 26.32 mmol) in the same solvent (20 ml). The reaction mixture was stirred at 95 °C for 3 d, and then quenched with water (10 ml). The mixture was extracted with diethyl ether (2 x 30 ml). The combined organic layer was washed with saturated sodium chloride solution and then dried over magnesium sulphate. All the volatiles were removed under reduced pressure to give a brown solid. The crude product was purified by column chromatography (CH_2Cl_2) to give compound **41** as a pale yellow solid. Yield: 5.64 g, 21.06 mmol, 80 %. ^{1}H NMR (300.13 MHz, $CDCl_3$): δ 7.32 (dd, *J* = 6.6, 8.6 Hz, 1H, *p*–Ar*H*), 7.26-7.20 (m, 3H, *m*–Ar*H* and Py*H*), 6.48 (d, *J* = 7.3 Hz, 1H, Py*H*), 6.05 (br, 1H, NH), 5.74 (d, *J* = 8.3 Hz, 1H, Py*H*), 3.21 (sept, *J* = 6.9 Hz, 2H, C*H*Me_2), 2.43 (s, 3H, Py*Me*), 1.13 (d, *J* = 6.9 Hz, 12H, CH*Me*$_2$).

^{13}C NMR (75.47 MHz, $CDCl_3$): δ 159.0, 157.2, 148.1, 138.2, 133.7, 128.1, 124.1, 112.9, 102.6 (*Ar* and *Py*), 28.4 (CH*Me*$_2$), 24.4 (C*H*Me$_2$), 24.0 (Py*Me*). MS (E.I. 70 eV): *m/z* (%) $[M]^+$ 268 (17), $[M–CH_3]^+$ 253 (11), $[M–Pr^i]^+$ 225 (100). HRMS: Calc. for $C_{18}H_{24}N_2$ $[M+H]^+$: *m/z* =268.1934. Found: *m/z* = 268.1940.*

Synthesis of $[\{KL^4(Et_2O)\}_2]$ (42)

A solution of compound **41** (5.48 g, 20.46 mmol) in diethyl ether (15 ml) was added to a slurry of KH (0.99 g, 24.75 mmol) in the same solvent (10 ml) at 0 °C. The reaction mixture was stirred at room temperature for 1 d, filtered, and the filtrate was concentrated *in vacuo* to *ca*. 10 ml. The *title* compound was obtained as colorless crystals at room temperature. Yield: 6.21 g, 16.32 mmol, 80 %. M.p. = 261-266 °C. ^{1}H NMR (400.13 MHz, C_6D_6): δ 7.22-7.11 (m, 3H, Ar*H*), 6.93 (dd, *J* = 6.7, 8.6 Hz, 1H, Py*H*), 5.93 (d, *J* = 6.7 Hz, 1H, Py*H*), 5.64 (d, *J* = 8.6 Hz, 1H, Py*H*), 3.25 (q, *J* = 7.0 Hz, 4H, OC*H*$_2$CH$_3$), 2.92 (sept, *J* = 6.9 Hz, 2H, C*H*Me$_2$), 2.25 (s, 3H, Py*Me*), 1.18 (br, 6H, CH*Me*$_2$), 1.11 (t, *J* = 7.0 Hz, 6H, OCH$_2$C*H*$_3$), 0.93 (br, 6H, CH*Me*$_2$). ^{13}C NMR (100.61 MHz, C_6D_6): δ 166.8, 155.8, 150.1, 141.7, 137.3, 123.8, 121.4, 105.4, 102.8 (*Ar* and *Py*), 65.9 (OCH$_2$CH$_3$), 28.1 (CHMe$_2$), 25.9 (Py*Me*), 24.1 (CH*Me*$_2$), 15.5 (OCH$_2$*C*H$_3$). Anal.: Calc. for $C_{44}H_{66}K_2N_4O_2$: C, 69.43; H, 8.74; N, 7.36%. Found: C, 69.02; H, 8.97; N, 7.88%.

Synthesis of $KL^4(thf)_2$ (43)

Compound **43** was prepared by a similar procedure as described above for complex **42**, except that thf was used as the solvent. $[HL^4]$ (**41**): 3.77 g, 14.08

* Attempts to obtain satisfactory elemental analysis results for this compound were not successful. Therefore, the compound was also characterized by high-resolution mass spectrometry.

mmol; KH: 0.64 g, 16.03 mmol. Yield: 4.62 g, 10.26 mmol, 73%. M.p.: 261–266 °C. ^{1}H NMR (400.13 MHz, C_6D_6): δ 7.25 (d, *J* = 7.6 Hz, 2H, *m*–Ar*H*), 7.14 (m, 1H, *p*–Ar*H*), 6.92 (dd, *J* = 6.7, 8.6 Hz, 1H, Py*H*), 5.88(d, *J* = 6.7 Hz, 1H, Py*H*), 5.67 (d, *J* = 8.6 Hz, 1H, Py*H*), 3.48 (m, 8H, thf), 3.03 (sept, *J* = 6.9 Hz, 2H, C*H*Me$_2$), 2.21 (s, 3H, Py*Me*), 1.38 (m, 8H, thf), 1.23 (br, 6H, CH*Me*$_2$), 1.00 (br, 6H, CH*Me*$_2$). ^{13}C NMR (100.62 MHz, C_6D_6): δ 166.8, 156.0, 150.3, 141.8, 137.3, 123.8, 121.4, 105.4, 102.7, 67.8, 28.2, 25.8, 25.7, 24.3, 24.1. Anal.: Calc. for $C_{26}H_{39}KN_2O_2$: C, 69.29; H, 8.72; N, 6.21%. Found: C, 69.03; H, 8.64; N, 6.55%.

Synthesis of [Yb(L^4)$_2$(thf)$_2$] (44)

To a solution of $YbI_2(thf)_2$ (2.21 g, 3.86 mmol) in thf (15 ml) was added a solution of [{KL^4(Et$_2$O)}$_2$] (**42**) (2.30 g, 3.02 mmol) in the same solvent (15 ml) at room temperature. The reaction mixture was stirred at room temperature for 1 d. After that, all the volatiles were removed by vacuum to give a dark purple solid residue. Extraction of the residue with toluene, followed by filtration and concentration of the toluene solution yielded complex **44** as dark purple block-shaped crystals. Yield: 1.98 g, 2.33 mmol, 77%. M.p.: 216–219 °C. ^{1}H NMR (400.13 MHz, C_6D_6): δ 7.28 (d, *J* = 7.5 Hz, 4H, *m*–Ar*H*), 7.21–7.12 (m, 5H, *Ph*Me), 7.03 (t, *J* = 7.5 Hz, 2H, *p*–Ar*H*), 6.89 (dd, *J* = 6.9, 8.6 Hz, 2H, Py*H*), 5.86 (d, *J* = 6.9 Hz, 2H, Py*H*), 5.66 (d, *J* = 8.6 Hz, 2H, Py*H*), 3.49 (br, 12H, thf and C*H*Me$_2$), 2.18 (s, 6H, Py*Me*), 2.11 (s, 3H, Ph*Me*), 1.27 (d, J = 6.8 Hz, 12H, CH*Me*$_2$), 1.22 (br, 8H, thf), 1.11 (d, J = 6.8 Hz, 12H, CH*Me*$_2$). ^{13}C NMR (100.62 MHz, C_6D_6): δ 168.7, 153.8, 147.9, 143.5, 138.0, 123.6, 122.8, 105.2, 104.1, 68.7, 28.1, 25.4, 25.2, 24.3, 23.9, 21.4. Anal.: Calc. for $C_{44}H_{62}N_4O_2Yb \cdot C_7H_8$: C, 64.88; H, 7.47; N, 5.93%. Found: C, 64.42; H, 7.61; N, 6.19%.

Synthesis of $[Eu(L^4)(\mu\text{–}L^4)_2K(thf)]$ (45)

A solution of $[\{KL^4(Et_2O)\}_2]$ (**42**) (1.67 g, 4.38 mmol) in thf (15 ml) was added to a solution of $EuI_2(thf)_2$ (1.21 g, 2.20 mmol) in the same solvent (15 ml). The reaction mixture was stirred at room temperature for 1 d to give a orange-red suspension. The solution was pumped to dryness and the residue was extracted with hexane. The solution was filtered and concentrated to give the *title* compound as orange crystals. Yield: 0.90 g, 0.85 mmol, 39%. M.p.: 190–193 °C. Anal.: Calc. for $C_{58}H_{77}EuKN_6O$: C, 65.39; H, 7.28; N, 7.88%. Found: C, 64.79; H, 7.98; N, 8.45%.

Reaction of $SmI_2(thf)_2$ with $[\{KL^4(Et_2O)\}_2]$ (42)

To a thf solution (15 ml) of $SmI_2(thf)_2$ (1.56 g, 2.84 mmol) was added a solution of $[\{KL^4(Et_2O)\}_2]$ (**42**) (1.95 g, 5.12 mmol) in the same solvent (15 ml). The reaction mixture was then stirred at room temperature for 1 d, whereupon its color changed from dark blue to dark brown. The solution was pumped to dryness and the residue was extracted with hexane. Concentration of the solution yielded complex $[Sm(L^4)_3]$ (**46**) as yellow crystals. Yield: 0.72 g, 0.763 mmol, 30%. M.p.: decomposed at 357–359 °C without melting. ^{1}H NMR (400.13 MHz, C_6D_6): δ 12.55 (br, 3H, C*H*Me$_2$), 9.02 (d, *J* = 8.6 Hz, 3H, Py*H*), 8.19 (dd, *J* = 7.2, 8.6 Hz, 3H, Py*H*), 8.04 (dd, *J* = 1.3, 7.7 Hz, 3H, *m*–Ar*H*), 7.18–7.14 (m, 3H, *p*–Ar*H*), 5.59 (dd, *J* = 1.3, 7.7 Hz, 3H, *m*–Ar*H*), 5.47 (d, *J* = 7.2 Hz, 3H, Py*H*), 3.86 (d, *J* = 6.5 Hz, 9H, CH*Me*$_2$), 3.11 (d, *J* = 6.5 Hz, 9H, CH*Me*$_2$), 1.16 (d, *J* = 6.3 Hz, 9H, CH*Me*$_2$), 0.7 (br, 3H, C*H*Me$_2$), –3.9 (s, 9H, Py*Me*), –6.5 (d, J = 6.3 Hz, 9H CH*Me*$_2$). ^{13}C NMR (100.62 MHz, C_6D_6): δ 151.0, 146.9, 144.9, 141.8, 140.5, 125.6, 123.5, 111.3, 104.5, 34.5, 27.8, 27.1, 26.3, 24.0, 19.3, 17.0. Anal.: Calc. for $C_{54}H_{69}N_6Sm$: C, 68.09; H, 7.30; N, 8.82%. Found: C,

67.55; H, 7.36; N, 9.59%.

Reaction of [Eu(L^4)(μ–L^4)$_2$K(thf)] (45) with I_2

To a solution of complex **45** (1.96 g, 1.84 mmol) in thf (20 ml) at 0 °C was slowly added a solution of I_2 (0.23 g, 0.89 mmol) in the same solvent (10 ml). The solution was stirred at room temperature 1 d. All the volatiles were removed in *vacuo.* The solid residue was extracted with hexane. Concentration of the solution gave [Eu(L^4)$_3$] (**48**) as purple crystals. Yield: 1.12 g, 1.17 mmol, 64%. M.p.: 378–380 °C (dec.). Anal.: Calc. for $C_{54}H_{69}EuN_6$: C, 67.98; H, 7.29; N, 8.80%. Found: C, 67.55; H, 7.58; N, 8.92%.

Reaction of [Yb(L^4)$_2$(thf)$_2$] (44) with I_2

To a solution of complex **44** (1.64 g, 1.92 mmol) in thf (20 ml) at 0 °C was slowly added a solution of I_2 (0.25 g, 0.97 mmol) in the same solvent (10 ml). The reaction mixture was allowed to warm to room temperature and stirring was continued for 1 d. The solution was filtered and concentrated to give [Yb(L^4)$_2$(I)(thf)] (**47**) as orange-red crystals. Yield: 0.78 g, 0.86 mmol, 45%. M.p.: 241–243 °C (dec.). Anal.: Calc. for $C_{40}H_{54}N_4OIYb$: C, 52.98; H, 6.00; N, 6.18%. Found: C, 52.69; H, 6.15; N, 6.29%.

Reaction of [Yb(L^4)$_2$(thf)$_2$] (44) with CuI

A solution of complex **44** (1.41 g, 1.65 mmol) in thf (20 ml) was added slowly to a slurry of CuI (0.32 g, 1.67 mmol) in the same solvent (10 ml). The reaction mixture was stirred at room temperature for 1 d, whereupon its color changed from dark purple to orange-red. The reaction mixture was filtered and concentrated to give [Yb(L^4)$_2$(I)(thf)] (**47**) as orange-red crystals. Yield: 0.83g, 0.92 mmol, 56%.

Reaction of [Yb(L^4)$_2$(thf)$_2$] (44) with PhSSPh

To a solution of PhSSPh (0.12 g, 0.54 mmol) in thf (10 ml) at 0 °C was added dropwise a solution of [Yb(L^4)$_2$(thf)$_2$] (**44**) (0.87 g, 1.02 mmol) in the same solvent (20 ml). After stirring at room temperature for 1 d, all the volatiles were removed in *vacuo*. The solid residue was extracted with toluene and then filtered. Concentration of the filtrate afforded the yellow crystalline [Yb(L^4)$_3$] (**49**). Yield: 0.16 g, 0.16 mmol, 16%. M.p.: 219–220 °C (dec.). ^{1}H NMR (400.13 MHz, C_6D_6): δ 67.00 (s, 9H, *Me*), 61.84 (s, 9H, *Me*), 43.49 (br, 3H, C*H*Me$_2$), 19.07 (s, 3H, Ar*H* or Py*H*), 8.60 (s, 3H, Ar*H* or Py*H*), 6.60 (s, 3H, Ar*H* or Py*H*), –1.27 (s, 9H, *Me*), –2.85 (s, 3H, Ar*H* or Py*H*), –8.76 (s, 3H, Ar*H* or Py*H*), –20.11 (s, 9H, *Me*), –34.19 (s, 3H, Ar*H* or Py*H*), –98.47 (br, 3H, C*H*Me$_2$). Anal.: Calc. for $C_{54}H_{69}N_6Yb$: C, 66.51; H, 7.31; N, 8.61%. Found: C, 65.81; H, 7.59; N, 8.93%.

Reaction of [Yb(L^4)$_2$(thf)$_2$] (44) with PhSeSePh

Treatment of complex **44** with PhSeSePh according to a similar procedure as described above yielded complex **49** as the only isolable product. [Yb(L^4)$_2$(thf)$_2$] (**44**): 1.59 g, 1.87 mmol; PhSeSePh: 0.29 g, 0.92 mmol. Yield: 0.21 g, 0.22 mmol, 23%.

Reaction of [Yb(L^4)$_2$(thf)$_2$] (44) with PhTeTePh

Treatment of complex **44** with PhTeTePh according to a similar procedure as described above yielded complex **49** as the only isolable product. [Yb(L^4)$_2$(thf)$_2$] (**44**): 1.59 g, 1.87 mmol; PhTeTePh: 0.38 g, 0.94 mmol. Yield: 0.12 g, 0.12 mmol, 13%.

Reaction of $[Yb(L^4)_2(I)(thf)]$ (47) with $KOBu^t$

To a solution of $KOBu^t$ (0.83 g, 0.92 mmol) in thf (10 ml) at 0 °C was slowly added a solution of $[Yb(L^4)_2(I)(thf)]$ (**47**) (0.12 g, 1.06 mmol) in the same solvent (20 ml). The reaction mixture was stirred at room temperature for 1 d. All the volatiles were removed in *vacuo* and the solid residue was extracted with toluene. Filtration and concentration of the solution gave $[Yb(L^4)_3]$ (**49**) as yellow crystals. Yield: 0.20 g, 0.20 mmol, 22%.

References for Chapter 4

1. Evans, W. J. *Coordination Chemistry Reviews* **2000**, *206-207*, 263-283.
2. Heitmann, D.; Jones, C.; Junk, P. C; Lippert, K. -A.; Stasch, A. *Dalton Trans.* **2007**, 187-189.
3. Deng, M.; Yao, Y.; Zhang, Y.; Shen, Q. *Inorg. Chem.* **2004**, 2742-2743.
4. Evans, W. J.; Drummond, D. K.; Chamberlain, L. R.; Doedens, R. J.; Bott, S. G.; Zhang, H.; Atwood, J. L. *J. Am. Chem. Soc.* **1988**, *110*, 4983–4994.
5. Evans, W. J.; Drummond, D. K.; Bott, S. G.; Atwood, J. L. *Organometallics* **1986**, *5*, 2389–2391.
6. Guillaume, S. M.; Schappacher, M.; Scott, N. M.; Kempe, R. J. *Polym. Sci., Part A: Polym. Chem.* **2007**, *45*, 3611-3619.
7. Berg, D. J.; Burns, C. J.; Andersen, R. A.; Zalkin, A. *Organometallics* **1989**, *8*, 1865–1870.
8. Berg, D. J.; Burns, C. J.; Andersen, R. A. *Organometallics* **2003**, *11*, 627–632.
9. Evans, W. J.; Miller, K. A.; Lee, D. S.; Ziller, J. W. *Inorg. Chem.* **2005**, *44*, 4326–4332.
10. Tilley, T. D.; Zalkin, A.; Andersen, R. A.; Templeton, D. H. *Inorg. Chem.* **1981**, *20*, 551–554.
11. Evans, W. J.; Drummond, D. K.; Zhang, H.; Atwood, J. L. *Inorg. Chem.* **1988**, *27*, 575–579.
12. Hitchcock, P. B.; Khvostov, A. V.; Lappert, M. F.; Protchenko, A. V. *J. Organomet. Chem.* **2002**, *647*, 198–204.
13. Boncella, J. M.; Andersen, R. A. *Organometallics* **1985**, *4*, 205–206.
14. Tilley, T. D.; Andersen, R. A.; Zalkin, A. *Inorg. Chem.* **1984**, *23*, 2271–2276.
15. Hitchcock, P. B.; Khvostov, A. V.; Lappert, M. F.; Protchenko, A. V. *J. Organomet. Chem.* **2002**, *647*, 198–204.
16. Zhou, L.; Wang, J.; Zhang, Y.; Yao, Y. Shen, Q. *Inorg. Chem.* **2007**, *46*, 5763–5772.
17. Deacon, G. B.; Fallon, G. D.; Forsyth, C. M.; Schumann, H.; Weimann, R. *Chem. Ber.* **1997**, *130*, 409–415.
18. Bourget–Merie, L.; Lappert, M. F.; Severn, J. R. *Chem. Rev.* **2002**, *102*, 3031–3065.
19. Hitchcock, P. B.; Khvostov, A. V.; Lappert, M. F.; Protchenko, A. V. *Dalton Trans.* **2009**, 2383–2391.
20. Jiao, R.; Shen, X.; Xue, M.; Zhang, Y.; Yao, Y.; Shen, Q. *Chem. Commun.* **2010**, *46*, 4118–4120.
21. Cole, M. L.; Junk, P. C. *Chem. Commun.* **2005**, 2695–2697.
22. Wedler, M.; Noltemeyer, M.; Pieper, U.; Schmidt, H. –G.; Stalke, D. Edelmann. F. T. *Angew. Chem. Int. Ed. Engl.* **1990**, *29*, 894–896.
23. Wedler, M.; Recknagel, A.; Gilje, J. W.; Noltemeyer, M.; Edelmann. F. T. J. Organomet. Chem. **1992**, *462*, 295–306.
24. Yao, S.; Chan, H. –S.; Lam, C. –K.; Lee, H. K. *Inorg. Chem.* **2009**, *48*, 9936–9946.
25. Heitmann, D.; Jones, C.; Junk, P. C.; Lippert, K. –A.; Stasch, A. *Dalton Trans.* **2007**, 187–189.
26. Heitmann, D.; Jones, C.; Milla, D. P.; Stasch, A. *Dalton Trans.* **2010**, *39*, 1877–1882.
27. Scott, N. M.; Kempe, R. *Eur. J. Inorg. Chem.* **2005**, 1319–1324.

28. Qayyum, S.; Noor, A.; Glatz, G.; Kempe, R. *Z. Anorg. Allg. Chem.* **2009**, *635*, 2455–2458.
29. Qayyum, S.; Haberland, K.; Forsyth, C. M.; Junk, P. C.; Deacon, G. B.; Kempe, R. *Eur. J. Inorg. Chem.* **2008**, 557–562.
30. Wagaw, S.; Buchwald, S. L. *J. Org. Chem.* **1996**, *61*, 7240–7241.
31. Kui, S. C. F.; Li, H. –W.; Lee, H. K. *Inorg. Chem.* **2003**, *42*, 2824–2826.
32. Liddle, S. T.; Clegg, W. *J. Chem. Soc., Dalton Trans.* **2001**, 402–408.
33. Liddle, S. T.; Clegg, W.; Morrison, C. A. *Dalton Trans.* **2004**, 2514–2525.
34. Antolini, F.; Hitchcock, P. B.; Khvostov, A. V.; Lappert, M. F. *Eur. J. Inorg. Chem.* **2003**, 3391–3400.
35. Qayyum, S.; Skvortsov, G. G.; Fukin, G. K.; Trifonov, A. A>; Kretschmer, W. P.; Dõring, C.; Kempe, R. *Eur. J. Inorg. Chem.* **2010**, 248–257.
36. Dietel, A. M.; Dõring, C.; Glatz, G.; Butovskii, M. V.; Tok, O.; Schappacher, F. M.; Põttgen, R.; Kempe, R. *Eur. J. Inorg. Chem.* **2009**, 1051–1059.
37. Ghotra, J. S.; Hursthouse, M. B.; Welch, A. J. *J. Chem. Soc., Chem. Commun.* **1973**, 669–670.
38. Namy, J. L.; Girard, P.; Kagan, H. B. *Nouv. J. Chim.* **1981**, *5*, 479–484.
39. Namy, J. L.; Girard, P.; Kagan, H. B. *Nouv. J. Chim.* **1977**, *1*, 5–7.
40. Watson, P. L.; Tulip, T. J.; Williams, I. *Organometallics* **1990**, *9*, 1999–2009.
41. Evans, W. J.; Drummond, D. K.; Zhang, H.; Atwood, J. L. *Inorg. Chem.* **1988**, *27*, 575-579.

Chapter 5

Conclusion

The first part of this research work covers the synthesis, structure and reactivity of Group 4 metal complexes supported by the *N*-alkylated arylamido ligands $[N(C_6H_3Me_2\text{–}2,6)(CH_2Bu^t)]^-$ (L^1) and $[N(C_6H_3Pr^i_2\text{–}2,6)(CH_2Bu^t)]^-$ (L^2). Recently, the coordination chemistry of the L^1 and L^2 ligands has been investigated by our research group.[1] This earlier work in out group has shown that the L^1 and L^2 ligands can support metal complexes with very interesting structures and reactivity. In the present research work, we extended out studies to the Group 4 transition metals. The majority of reports on Group 4 metal amides were focusesd on theit catalytic properties towards alkene polymerization.[2] Results of our work can provide insights to the reactivity of Group 4 metal complexes supported by monodentate arylamido ligainds. Moreover, the reaction chemistry of complexes **13** and **14** shows that the L^1 and L^2 ligands are compatible with a variety of amide, halide and methyl ligands in Group 4 metal complexes. The bis(amido) Zr(IV) and Hf(IV) complexes **21** and **22** represent rare examples of Group 4 dimethyl complexes supported by monodentate amido ligands.

The second part of our work was focused on the synthesis, structure and reactivity of Group 4 metal complexes supported by the unsymmetrical benzamidinate ligand $[PhC(NC_6H_3Pr^i_2\text{–}2,6)(NSiMe_3)]^-$ (L^3). Similar ligands have been employed to stabilize late transition-metal[3] and lanthanide complexes.[4] It is

noteworthy that the use of unsymmetrical amidinate ligands can provide a wide range of ligand modification via the introduction of substituents with different electronic and steric properties. It is interesting to note that a few methyl and benzyl complexes of the Group 4 metals supported by L^3 were successfully isolated in our studies.

The third part of this work was focused on the synthesis, structure and reactivity of divalent lanthanide complexes supported by a new *2*-pyridylamido ligand $[N(C_6H_3Pr^i_2\text{–}2,6)(2\text{–}C_5H_3N\text{–}6\text{–}Me)]^-$ (L^4). The coordination chemistry of *2*-pyridylamido ligands has attracted considerable attention in the past decades.[5] This class of ligands can exhibit flexible coordination modes. A number of metal complexes with interesting molecular structures and oxidation states have been reported by others as well as our research group.[6] Divalent europium and ytterbium complexes containing bulky *2*-pyridylamido ligands have been reported earlier by Kempe and co-workers.[7] However, a detailed investigation on theis reaction chemistry remains elusive. Our work represents the first systematic study on the reaction chemistry of divalent lanthanide complexes supported by *2*-pyridylamido ligands.

References for Chapter 5

1. (a) Au–Yeung, H. Y.; Lam, C. H.; Lam, C. –K.; Wong, W. –Y.; Lee, H. K. *Inorg. Chem.* **2007**, *46*, 7695–7697.
   (b) Au-Yeung, H. Y. *M. Phil. Thesis*, The Chinese University of Hong Kong, 2006.
   (c) Wong, G. F. *M. Phil. Thesis*, The Chinese University of Hong Kong, 2008.
2. See for example:
   (a) Nomura, K.; Fujii, K. *Organometallics* **2002**, *21*, 3042–3049.
   (b) Shah, S. A. A.; Dorn, H.; Voigt, A.; Roesky, H. W.; Parisini, E.; Schmidt, H. –G.; Noltemeyer, M. *Organometallics* **1996**, *15*, 3176–3181.
   (c) Shah, S. A. A.; Dorn, H.; Roesky, H. W.; Parisini, E.; Schmidt, H. –G.; Noltemeyer, M. *J. Chem. Soc., Dalton Trans.* **1996**, 4143–4146.
3. (a) Lee, H. K.; Lam, T. S.; Lam, C. –K.; Li, H. –W.; Fung, S. M. *New J. Chem.* **2003**, *27*, 1310–1318.
   (b) Lam, T. S. *M. Phil. Thesis*, The Chinese University of Hong Kong, 2002.
4. (a) Yao, S.; Chan, H. –S.; Lam, C. –K.; Lee, H. K. *Inorg. Chem.* **2009**, *48*, 9936–9946.
   (b) Yao, S. *PhD. Thesis*, The Chinese University of Hong Kong, 2009.
5. (a) Kempe, R. *Angew. Chem. Int. Ed.* **2000**, *39*, 468–493.
   (b) Deeken, S.; Motz, G.; Kempe, R. *Z. Anorg. Allg. Chem.* **2007**, *633*, 320–325.
6. (a) Cheng, P. S. *M. Phil. Thesis*, The Chinese University of Hong Kong, 2004.
   (b) Lee, H. K.; Wong, Y. –L.; Zhou, Z. –Y.; Zhang, Z. –Y.; Ng, D. K. P.; Mak, T. C. W. *J. Chem. Soc., Dalton Trans.* **2000**, 539–544.
   (c) Lee, H. K.; Lam, C. H.; Li, S. –L.; Zhang, Z. –Y.; Mak, T. C. W. *Inorg. Chem.* **2001**, *40*, 4691–4695.
   (d) Lam, C. H. *M. Phil. Thesis*, The Chinese University of Hong Kong, 2001.
   (e) Lam, T. S. *M. Phil. Thesis*, The Chinese University of Hong Kong, 2002.
   (f) Lam, P. C. *M. Phil. Thesis*, The Chinese University of Hong Kong, 2006.
   (g) Kui, S. C. F.; Li, H. –W.; Lee, H. K. *Inorg. Chem.* **2003**, *42*, 2824–2826.
   (h) Kui, S. C. F. *M. Phil. Thesis*, The Chinese University of Hong Kong, 2001.
7. (a) Scott, N. M.; Kempe, R. *Eur. J. Inorg. Chem.* **2005**, 1319–1324.
   (b) Qayyum, S.; Noor, A.; Glatz, G.; Kempe, R. *Z. Anorg. Allg. Chem.* **2009**, *635*, 2455–2458.
   (c) Qayyum, S.; Haberland, K.; Forsyth, C. M.; Junk, P. C.; Deacon, G. B.; Kempe, R. *Eur. J. Inorg. Chem.* **2008**, 557–562.

Appendix 1

General Procedures, Physical Measurements, and X-Ray Diffraction Analysis

All manipulations were carried out using standard Schlenk techniques or in a Braun MB 150-M drybox under an atmosphere of purified nitrogen. Solvents were dried over sodium wire and distilled under nitrogen from sodium benzophenone (diethyl ether and thf) or Na/K alloy (hexane and toluene), and degassed twice by freeze-thaw cycles before use.

^{1}H and ^{13}C NMR spectra were recorded on a Bruker DPX300 NMR Spectrometer (at 300.13 and 75.47 MHz) or a Bruker Advance III 400 NMR Spectrometer (at 400.13 and 100.61 MHz). Chemical shifts were referenced to residue protons of $CDCl_3$ and C_6D_6 at 7.26 and 7.16 ppm (in ^{1}H NMR), and 77.16 and 128.06 ppm (in ^{13}C NMR), respectively. Melting-points were recorded on an Electrothermal melting point apparatus and were uncorrected. Mass spectra were obtained on a ThermoFinnigan MAT 95 XP Mass Spectrometer (E.I. 70 eV). Elemental analysis (C, H, N) were performed by MEDAC Ltd., Brunel University, U.K.

Single-crystals of compounds **8–19**, **21–24**, **31–42** and **44–49** suitable for X-ray diffraction studies were mounted in glass capillaries and sealed under nitrogen. Data were collected on a Bruker SMART CCD diffractometer or a Bruker KAPPA APEX II diffractometer with graphite-monochromatized Mo–K_α radiation (λ = 0.71073 Å) using ω scan. The structures were solved by direct phase determination using the computer program SHELX-97 and refined by full-matrix

least squares with anisotropic thermal parameters for the non-hydrogen atoms.[2] Hydrogen atoms were introduced in their idealized positions and included in structure factor calculations with assigned isotropic temperature factors.

---

[2] Scheldrick, G. M. *SHELX-97*; *Package for Crystal Structure Solution and Refinement*; University of Göttingen: Göttingen, Germany, **1997**.

Appendix 2

NMR Spectra of Compounds

^{1}H NMR Spectrum of $[Zr(L^{1})_2Cl(\mu\text{–}Cl)_2Li(tmeda)]$ (**8**)

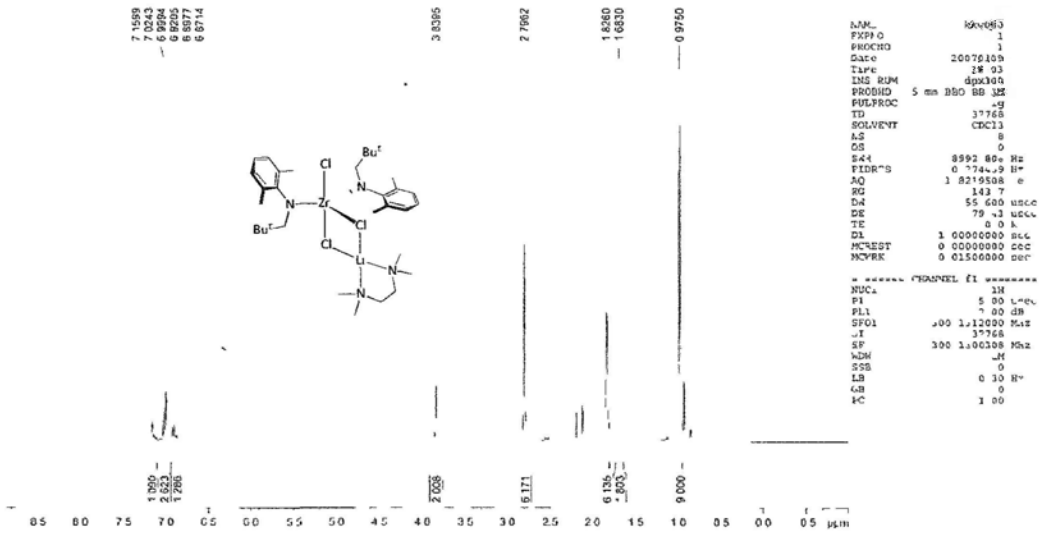

Figure A2–1

^{13}C NMR Spectrum of $[Zr(L^{1})_2Cl(\mu\text{–}Cl)_2Li(tmeda)]$ (**8**)

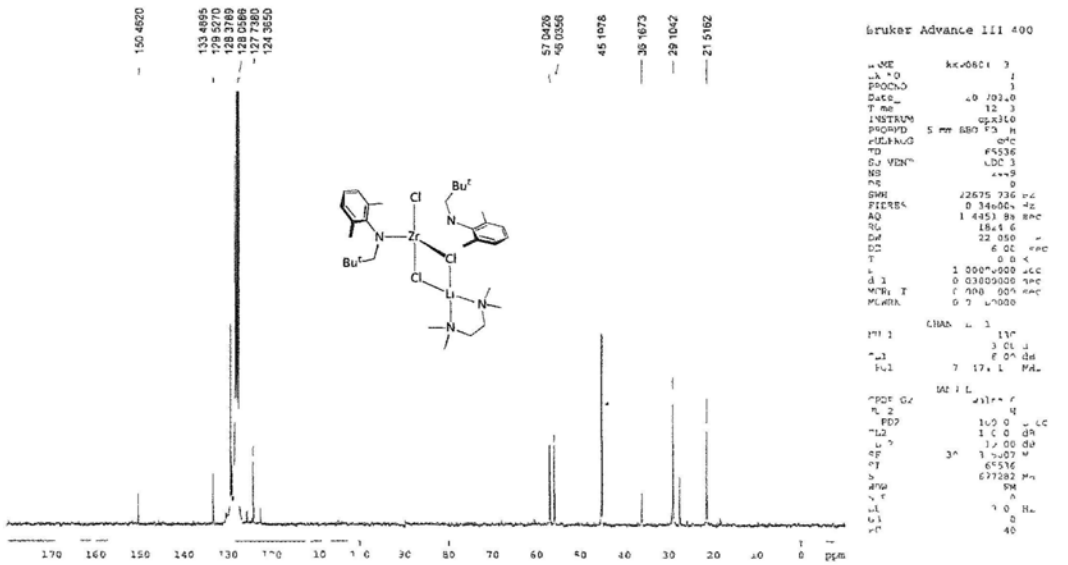

Figure A2–2

^{1}H NMR Spectrum of $[Zr(L^{2})_{2}Cl(\mu\text{–}Cl)_{2}Li(tmeda)]$ (**9**)

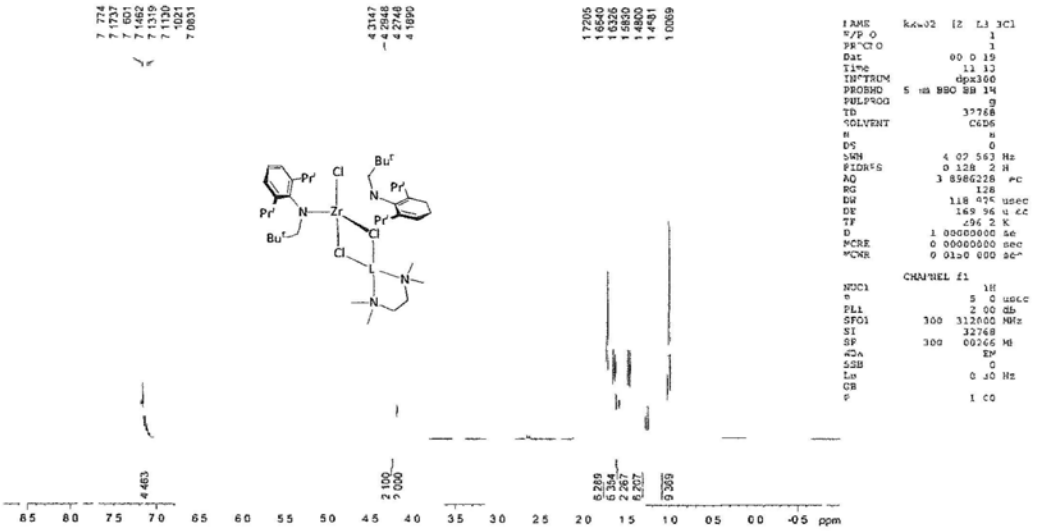

Figure A2–3

^{13}C NMR Spectrum of $[Zr(L^{2})_{2}Cl(\mu\text{–}Cl)_{2}Li(tmeda)]$ (**9**)

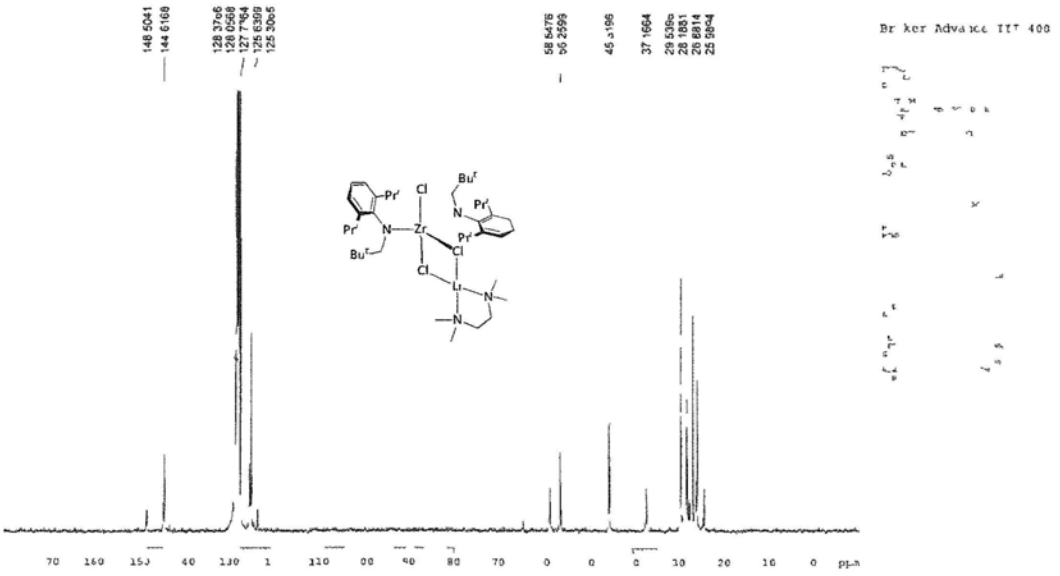

Figure A2–4

^{1}H NMR Spectrum of [Hf(L^{1})$_{2}$Cl(μ–Cl)$_{2}$Li(tmeda)] (**10**)

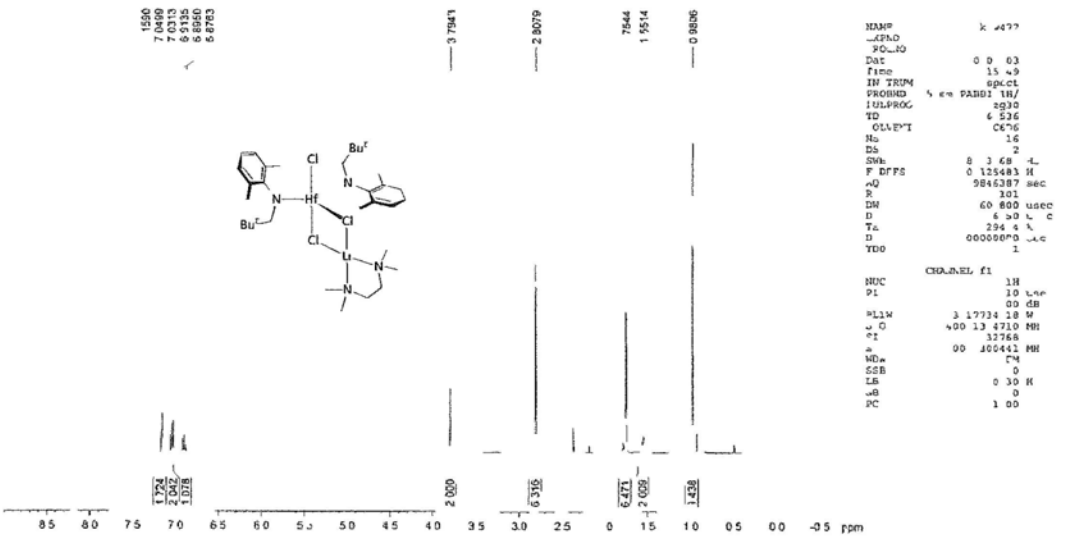

Figure A2–5

^{13}C NMR Spectrum of [Hf(L^{1})$_{2}$Cl(μ–Cl)$_{2}$Li(tmeda)] (**10**)

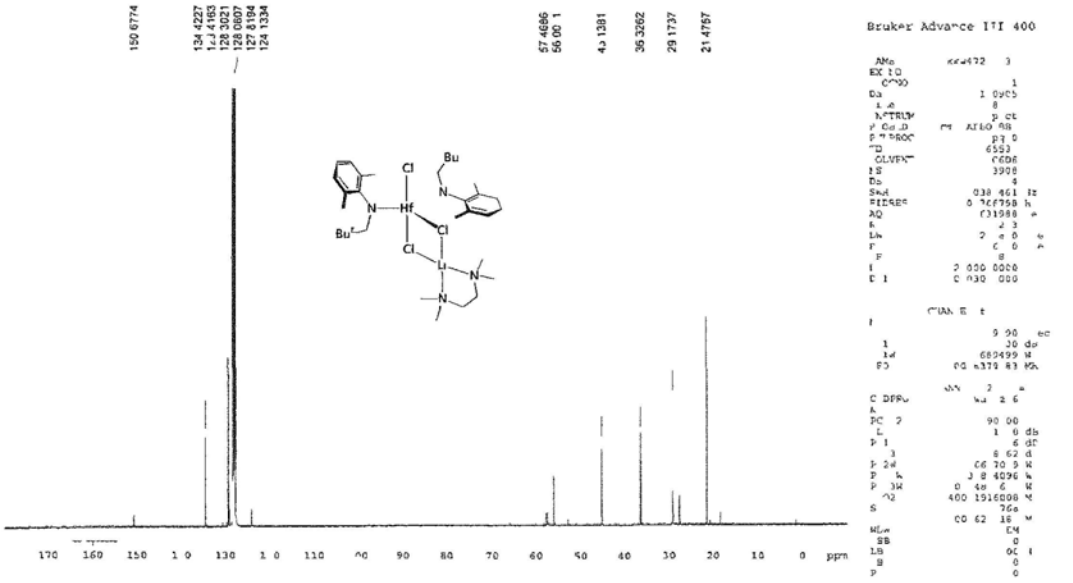

Figure A2–6

^{1}H NMR Spectrum of $[Hf(L^{2})_{2}Cl(\mu\text{–}Cl)_{2}Li(tmeda)]$ (**11**)

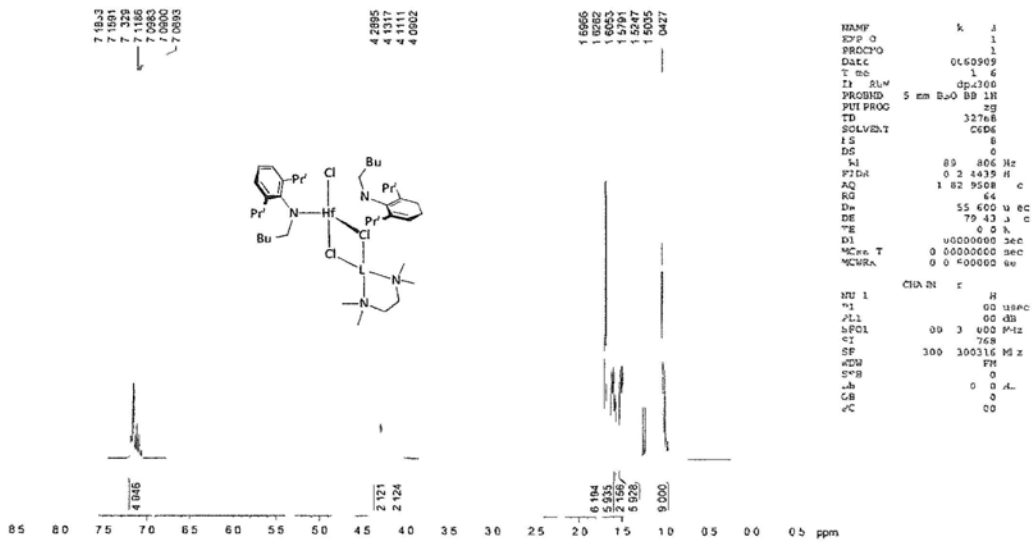

Figure A2–7

^{13}C NMR Spectrum of $[Hf(L^{2})_{2}Cl(\mu\text{–}Cl)_{2}Li(tmeda)]$ (**11**)

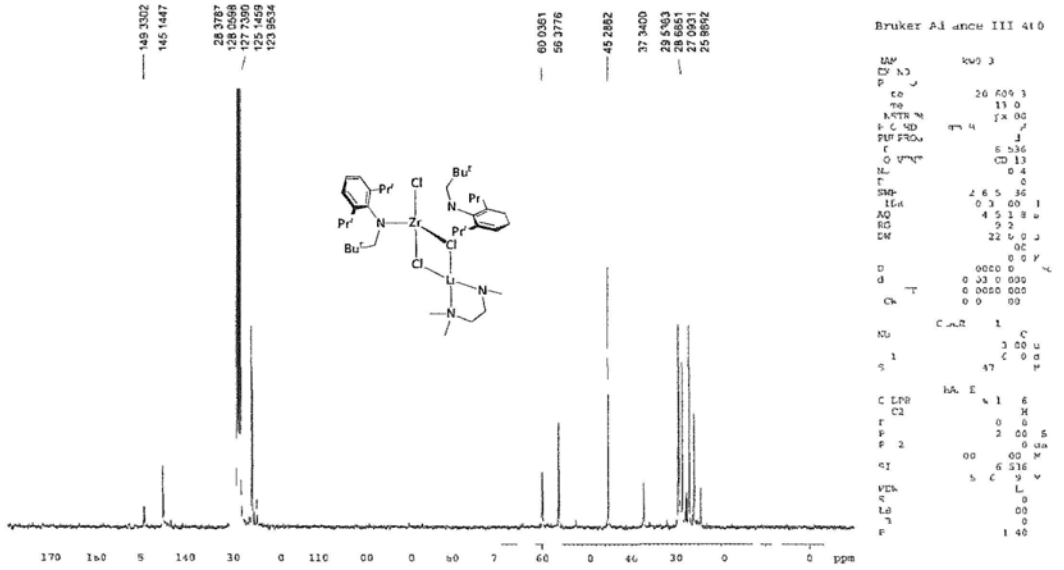

Figure A2–8

^{1}H NMR Spectrum of $[Ti(L^{2})_{2}Cl_{2}]$ (**12**)

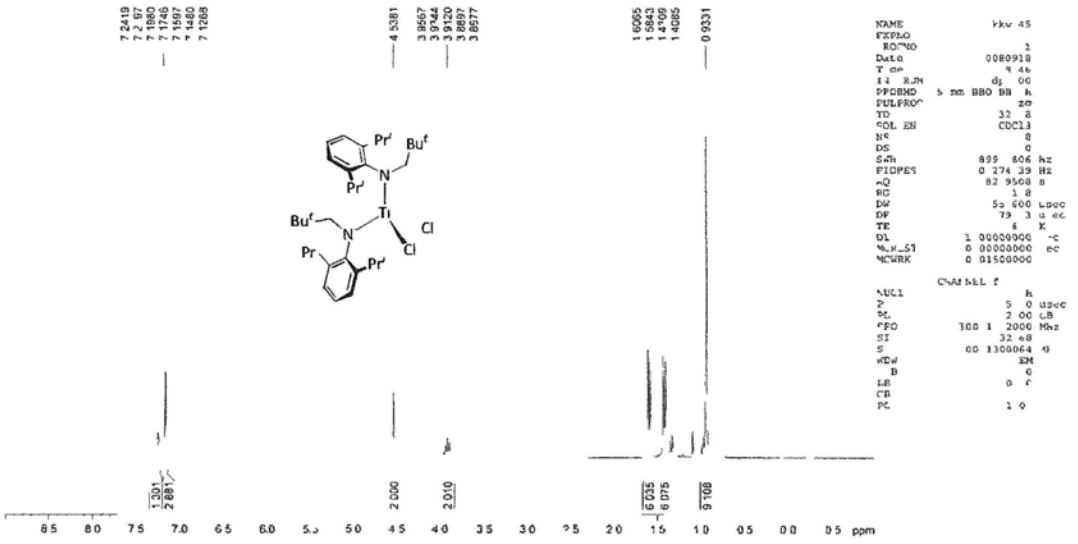

Figure A2–9

^{13}C NMR Spectrum of $[Ti(L^{2})_{2}Cl_{2}]$ (**12**)

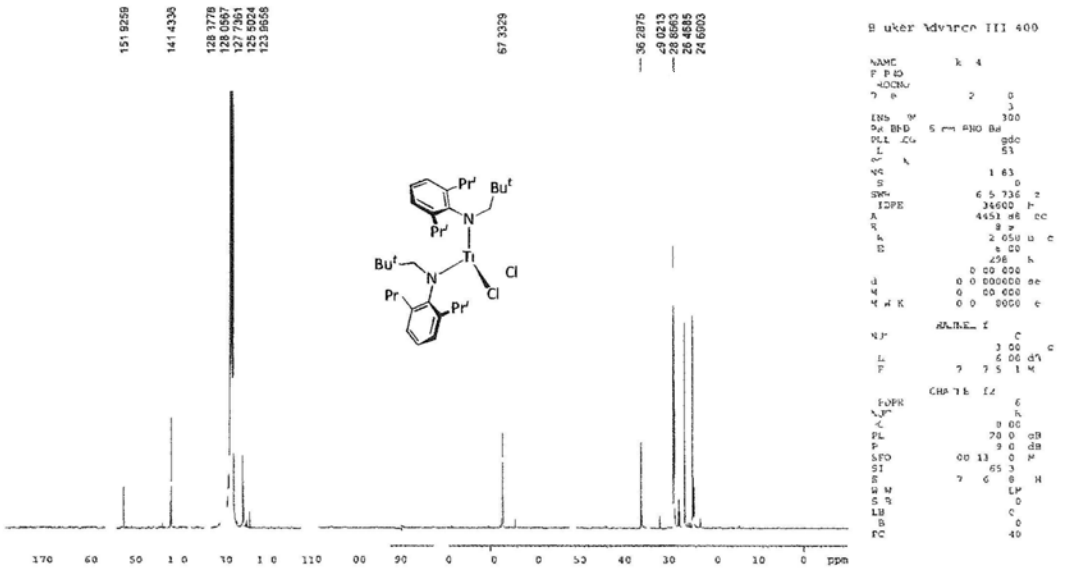

Figure A2–10

^{1}H NMR Spectrum of $[Zr(L^{2})_{2}Cl_{2}]$ (**13**)

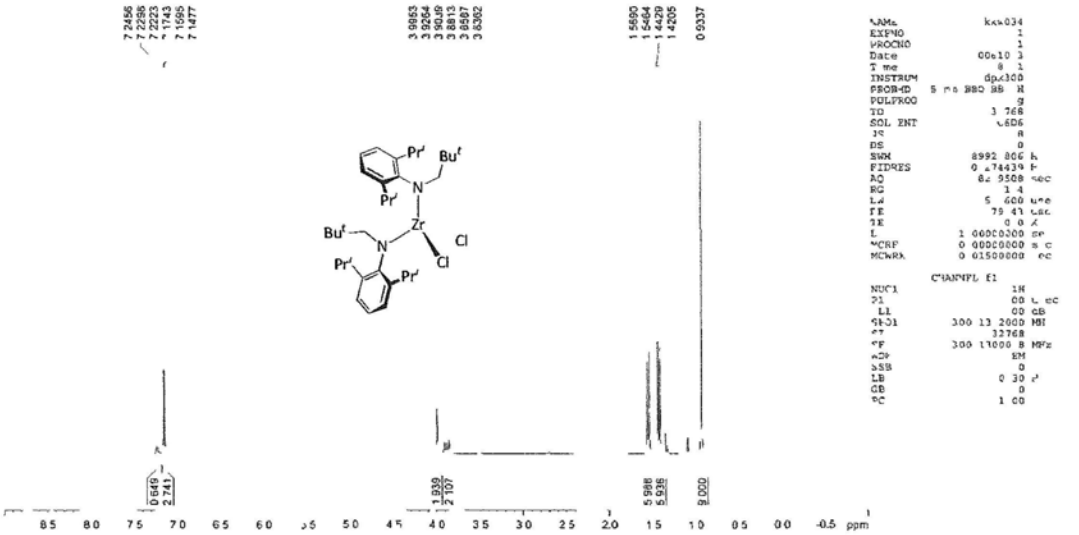

Figure A2–11

^{13}C NMR Spectrum of $[Zr(L^{2})_{2}Cl_{2}]$ (**13**)

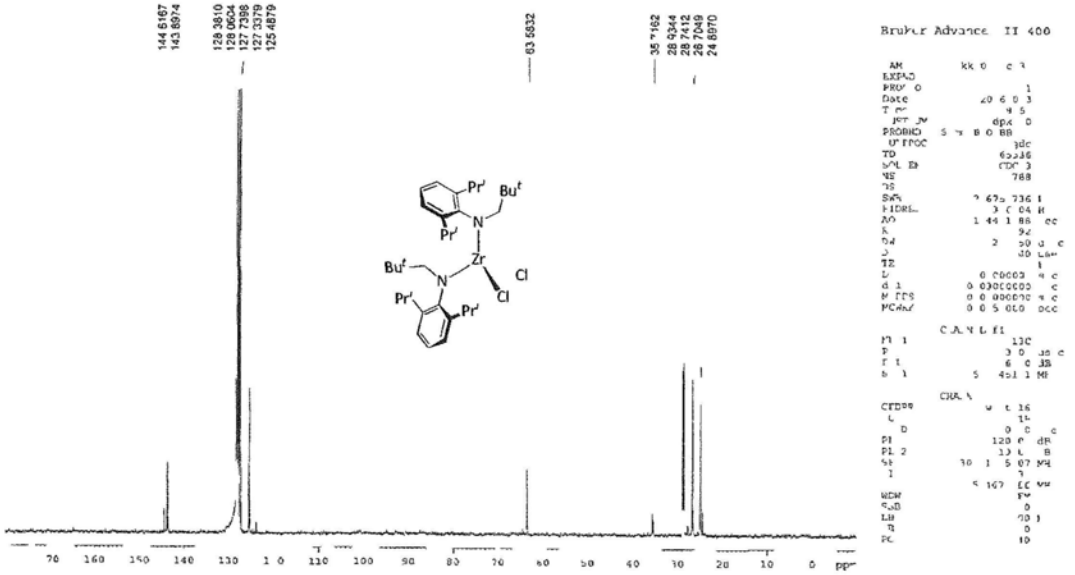

Figure A2–12

^{1}H NMR Spectrum of $[Hf(L^{2})_{2}Cl_{2}]$ (**14**)

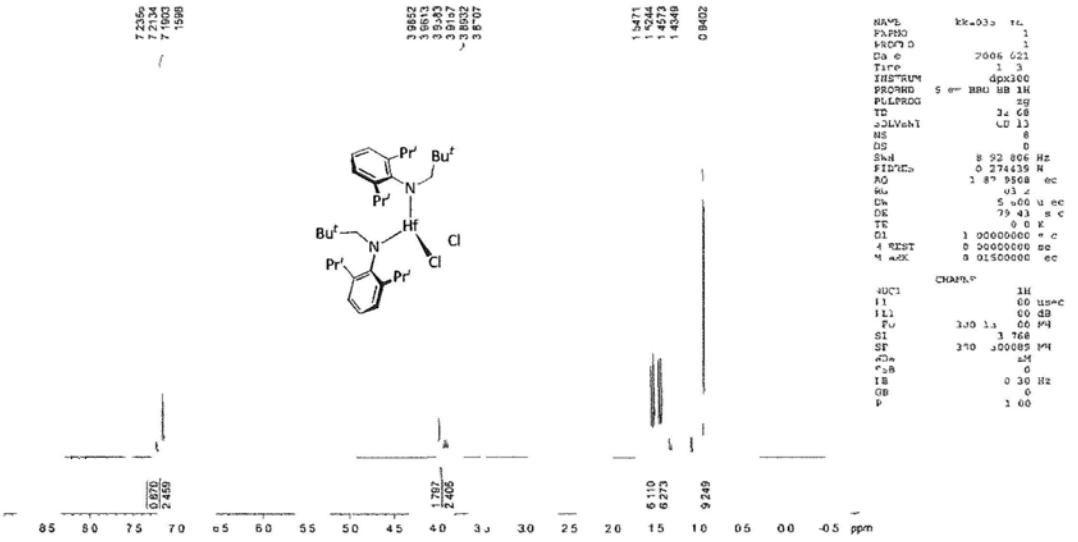

Figure A2–13

^{13}C NMR Spectrum of $[Hf(L^{2})_{2}Cl_{2}]$ (**14**)

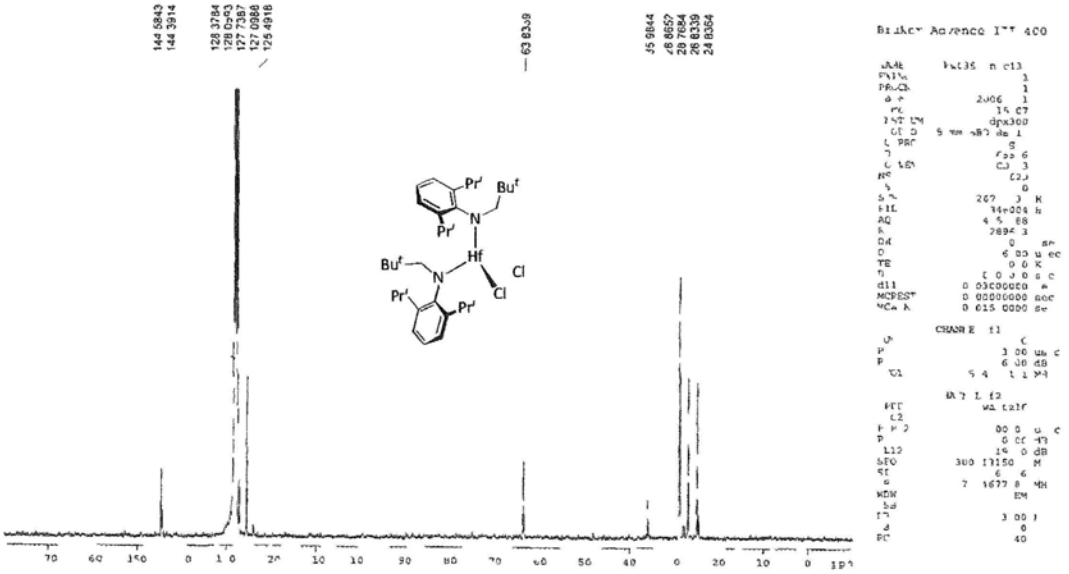

Figure A2–14

^{1}H NMR Spectrum of $[Zr(L^2)_2(NMe_2)_2]$ (**15**)

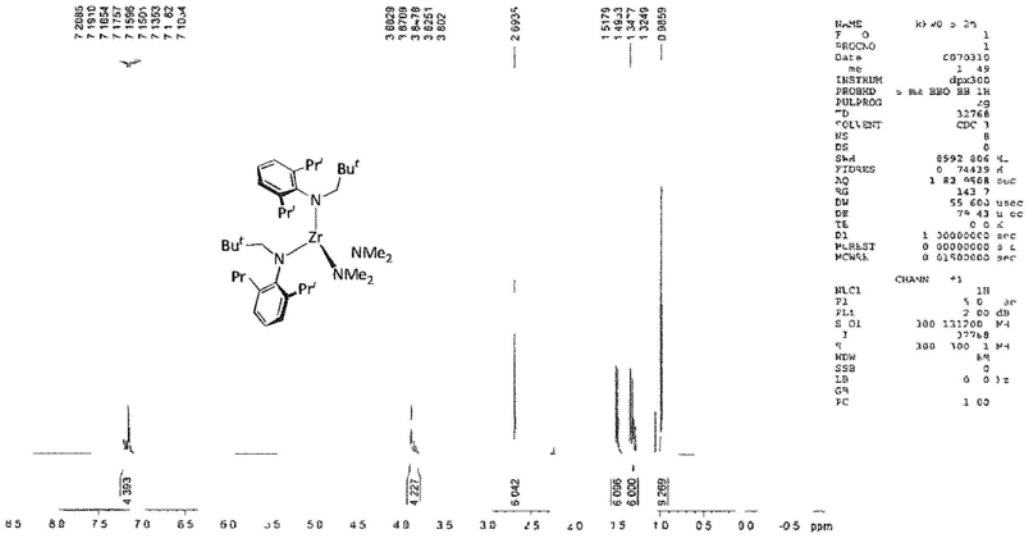

Figure A2–15

^{13}C NMR Spectrum of $[Zr(L^2)_2(NMe_2)_2]$ (**15**)

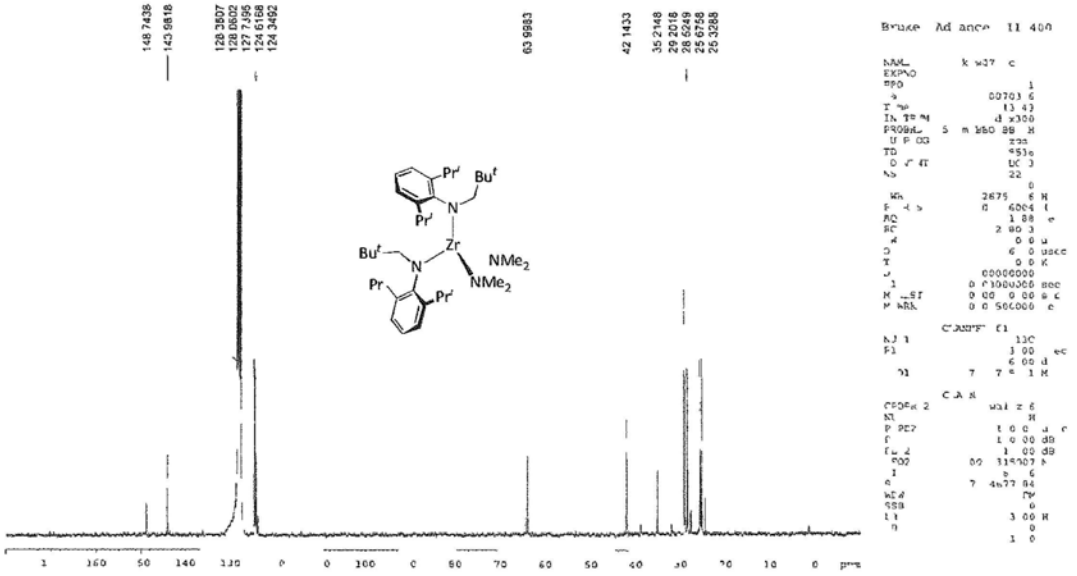

Figure A2–16

^{1}H NMR Spectrum of $[Hf(L^2)_2(NMe_2)_2]$ (**16**)

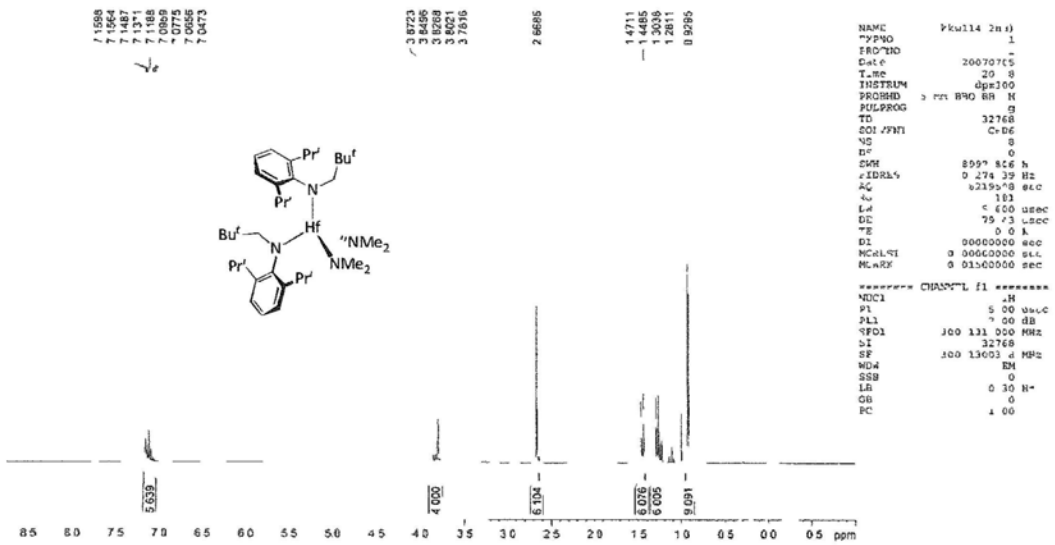

Figure A2–17

^{13}C NMR Spectrum of $[Hf(L^2)_2(NMe_2)_2]$ (**16**)

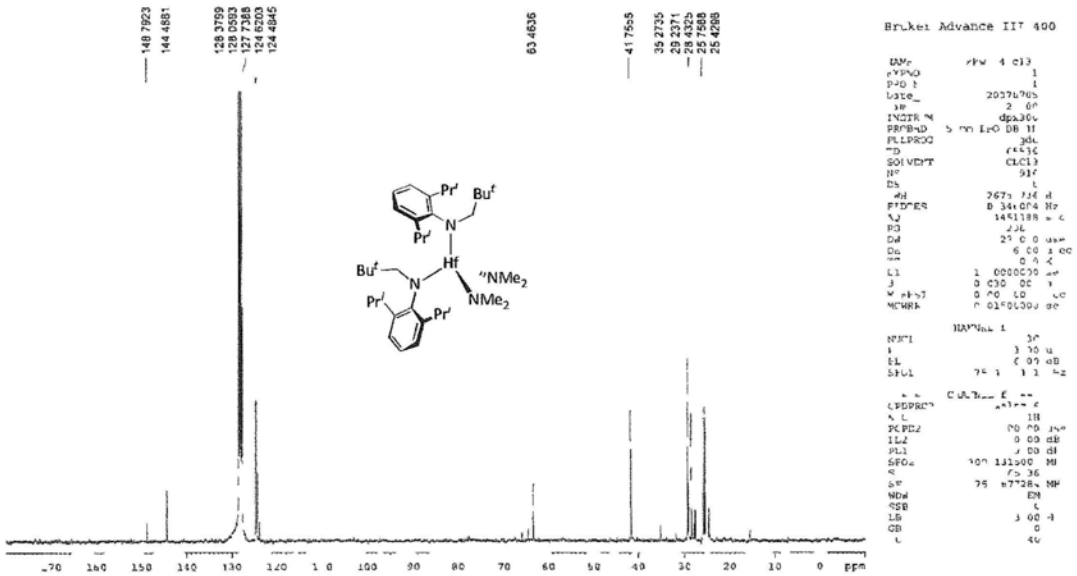

Figure A2–18

^{1}H NMR Spectrum of $[Zr(L^{2})_{2}(NMe_{2})(I)]$ (**17**)

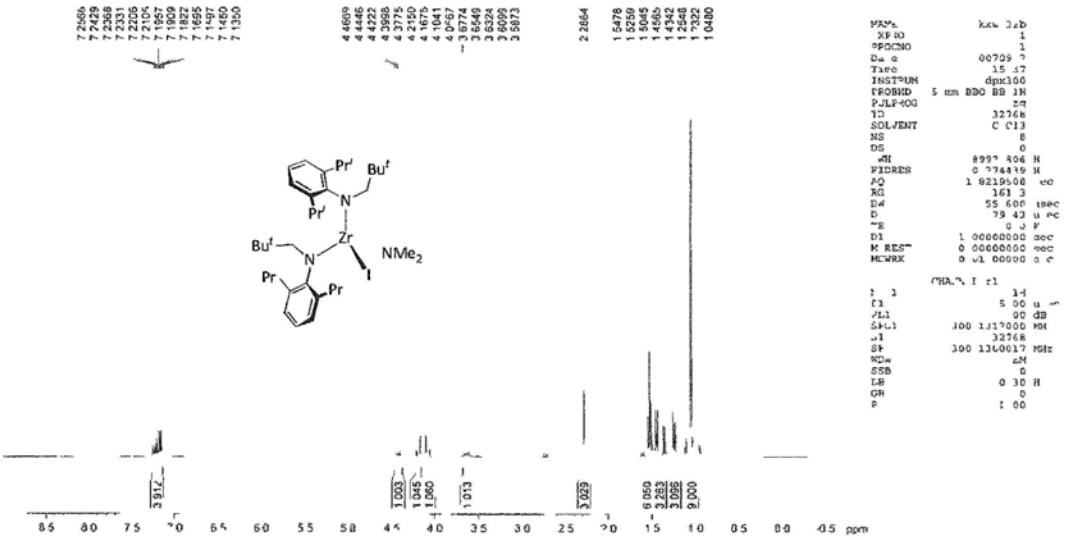

Figure A2–19

^{13}C NMR Spectrum of $[Zr(L^{2})_{2}(NMe_{2})(I)]$ (**17**)

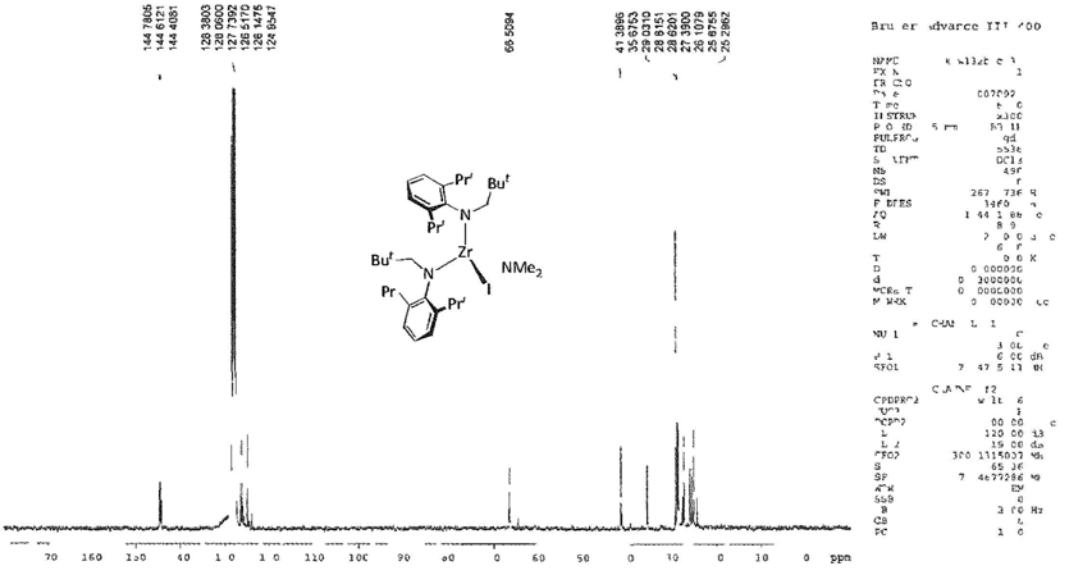

Figure A2–20

^{1}H NMR Spectrum of $[Zr(L^{2})_{2}I_{2}]$ (**18**)

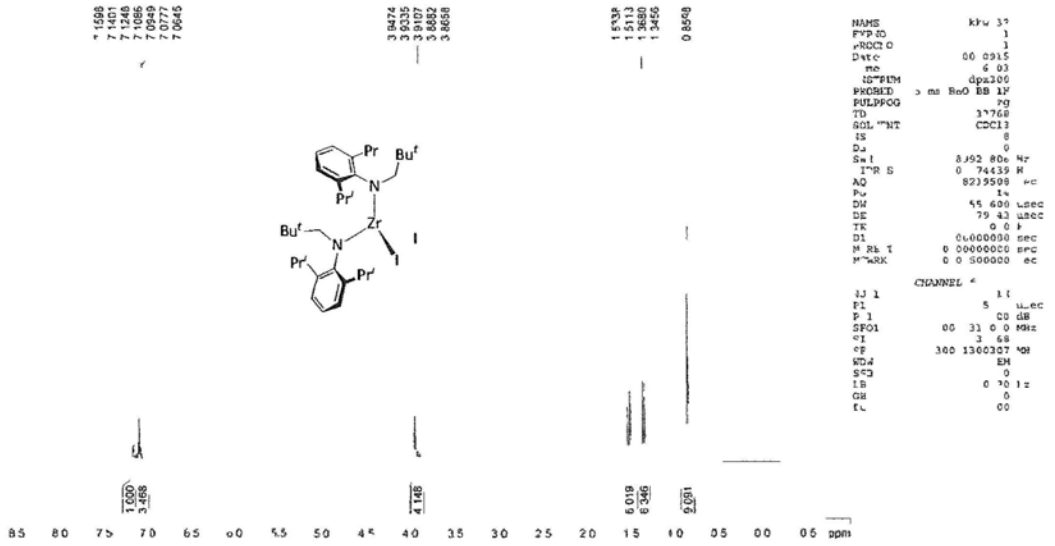

Figure A2–21

^{13}C NMR Spectrum of $[Zr(L^{2})_{2}I_{2}]$ (**18**)

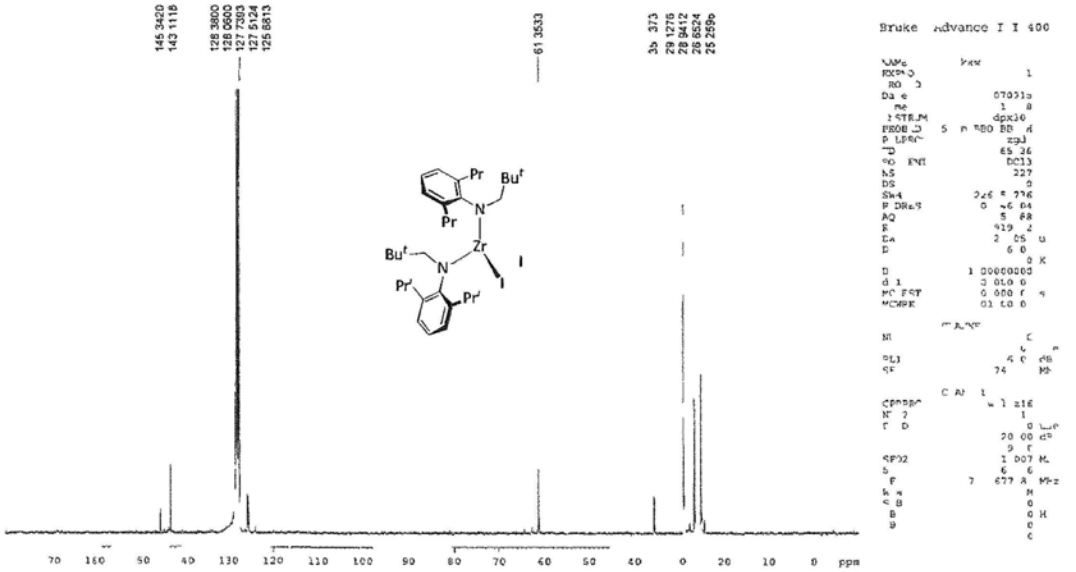

Figure A2–22

^{1}H NMR Spectrum of [Hf(L^{2})$_{2}$(NMe$_{2}$)(I)] (**19**)

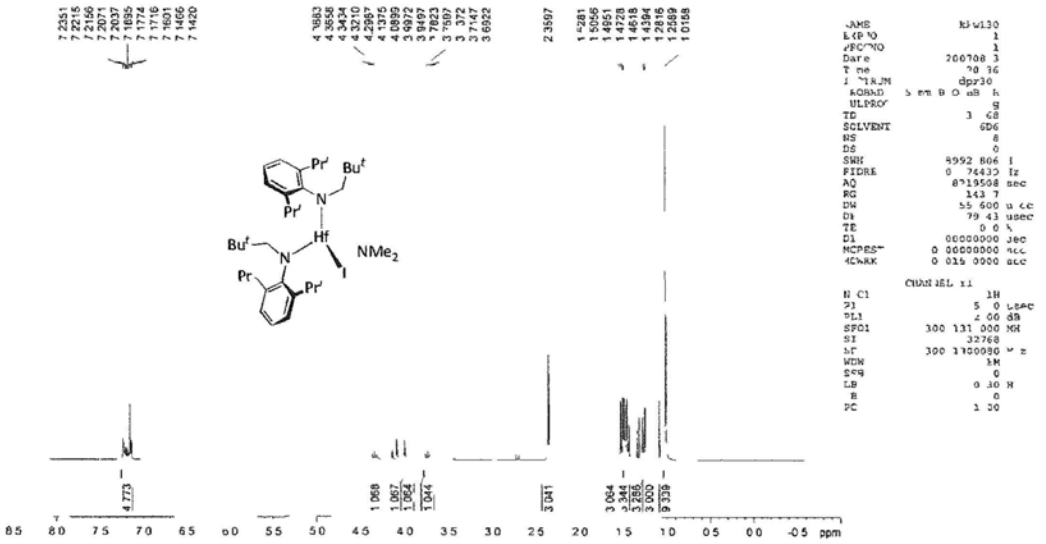

Figure A2–23

^{13}C NMR Spectrum of [Hf(L^{2})$_{2}$(NMe$_{2}$)(I)] (**19**)

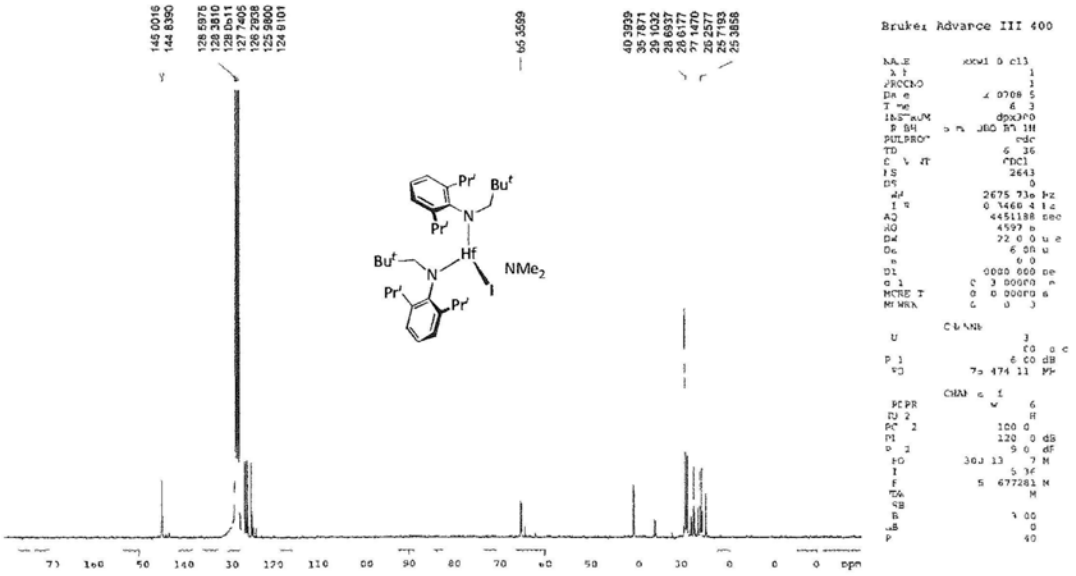

Figure A2–24

^{1}H NMR Spectrum of $[Hf(L^{2})_{2}I_{2}]$ (**20**)

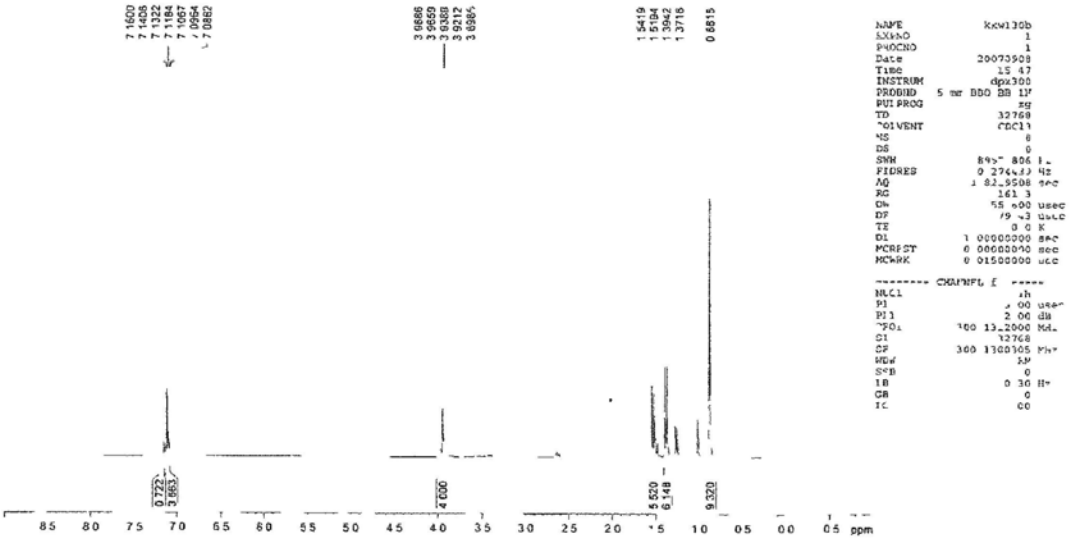

Figure A2–25

^{13}C NMR Spectrum of $[Hf(L^{2})_{2}I_{2}]$ (**20**)

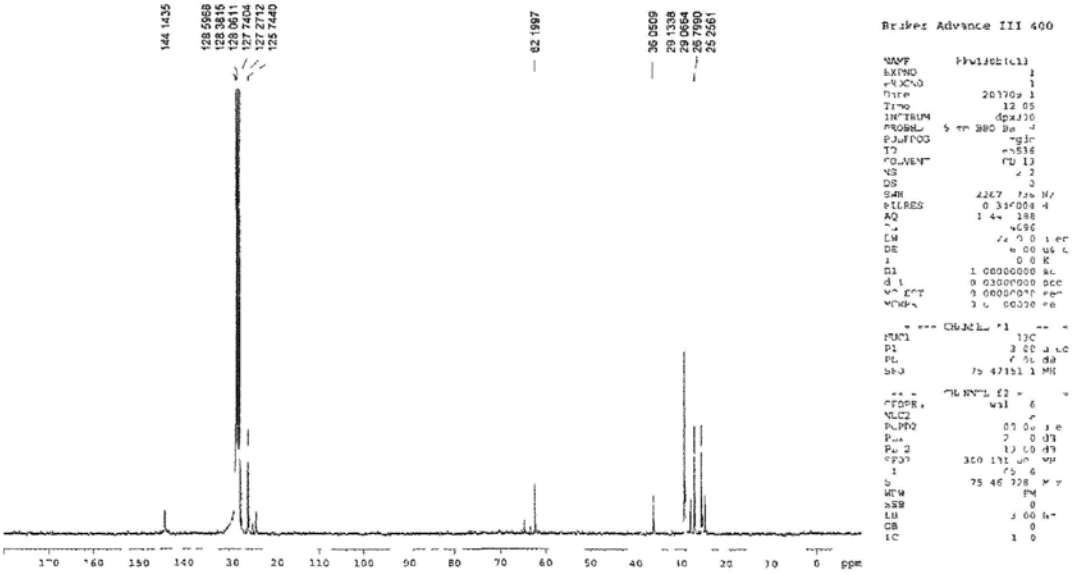

Figure A2–26

^{1}H NMR Spectrum of $[Zr(L^{2})_{2}Me_{2}]$ (**21**)

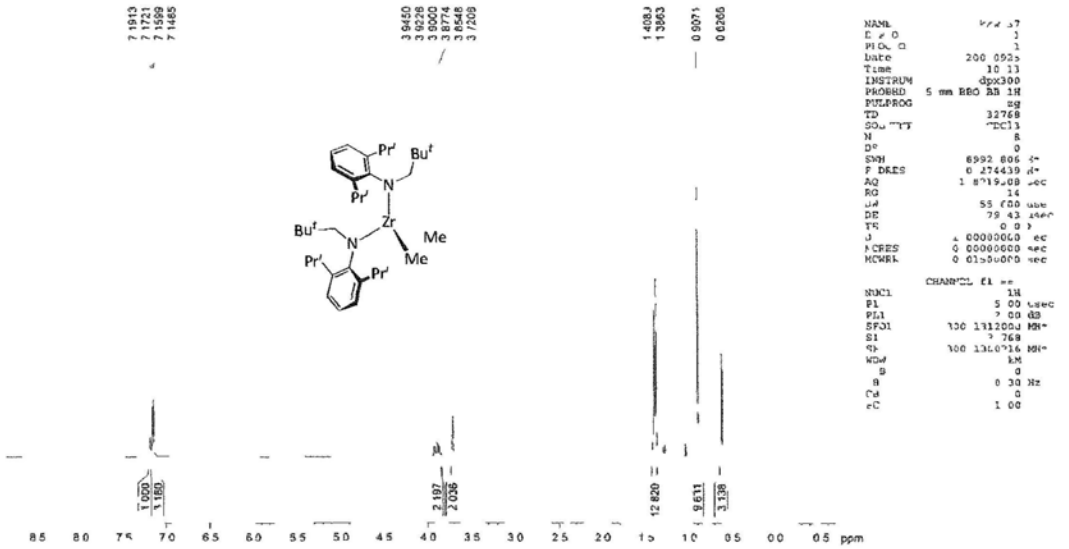

Figure A2–27

^{13}C NMR Spectrum of $[Zr(L^{2})_{2}Me_{2}]$ (**21**)

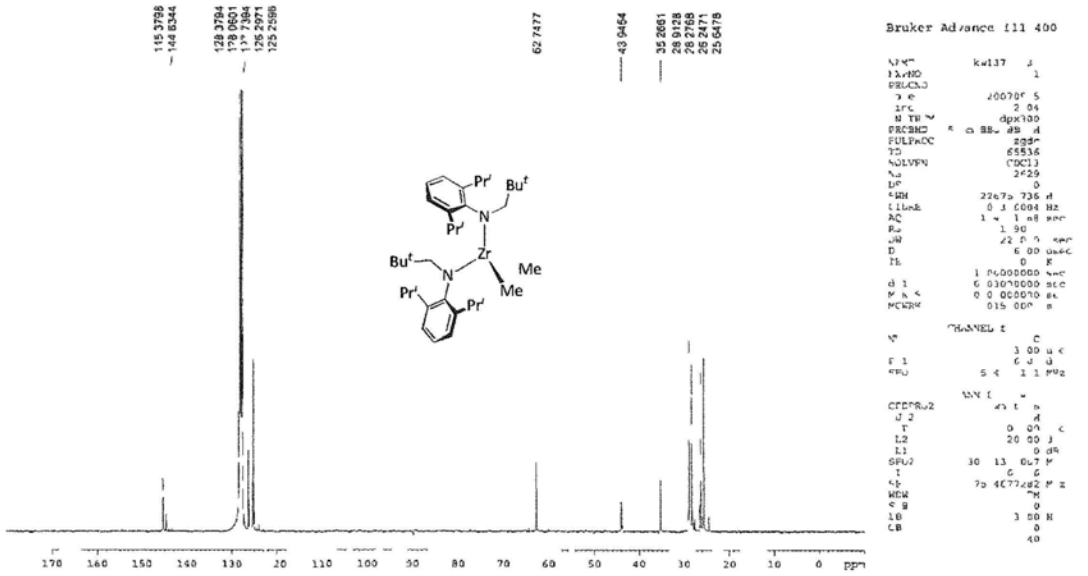

Figure A2–28

^{1}H NMR Spectrum of [Hf(L^{2})$_{2}$Me$_{2}$] (**22**)

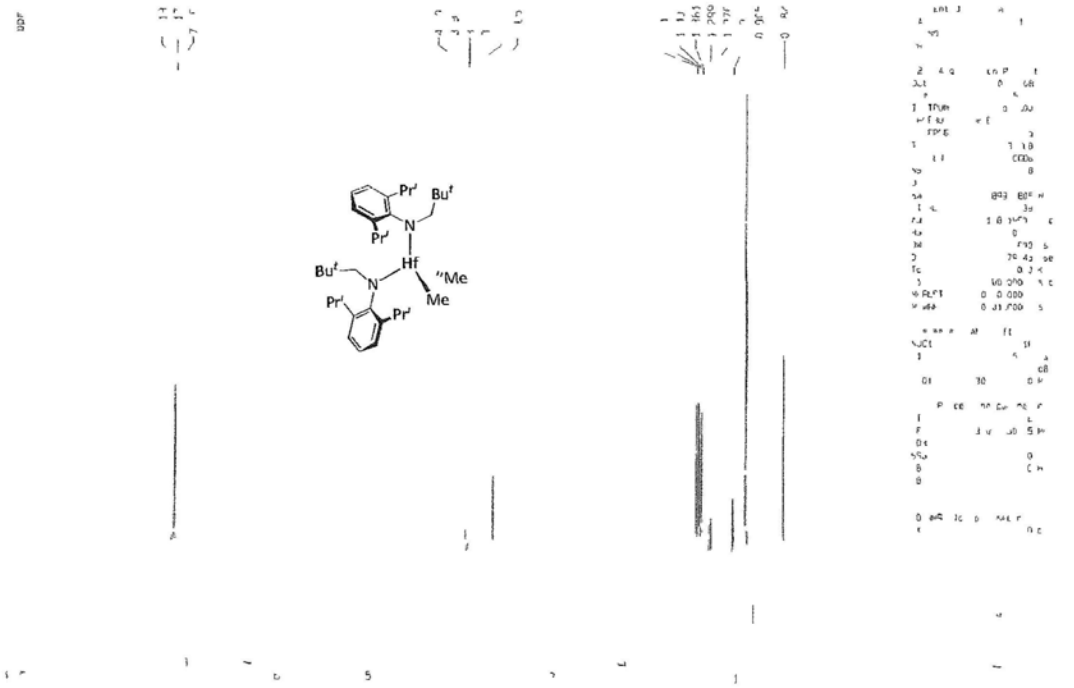

Figure A2–29

^{13}C NMR Spectrum of [Hf(L^{2})$_{2}$Me$_{2}$] (**22**)

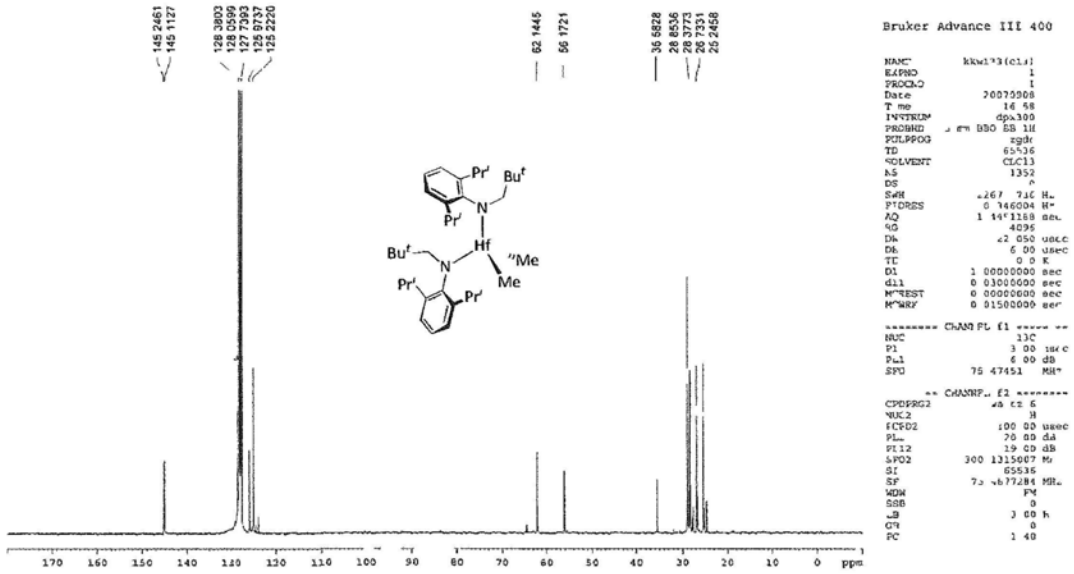

Figure A2–30

^{1}H NMR Spectrum of LiL^{3}(thf)$_2$ (**29**)

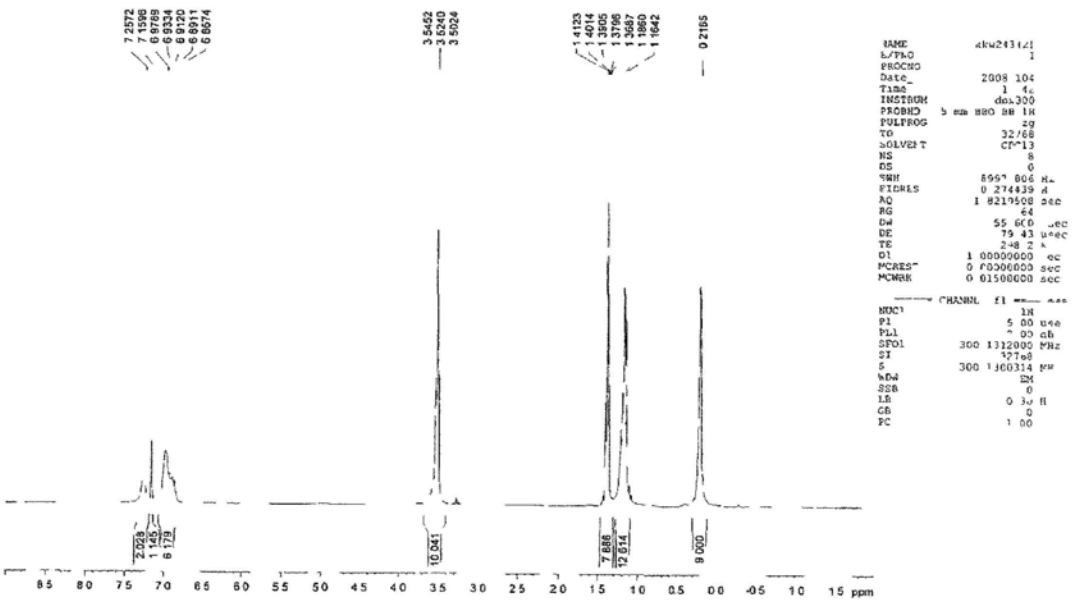

Figure A2–31

^{13}C NMR Spectrum of LiL^{3}(thf)$_2$ (**29**)

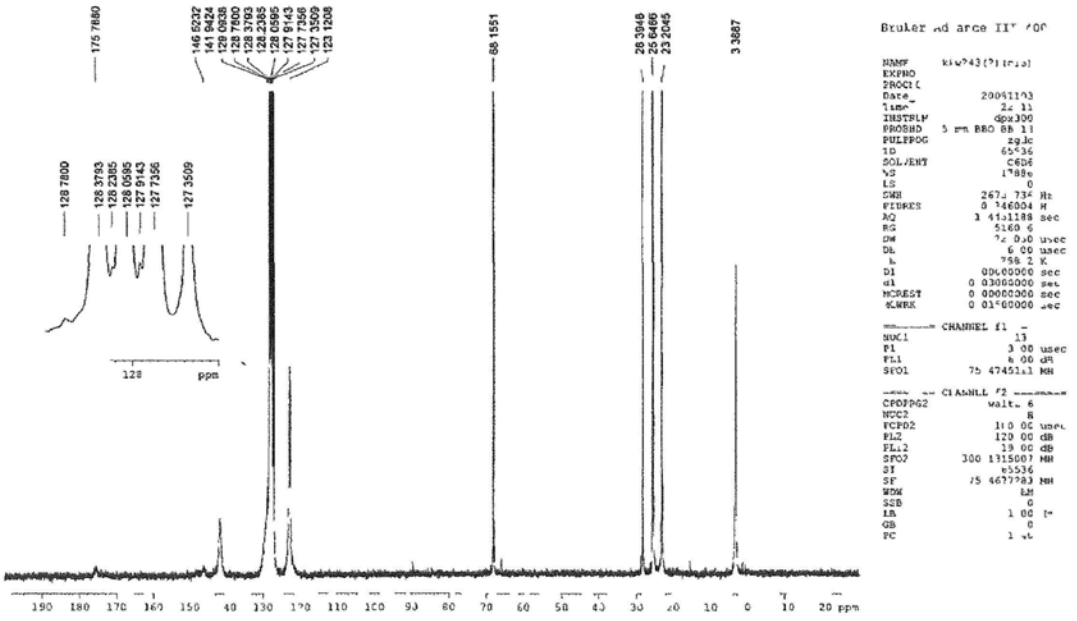

Figure A2–32

^{1}H NMR Spectrum of [Ti(L^{3})(NC$_{6}$H$_{3}$Pr$^{i}_{2}$–2,6)(μ–Cl)$_{2}$Li(tmeda)] (**33**)

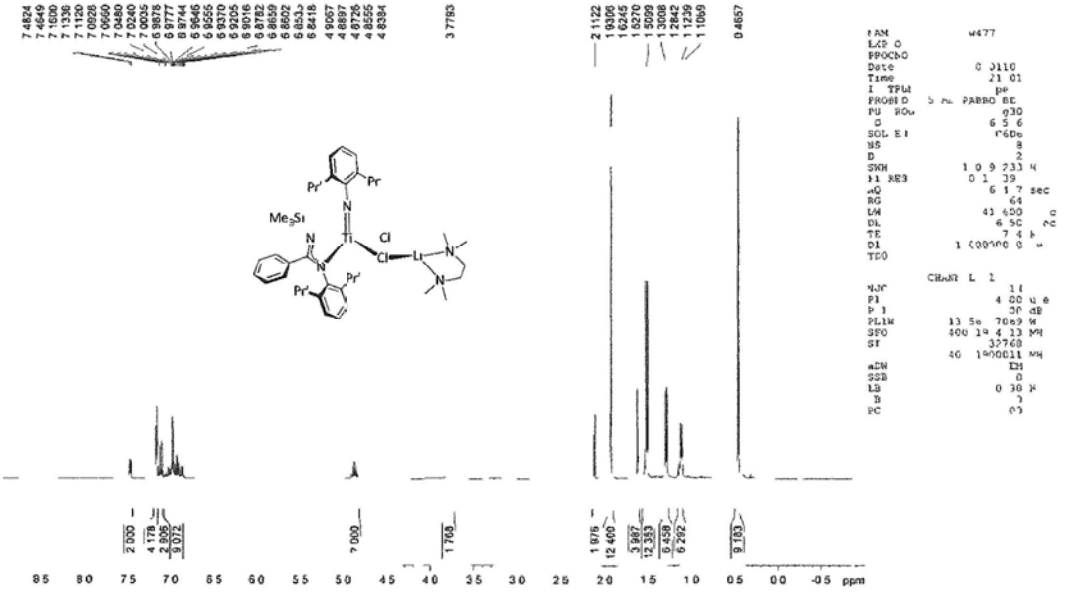

Figure A2–33

^{13}C NMR Spectrum of [Ti(L^{3})(NC$_{6}$H$_{3}$Pr$^{i}_{2}$–2,6)(μ–Cl)$_{2}$Li(tmeda)] (**33**)

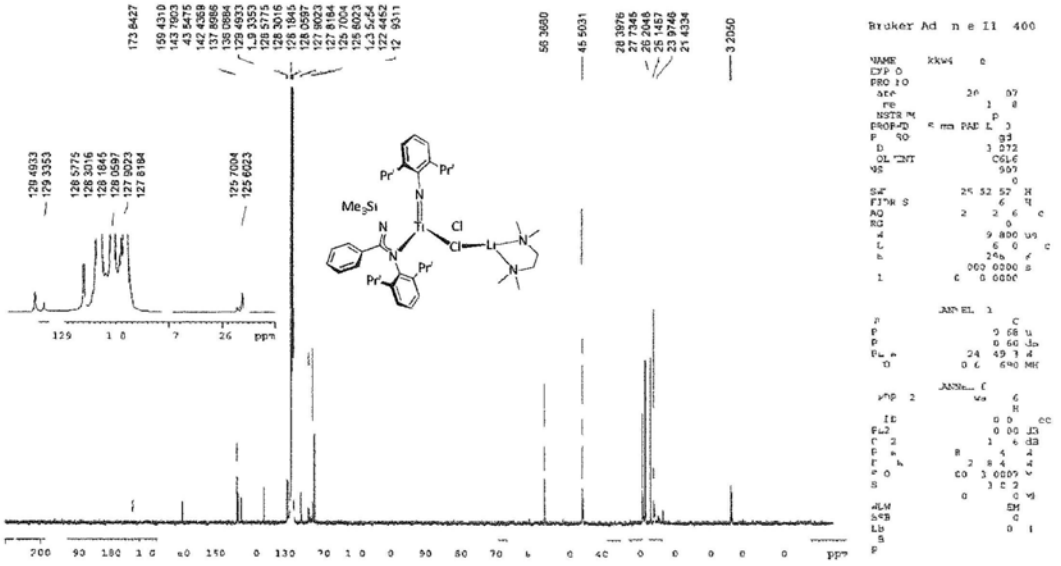

Figure A2–34

^{1}H NMR Spectrum of $[Zr(L^{3})_{2}Cl_{2}]$ (**34**)

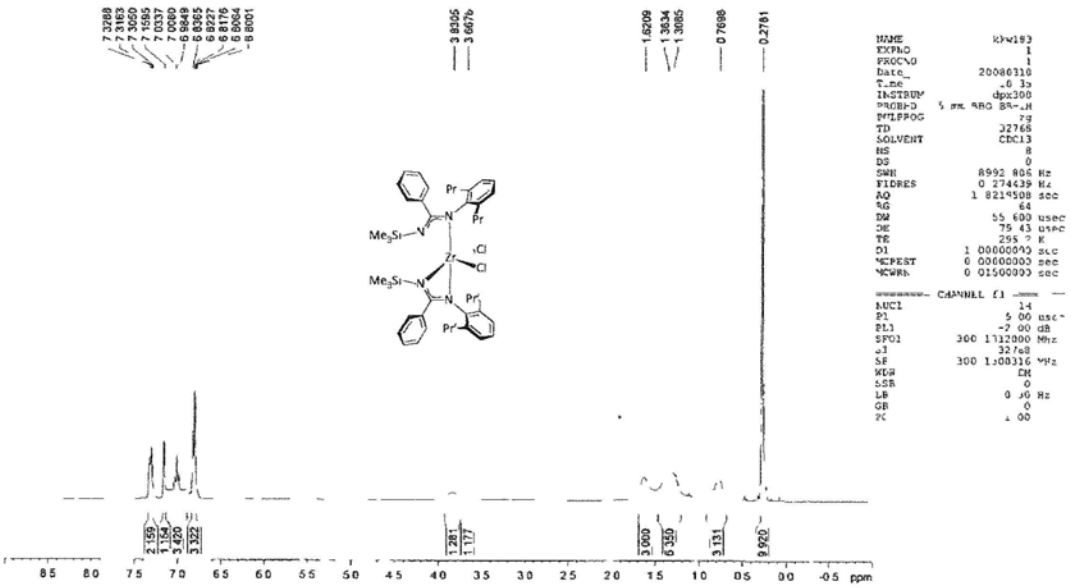

Figure A2–35

^{13}C NMR Spectrum of $[Zr(L^{3})_{2}Cl_{2}]$ (**34**)

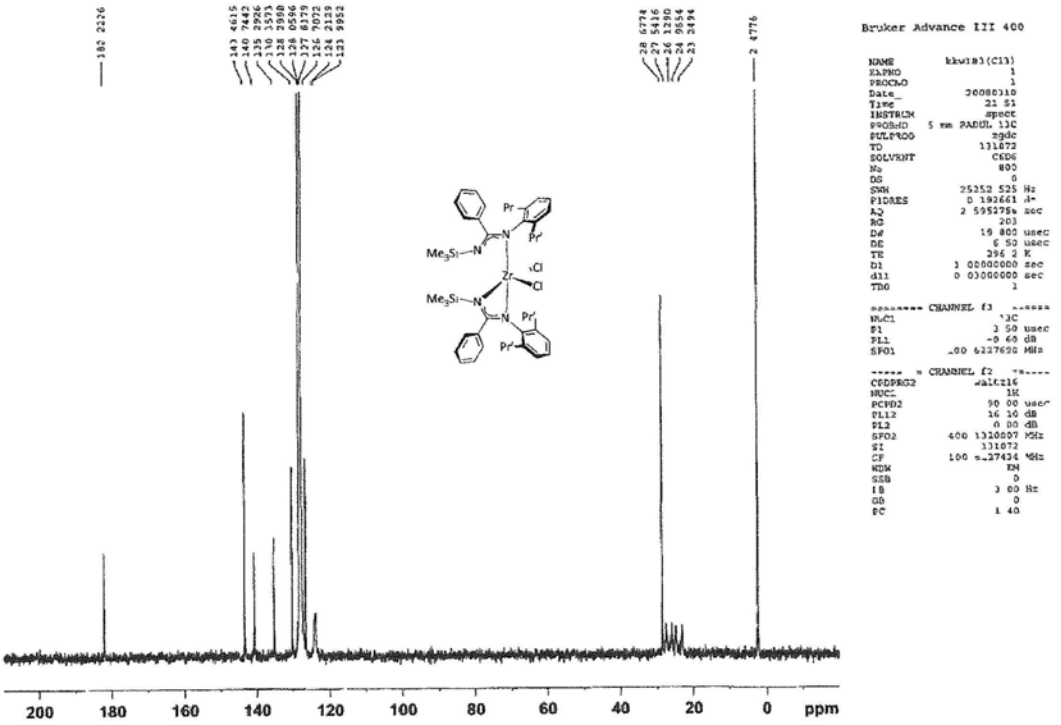

Figure A2–36

^{1}H NMR Spectrum of $[Hf(L^{3})_{2}Cl_{2}]$ (**35**)

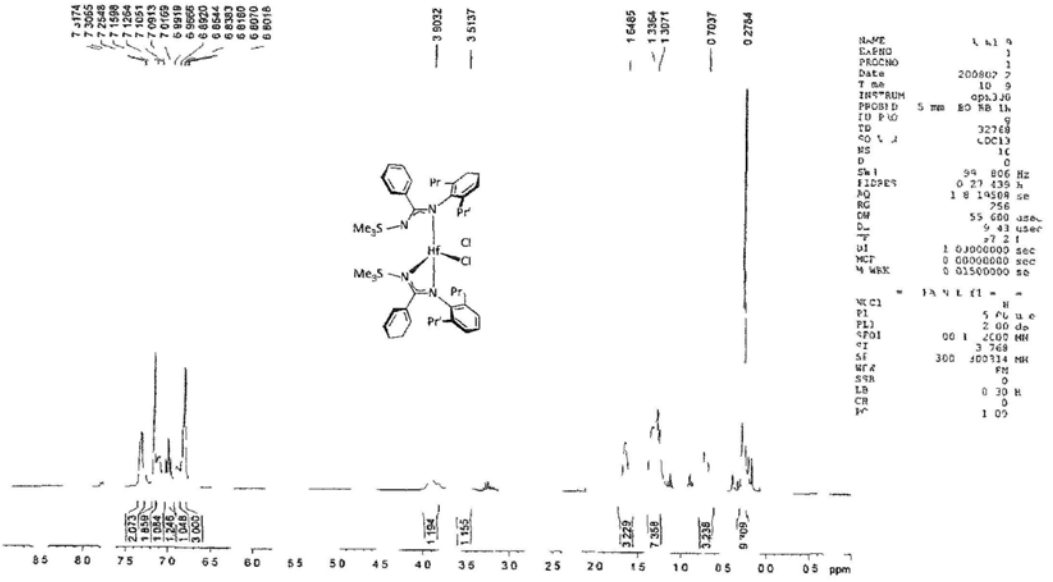

Figure A2–37

^{13}C NMR Spectrum of $[Hf(L^{3})_{2}Cl_{2}]$ (**35**)

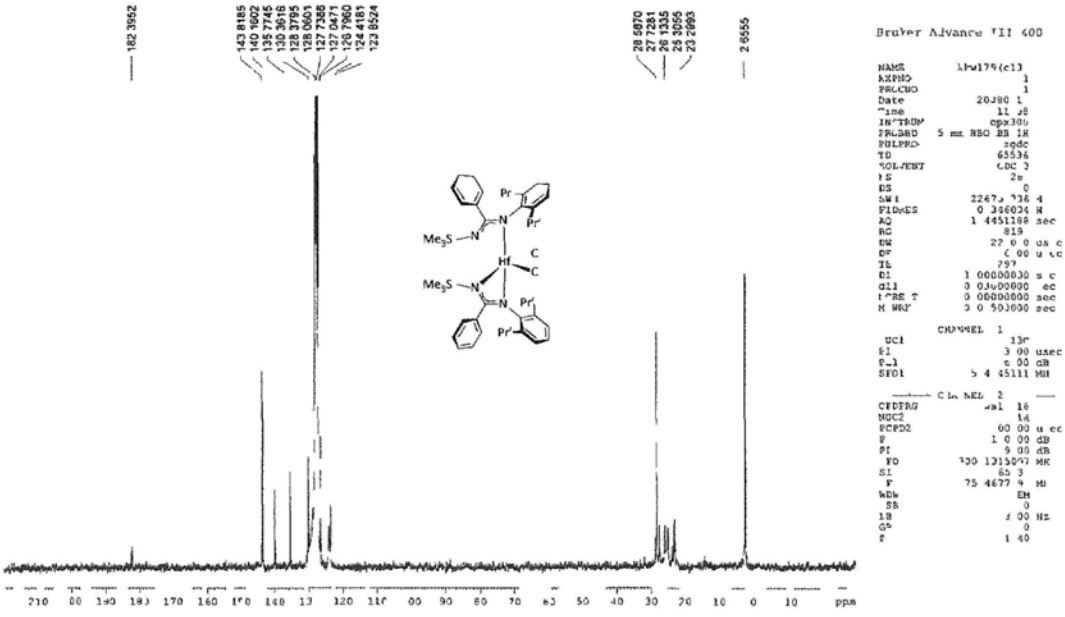

Figure A2–38

^{1}H NMR Spectrum of [Zr(L^{3})$_{2}$Me$_{2}$] (**36**)

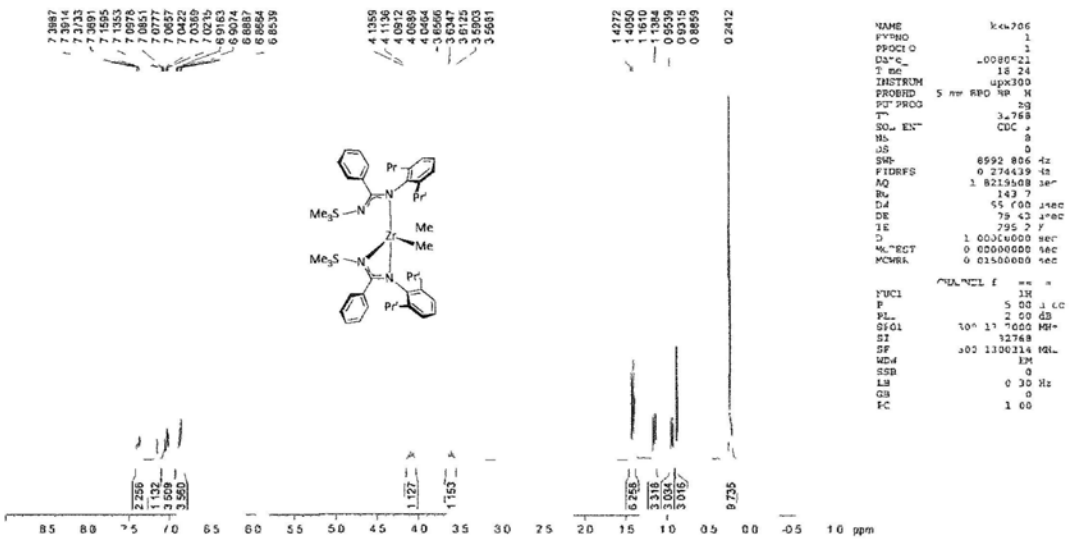

Figure A2–39

^{13}C NMR Spectrum of [Zr(L^{3})$_{2}$Me$_{2}$] (**36**)

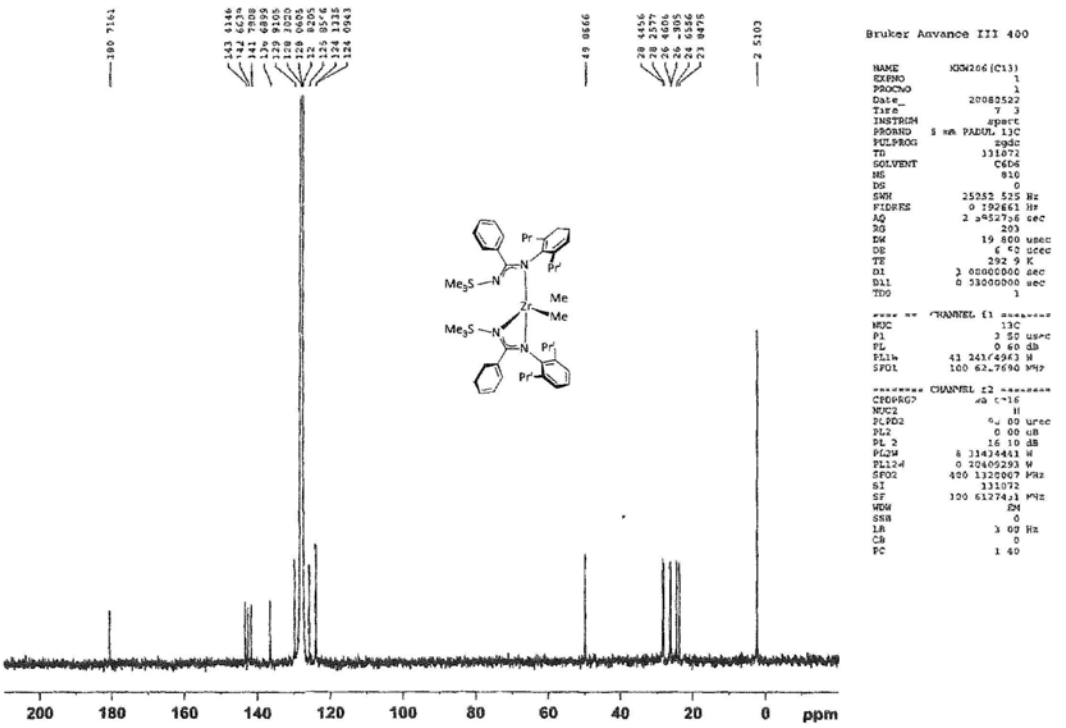

Figure A2–40

^{1}H NMR Spectrum of $[Zr(L^{3})_{2}(CH_{2}Ph)Cl]$ (**37**)

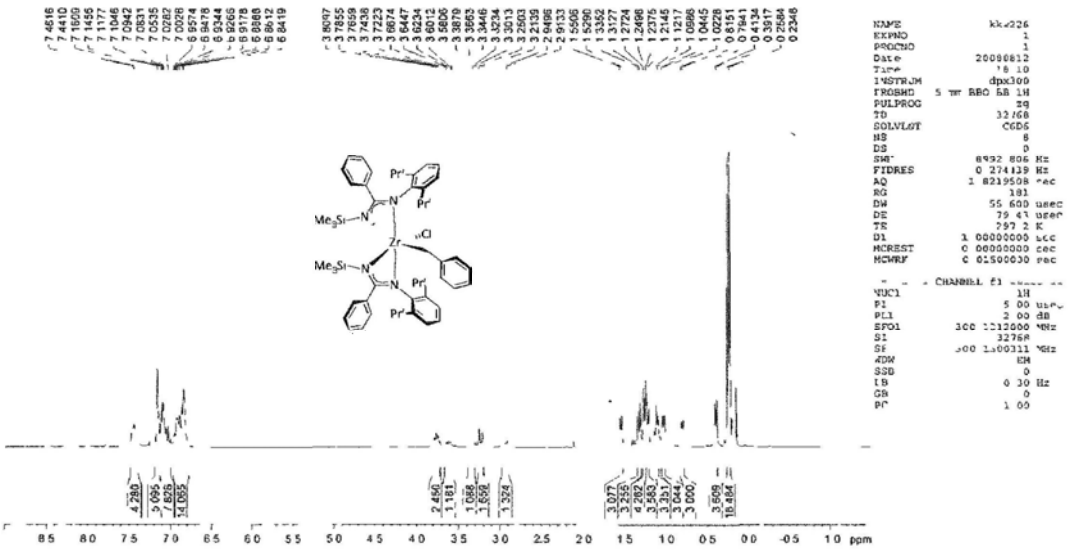

Figure A2–41

^{13}C NMR Spectrum of $[Zr(L^{3})_{2}(CH_{2}Ph)Cl]$ (**37**)

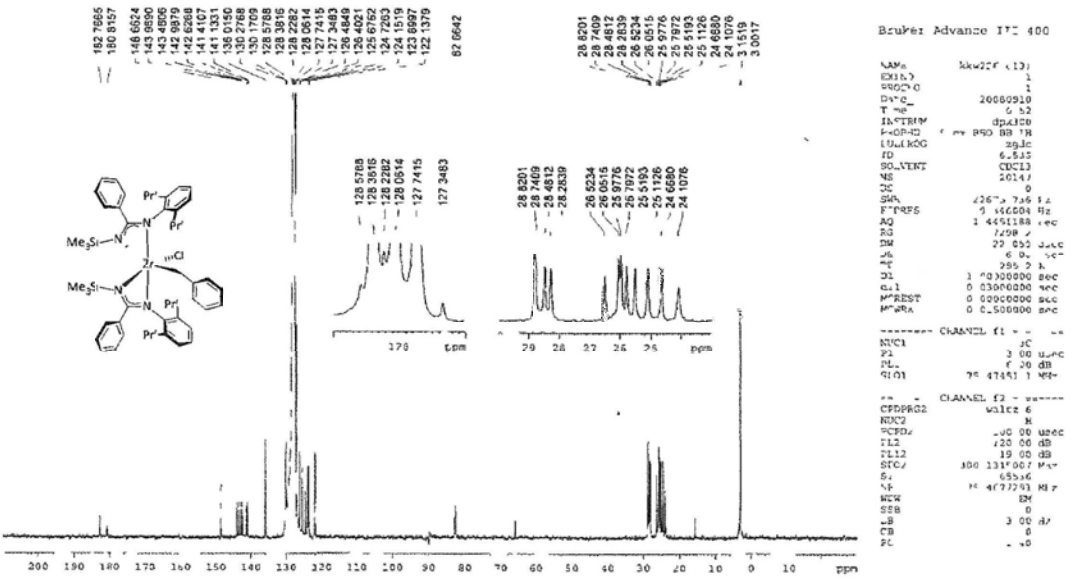

Figure A2–42

^{1}H NMR Spectrum of [Mg(L^{3})$_{2}$(thf)] (**39**)

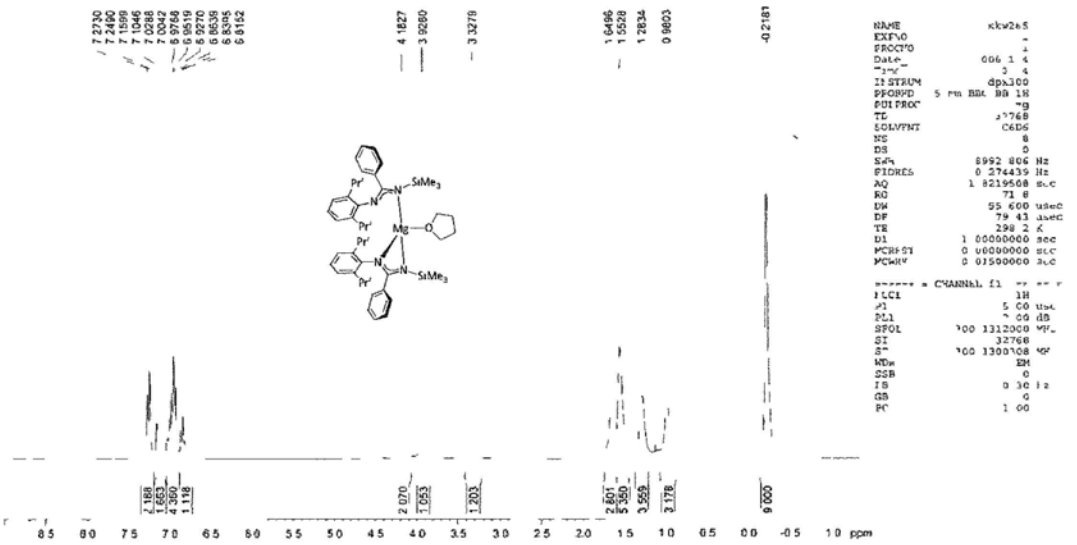

Figure A2–43

^{13}C NMR Spectrum of [Mg(L^{3})$_{2}$(thf)] (**39**)

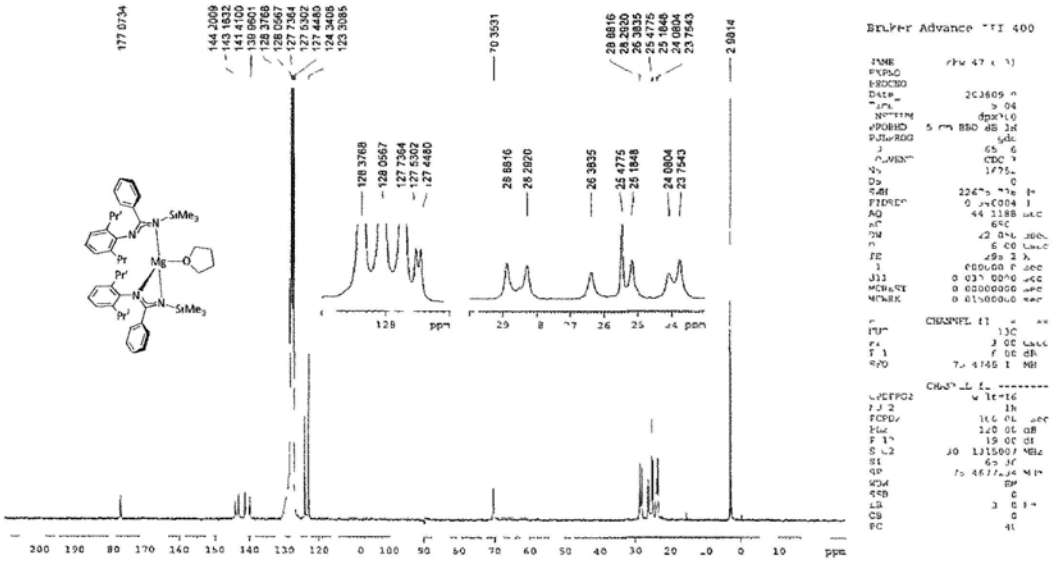

Figure A2–44

^{1}H NMR Spectrum of [Ca(L^{3})$_{2}$(thf)] (**40**)

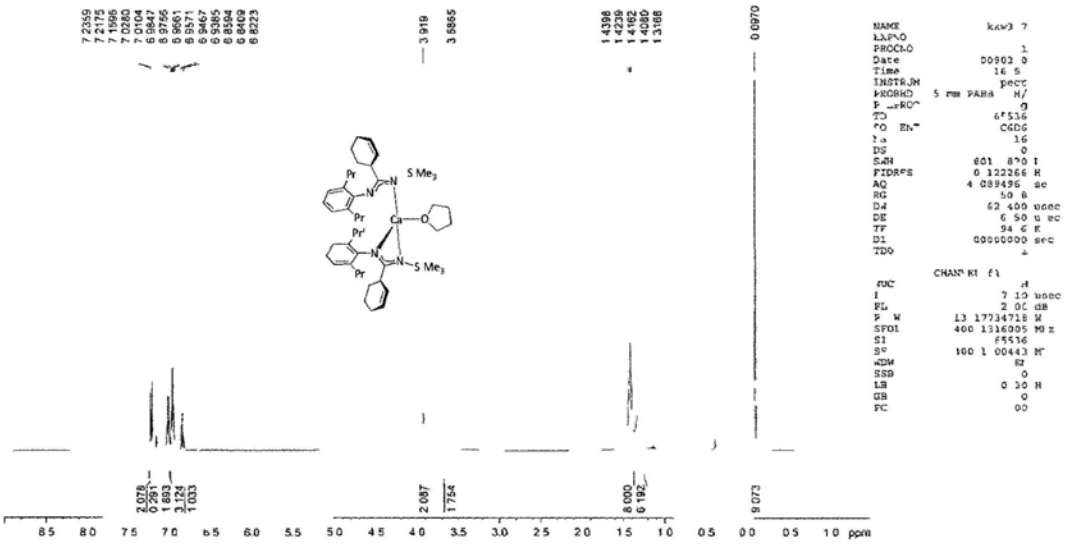

Figure A2–45

^{13}C NMR Spectrum of [Ca(L^{3})$_{2}$(thf)] (**40**)

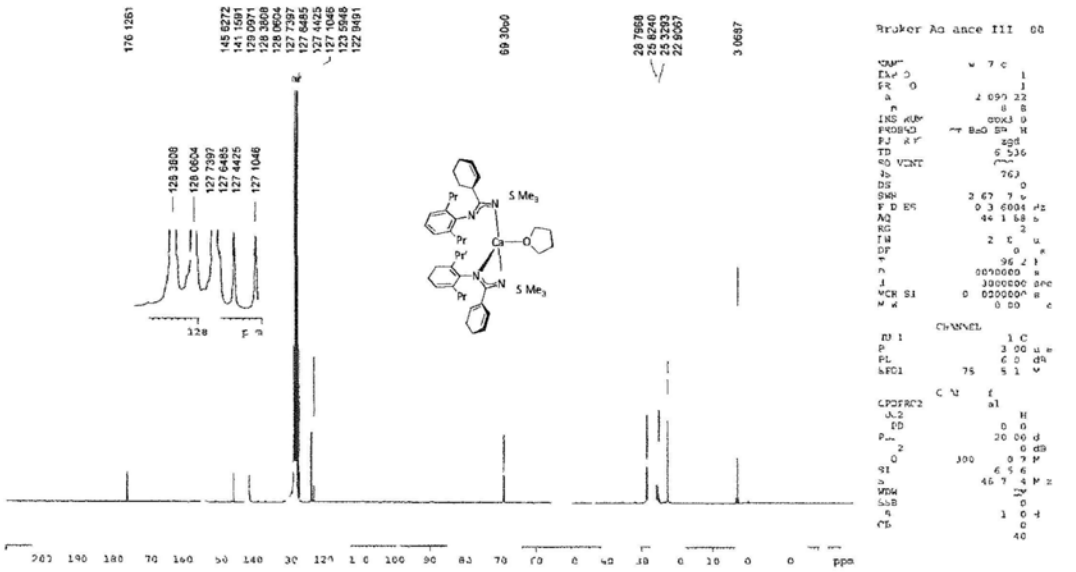

Figure A2–46

^{1}H NMR Spectrum of [HL^{4}] (**41**)

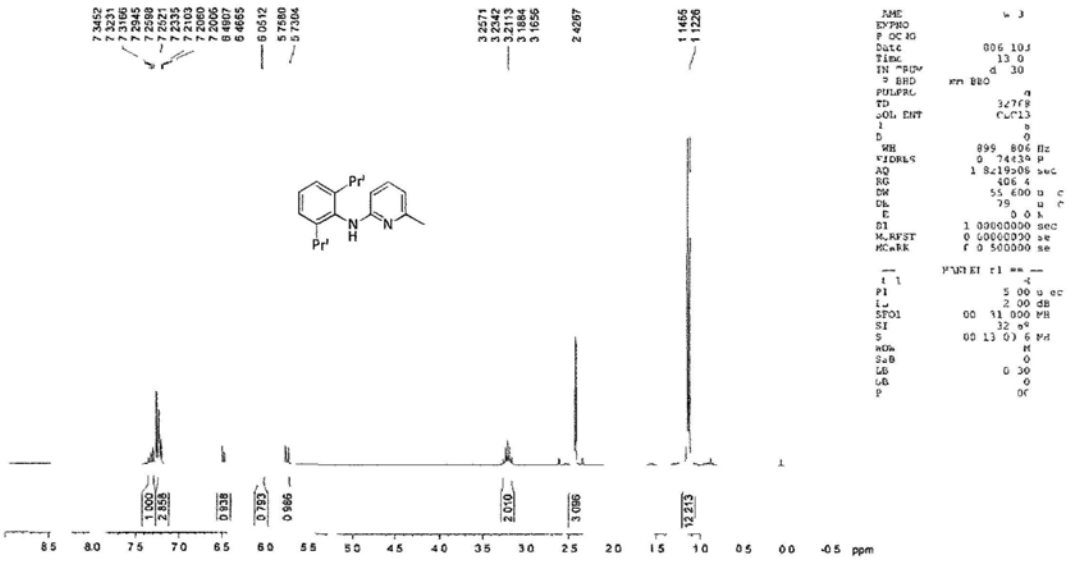

Figure A2–47

^{13}C NMR Spectrum of [HL^{4}] (**41**)

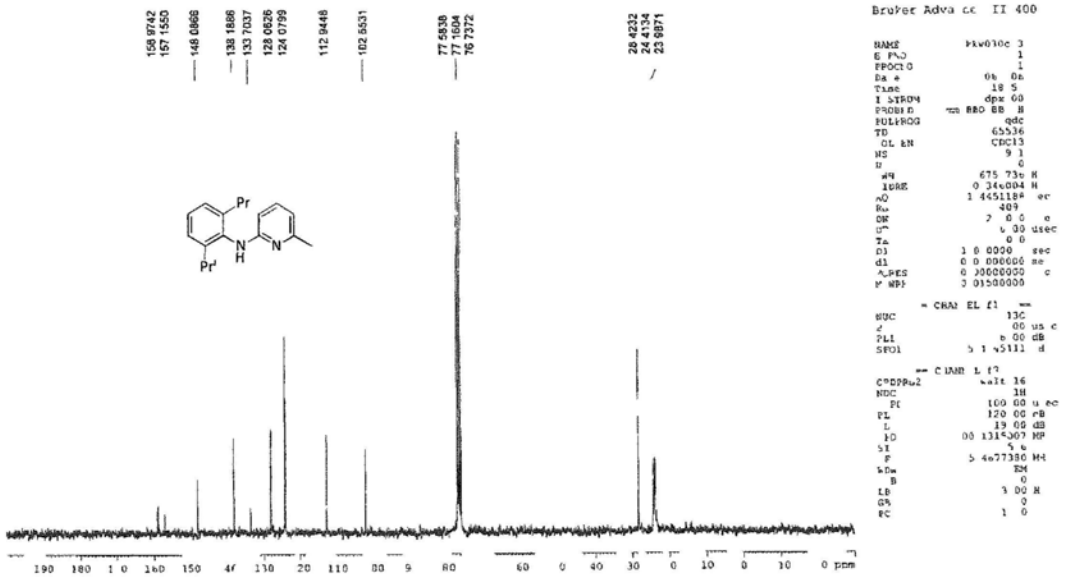

Figure A2–48

^{1}H NMR Spectrum of [{KL^{4}(OEt$_{2}$)}$_{2}$] (**42**)

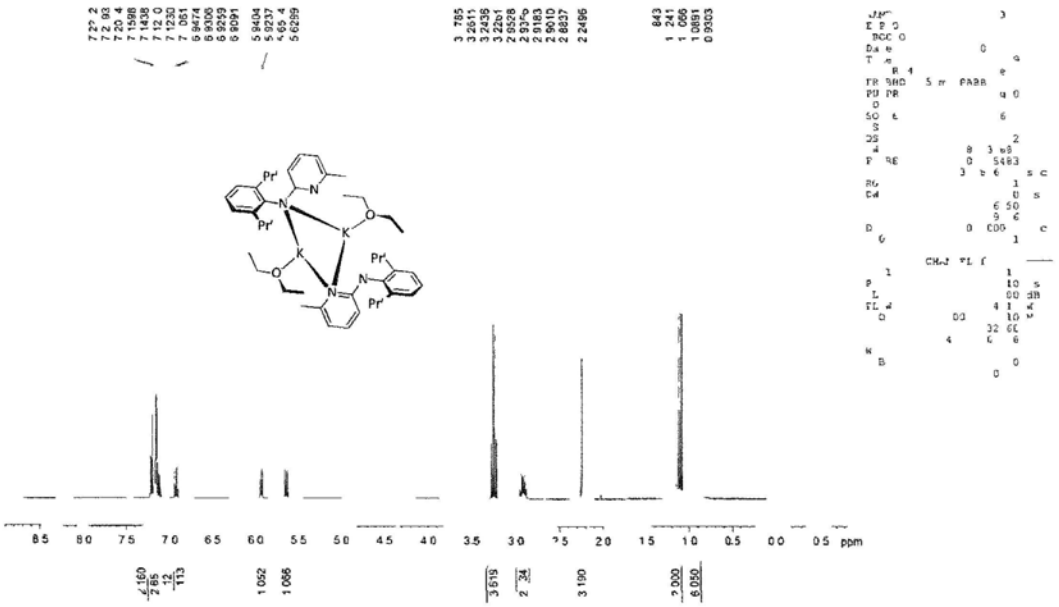

Figure A2–49

^{13}C NMR Spectrum of [{KL^{4}(OEt$_{2}$)}$_{2}$] (**42**)

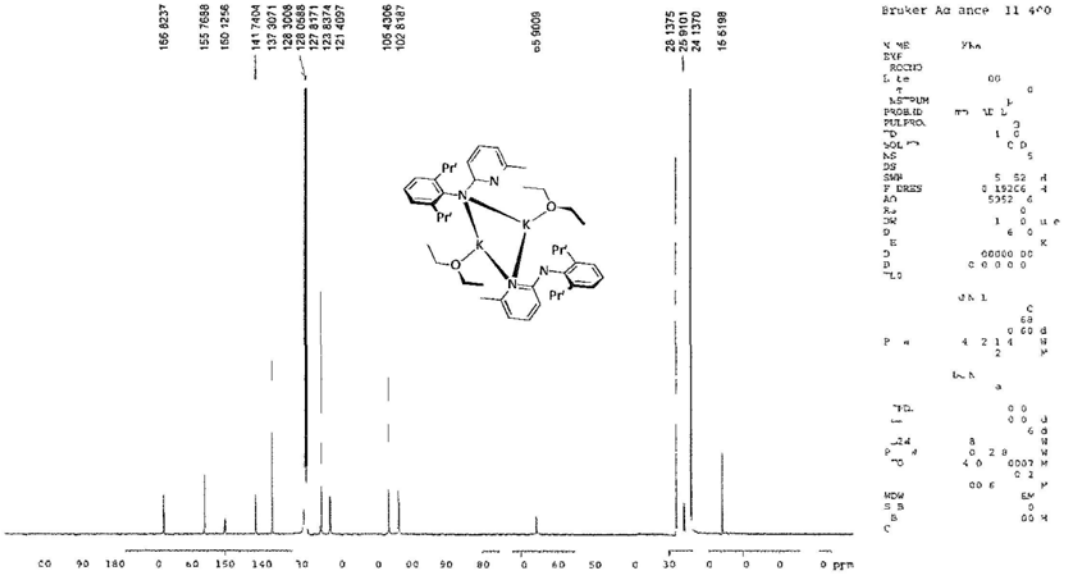

Figure A2–50

^{1}H NMR Spectrum of KL^{4}(thf)$_2$ (**43**)

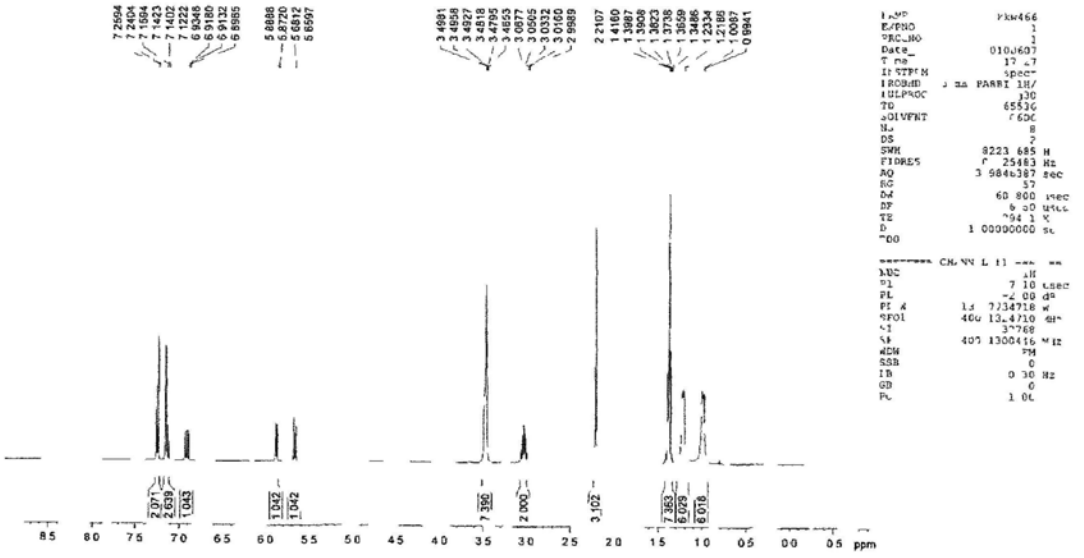

Figure A2–51

^{13}C NMR Spectrum of KL^{4}(thf)$_2$ (**43**)

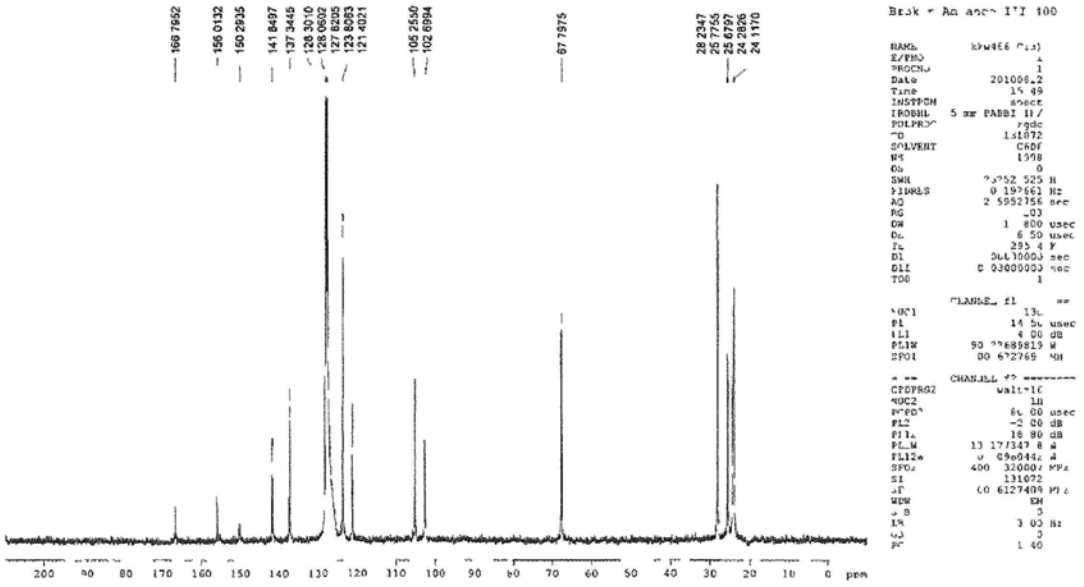

Figure A2–52

^{1}H NMR Spectrum of [Yb(L^{4})$_{2}$(thf)$_{2}$] (**44**)

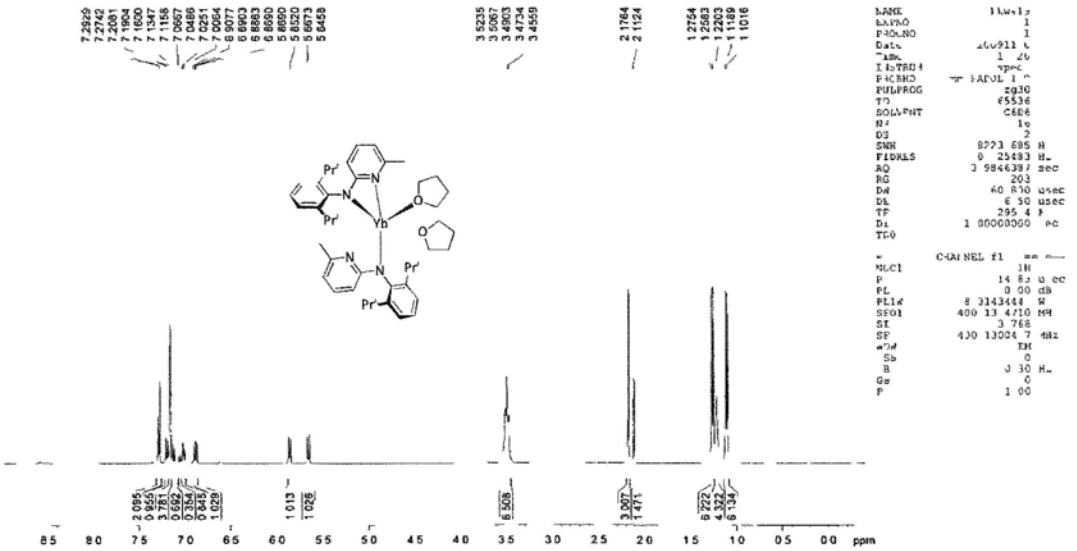

Figure A2–53

^{13}C NMR Spectrum of [Yb(L^{4})$_{2}$(thf)$_{2}$] (**44**)

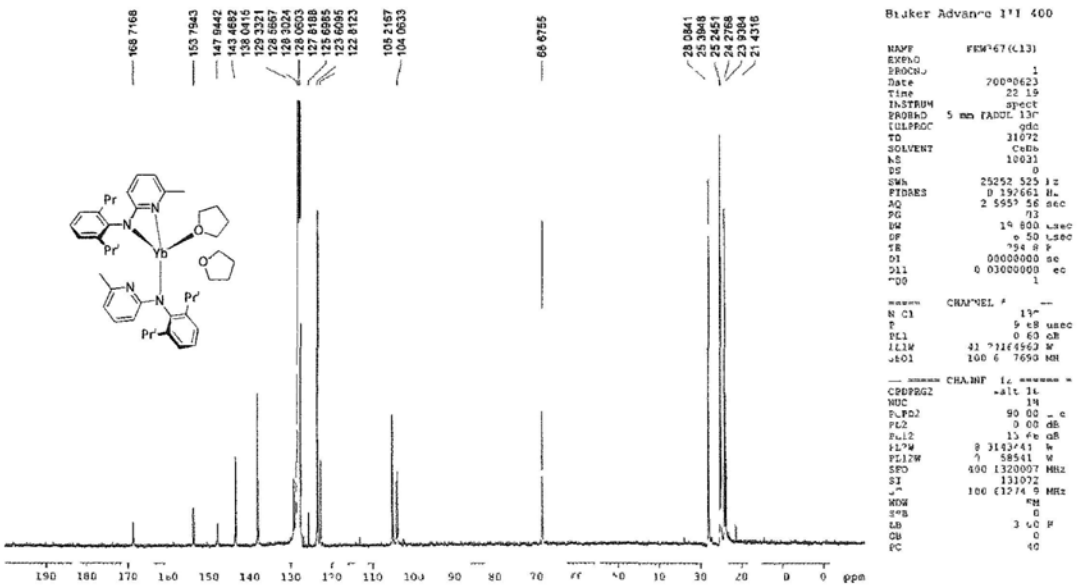

Figure A2–54

^{1}H NMR Spectrum of [Sm(L^{4})$_{3}$] (**46**)

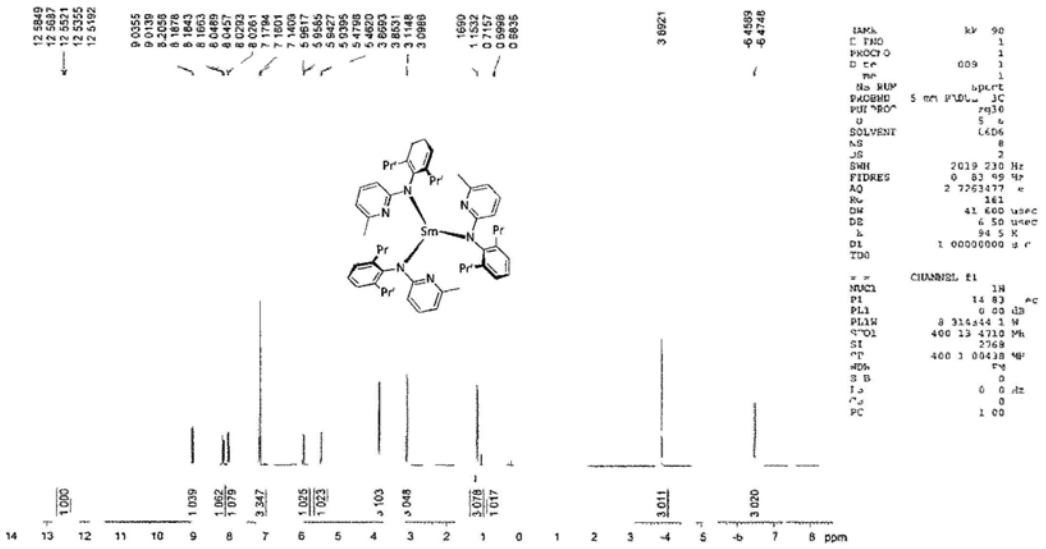

Figure A2–55

^{13}C NMR Spectrum of [Sm(L^{4})$_{3}$] (**46**)

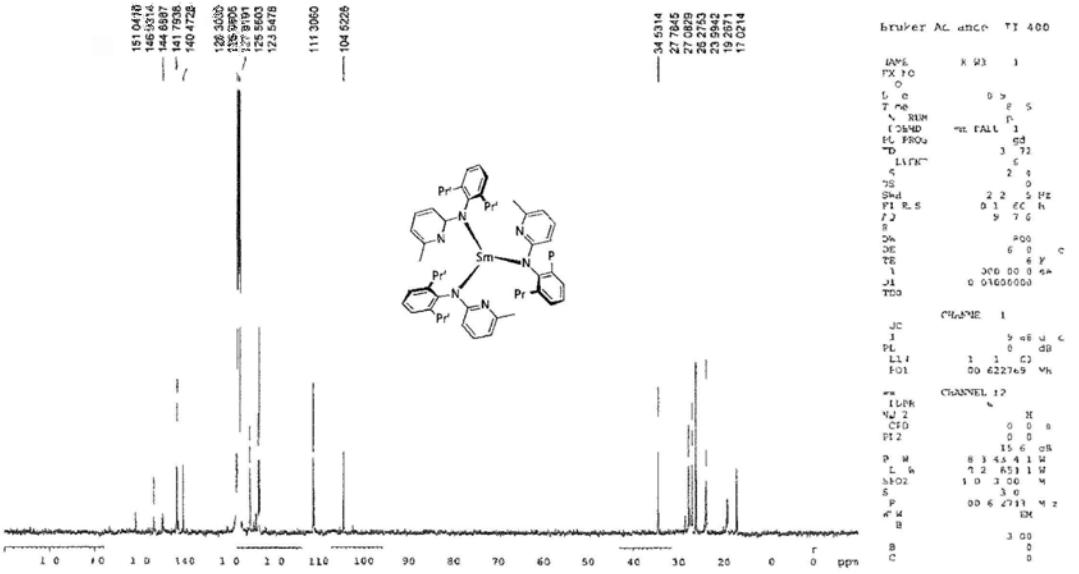

Figure A2–56

^{1}H NMR Spectrum of [Yb(L^{4})$_{3}$] (**49**)

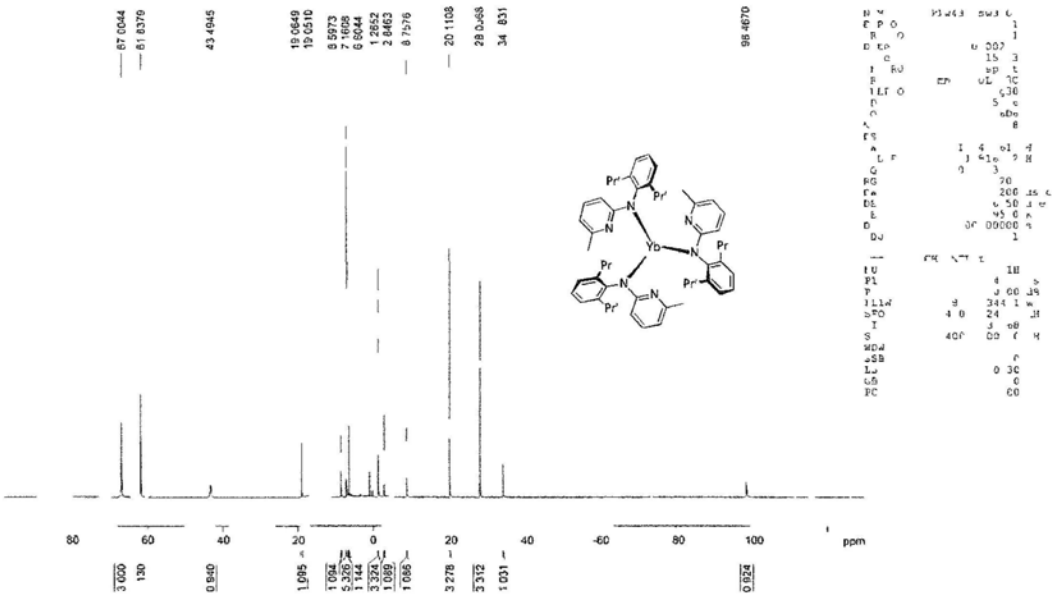

Figure A2–56

Appendix 3

Selected Crystallographic Data

Table A3–1 Selected Crystallographic Data for Compounds **8**•0.5PhMe and **9**.

	8•0.5PhMe	**9**
Molecular formula	$C_{35.5}H_{60}Cl_3LiN_4Zr$	$C_{40}H_{72}Cl_3LiN_4Zr$
Formula weight	747.39	813.53
Crystal size, mm^3	0.50 × 0.40 × 0.30	0.30 × 0.20 × 0.10
Crystal system	Triclinic	Monoclinic
Space group	$P\bar{1}$	$P2_1/n$
a, Å	12.209(2)	13.842(3)
b, Å	12.455(3)	15.560(3)
c, Å	15.394(3)	21.736(4)
α, Å	79.857(4)	90
β, deg	88.340(4)	91.86(3)
γ, deg	76.929(4)	90
Z	2	4
V, $Å^3$	2244.4(8)	4679(1)
Density, g cm^{-3}	1.106	1.155
Abs coeff., mm^{-1}	0.448	0.435
Temperature, K	293(2)	293(2)
Reflections collected	12219	13355
Independent reflections	7866 (R_{int} = 0.0365)	7864 (R_{int} = 0.0416)
Obs. data with $I \geq 2\sigma(I)$	4919	6992
Final R indices [$I \geq 2\sigma(I)$]	$R1$ = 0.0710	$R1$ = 0.0499
	$wR2$ = 0.1990	$wR2$ = 0.1222
R indices (all data)*	$R1$ = 0.1228	$R1$ = 0.0614
	$wR2$ = 0.2519	$wR2$ = 0.1288

* $R1 = \sum \big| \, |F_o| - |F_c| \, \big| \, / \sum |F_o|$; $wR2 = \{\sum [w(F_o^2 - F_c^2)^2] \, / \sum [w(F_o^2)^2]\}^{1/2}$

Table A3–2 Selected Crystallographic Data for Compounds **10**•PhMe, **11** and **13a**.

	10•PhMe	**11**	**13a**
Molecular formula	$C_{39}H_{64}Cl_3HfLiN_4$	$C_{40}H_{72}Cl_3HfLiN_4$	$C_{42}H_{72}Cl_3LiN_2O_2Zr$
Formula weight	880.72	900.80	841.53
Crystal size, mm^3	0.40 × 0.30 × 0.20	0.50 × 0.40 × 0.30	0.40 × 0.30 × 0.20
Crystal system	Triclinic	Monoclinic	Monoclinic
Space group	$P\bar{1}$	$P2_1/n$	C_c
a, Å	12.281(1)	13.282(1)	24.705(5)
b, Å	12.406(1)	14.021(1)	10.465(2)
c, Å	15.427(1)	25.536(3)	20.046(4)
α, Å	79.971(2)	90	90
β, deg	88.245(2)	100.733(2)	113.37(3)
γ, deg	76.368(2)	90	90
Z	2	4	4
V, $Å^3$	2249.2(4)	4672.5(9)	4758(1)
Density, g cm^{-3}	1.300	1.281	1.175
Abs coeff., mm^{-1}	2.526	2.433	0.432
Temperature, K	293(2)	293(2)	293(2)
Reflections collected	15479	31253	7082
Independent reflections	10673 (R_{int} = 0.0354)	11294(R_{int} = 0.0366)	3887 (R_{int} = 0.0249)
Obs. data with $I \geq 2\sigma(I)$	7109	8218	3764
Final R indices [$I \geq 2\sigma(I)$]	$R1$ = 0.0474	$R1$ = 0.0336	$R1$ = 0.0348
	$wR2$ = 0.1009	$wR2$ = 0.0742	$wR2$ = 0.0877
R indices (all data)*	$R1$ = 0.0874	$R1$ = 0.0578	$R1$ = 0.0371
	$wR2$ = 0.1204	$wR2$ = 0.0841	$wR2$ = 0.0897

* $R1 = \sum \mid |F_o| - |F_c| \mid / \sum |F_o|$; $wR2 = \{\sum [w(F_o^2 - F_c^2)^2] / \sum [w(F_o^2)^2]\}^{1/2}$

Table A3–3 Selected Crystallographic Data for Compounds **12–14**.

	12	**13**	**14**
Molecular formula	$C_{34}H_{56}Cl_2N_2Ti$	$C_{34}H_{56}Cl_2N_2Zr$	$C_{34}H_{56}Cl_2HfN_2$
Formula weight	611.61	654.93	742.20
Crystal size, mm^3	0.40 × 0.30 × 0.20	0.50 × 0.40 × 0.20	0.50 × 0.30 × 0.20
Crystal system	Orthorhombic	Orthorhombic	Orthorhombic
Space group	$P2_12_12_1$	$P2_12_12_1$	$P2_12_12_1$
a, Å	10.950(1)	10.980(1)	10.972(1)
b, Å	12.618(1)	12.715(1)	12.709(1)
c, Å	25.985(3)	26.078(3)	26.079(3)
α, Å	90	90	90
β, deg	90	90	90
γ, deg	90	90	90
Z	4	4	4
V, $Å^3$	3590.3(6)	3640.9(6)	3636.7(7)
Density, g cm^{-3}	1.132	1.195	1.356
Abs coeff., mm^{-1}	0.410	0.471	3.038
Temperature, K	293(2)	293(2)	293(2)
Reflections collected	24598	24846	24749
Independent reflections	8661 (R_{int} = 0.0467)	8765 (R_{int} = 0.0514)	8782 (R_{int} = 0.0382)
Obs. data with $I \geq 2\sigma(I)$	5833	5814	7137
Final R indices [$I \geq 2\sigma(I)$]	$R1$ = 0.0412	$R1$ = 0.0423	$R1$ = 0.0258
	$wR2$ = 0.0902	$wR2$ = 0.0766	$wR2$ = 0.0485
R indices (all data)*	$R1$ = 0.0822	$R1$ = 0.0880	$R1$ = 0.0407
	$wR2$ = 0.1077	$wR2$ = 0.0939	$wR2$ = 0.0535

* $R1 = \sum \big| \, |F_o| - |F_c| \, \big| / \sum |F_o|$; $wR2 = \{\sum [w(F_o^2 - F_c^2)^2] / \sum [w(F_o^2)^2]\}^{1/2}$

Table A3–4 Selected Crystallographic Data for Compounds **15** and **16**.

	15	**16**
Molecular formula	$C_{38}H_{68}N_4Zr$	$C_{38}H_{68}HfN_4$
Formula weight	672.18	759.45
Crystal size, mm^3	0.40 × 0.30 × 0.20	0.50 × 0.40 × 0.30
Crystal system	Monoclinic	Monoclinic
Space group	$P2_1/c$	$P2_1/c$
a, Å	14.882(1)	14.896(3)
b, Å	11.385(1)	11.387(2)
c, Å	23.651(2)	23.663(4)
α, Å	90	90
β, deg	92.211(2)	92.236(3)
γ, deg	90	90
Z	4	4
V, $Å^3$	4004.3(7)	4004(1)
Density, g cm^{-3}	1.115	1.260
Abs coeff., mm^{-1}	0.302	2.634
Temperature, K	293(2)	293(2)
Reflections collected	26561	26520
Independent reflections	9668 (R_{int} = 0.0611)	9587 (R_{int} = 0.0364)
Obs. data with $I \geq 2\sigma(I)$	5465	6935
Final R indices [$I \geq 2\sigma(I)$]	$R1$ = 0.0490	$R1$ = 0.0323
	$wR2$ = 0.1110	$wR2$ = 0.0791
R indices (all data)*	$R1$ = 0.1110	$R1$ = 0.0543
	$wR2$ = 0.1426	$wR2$ = 0.0927

* $R1 = \sum \big| \, |F_o| - |F_c| \, \big| \, / \sum |F_o|$; $wR2 = \{\sum [w(F_o^2 - F_c^2)^2] \, / \sum [w(F_o^2)^2]\}^{1/2}$

Table A3–5 Selected Crystallographic Data for Compounds **17–19**.

	17	**18**	**19**
Molecular formula	$C_{36}H_{62}IN_3Zr$	$C_{34}H_{56}I_2N_2Zr$	$C_{36}H_{62}HfIN_3$
Formula weight	755.01	837.83	842.28
Crystal size, mm^3	0.50 × 0.40 × 0.30	0.40 × 0.30 × 0.20	0.50 × 0.40 × 0.30
Crystal system	Monoclinic	Orthorhombic	Monoclinic
Space group	$P2_1/n$	$P2_12_12_1$	$P2_1/n$
a, Å	10.540(1)	11.260(1)	10.543(1)
b, Å	17.018(1)	13.061(1)	16.956(1)
c, Å	22.161(2)	26.242(3)	22.198(3)
α, Å	90	90	90
β, deg	99.099(2)	90	99.059(2)
γ, deg	90	90	90
Z	4	4	4
V, $Å^3$	3924.8(7)	3859.3(8)	3918.5(8)
Density, g cm^{-3}	1.278	1.442	1.428
Abs coeff., mm^{-1}	1.092	1.907	3.475
Temperature, K	293(2)	293(2)	293(2)
Reflections collected	26278	26299	26069
Independent reflections	9491 (R_{int} = 0.0405)	9345 (R_{int} = 0.0518)	9465 (R_{int} = 0.0350)
Obs. data with $I \geq 2\sigma(I)$	7123	6385	7492
Final R indices [$I \geq 2\sigma(I)$]	$R1$ = 0.0390	$R1$ = 0.0405	$R1$ = 0.0272
	$wR2$ = 0.0928	$wR2$ = 0.0837	$wR2$ = 0.0619
R indices (all data)*	$R1$ = 0.0592	$R1$ = 0.0791	$R1$ = 0.0420
	$wR2$ = 0.1046	$wR2$ = 0.0988	$wR2$ = 0.0690

* $R1 = \sum \big| \, |F_o| - |F_c| \, \big| \, / \sum |F_o|$; $wR2 = \{\sum [w(F_o^2 - F_c^2)^2] \, / \sum [w(F_o^2)^2]\}^{1/2}$

Table A3–6 Selected Crystallographic Data for Compounds **21** and **22**.

	21	**22**
Molecular formula	$C_{36}H_{62}N_2Zr$	$C_{36}H_{62}HfN_2$
Formula weight	614.10	701.37
Crystal size, mm^3	0.50 × 0.30 × 0.20	0.50 × 0.40 × 0.30
Crystal system	Orthorhombic	Orthorhombic
Space group	$P2_12_12_1$	*Pnma*
a, Å	11.006(1)	26.207(3)
b, Å	12.827(1)	10.994(1)
c, Å	26.223(3)	12.812(1)
α, Å	90	90
β, deg	90	90
γ, deg	90	90
Z	4	4
V, $Å^3$	3701.8(7)	3691.4(8)
Density, g cm^{-3}	1.102	1.262
Abs coeff., mm^{-1}	0.320	2.849
Temperature, K	293(2)	293(2)
Reflections collected	25350	23888
Independent reflections	8973 (R_{int} = 0.0522)	4698 (R_{int} = 0.0424)
Obs. data with $I \geq 2\sigma(I)$	5844	4110
Final R indices [$I \geq 2\sigma(I)$]	$R1$ = 0.0395	$R1$ = 0.0419
	$wR2$ = 0.0820	$wR2$ = 0.1457
R indices (all data)*	$R1$ = 0.0854	$R1$ = 0.0479
	$wR2$ = 0.1010	$wR2$ = 0.1485

* $R1 = \sum \mid |F_o| - |F_c| \mid / \sum |F_o|$; $wR2 = \{\sum [w(F_o^2 - F_c^2)^2] / \sum [w(F_o^2)^2]\}^{1/2}$

Table A3–7 Selected Crystallographic Data for Compounds **23** and **24**.

	23	**24**
Molecular formula	$C_{32}H_{56}Cl_2LiN_4Ti$	$C_{46}H_{88}Cl_2LiN_6Ti$
Formula weight	622.55	850.96
Crystal size, mm^3	0.40 × 0.30 × 0.20	0.30 × 0.20 × 0.20
Crystal system	Monoclinic	Monoclinic
Space group	$P2_1/n$	Cc
a, Å	15.704(1)	23.603(2)
b, Å	11.897(1)	10.454(9)
c, Å	20.145(2)	24.714(2)
α, Å	90	90
β, deg	93.126(2)	114.715(2)
γ, deg	90	90
Z	4	4
V, $Å^3$	3758.2(7)	5539.5(8)
Density, g cm^{-3}	1.100	1.020
Abs coeff., mm^{-1}	0.394	0.283
Temperature, K	293(2)	293(2)
Reflections collected	19946	18503
Independent reflections	6620 (R_{int} = 0.0520)	11227 (R_{int} = 0.0530)
Obs. data with $I \geq 2\sigma(I)$	4092	5220
Final R indices [$I \geq 2\sigma(I)$]	$R1$ = 0.0489	$R1$ = 0.0685
	$wR2$ = 0.1203	$wR2$ = 0.1675
R indices (all data)*	$R1$ = 0.0969	$R1$ = 0.1625
	$wR2$ = 0.1534	$wR2$ = 0.2258

* $R1 = \sum \mid |F_o| - |F_c| \mid / \sum |F_o|$; $wR2 = \{\sum [w(F_o^2 - F_c^2)^2] / \sum [w(F_o^2)^2]\}^{1/2}$

Table A3–8 Selected Crystallographic Data for Compounds **31** and **32**.

	31	**32**
Molecular formula	$C_{44}H_{62}ClN_4Si_2Ti$	$C_{45}H_{65}N_4Si_2Ti$
Formula weight	786.51	766.09
Crystal size, mm^3	0.50 × 0.40 × 0.30	0.50 × 0.30 × 0.20
Crystal system	Monoclinic	Triclinic
Space group	$P2_1/c$	$P\bar{1}$
a, Å	10.317(3)	10.7869(5)
b, Å	29.933(8)	10.9068(6)
c, Å	29.920(8)	20.346(1)
α, Å	90	92.464(1)
β, deg	91.628(5)	98.726(1)
γ, deg	90	103.842(1)
Z	8	2
V, $Å^3$	9236(4)	2289.4(2)
Density, g cm^{-3}	1.131	1.111
Abs coeff., mm^{-1}	0.327	0.272
Temperature, K	293(2)	296(2)
Reflections collected	49534	22750
Independent reflections	16281 (R_{int} = 0.0989)	8059 (R_{int} = 0.0445)
Obs. data with $I \geq 2\sigma(I)$	7356	5492
Final R indices [$I \geq 2\sigma(I)$]	$R1$ = 0.0780	$R1$ = 0.2212
	$wR2$ = 0.2019	$wR2$ = 0.5464
R indices (all data)*	$R1$ = 0.1828	$R1$ = 0.2510
	$wR2$ = 0.2810	$wR2$ = 0.5714

* $R1 = \sum \mid |F_o| - |F_c| \mid / \sum |F_o|$; $wR2 = \{\sum [w(F_o^2 - F_c^2)^2] / \sum [w(F_o^2)^2]\}^{1/2}$

Table A3–9 Selected Crystallographic Data for Compounds **33**·0.5C_6H_{14}–**35**.

	33·0.5C_6H_{14}	**34**	**35**
Molecular formula	$C_{43}H_{71}Cl_2LiN_5SiTi$	$C_{44}H_{62}Cl_2N_4Si_2Zr$	$C_{44}H_{62}Cl_2HfN_4Si_2$
Formula weight	811.87	865.28	952.55
Crystal size, mm^3	0.50 × 0.40 × 0.30	0.50 × 0.40 × 0.30	0.50 × 0.40 × 0.30
Crystal system	Triclinic	Monoclinic	Monoclinic
Space group	$P\bar{1}$	$P2_1/n$	$P2_1/n$
a, Å	12.800(2)	10.764(2)	10.7493(3)
b, Å	14.066(2)	27.472(5)	27.3816(8)
c, Å	14.338(2)	16.172(3)	16.1909(4)
α, Å	89.893(3)	90	90
β, deg	70.746(3)	95.272(3)	95.100(1)
γ, deg	84.914(3)	90	90
Z	2	4	4
V, $Å^3$	2426.5(7)	4762(1)	4746.7(2)
Density, g cm^{-3}	1.110	1.207	1.333
Abs coeff., mm^{-1}	0.343	0.426	2.393
Temperature, K	293(2)	293(2)	296(2)
Reflections collected	13259	31969	40146
Independent reflections	8507 (R_{int} = 0.0467)	11415 (R_{int} = 0.0598)	11237 (R_{int} = 0.0243)
Obs. data with $I \geq 2\sigma(I)$	4171	6316	9080
Final R indices [$I \geq 2\sigma(I)$]	$R1$ = 0.0647	$R1$ = 0.0488	$R1$ = 0.0260
	$wR2$ = 0.1515	$wR2$ = 0.1122	$wR2$ = 0.0595
R indices (all data)*	$R1$ = 0.1476	$R1$ = 0.1160	$R1$ = 0.0388
	$wR2$ = 0.2019	$wR2$ = 0.1504	$wR2$ = 0.0672

* $R1 = \sum \big| \, |F_o| - |F_c| \, \big| \, / \sum |F_o|$; $wR2 = \{\sum [w(F_o^2 - F_c^2)^2] \, / \sum [w(F_o^2)^2]\}^{1/2}$

Table A3–10 Selected Crystallographic Data for Compounds **36** and **37**.

	36	**37**
Molecular formula	$C_{46}H_{68}N_4Si_2Zr$	$C_{51}H_{69}ClN_4Si_2Zr$
Formula weight	824.44	920.95
Crystal size, mm^3	0.50 × 0.30 × 0.20	0.40 × 0.30 × 0.20
Crystal system	Monoclinic	Monoclinic
Space group	$P2_1/n$	$P2_1/c$
a, Å	10.782(1)	13.612(2)
b, Å	27.754(4)	22.575(4)
c, Å	16.136(2)	16.741(3)
α, Å	90	90
β, deg	95.461(2)	94.918(3)
γ, deg	90	90
Z	4	4
V, $Å^3$	4807(1)	5125.(1)
Density, g cm^{-3}	1.139	1.193
Abs coeff., mm^{-1}	0.311	0.349
Temperature, K	293(2)	293(2)
Reflections collected	32513	34580
Independent reflections	11630 (R_{int} = 0.0497)	12372 (R_{int} = 0.0629)
Obs. data with $I \geq 2\sigma(I)$	7177	6729
Final R indices [$I \geq 2\sigma(I)$]	$R1$ = 0.0468	$R1$ = 0.0504
	$wR2$ = 0.1124	$wR2$ = 0.1163
R indices (all data)*	$R1$ = 0.0940	$R1$ = 0.1181
	$wR2$ = 0.1407	$wR2$ = 0.1505

* $R1 = \sum \big| \, |F_o| - |F_c| \, \big| \, / \sum |F_o|$; $wR2 = \{\sum [w(F_o^2 - F_c^2)^2] \, / \sum [w(F_o^2)^2]\}^{1/2}$

Table A3–11 Selected Crystallographic Data for Compounds **39** and **40**.

	39	**40**
Molecular formula	$C_{48}H_{70}MgN_4OSi_2$	$C_{48}H_{70}CaN_4OSi_2$
Formula weight	799.57	825.34
Crystal size, mm^3	0.50 × 0.40 × 0.30	0.50 × 0.40 × 0.30
Crystal system	Monoclinic	Triclinic
Space group	$P2_1/n$	$P\bar{1}$
a, Å	11.867(1)	11.50(1)
b, Å	28.045(4)	13.13(1)
c, Å	15.009(2)	17.88(1)
α, Å	90	87.6(1)
β, deg	96.889(3)	77.94(1)
γ, deg	90	72.91(1)
Z	4	2
V, $Å^3$	4959(1)	2523(4)
Density, g cm^{-3}	1.071	1.073
Abs coeff., mm^{-1}	0.120	0.207
Temperature, K	293(2)	293(2)
Reflections collected	33733	13705
Independent reflections	11986 (R_{int} = 0.1012)	8834 (R_{int} = 0.0656)
Obs. data with $I \geq 2\sigma(I)$	4072	3491
Final R indices [$I \geq 2\sigma(I)$]	$R1$ = 0.0626	$R1$ = 0.0707
	$wR2$ = 0.1548	$wR2$ = 0.1709
R indices (all data)*	$R1$ = 0.2187	$R1$ = 0.1765
	$wR2$ = 0.2266	$wR2$ = 0.2415

* $R1 = \sum \big| \, |F_o| - |F_c| \, \big| \, / \sum |F_o|$; $wR2 = \{\sum [w(F_o^2 - F_c^2)^2] \, / \sum [w(F_o^2)^2]\}^{1/2}$

Table A3–12 Selected Crystallographic Data for Compounds **41** and **42**.

	41	**42**
Molecular formula	$C_{18}H_{24}N_2$	$C_{44}H_{66}K_2N_4O_2$
Formula weight	268.39	761.21
Crystal size, mm^3	0.50 × 0.40 × 0.30	0.40 × 0.30 × 0.20
Crystal system	Orthorhombic	Triclinic
Space group	*Pcca*	$P\bar{1}$
a, Å	21.158(4)	10.3277(6)
b, Å	10.620(2)	11.1184(7)
c, Å	14.846(3)	11.8225(7)
α, Å	90	115.875(1)
β, deg	90	90.585(1)
γ, deg	90	102.495(1)
Z	8	1
V, $Å^3$	3335(1)	1184.0(1)
Density, g cm^{-3}	1.069	1.068
Abs coeff., mm^{-1}	0.063	0.236
Temperature, K	293(2)	296(2)
Reflections collected	2932	13203
Independent reflections	2932 (R_{int} = 0.0000)	4037 (R_{int} = 0.0295)
Obs. data with $I \geq 2\sigma(I)$	1273	2601
Final R indices [$I \geq 2\sigma(I)$]	$R1$ = 0.0663	$R1$ = 0.0449
	$wR2$ = 0.1786	$wR2$ = 0.1176
R indices (all data)*	$R1$ = 0.1876	$R1$ = 0.0873
	$wR2$ = 0.2242	$wR2$ = 0.1425

* $R1 = \sum \big| \, |F_o| - |F_c| \, \big| \, / \sum |F_o|$; $wR2 = \{\sum [w(F_o^2 - F_c^2)^2] \, / \sum [w(F_o^2)^2]\}^{1/2}$

Table A3–13 Selected Crystallographic Data for Compounds **44–46**.

	44	**45**	**46**
Molecular formula	$C_{44}H_{62}N_4O_2Yb$	$C_{58}H_{77}EuKN_6O$	$C_{54}H_{69}N_6Sm$
Formula weight	852.02	1065.32	952.50
Crystal size, mm^3	0.40 × 0.30 × 0.20	0.50 × 0.40 × 0.30	0.40 × 0.30 × 0.20
Crystal system	Triclinic	Triclinic	Hexagonal
Space group	$P\bar{1}$	$P\bar{1}$	$P3$
a, Å	10.463(1)	11.870(2)	12.673(2)
b, Å	12.008(1)	13.542(2)	12.673(2)
c, Å	20.892(3)	22.292(4)	18.424(3)
α, Å	92.854(3)	98.072(3)	90
β, deg	90.430(3)	99.164(3)	90
γ, deg	110.628(2)	112.940(3)	120
Z	2	2	2
V, $Å^3$	2452.6(7)	3175.8(9)	2562.7(8)
Density, g cm^{-3}	1.154	1.114	1.234
Abs coeff., mm^{-1}	1.904	1.090	1.185
Temperature, K	293(2)	293(2)	293(2)
Reflections collected	13360	17254	13910
Independent reflections	8588 (R_{int} = 0.0340)	11114 (R_{int} = 0.0354)	6026 (R_{int} = 0.0441)
Obs. data with $I \geq 2\sigma(I)$	7238	8868	4985
Final R indices [$I \geq 2\sigma(I)$]	$R1$ = 0.0393	$R1$ = 0.0429	$R1$ = 0.0381
	$wR2$ = 0.0909	$wR2$ = 0.0986	$wR2$ = 0.0901
R indices (all data)*	$R1$ = 0.0489	$R1$ = 0.0578	$R1$ = 0.540
	$wR2$ = 0.0947	$wR2$ = 0.1048	$wR2$ = 0.1122

* $R1 = \sum \mid |F_o| - |F_c| \mid / \sum |F_o|$; $wR2 = \{\sum [w(F_o^2 - F_c^2)^2] / \sum [w(F_o^2)^2]\}^{1/2}$

Table A3–14 Selected Crystallographic Data for Compounds **47–49**.

	47	**48**	**49**
Molecular formula	$C_{40}H_{54}IN_4OYb$	$C_{54}H_{69}N_6Eu$	$C_{54}H_{69}N_6Yb$
Formula weight	906.81	954.11	975.19
Crystal size, mm^3	0.40 × 0.30 × 0.20	0.40 × 0.30 × 0.30	0.40 × 0.30 × 0.20
Crystal system	Monoclinic	Hexagonal	Triclinic
Space group	$P2_1/c$	$P3$	$P\bar{1}$
a, Å	19.2421(5)	12.6538(8)	11.742(1)
b, Å	12.6237(3)	12.6538(8)	11.847(1)
c, Å	17.8425(4)	18.422(1)	41.537(5)
α, Å	90	90	90.019(3)
β, deg	100.408(1)	90	93.601(2)
γ, deg	90	90	112.801(2)
Z	4	2	4
V, $Å^3$	4262.7(1)	2554.5(3)	5314(1)
Density, g cm^{-3}	1.413	1.240	1.219
Abs coeff., mm^{-1}	2.950	1.267	1.798
Temperature, K	296(2)	296(2)	296(2)
Reflections collected	39618	21005	47950
Independent reflections	7711	6204	19087
	(R_{int} = 0.0376)	(R_{int} = 0.0379)	(R_{int} = 0.0513)
Obs. data with $I \geq 2\sigma(I)$	6818	5424	14896
Final R indices [$I \geq 2\sigma(I)$]	$R1$ = 0.0253	$R1$ = 0.0240	$R1$ = 0.0727
	$wR2$ = 0.0629	$wR2$ = 0.0561	$wR2$ = 0.1978
R indices (all data)*	$R1$ = 0.0299	$R1$ = 0.0323	$R1$ = 0.0897
	$wR2$ = 0.0647	$wR2$ = 0.0589	$wR2$ = 0.2037

* $R1 = \sum \mid |F_o| - |F_c| \mid / \sum |F_o|$; $wR2 = \{\sum [w(F_o^2 - F_c^2)^2] / \sum [w(F_o^2)^2]\}^{1/2}$